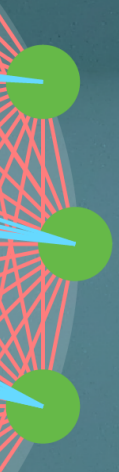


Systemic risk in ecosystems



J. Jelle Lever



Propositions

- 1) When species continue to support each other under increasingly harsh conditions they may, eventually, collapse simultaneously because they depend on each other for survival.
(this thesis)
- 2) Delayed negative feedbacks are underestimated as a potential cause of critical transitions in complex ecosystems.
(this thesis)
- 3) Measures to prevent small-scale failures in complex systems should not be taken because they undermine a system's capacity to adapt to changing circumstances.
- 4) Field observations of complex ecosystems should focus on the rates at which different processes occur rather than on diversity and species abundances.
- 5) Scientists should be as engaged in defending scientific freedom, the freedom to imagine, explore, and discover, as artists are in defending artistic freedom.
- 6) Rather than well-planned scientific research we should promote a process of scientific evolution where progress is made by making random mistakes.
- 7) Future generations will criticize us for defining efficiency in terms of productivity rather than in terms of minimum wasted time, effort, or resources.
- 8) All social developments start with education or a lack thereof.

Propositions accompanying the PhD thesis:

Systemic Risk in Ecosystems

J. Jelle Lever

Wageningen, 19 February 2020

Systemic Risk in Ecosystems

J. Jelle Lever

Thesis committee

Promotors:

Prof. Dr M. Scheffer

Distinguished professor of Aquatic Ecology and Water Quality Management
Wageningen University & Research

Prof. Dr J. Bascompte

Professor of Ecology
University of Zurich, Switzerland

Co-promotor:

Dr E.H. van Nes

Associate professor, Aquatic Ecology and Water Quality Management Group
Wageningen University & Research

Other members:

Prof. Dr J.C. Biesmeijer, Naturalis Biodiversity Center, Leiden

Prof. Dr P. Hogeweg, Utrecht University

Prof. Dr A.M. de Roos, University of Amsterdam

Prof. Dr P.C. de Ruiter, Wageningen University & Research

This research was conducted under the auspices of the Graduate School for Socio-Economic and Natural Sciences of the Environment (SENSE)

Systemic Risk in Ecosystems

J. Jelle Lever

Thesis

submitted in fulfilment of the requirements for the degree of doctor

at Wageningen University

by the authority of the Rector Magnificus

Prof. Dr A.P.J. Mol,

in the presence of the

Thesis Committee appointed by the Academic Board

to be defended in public

on Wednesday 19 February 2020

at 4 p.m. in the Aula.

J. Jelle Lever
Systemic Risk in Ecosystems
194 pages.

PhD thesis, Wageningen University, Wageningen, NL (2020)
With references, with summary in English

ISBN: 978-94-6395-263-7
DOI: <https://doi.org/10.18174/510243>

Contents

	Page
Chapter 1 General Introduction	7
Chapter 2 The sudden collapse of pollinator communities	25
Chapter 3 Critical transitions in complex food webs	49
Chapter 4 Foreseeing the future of mutualistic communities beyond collapse	89
Chapter 5 Synthesis	157
References	165
Summary	183
Acknowledgements	187
About the author	191
SENSE Diploma	192

Chapter 1

General Introduction

J. Jelle Lever

1.1 A HISTORY OF NETWORKS IN ECOLOGY

The earliest evidence of life on Earth dates from at least 3,770 million years ago (Rosing 1999; Ohtomo et al. 2014; Dodd et al. 2017) and, today, the Earth is inhabited by an estimated 8.7 million species (Mora et al. 2011). The far majority of these species still awaits description. It is, therefore, only logical that we continue to try to understand more about the world in which we live by classifying and describing the intrinsic, e.g. the morphological, physiological, and genetic, properties of species and their common ancestors. The description and classification of species, however, only provides limited insight. Observations need to be accompanied by the development of theories that explain observed patterns in order to achieve real understanding, and species are embedded in complex ecosystems of many interacting species and of interactions between species and their environment that have properties of their own. Network approaches towards studying ecosystems attempt to study these properties, for example, by describing the patterns of interactions among species, i.e. the way in which these interactions are arranged in complex ‘ecological networks’. These patterns are likely to be crucial for the maintenance of biodiversity because they allow species to coexist, and may affect the specific way in which ecosystems may respond to changing environmental conditions.

An early, perhaps the first, graphical representation of a network of interacting species was made by Lorenzo Camerano in 1880 (Camerano 1880, 1994; Cohen 1994 and Fig. 1.1). Other relatively early studies included descriptions of such networks as well (e.g. Forbes 1925 and Shelford 1913). Ecological networks, however, only became central to ecology when Charles Elton proposed four main organizing principles by which species communities are organized; food chains, ecological niches, food size ranges, and trophic pyramids (Elton, 1927). These principles were an attempt to describe general patterns in ecosystems, varying from the observation that different species may occupy a similar place or ‘niche’ in food webs, i.e. networks of predator-prey relationships, that species tend to eat food between certain size limits, and the idea that species at the base of food chains tend to be more abundant than those at the top. An important further step was made by Lindeman (1942), who described ecosystems as systems that transform energy obtained from sunlight by plants. Lindeman (1942) suggested that this transfer of energy to higher trophic levels is inefficient: a potential explanation for the loss in abundance as trophic levels increase as described by Elton (1927). When describing flows of energy in lakes, Lindeman proposed, following Tansley (1935), that lakes should be seen as integrated systems of biotic and abiotic interactions, and, as such, provided the basis for our modern understanding of the word ‘ecosystem’.

The work of Lindeman (1942) was developed further by the brothers Howard and Eugene Odum. Howard was the first to use an energy flow diagram to describe the trophic structure and productivity of ecosystems (Odum, 1957), and Eugene wrote, with the help of his brother, several revised editions of an influential textbook that introduced the holistic,

other species.

While the previous work focused on the upward flows of energy through food webs, little attention was given to the top-down effects of predators on prey until Hairston et al. (1960) published their influential work on food chains in terrestrial communities. Hairston et al. (1960) argued that predators reduce the abundance of herbivores and therefore allow plants to flourish, an hypothesis referred to as the ‘green world hypothesis’. The importance of top-down effects was later confirmed by Paine (1966), who showed experimentally that the removal of a top-predator may lead to secondary extinctions due to increased competition between species on lower trophic levels. He later coined the terms keystone species (Paine, 1969) and trophic cascade (Paine, 1980) to describe species that have a disproportionately large effect on the integrity and stability of species communities and the indirect effects these species may have on other species.

By explicitly incorporating, and showing the relevance of, top-down effects in species communities, Hairston et al. (1960) and Paine (1969) paved the way for a re-evaluation of the relationship between the complexity and stability of ecosystems. Eventually, it was May (1972, 1973) who suggested that a general study of Gardner & Ashby (1970) on the relationship between the complexity and stability of complex systems, was of relevance for ecology as well. With model systems they showed that, when randomly taking interaction strengths from a normal distribution with mean zero, the chance of a system to be stable, i.e., to exhibit a stable nontrivial equilibrium point at which all species may coexist stably, declines rapidly when the number of interactions or species passes a critical value.

The analysis of May (1972, 1973) triggered a longstanding debate in ecology on the relationship between the complexity and stability of ecosystems, because the observation that simple systems are more likely to be stable than large, complex ones, was the opposite of what was commonly believed and previously suggested by Odum (1953) and MacArthur (1955). The model systems of May (1972, 1973), however, did not include much ecological realism as interactions were assigned randomly and allowed for negative nontrivial equilibrium abundances (Roberts, 1974), and May hinted in his 1972 paper that alternative arrangements, i.e. a modular ‘block’ structure, could promote the stability of complex ecosystems. Eventually, it was Yodzis (1981), building on the work of Pimm & Lawton (1978), who showed that model systems to which interactions are assigned such that they mimic real ecosystems are more likely to exhibit a stable nontrivial equilibrium point than their randomized counterparts. A strong suggestion that the non-random way in which interactions are arranged in complex ecological networks may provide an explanation for the stable coexistence of species in complex ecosystems.

1.2 THE STRUCTURE OF ECOLOGICAL NETWORKS

One of the pioneers in searching for structural patterns in complex ecological networks was Joel Cohen. Cohen used a framework provided by Hutchinson (1957), who defined a

species' niche as an n -dimensional hypervolume in a space with environmental conditions or resource traits on the axes to study the niche structure of species communities (Cohen, 1977; Cohen & Stephens, 1978). By determining the prey shared by predators, Cohen determined the overlap in the trophic niche occupied by predators and suggested that a single niche axis is usually sufficient to explain who interacts with whom in complex food webs. Discussions continue about what this single axis might represent, some have suggested that it could simply be the body-size of prey (Warren & Lawton, 1987; Lawton & Warren, 1988; Cohen et al., 1993, 2003), but it might differ among ecosystems.

A way to test whether basic rules based on the aforementioned organizing principle may explain observed patterns is to generate model networks and comparing them with data. Cohen & Newman (1985) made a first attempt to generate such networks by arranging species in a 'cascade' or hierarchical order and assuming that species feed, with a certain probability, only on species that are lower in hierarchy (Cohen & Newman, 1985; Cohen et al., 1990). The approach of Cohen & Newman (1985) was developed further by Williams & Martinez (2000), who randomly assigned species with a 'niche value' and assumed species to feed on species within a niche range of which the mean is lower than a species own value. Other notable work building on the work of Cohen (1977) can be found in Sugihara (1980, 1983), Cattin et al. (2004), and Stouffer et al. (2005). In this work, other, similar methods to generate model networks are proposed that were, to a more or lesser extent, able to reproduce several features common to all food webs, such as the fractions of species at top, intermediate and basal levels, the variability in the number of interactions per prey and predator species, and the degrees of cannibalism, omnivory, and trophic similarity. Stouffer et al. (2005) suggests that this will be the case for any model satisfying two conditions: (1) the species' niche values form a totally ordered set and (2) each species has a specific exponentially decaying probability of preying on a given fraction of the species with lower niche values.

Another approach to detect commonalities in food-web structure is to study the frequency of network motifs, i.e. subnetworks of n species within larger food webs. In ecology, several simple patterns of interactions involving three or more species received a lot of attention, i.e. trophic cascades in food chains, omnivory, exploitative competition, and apparent competition (Elton, 1927; Hairston et al., 1960; Holt, 1977; Pimm & Lawton, 1978; Tilman, 1982; Holt et al., 1994). Following earlier work by Milo et al. (2002), Stouffer et al. (2007) were the first to rigorously explore whether such relationships are common in empirical and model-generated food webs by studying the frequency of three-species motifs. Stouffer et al. (2007) found that simple food chains and omnivory were over-represented in most empirical and in model-generated food webs, while exploitative and apparent competition were under-represented relative to randomized versions of the same food webs. A notable exception, however, did occur in some empirical networks where omnivory was under-represented and exploitative and apparent competition were over-represented. The implications of these patterns for the dynamics of complex food-webs

are still part of ongoing research (Prill et al., 2005; Kondoh, 2008; Stouffer & Bascompte, 2010).

A further understanding of why some patterns are more likely to occur in ecological networks can, most likely, be obtained when studying feedbacks in complex ecosystems. Three types of feedbacks are of importance; direct negative feedbacks, positive feedbacks, and delayed negative feedbacks (Levins, 1974). Direct negative feedbacks, e.g. intraspecific competition, have stabilizing effects. Positive or ‘reinforcing’ feedbacks, e.g. the feedback between two mutualistically interacting species, amplify change away from an existing equilibrium and are thus destabilizing. Delayed negative feedbacks, i.e. negative feedbacks with a time lag usually occurring as the result of an uneven number of negative interactions in feedback loops of two or more species, can lead to oscillating dynamics, and the interplay between several delayed negative feedbacks may cause chaotic or other complex dynamics. A well-known example is provided by Rosenzweig & MacArthur (1963) and Rosenzweig (1971) who showed that ‘enriching’ a prey population by providing it with more resources could destabilize predator-prey systems, a phenomenon referred to as the ‘paradox of enrichment’. When providing prey with more resources, the direct negative feedback due to intraspecific competition becomes weaker relative to the delayed, indirect negative effect due to a prey’s interaction with a predator. Such a change in the balance between direct and delayed negative feedbacks may lead to oscillations in the abundances of predators and prey (Levins, 1974; Puccia & Levins, 1985). McCann et al. (1998) later suggested that weak trophic interactions may stabilize subsystems of strongly interacting prey and predator species that would show oscillating or chaotic dynamics in isolation, an idea that was later built further upon by Berlow (1999), Neutel et al. (2002), and Bascompte et al. (2005). Delayed negative feedback may also undermine the resilience of systems with strong positive feedbacks, such as shallow lakes. The interplay between a delayed negative feedback and such a positive feedback may lead to a ‘slow-fast cycle’, causing a system to repeatedly switch between alternative states, e.g. a clear-water and a turbid state (Van Nes et al., 2007).

Networks of trophic, predator-prey interactions remained the main object of study when describing ecological network structure until Jordano (1987) presented his work on complex communities of mutualistically interacting plant and pollinator species or seed dispersers. Jordano (1987) found, among other patterns, that the distribution of relative mutualistic interaction strengths is highly skewed. Most interactions were found to be weak, and the few cases in which species depended strongly on a single species did not necessarily imply a strong mutual dependence. Pairwise dependencies were, instead, found to be asymmetric, i.e., plant species depend relatively strongly on seed dispersers that do not depend strongly on them and vice versa. Building further on the work of Jordano (1987), Bascompte et al. (2006) showed that such asymmetric relationships promote the stability of mutualistic networks. The work of Jordano (1987) paved the way for the later finding that mutualistic networks tend to be highly nested, i.e., specialists tend to interact with

a subset of the species interacting with the more generalist species (Bascompte et al., 2003). An automatic consequence of such a structure is that specialist species depend relatively strongly on generalist species, thus explaining the asymmetry in relative interaction strengths as described by Jordano (1987). Bastolla et al. (2009) later showed that nestedness reduces effective interspecific competition and promotes indirect facilitation in mutualistic communities which, in turn, enhances the number of species that may coexist stably. These findings may have wider implications for other disassortative networks, i.e., networks in which nodes with few interactions tend to interact with nodes that have many interactions, such as scale-free networks in social, economic, technological, biological, and physical systems (Barabási & Albert 1999; May et al. 2008, but see Jordano et al. 2003). Such disassortative structures were found to promote the robustness of networks to the random removal, but increases the dependence of networks on a few highly connected nodes (Albert et al., 2000; Memmott et al., 2004).

Studies on the structural properties of communities dominated by other interaction types are less common. An early exception is the work of Cody (1974) on competitive bird communities further analyzed by Sugihara (1983). More recent work has focused on the ways in which networks of trophic, mutualistic, competitive and/or other interaction types combine into larger networks (Chase et al., 2002; Arim & Marquet, 2004; Lafferty et al., 2008; Melián et al., 2009; Poccock et al., 2012; Mougi & Kondoh, 2012; Pilosof et al., 2017). Our knowledge, in particular of the structural patterns and dynamic behavior of such complex ‘multilayer’ systems, is however still far from complete.

1.3 STABILITY CONCEPTS

The search for common patterns in the structure of ecological networks, i.e. the way in which interactions are arranged, is a first step towards understanding the rules determining the dynamics and stability of ecosystems. It is, however, certainly not the last step. Ecosystems may exhibit a wide variety of dynamical properties that may correspond to different aspects of stability. When studying the interrelationship between the structure and stability of ecological networks, it is thus of importance to determine which aspects of stability are of interest, and whether these aspects are interrelated.

In one of few field experiments on the relationship between the complexity and stability of ecosystems, Tilman et al. (2006) showed, for example, that greater numbers of plant species increase the temporal stability of grassland communities. Temporal stability was defined as the mean divided by the standard deviation of fluctuating plant abundances, a measure of stability that roughly corresponds to the way in which the early contributors to the diversity-stability debate thought of stability (e.g. MacArthur 1955 and Elton 1958). An important distinction between the level at which a system’s temporal stability is measured, however, needs to be made. While the temporal stability of the community’s total biomass was found to increase, the temporal stability of individual species was

found to decrease with increasing species number. A greater temporal stability of the total biomass of diverse communities may be caused by a higher productivity, statistical averaging, and negative correlations between species abundances (Tilman et al., 1998; Lehman & Tilman, 2000). In Fig. 1.2 and Fig. A1.1 in Supplementary Information, I show that similar differences in temporal stability may be found in food webs. Strong correlations between species abundances can be expected when species recover slowly from perturbations along a particular line in a system's phase space, i.e. a multidimensional space in which each axis corresponds to the abundance of a species. Such slow recovery may occur when the dominant eigenvalue of the Jacobian matrix corresponding to a system's nontrivial equilibrium is close to zero, a measure used by May (1972, 1973) to distinguish between stable and unstable ecosystems. A slow recovery from perturbations along a particular line in the system's phase space, which is generally seen as 'unstable', may thus simultaneously lead to relatively small fluctuations in the total abundance of species groups, which is seen as 'stable', when abundances are negatively correlated. Discussions on whether certain ecosystem properties, e.g. the number of species, promote or undermine stability may only be clarified when such different aspects of stability are clearly defined.

Other notions of stability exist. For instance, the aforementioned method used by May (1972, 1973), i.e. the local stability of a system's nontrivial equilibrium, has the drawback that it misses non-equilibrium attractors that may allow species to coexist while abundances are oscillating or following other more complex dynamics. A criterion used to determine whether the coexistence of species is possible, even when there is no stable nontrivial equilibrium, is referred to as 'permanence'. A permanent set of species has the property that all species may persist over time, i.e. have nonzero abundances, even when dynamics are fairly complex because the boundaries to the system's phase space are repelling (Hutson & Vickers, 1983; Hutson & Law, 1985; Hofbauer & Sigmund, 1988; Law & Morton, 1996). Others may want to use a more strict definition of stability, and want to check whether a system's nontrivial equilibrium point is 'globally stable', i.e. there are no alternative attractors to which a system may shift. Conditions to determine whether a nontrivial equilibrium of a Lotka-Volterra competition model is globally stable can be found in Goh (1977) and Logofet (1993). Both definitions of permanence and global stability are conceptually attractive. Determining whether a set of species is permanent, or whether a system's nontrivial equilibrium is globally stable is, however, usually not easy and may often be impossible. Evaluating the local stability of a system's nontrivial equilibrium is, perhaps for this reason, the most commonly used method when studying the interrelationship between the complexity and stability of ecosystems. In addition to the here described methods, graph theoretical approaches are used to study the stability of complex ecosystems, e.g. the likelihood of co-extinctions when species are removed from a network (Albert et al., 2000; Solé & Montoya, 2001; Memmott et al., 2004; Rezende et al., 2007).

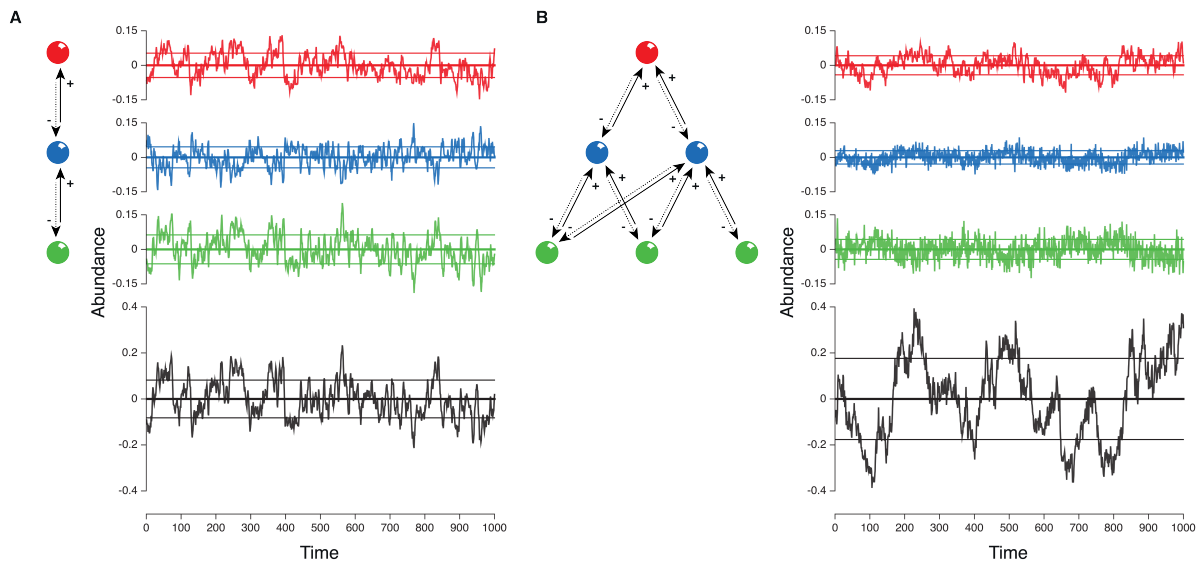


Figure 1.2: Fluctuations in the abundances of primary producers (green), consumers (blue) and top-predators (red) when forming part of a simple food chain (**A**) and a more complex food web (**B**). Colored time series show the sum of all species belonging to a single trophic level. Time series in black show the fluctuations in species abundances when they are projected on the line in the network's phase space along which variance is highest, i.e. the first principal component as determined with a principal component analysis. A similar regime of random perturbations leads to relatively large fluctuations in the abundances of basal and consumer species in the simple food chain when compared to the total biomass of basal and consumer species in the more complex food web. Fluctuations along the system's first principal component are, however, substantially smaller. These opposing patterns in variability may occur when the abundances of species belonging to the same trophic level are anti-correlated. Relatively large fluctuations along a system's first principal component and strong (anti-)correlations in species abundances can be expected when the dominant eigenvalue of a system's Jacobian matrix is close to zero (see **Chapter 4**). Horizontal lines indicate the mean and standard deviations. Competition among primary produces and the feeding rates of consumers and predators are assumed to be substantially lower in the simple food chain (see Appendix A1.1 and Fig. A1.1 in Supporting Information).

Apart from stability concepts that were developed in the context of the aforementioned complexity-stability debate, two important theories, i.e. chaos theory and catastrophe theory, are of major importance for the way in which ecologists evaluate ecosystem stability. Chaos theory deals with the fact that even relatively simple systems may show complex dynamical behavior that never repeats itself (Poincaré, 1890; Lorenz, 1963; May, 1976). More importantly, small differences in a system's initial state, or small external perturbations to this state, will expand exponentially over time and may lead to a wide variety of outcomes when systems exhibit such chaotic dynamics, which makes it hard to predict their long-term behavior. This complex behavior is determined by the deter-

ministic rules governing a system's dynamics and not the result of a stochastic process. Catastrophe theory deals with another type of perturbations, namely with changes in the parameters of a system and is embedded in a wider framework on the structural stability of complex biological systems developed by René Thom (Thom, 1972, 1975). A system is structurally unstable when infinitely small changes to a system's parameters lead to qualitative changes in the dynamical behavior of a system (such as the existence of equilibrium points, limit cycles, or deterministic chaos). The size of the area in a system's parameter space within which a system exhibits the same qualitative behavior is used as a measure of the extent in which a system's dynamical behavior is structurally stable (Thom, 1972; Vandermeer, 1975; Thom, 1977; Alberch, 1989; Bastolla et al., 2005, 2009; Rohr et al., 2014). Catastrophe theory deals with the nature of the boundaries to such areas and in particular with the cases in which gradual changes in the properties of a system lead to abrupt changes in behavior, e.g. a shift from one stable state to another. Thom (1972) shows that there are seven 'elementary' catastrophes, i.e. catastrophes that involve stable equilibrium points, when dynamics are controlled by no more than four parameters. The simplest of these elementary catastrophes, and the most commonly used when explaining abrupt shifts in ecosystems, are the fold and cusp catastrophe that are controlled by 1 and 2 parameters respectively (Fig. 1.3). Despite some controversy in the past (Zahler & Sussmann, 1977), the cusp and fold catastrophe are now considered to capture the essence of a wide variety of systems varying from ecosystems (May, 1977; Wilson & Agnew, 1992; Scheffer et al., 2001), to human cells (Hasty et al., 2002; Ferrell Jr, 2002; Lee et al., 2002; Tyson et al., 2003; Angeli et al., 2004), and the climate (Hare & Mantua, 2000; Clark et al., 2002; Alley et al., 2003; Lenton et al., 2008).

Published around the same time, and highly related to the work of René Thom, is the work of Buzz Holling (Holling, 1973, 1996). Holling (1973) uses several examples to illustrate that abrupt regime shifts or 'critical transitions' may occur in ecosystems, e.g. towards a eutrophic or 'highly productive' state under the influence of nutrient enrichment in lakes, in fish populations due to harvesting (Ricker, 1963; Smith, 1968; Hutchinson et al., 1970), and in tree cover due to grazing in terrestrial ecosystems (Glendening, 1952). Holling (1973) noted that for such systems the important question is not how stable a system is in the classical sense as described by MacArthur (1955) and Elton (1958), but how likely it is for a system to switch from one state to another. As a way to estimate such probability, he proposes to use the size of the domain of attraction in a system's phase space (Fig. 1.4). In later work, Holling refers to the magnitude of a disturbance that can be absorbed before a system shifts into another stability domain as 'ecological resilience', and to the resistance to disturbance or the speed of return to equilibrium as 'engineering resilience' (Holling 1996, Fig. 1.4, and 1.5). More loose definitions of ecological resilience are, however, also used such as: 'a system's ability to absorb changes of state variables, driving variables, and parameters, and still persist' (Holling, 1973) and 'the capacity of a system to absorb disturbance and reorganize while undergoing change so as to still retain

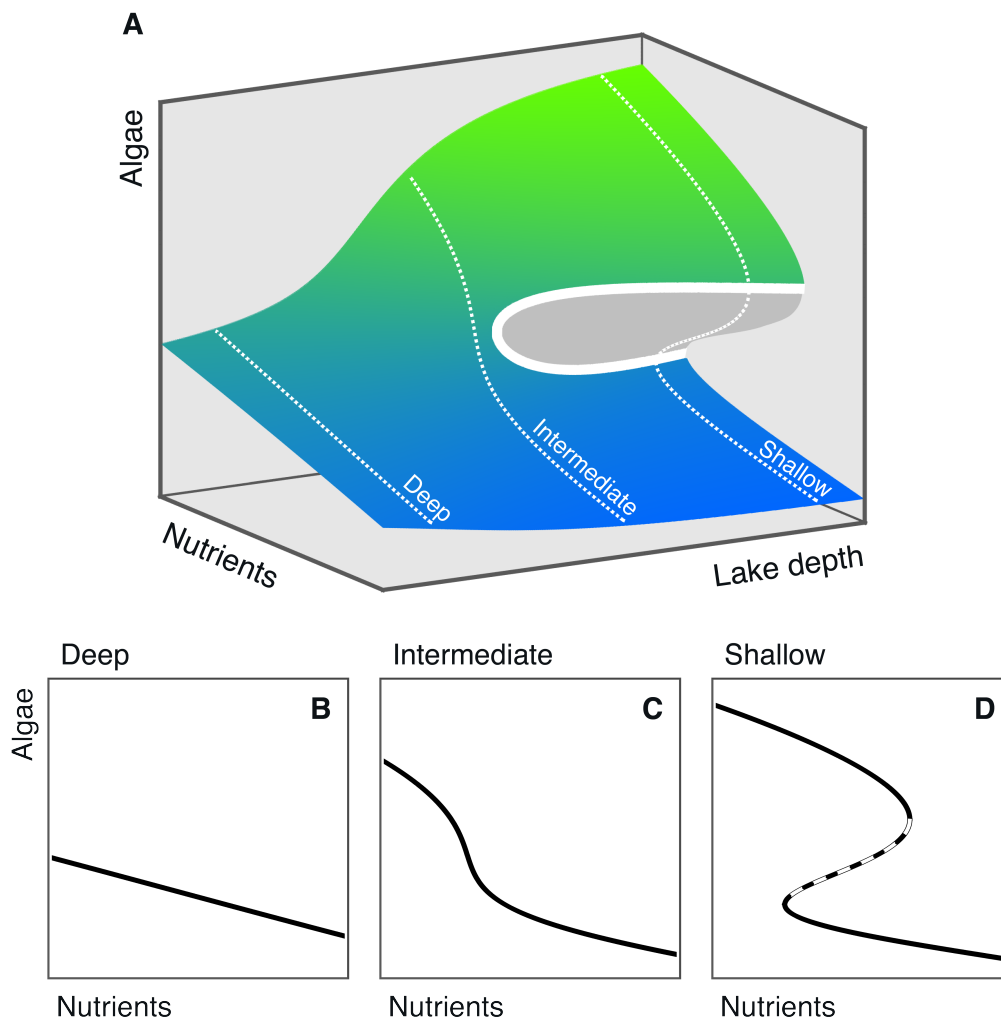


Figure 1.3: The density of algae as described by a model with two control parameters; nutrient availability and lake depth. (A) Cusp catastrophe in which two alternative stable states, i.e. a non-turbid state with low algae density and a turbid state with high algae density, may exist depending on nutrient availability and lake depth. The surface corresponds to the algae's equilibrium density. Unstable equilibrium densities are plotted in grey. (B-D) Ways in which the algae's equilibrium density depends on nutrient availability in a deep (B), intermediate (C), and shallow lake (D). Panel D corresponds to a fold catastrophe. The dashed middle section in panel D corresponds to an unstable equilibrium. This figure is based on a model in Scheffer (1990), and Scheffer et al. (1993).

essentially the same function, structure, identity, and feedbacks' (Walker et al., 2004). The work of Thom (1972) and Holling (1973) was further introduced to ecology by May (1977) and Scheffer et al. (2001). This work shows that, as conditions change, ecological resilience might be lost until a 'critical point' is reached beyond which a transition towards an alternative state becomes inevitable (Fig. 1.4). Recovery from such shifts may require

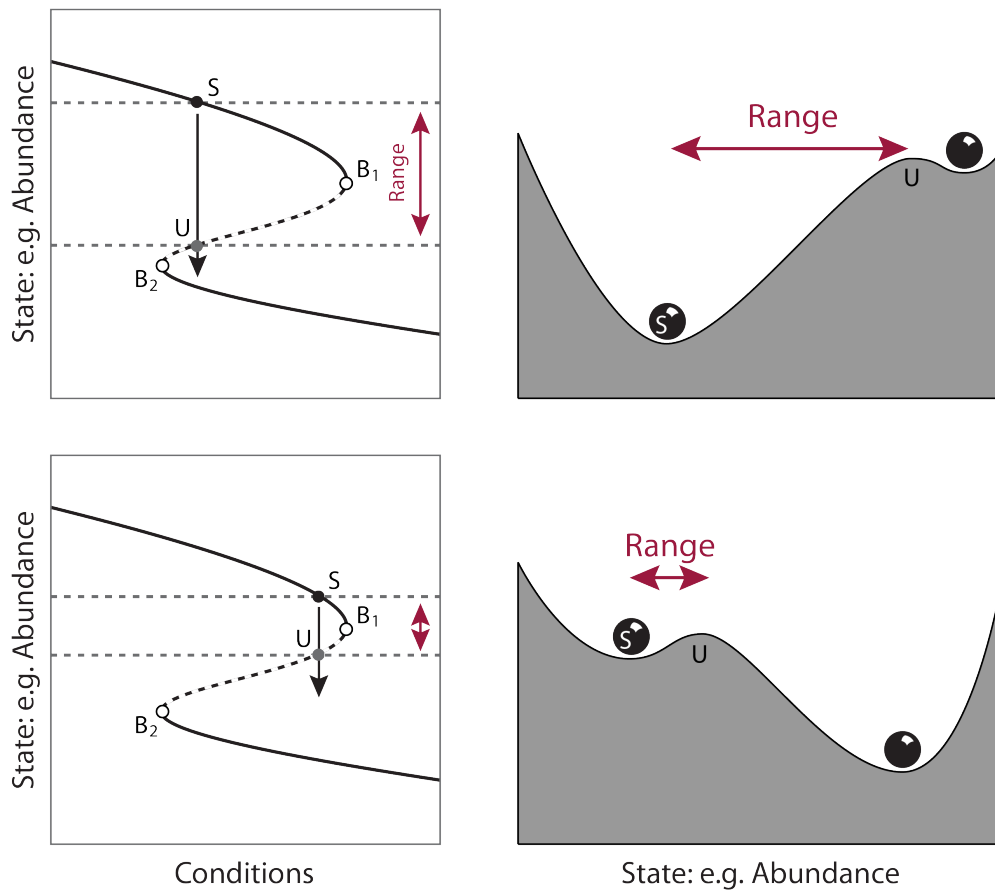


Figure 1.4: Ecological resilience far from (top panels) and close to a bifurcation point (bottom panels) as determined by the size of a system's attraction basin. Left panels show the equilibrium curve of a system with two alternative stable states, i.e. a fold catastrophe as in Fig. 1.3.D. Dots indicate stable (S) and unstable equilibrium points (U) far from (top panel) and close to a bifurcation point B_1 (bottom panel). Ecological resilience is large, i.e. the indicated range or amount of change in abundance a system may tolerate without shifting into an alternative attraction basin, is large far from a bifurcation point. When conditions change further towards a bifurcation point, the amount of change a system can handle goes to zero and a regime shift or 'critical transition' toward an alternative state becomes inevitable. Right panels show stability landscapes for the conditions at which stable and unstable equilibrium points are indicated on the fold catastrophe. Balls correspond to stable and hilltops to unstable equilibrium points.

more than a simple return to the conditions at which a transition occurred, a phenomenon called 'hysteresis'.

One of the challenges when dealing with such critical transitions is that it might be hard to know whether a system is approaching a critical point because the state of a system may show little change before a tipping point is reached. A concern for those who may

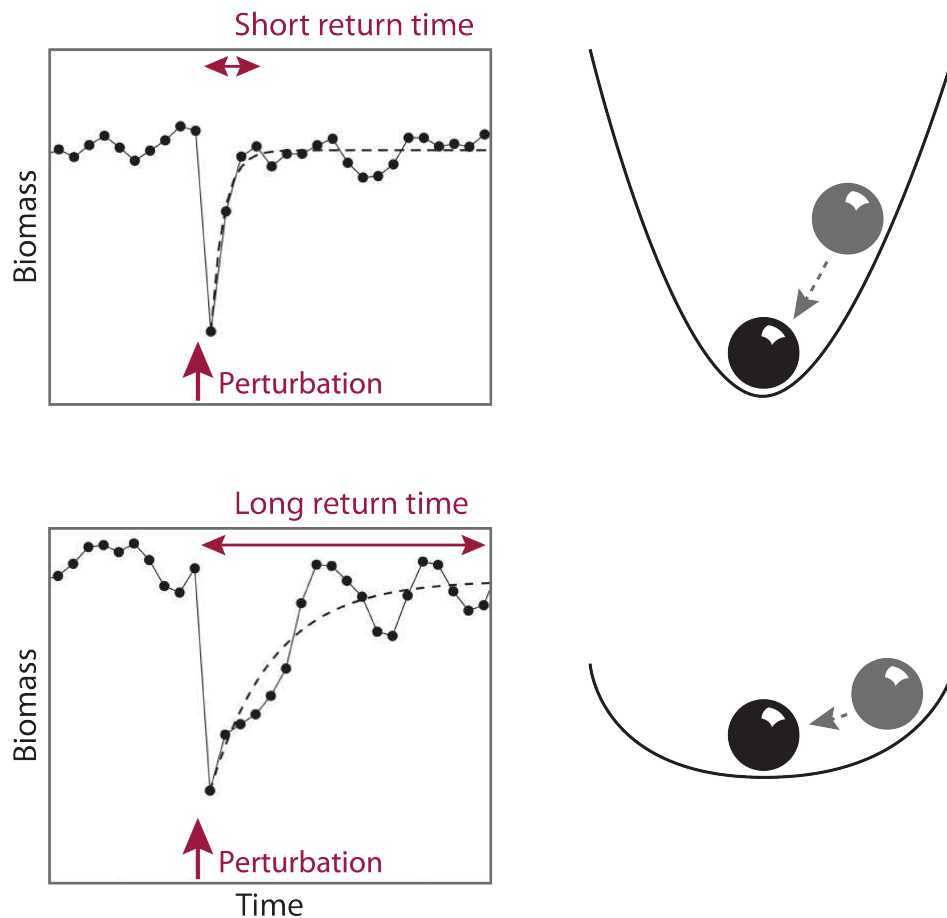


Figure 1.5: Engineering resilience, or the speed at which a system returns to equilibrium after a perturbation. Top panels correspond to a system with a high engineering resilience, lower panels to a system with a low engineering resilience. The speed of recovery, and thus the time it takes to return to equilibrium, is roughly determined by the slope of a system's stability landscape. This figure is based on work in Van Nes & Scheffer (2007).

want to prevent critical transitions from happening. Wissel (1984) and Van Nes & Scheffer (2007), however, showed that an increasingly slow recovery from small disturbances may be indicative of a loss of ecological resilience prior to a critical transition, a phenomenon known as 'critical slowing down'. This work, in turn, provided the basis for a wide variety of indicators often obtained through time series analysis, e.g. an increase in variance, autocorrelation, and skewness, that may serve to detect an increase in the likelihood of critical transitions (reviewed in Scheffer et al. 2009 and Dakos et al. 2012).

1.4 NETWORK THEORY AND CRITICAL TRANSITIONS

Despite a longstanding interest in the structure and stability ecological networks, the common ground between studying the structure of ecological networks and the potential causes and consequences of critical transitions remains largely unexplored. Or, more

specifically, most studies on the structure and stability of ecological networks have focused on stability concepts that are unrelated with critical transitions, while studies of critical transitions have often focused on the dynamics of individual populations rather than on the complex networks of interactions between species that maintain them. This thesis aims to fill this gap by merging network theory with theory on critical transitions.

In **Chapter 2**, we build further on the work of Bastolla et al. (2009) and show that indirect facilitation occurring nested mutualistic networks may come at a cost; when pollinators continue to facilitate each other under increasingly harsh conditions they may eventually collapse simultaneously, because they depend on each other for survival. Recovery from such a simultaneous collapse may require a relatively large improvement in conditions. Findings that may have large implications for our view on the sustainability of pollinator communities and the services they provide in a time when pollinator populations are rapidly declining. Pollinator communities may, however, also be able to persist longer under increasingly harsh circumstances when indirect facilitation is strong. A trade-off between different aspects of stability, e.g. persistence and the potential for a large-scale systemic collapse, thus appears to exist.

In **Chapter 3**, we build further on previous work (implicitly) pointing towards delayed negative feedbacks as a potential cause of instability in complex food webs, e.g. McCann et al. (1998), Berlow (1999), and Neutel et al. (2002). Inspired by previous work on critical transitions and the structural stability of dynamical systems, e.g. Thom (1972) and Kuznetsov (1995), we describe a variety of transitions, associated with different types of boundaries in parameter space, that may occur when stabilizing, damping patterns in complex food webs are undermined, and explore how structural network patterns, i.e. species number, connectance, and variability in interaction strength, might influence the occurrence of such transitions. The findings in this chapter are of importance because most previous work on critical transitions in ecosystems has focused on positive feedbacks as a potential cause of instability. As such, this chapter may thus point towards an important other potential cause of critical transitions in complex ecosystems.

In **Chapter 4**, we build further on previous work on critical slowing down prior to critical transitions, e.g. Wissel (1984) and Van Nes & Scheffer (2007). Previous studies on critical slowing down aimed to detect a change in the proximity to a critical point (Scheffer et al., 2009; Dakos et al., 2012) and did not address the question of what a system's future state might be like after an impending critical transition. Complex ecosystems may, however, shift to many different, alternative states. Whether impending transitions in such systems have minor, positive or catastrophic effects thus remains unclear. Predicting a system's future state is difficult in particular when complex, unpredictable dynamics occur when a critical point is passed. Some systems may, however, behave more predictably than others. The dynamics of mutualistic communities can, for example, be expected to be relatively simple, because delayed negative feedbacks leading to oscillatory or other com-

plex dynamics are weak. This relative simplicity may allow us to look beyond impending critical transitions and foresee a community's future state. To predict the future state of complex mutualistic communities, we take advantage of the fact that resilience is not lost equally in all directions. Disturbances have a size (i.e. the total amount of change) and a direction (i.e. the relative amount of change in each species). The more similar a disturbance's direction to the direction in which increasingly small perturbations may cause critical transitions, the stronger the effect of critical slowing down. Provided that there are no oscillating, chaotic or other complex dynamics, a system's future state will most likely lie in the same approximate direction.

In **Chapter 5**, the final chapter of this thesis, I reflect on the findings in the previous chapters and place them in a broader context. In a time when ecosystems are confronted with rapid environmental change, it is becoming increasingly clear that predicting the consequences of changing environmental conditions requires a fundamental understanding of the processes occurring in ecosystems. In particular, because such changes are likely to bring ecosystems outside of the range in conditions for which data are available. Applied questions on the stability of a particular ecosystem in the context of such changes may thus require the development of novel, fundamental theories and hypothesis that may apply to a wide variety of ecosystems. In this thesis, I hope to have contributed to the development of such theories and hypothesis.

A1.1 A SIMPLE FOOD CHAIN AND A MORE COMPLEX WEB

We use a Lotka-Volterra style model to describe the dynamics of primary producers, consumers and top-predators. Primary producers obtain resources from abiotic sources, e.g. soil nutrients and sunlight, consumers feed on primary producers and predators prey on consumers. Changes in the biomass of species are described as follows:

$$\begin{aligned}\frac{dB_i}{dt} &= r_i B_i - \sum_{k=cons} \frac{\gamma_{ik}}{1 - \delta_{ik}} B_i C_k - \sum c_{ij} B_i B_j + \epsilon_i, \\ \frac{dC_k}{dt} &= \gamma_{ik} B_i C_k - \sum_{l=pred} \frac{\gamma_{kl}}{1 - \delta_{kl}} C_k P_l - t_k C_k + \epsilon_k, \\ \frac{dP_l}{dt} &= \gamma_{kl} C_k P_l - t_l P_l \epsilon_l,\end{aligned}\tag{A1.1}$$

in which primary producer i has abundance B_i , consumer k abundance B_k , and top-predator l abundance P_l . The rate at which primary producers grow in abundance is described by growth rate r_i , and competition among basal species is described by competitive interaction strength c_{ij} . Trophic interactions are described by feeding rate, γ_{ik} , and the fraction of ingested biomass lost to feces and other losses, δ_{ik} . The rate at which biomass production is lost due to respiration and other losses, e.g. death, is described by mortality rate, t_k . Species experience small stochastic perturbations incorporated through noise term ϵ_i :

$$\epsilon_i = \delta_i \frac{dW}{dt}.\tag{A1.2}$$

ϵ_i fluctuates in time due to Wiener process, W , with mean zero and standard deviation δ_i . The Wiener process is a continuous-time stochastic process generating white noise. To prevent noise leading to negative abundances, we assume that $dN/dt = 0$ when $N < 0.001$.

Parameters settings of the simple food chain in Fig. 1.2.A are as follows: $\hat{B}_1 = 3$, $\hat{C}_2 = 2$, $\hat{P}_3 = 1$, $c_{11} = 0.17$, $\gamma_{12} = 0.12$, $\gamma_{23} = 0.1$, $\delta_{12} = 0.55$, and $\delta_{23} = 0.15$, and the parameter settings of the more complex food web in Fig. 1.2.B as follows: $\hat{B}_1 = 1$, $\hat{B}_2 = 1$, $\hat{B}_3 = 1$, $\hat{C}_4 = 1$, $\hat{C}_5 = 1$, $\hat{P}_6 = 1$, $c_{11} = 0.9$, $c_{12} = 2.1$, $c_{13} = 0$, $c_{21} = 0.3$, $c_{22} = 0.9$, $c_{23} = 1.8$, $c_{31} = 1.5$, $c_{32} = 0$, $c_{33} = 1.5$, $\gamma_{14} = 1.2$, $\gamma_{24} = 1.8$, $\gamma_{15} = 1.2$, $\gamma_{25} = 0.9$, $\gamma_{35} = 0.9$, $\gamma_{46} = 0.4$, $\gamma_{56} = 0.6$, $\delta_{13} = 0.55$, $\delta_{14} = 0.55$, $\delta_{24} = 0.55$, $\delta_{15} = 0.55$, $\delta_{25} = 0.55$, $\delta_{35} = 0.55$, $\delta_{46} = 0.15$, $\delta_{56} = 0.15$. The growth rates of primary producers, r_i , and mortality rates, t_k ,

of consumers and top-predators are assigned such that $d\hat{B}_i/dt$, $d\hat{C}_i/dt$, and $d\hat{P}_i/dt$, are zero. \hat{B} , \hat{C} , and \hat{P} correspond to the species' nontrivial equilibrium abundances.

A1.2 SUPPLEMENTARY FIGURE

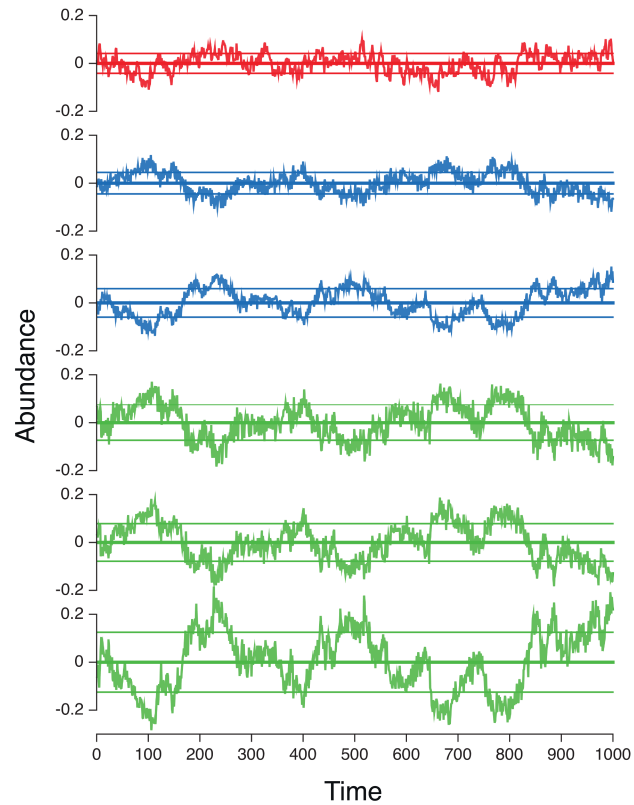


Figure A1.1: Fluctuations in the abundances of individual species belonging to the more complex food web described in Appendix A1.1 and displayed in Fig. 1.2.B. The abundances of primary producers (green) and consumers (blue) are (anti-)correlated. The bottom time series belongs to primary producer ‘1’ and the top time series to top-predator ‘6’ as described in Appendix A1.1. Horizontal lines indicate the mean and standard deviations.

Chapter 2

The sudden collapse of pollinator communities

J. Jelle Lever,

Egbert H. van Nes,

Marten Scheffer,

and Jordi Bascompte

This chapter is based on: Lever, J.J., Van Nes, E.H., Scheffer, M., & Bascompte, J. (2014). The sudden collapse of pollinator communities. *Ecology letters*, 17(3), 350-359.

ABSTRACT

Declines in pollinator populations may harm biodiversity and agricultural productivity. Little attention has, however, been paid to the systemic response of mutualistic communities to global environmental change. By using a modelling approach and merging network theory with theory on critical transitions, we show that the scale and nature of critical transitions is likely to be influenced by the architecture of mutualistic networks. Specifically, we show that pollinator populations may collapse suddenly once drivers of pollinator decline reach a critical point. A high connectance and/or nestedness of the mutualistic network increases the capacity of pollinator populations to persist under harsh conditions. However, once a tipping point is reached, pollinator populations collapse simultaneously. Recovering from this single community-wide collapse requires a relatively large improvement of conditions. These findings may have large implications for our view on the sustainability of pollinator communities and the services they provide.

2.1 INTRODUCTION

Widespread declines in wild and domesticated pollinator populations raise concerns about the future of biodiversity and agricultural productivity (Allen-Wardell et al. 1998; Diaz et al. 2005; Biesmeijer et al. 2006; Potts et al. 2010; Burkle et al. 2013; Garibaldi et al. 2013). The majority of flowering plants depend on animals for pollination. Those plants are in turn at the basis of food webs and provide food for livestock and human populations (Klein et al. 2007; Ollerton et al. 2011). Pollinators thus provide an essential service to ecosystems and humanity. Assessing the potential for further degradation of this service is therefore of great importance.

A considerable effort is being made to identify the potential causes of declining pollinator abundances. Recently, field experiments showed how commonly used insecticides strongly increase pollinator mortality (Henry et al. 2012; Whitehorn et al. 2012). Habitat destruction, parasites, and disease are also seen as important drivers of pollinator decline. Most likely, a mix of those causes increases the mortality of pollinator populations (Diaz et al. 2005; Potts et al. 2010; Bryden et al. 2013).

The impact of a further increase in drivers of pollinator decline will depend strongly on the capacity of plant-pollinator communities to withstand a further increase in those drivers. Determination of the response of natural communities to environmental change is however notably hard, primarily because the response of these relatively complex systems depends on more than the intrinsic properties of species. A central role is likely to be played by the strength, number, and nature of interactions between species, and the way in which those interactions are arranged in ecological networks (May 1972; McCann 2000; Bascompte et al. 2006; May 2006; Ives & Carpenter 2007; Scheffer et al. 2012). When assessing the impact of a further increase in the drivers of pollinator decline, it is thus of fundamental importance to take the topology of mutualistic networks (i.e., the number and way in which mutualistic interactions are arranged) into account.

Mutualistic networks, such as those made out of the interactions between plants and pollinators, are known to display a high degree of nestedness, i.e., the more specialist species tend to interact with subsets of the species interacting with the more generalist species (Fig. 2.1; Bascompte et al. 2003; Bascompte & Jordano 2007). Theoretical work has shown that the nestedness of mutualistic networks increases the robustness of plant-pollinator communities to species extinctions (Memmott et al. 2004; Burgos et al. 2007) and habitat loss (Fortuna & Bascompte 2006), the proportion of coexisting species once an equilibrium is reached (Bastolla et al. 2009; Thébault & Fontaine 2010), and the speed at which the community returns to equilibrium after a perturbation (Okuyama & Holland 2008; Thébault & Fontaine 2010).

Little attention, however, is given to the influence of mutualistic network topology on potential critical transitions in the size of pollinator populations. Ecosystems may respond

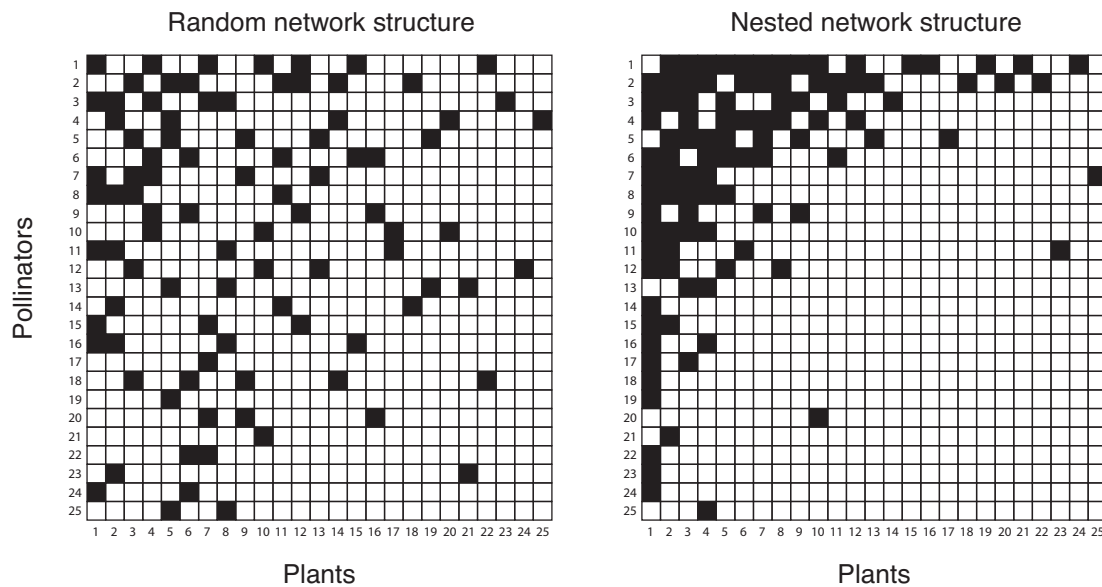


Figure 2.1: Matrix representations of a randomly structured network (left) and a nested network (right, $N=0.6$). Filled squares indicate interactions between species. Column and row numbers correspond to individual plant and pollinator species. Species are ordered based upon their number of interactions.

in various ways to changing environmental conditions, such as the change in conditions caused by a further increase in drivers of pollinator decline, which may have profound implications for their resilience to environmental change (Scheffer et al. 2001; Scheffer & Carpenter 2003). When conditions change gradually, the state of some systems (e.g., the size of populations) may change likewise, in a smooth, gradual manner. Other systems may respond strongly to change within a narrow range of environmental conditions, but are relatively insensitive to change outside of this range. Particularly sudden shifts may occur when a system has more than one stable state. Such a system cannot change smoothly from a one stable state (e.g., large population sizes) to an alternative stable state (e.g., small population sizes). Instead, a sudden shift occurs when environmental conditions pass a critical point. We refer to such shifts as ‘critical transitions’. To return back to the original state after a critical transition, a return to conditions prior to the transition is often not sufficient; instead, a larger change in conditions is needed until another critical point is reached at which the system shifts back to the original state. The existence of a difference between the critical conditions at which a forward and backward transition occurs, is known as ‘hysteresis’.

The notion that alternative stable states exist is supported by observations in a wide variety of ecological and experimental systems (Scheffer et al. 2001; Scheffer & Carpenter 2003; Rietkerk et al. 2004; Kefi et al. 2007; Drake & Griffen 2010; Veraart et al. 2011; Hirota et al. 2011; Dai et al. 2012). The complexity of many natural communities has however made it hard to develop the existing theory on alternative stable states further

into a framework that helps us to assess their resilience (Scheffer et al. 2012). Here, we try to contribute to the development of such a framework, by merging theory on alternative stable states with theory on the structure of ecological networks. Specifically, we do this by examining the potential occurrence of critical transitions in the size of pollinator populations due to a change in a driver of pollinator decline. Subsequently, we study the way in which the connectance and nestedness of mutualistic networks may affect the community-wide implications of these shifts between alternative stable states. This will be done with the help of a mathematical model.

2.2 METHODS

Nestedness algorithm

Networks with a different degree of nestedness were generated by using an algorithm similar to the one described by Medan et al. (2007). This algorithm was shown to generate networks that are similar to empirically studied plant-pollinator networks (also by Medan et al. 2007). The algorithm allows us to vary nestedness of networks with a given number of species, connectance and fraction of “forbidden links”. Connectance is the fraction of all possible interactions that is occurring in the network. Forbidden links are interactions that cannot occur, for example because of a morphological or phenological uncoupling (e.g., between late-flowering plant species and early seasonal pollinator species, see Jordano et al. 2003).

Initially, the algorithm assigns with a predefined probability mutualistic interactions and forbidden links between two species groups. This results in a network with a random structure, of which the probability of having an interaction corresponds to the connectance of the network and the probability of a forbidden link to the fraction of forbidden links. In case any of the species has no interactions, a new randomly structured network is generated.

In order to generate nested networks, interactions are re-arranged within the network. During each iteration the algorithm randomly selects an interaction between two species a and b . This interaction is changed into an interaction between species a and randomly selected species c , when this species has more interactions than species b . During the iterative process, species thus start to interact more with species that already have many interactions. This “rich get richer” mechanism increases the nestedness of the network. Iterations are continued until a desired nestedness is reached.

Two exceptions to the above mentioned rule exist. The interaction is not changed from an interaction with species b to an interaction with species c , when species b has only one interaction, or when the interaction between species a and c is forbidden. This ensures that each species remains having at least one interaction, and that the identity of forbidden links is not changed by the algorithm.

We derive the nestedness of the entire network, N , as in Bastolla et al. (2009):

$$N = \frac{\sum_{i<j}^{S_P} N_{ij} + \sum_{i<j}^{S_A} N_{ij}}{\frac{S_P(S_P - 1)}{2} + \frac{S_A(S_A - 1)}{2}}, \quad (2.1)$$

where the first sum is across all pairs of plant species, the second sum is across all pairs of pollinator species, S_P is the number of plant species, S_A is the number of pollinator species. N_{ij} is the nestedness of species pair i and j , which is derived as follows:

$$N_{ij} = \frac{n_{ij}}{\min(n_i, n_j)}, \quad (2.2)$$

where n_{ij} is the number of times species i and j interact with the same mutualistic partner, n_i is the number of interactions of species i and n_j is the number of interactions of species j .

All networks generated with the procedure above were checked for the potential presence of more than one component (i.e., a group of species that is completely disconnected from the rest of the network). If more than one component was found, the network was dismissed from our analysis, and replaced with a newly generated network, consisting of only one component.

Model of mutualistically interacting species

In an attempt to disentangle the relationship between network structure and the response of plant-pollinator communities to environmental change, we studied the impact of mutualistic network topology on the behaviour of a dynamic model. Our dynamic model describes two mutualistically interacting species groups; plants and pollinators. Species belonging to the same group are in direct competition with each other, while mutualistic interactions occur between species belonging to a different group. The pollinators are subjected to a gradual change in mortality and/or growth rate, caused by a change in one of the drivers of pollinator decline.

The model, describing a group of S_P plant species and S_A pollinator species, is as follows:

$$\begin{aligned} \frac{dP_i}{dt} &= r_i P_i + \frac{\sum_{k=1}^{S_A} \gamma_{ik} A_k}{1 + h_i \sum_{k=1}^{S_A} \gamma_{ik} A_k} P_i - \sum_{j=1}^{S_P} C_{ij} P_j P_i + \mu_P, \\ \frac{dA_k}{dt} &= (r_k - d_A) A_k + \frac{\sum_{i=1}^{S_P} \gamma_{ki} P_i}{1 + h_k \sum_{i=1}^{S_P} \gamma_{ki} P_i} A_k - \sum_{l=1}^{S_A} C_{kl} A_l A_k + \mu_A, \end{aligned} \quad (2.3)$$

where P_i represents the abundance of plant species i and A_k represents the abundance of pollinator species k . Intrinsic growth rates, i.e., the growth independent from mutualistic and competitive interactions, are represented by r , which is species-specific and can either be positive or negative. A general reduction of pollinator growth rates or increase in pollinator mortality rates, affecting all pollinator species, is included with driver of pollinator decline, d_A .

Population growth is enhanced by mutualistic partners (i.e. the pollinator or plant species providing a service or resource to the plant or pollinator population). Like Okuyama & Holland (2008) and Bastolla et al. (2009), we assume that the beneficial effect of mutualistic partners on population growth saturates when the abundance of mutualistic partners is high. The extent of this saturation is determined by half-saturation constants h . We assume mutualistic interactions to be either absent, in which case mutualistic interaction strength, γ , is equal to zero, or to be present, in which case the mutualistic interaction strength is assumed to depend on the degree of the node benefiting from the interaction in the following manner:

$$\gamma_{mn} = \frac{\gamma_0}{K_n^t}, \quad (2.4)$$

in which, for each interaction, γ_0 is taken from a uniform distribution, K_n is the number of interactions of the species benefiting from the interaction, and t determines strength of the trade-off between interaction strength and number of interactions. Both $t = 0$ (no trade-off) and $t = 1$ (full trade-off), represent “neutral” cases. Assuming no trade-off is neutral in the sense that the strength of mutualistic interactions is not changed by the topology of the network, while a full trade-off assumes that the gain species have from their mutualistic interactions is not changed by the topology of the network. Ecological reality is likely to lie somewhere in between those two extremes. The strength of competition between individuals of the same species group is determined by C . We study a system where species do not outcompete each other when mutualistic partners are absent (as in Van Nes & Scheffer 2004). Intraspecific competition, C_{ii} , is therefore assumed to be substantially stronger than interspecific competition C_{ij} . Lastly, a small immigration factor μ is incorporated in order to allow for the (re-)establishment of otherwise extinct species. μ is not supposed to influence the dynamics of the model.

Simulations and parameter settings

We examined the response of pollinator populations to increasingly harsh conditions, by gradually increasing the driver of pollinator decline, d_A . This gradual increase was simulated by a stepwise increase in the driver of pollinator decline, with step size 0.01. For each step, we ran our model until equilibrium was reached, by applying a Runge-Kutta method that numerically solves our model. We increased the driver of pollinator decline past the point where all pollinator species are extinct (i.e., have an abundance

lower than 0.01). After this point was reached, we simulated improving conditions by gradually decreasing the driver of pollinator decline, again with a step size of 0.01. This allowed us to check for hysteresis.

We scanned for the occurrence of sudden changes in pollinator abundance within a small range of change in the driver of pollinator decline. We defined a “sudden change” as a change in pollinator abundance that was larger than 0.2 over an increase or decrease in the driver of pollinator decline of 0.01 (one step in our simulations). This allowed us to differentiate between a sudden and a gradual extinction or recovery of pollinator populations.

In our default approach, we made simulations for communities consisting out of 25 plants and 25 pollinator species. The impact of connectance on the behaviour of the model was tested by varying the connectance of communities with a random network topology. The impact of nestedness was studied by comparing networks differing in nestedness, but equal in connectance ($D=0.15$) and fraction of forbidden links ($F=0.3$). We, however, made sure that the qualitative behaviour of our model does not depend on a specific number of species, connectance or fraction of forbidden links chosen (see Appendix A2.3 in Supporting Information). For each level of connectance and nestedness, we tested 250 different networks created with the above algorithm.

Unless stated otherwise, parameters were sampled from the following uniform distributions: $r_i \sim U(0.05, 0.35)$, $\gamma_{0,mn} \sim U(0.8, 1.2)$, $h_i \sim U(0.15, 0.3)$, $C_{ii} \sim U(0.8, 1.1)$, $C_{ij} \sim U(0.01, 0.05)$ or given the following values: $t = 0.5$, $\mu = 0.0001$.

The feasibility of networks

In order to allow for partial collapses of the plant-pollinator community, a substantial variation in growth rate, competition, and mutualistic interaction strength is needed. As a result of this variation, we did not always find a feasible solution, where the abundances of all species were higher than 0.01. If no feasible solution was found for a certain network, parameters were re-sampled until a feasible solution was found. If after 500 attempts no solution was found, the network was discarded as non-feasible.

The net effect of species on each other

Net relationships between pollinators were studied by numerically determining the influence of a small change in growth rate of species l on the abundance of species k (dA_k/dr_l). If an increase in growth rate of species l leads to an increased abundance of species k , the net effect of species l on species k is positive (following Stone & Roberts 1991).

2.3 RESULTS

The majority of pollinator populations collapse suddenly to extinction once the driver of pollinator decline, d_A , reaches a critical value. These sudden collapses occur due to a positive feedback mechanism that results from the positive interactions between plants and pollinators. A large pollinator population size enhances the growth and thus the population size of plants, which in turn enhances the growth of the pollinator populations. As the strength of the driver pollinator decline, d_A , increases, this positive feedback mechanism maintains pollinator populations under conditions where they cannot recover from extinction (see Appendix A2.1). Under these conditions, multiple alternative stable states may therefore exist, varying from a state where all pollinator populations are present to a state where some or all pollinator species are extinct. As the strength of the driver of pollinator decline, d_A , increases further, a critical point is reached at which the strength of this feedback mechanism is no longer sufficient to maintain pollinator populations. At this point a critical transition occurs, leading to the sudden collapse of some or all pollinator populations. In communities with a random network topology and a relatively low connectance, we typically observe several partial collapses involving the extinction of few species. Nested communities with an equal connectance, however, tend to exhibit only one point of collapse, involving the extinction of the entire community (Fig. 2.2).

Once the driver of pollinator decline has increased beyond the point where all pollinator populations have collapsed, a small decrease in mortality rates may not be sufficient for species to recover. As was the case with the sudden collapses, observed when the driver of pollinator decline, d_A , was *increased*, pollinator populations may also recover suddenly when the driver of pollinator decline is *decreased* (Fig. 2.3). Especially in nested communities, the difference between the first point of recovery and the final point of collapse can be substantial when compared to randomly structured communities. A considerable improvement of conditions might thus be necessary before species can recover from collapse, which is indicative of hysteresis.

Multiple points of recovery were typically observed within communities that also exhibited several network collapses. In randomly structured communities, with a connectance of 0.15, for example, multiple points of sudden recovery were found in 92% of the feasible communities in which also multiple collapses were observed. More than one sudden recovery was however only observed in 21% of the feasible communities that exhibited one point of collapse.

The ranking of species recovery was, in most feasible communities, similar to the order in which they collapsed. E.g., the species who were the last to collapse when the driver of pollinator decline, d_A , was increased, always recovered before or simultaneously with species that collapsed at a lower value of pollinator decline, in 79% of randomly structured communities with a connectance of 0.15.

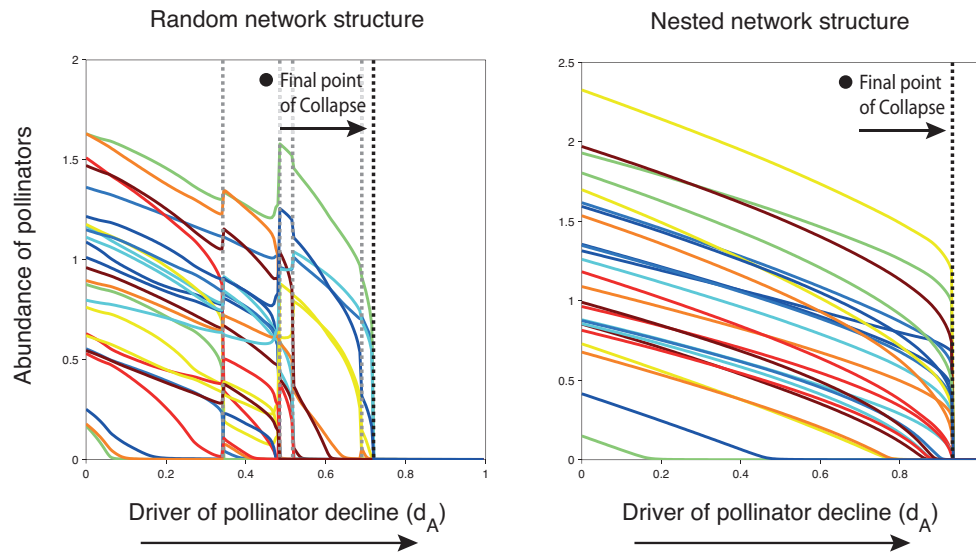


Figure 2.2: The collapse of pollinator populations when the driver of pollinator decline, d_A , affecting growth and/or mortality of pollinators, is gradually increased from zero to one. Results are shown for a random (left) and a nested (right, $N=0.6$) network. Connectance of both networks is equal ($D=0.15$). Several extinction events precede the final collapse of the randomly structured plant-pollinator community, while the nested community exhibits only one point of community-wide collapse.

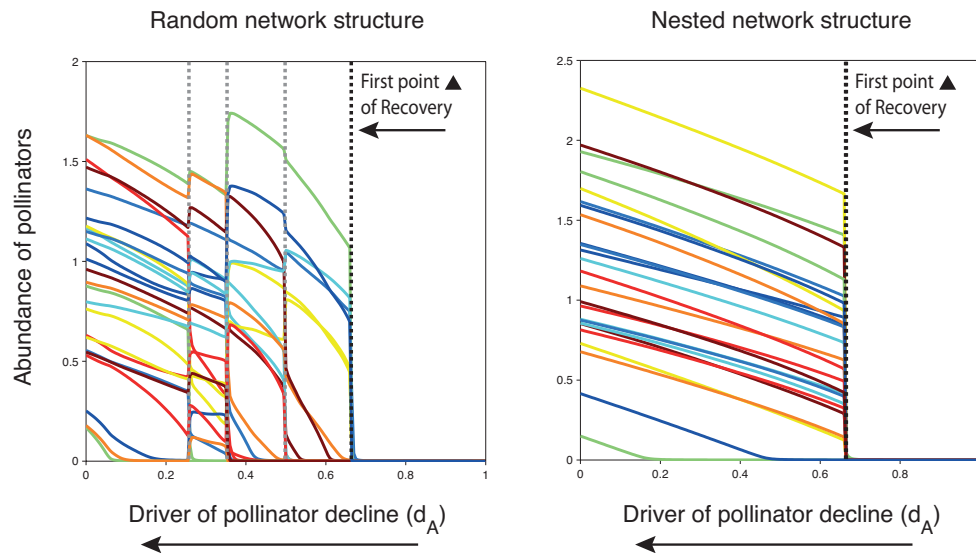


Figure 2.3: The recovery of pollinator populations when the driver of pollinator decline, d_A , is gradually decreased from one to zero. The points of recovery are not necessarily equal to the points of collapse (see Fig. 2.2). Especially in the nested community a large difference is observed between the final point of collapse and the first point of recovery. A substantial reduction of the driver of pollinator decline might thus be necessary for pollinator populations to recover from a collapse.

Further, sudden changes in the pollinator community always coincided with sudden changes in the plant community (see Appendix A2.2).

The potential for a single community-wide collapse

The probability of having a single community-wide collapse, instead of having several partial collapses, is strongly influenced by the connectance and/or nestedness of mutualistic networks. The fraction of networks, equal in connectance and nestedness, in which a single community-wide collapse was observed, can be seen as a measure of this probability.

The left panel of Fig. 2.4 shows the impact of connectance on the number of collapses that occur when the driver of pollinator decline, d_A , is increased. As the connectance of randomly structured communities increases, the fraction of communities that exhibit only one single point of community-wide collapse grows, until eventually almost no partial collapses are observed.

In the right panel of Fig. 2.4, we show what happens when the nestedness of communities with a connectance of 0.15 is increased. A small increase in nestedness from 0.2 to 0.25 is already sufficient to observe a substantial decrease in the occurrence of partial collapses. When nestedness is increased further, almost no partial collapses are observed any more. Consequently, by increasing the nestedness, we thus observe a strong reduction in the occurrence of partial collapses, even though the connectance of those networks was fixed.

The cases where we did find a partial collapse in a highly nested community represent an extreme case where a large fraction of specialists interacts only with one single generalist. This generalist may, together with the specialists associated to it, collapse independent of the rest of a highly nested community.

As described in the Methods section, we needed a substantial variation in growth rate, competition and mutualistic interaction strength in order to allow for partial collapses of the plant-pollinator community. As a result of this variation, the parameters drawn from uniform distributions did not always give a feasible solution. A large fraction of randomly structured networks with a connectance of 0.15, however, gave a feasible solution, and the majority of them also showed partial collapses. Surprisingly, the feasibility of networks was lowest for intermediate values of nestedness. Feasible solutions were thus most easily found in networks that were either fully random, or fully nested (Fig. 2.4 and Appendix A2.3). Networks for which it was hard to find a feasible solution, often had a small fraction of species that, during all attempts made to find a feasible solution, could not coexist with all others. Non-feasibility was thus almost always a property of this small fraction of species, rather than a property of the community as a whole.

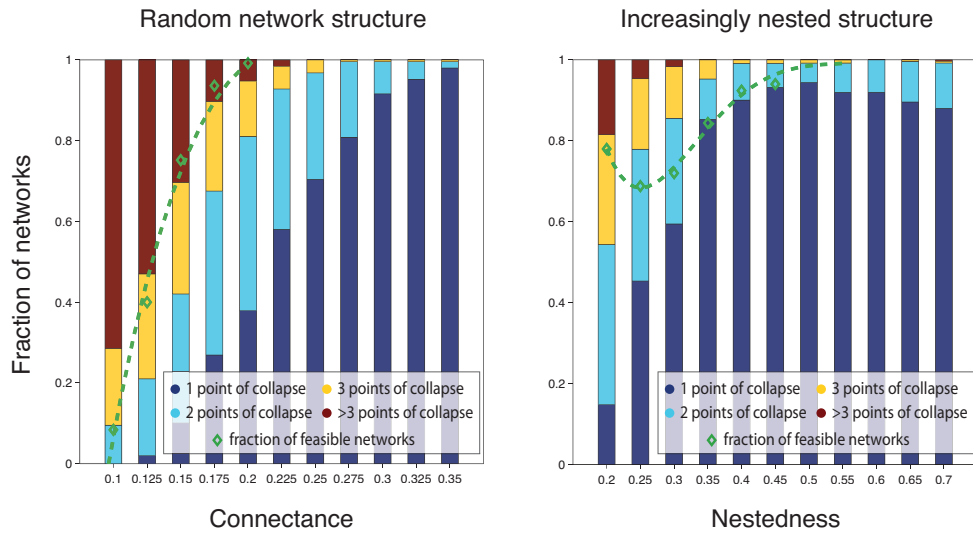


Figure 2.4: The number of collapses observed in randomly structured communities with different levels of connectance (left), and in communities with increasingly nested network topologies with a fixed connectance of 0.15 and fraction of forbidden links of 0.3 (right). The coloured bars represent the fraction of feasible networks in which a certain number of collapses is found. The fraction of networks for which feasible solutions are found is indicated with the green diamonds.

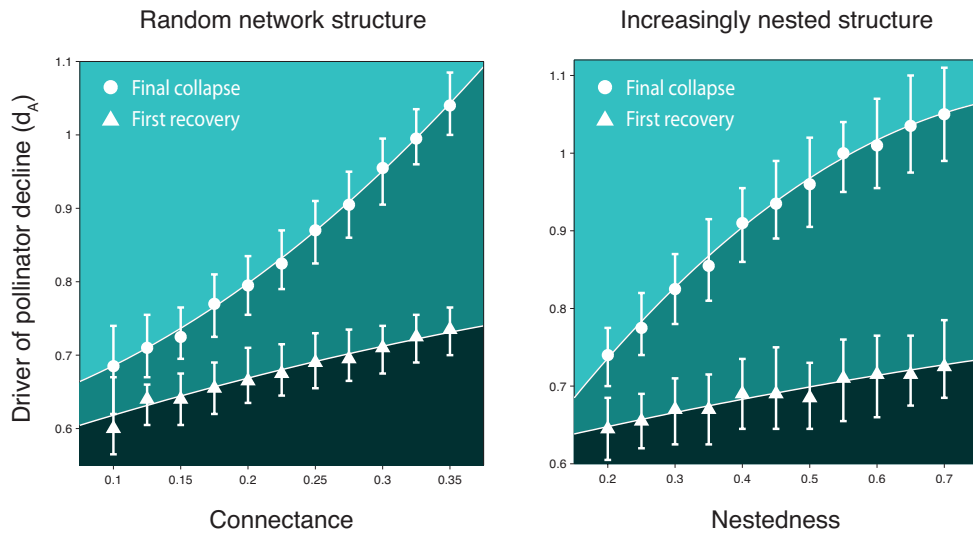


Figure 2.5: Points of collapse (circles) when the driver of pollinator decline, d_A , is increased, and points of recovery (triangles) when the driver of pollinator decline, d_A , is decreased. As in Fig. 2.4, results are shown for randomly structured networks that vary in connectance (left), and for increasingly nested networks with a connectance of 0.15 and fraction of forbidden links of 0.3 (right). In case of multiple collapses and/or recoveries, the final point of collapse and the first point of recovery was plotted.

Pollinator persistence under changing environmental conditions

Network topology influences not only the probability of a single community-wide collapse; it is also important for the capacity of pollinator communities to persist under increasingly harsh conditions. Here, we measure this capacity as the amount of increase in the driver of pollinator decline, d_A , needed to reach the “final point of collapse”. This final point of collapse is the point where the last pollinator collapses to extinction (as indicated in Fig. 2.2). Similarly, we can measure the ease of recovery by measuring the value of the driver of pollinator decline, where the first pollinator recovers from extinction. This would be the “first point of recovery” (as indicated in Fig. 2.3). The points of collapse and recovery as they were found for a certain value of connectance and nestedness are plotted in Fig. 2.5. For each value of connectance and nestedness, multiple networks were tested.

Connectance and nestedness both postpone the final point of collapse. Consequently, the persistence of the pollinator community to an increase in the driver of pollinator decline, d_A , increases with connectance and/or nestedness. Highly connected, and/or nested communities also recover from a collapse at higher values of the driver of pollinator decline. The distance between the final point of collapse and the first point of recovery, however, increases with connectance and/or nestedness. This means that a larger change in the driver of pollinator decline is needed for pollinators to recover, after the final threshold is passed.

The net effect of species on each other

Our results show that the connectance and/or nestedness of mutualistic networks affects the stability of pollinator communities in various ways. The different aspects of stability discussed so far are the fraction of networks in which feasible solutions are found, the number of collapses and persistence of pollinator populations when the driver of pollinator decline, d_A , is increased, and the ease of recovery when the driver of pollinator decline, d_A , is decreased. Fortunately, these very different implications of network topology can all be understood when studying the “net effects” of species on each other.

Pollinators have a direct negative effect on each other due to competition. An indirect positive effect between pollinators may however occur when pollinator species interact with the same plant species. It is the interplay between these direct and indirect effects that ultimately determines the net effect of pollinators on each other (Bastolla et al. 2009). In Fig. 2.6, two pollinators interacting with the same plant species are shown to have an increasingly strong positive effect on each other. Not surprisingly, these pollinators can endure a larger increase in the driver of pollinator decline, d_A , than the pollinator not benefiting from this facilitation (also shown in Fig. 2.6). Once the tipping point is reached, the two pollinators interacting with the same plant species, however, collapse simultaneously, because they both depend on the same plant species.

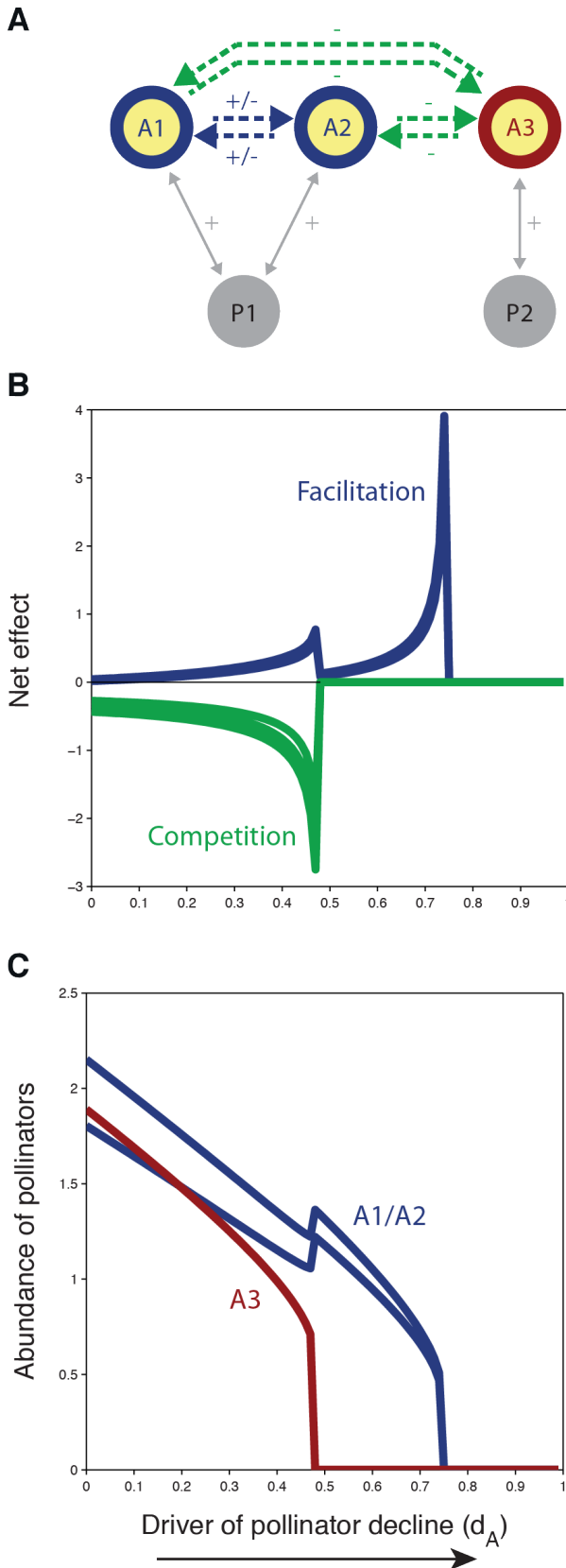


Figure 2.6: The net effect of species on each other while the driver of pollinator decline increases. Pollinators that share a mutualistic partner have an increasingly positive effect on each other and collapse simultaneously. Pollinators that do not share mutualistic partners have an increasingly negative effect on each other and collapse independently. **(A)** A simple network of mutualistic interactions between plants and pollinators. Pollinator A1 and A2 share mutualistic partner P1, while pollinator A3 does not share its mutualistic partner P2. Dashed lines indicate net relationships between pollinators. Although pollinators are in direct competition with each other, net positive relationships may exist between pollinator A1 and A2. **(B)** Net effect (dA_k/dr_l) of pollinator species on each other. In blue the net effects of pollinators A1 and A2 on each other. In green the net relationships between pollinator A3 and the other two pollinators. **(C)** Abundance of pollinators A1 and A2 (blue), and pollinator A3 (red). **Parameter settings:** $r_i \sim U(0.15, 0.25)$, $\gamma_{0,mn} \sim U(0.9, 1.1)$, $t = 0.5$, $h_i \sim U(0.5, 0.6)$, $C_{ii} \sim U(0.4, 0.6)$, $C_{ij} \sim U(0.025, 0.075)$, and $\mu = 0.0001$.

Increased connectance and nestedness both increase the fraction of mutualistic partners shared by pollinators. The behaviour of highly connected, and/or highly nested communities, is therefore similar to the behaviour of the two pollinator species who share an interaction with the same plant species (Fig. 2.6). With increasing connectance the “overlap” in identity of the mutualistic partners of pollinators is simply increased because a larger number of interactions has to be distributed over an equal number of plant species. The “rich get richer” mechanism that lies at the basis of the algorithm we used to generate nested networks, makes pollinators interact with mutualistic partners where many other pollinators already interact with. With the algorithm we thus achieve a similar increase in overlap while maintaining the number of interactions equal. As with the two species sharing an interaction with the same mutualistic partner in Fig. 2.6, pollinators who form part of a nested and/or highly connected community indirectly support each other when stress levels are high. This makes the community survive higher levels of the driver of pollinator decline, d_A , but also leads to a simultaneous collapse, because species depend on each other when stress levels are high.

Feasible solutions can be found in two types of regimes. The first regime would be one in which the combined effect of direct and indirect effects between pollinators is positive. An alternative regime is one where these net effects are mostly negative. This second regime is only feasible when these negative effects are relatively equal in strength. With increasing nestedness we move from the second to the first regime. Intermediate values of nestedness might be less likely to be in either of the two regimes. Some species have already benefited from the increase in nestedness, while others have not, which leads to an unbalanced community. This may explain why the probability of finding a feasible solution is smallest for intermediate values of nestedness (Fig. 2.4 and Appendix A2.3).

2.4 DISCUSSION

Studies addressing the occurrence of critical transitions between alternative stable states in ecosystems have provided us with myriad examples of potential positive feedback mechanisms that might lay at the basis of them (May 1977; Scheffer et al. 2001; Scheffer & Carpenter 2003; Rietkerk et al. 2004; Kefi et al. 2007; Hirota et al. 2011). These positive feedback mechanisms propel change towards an alternative stable state when environmental conditions pass a critical point (e.g., when a decline in population size reduces the growth of a population). It has, however, been challenging to understand how such mechanisms may affect the response of structurally complex systems, such as plant-pollinator communities, to changing environmental conditions (Scheffer et al. 2012). In this paper, we try to address this challenge by merging theory on alternative stable states with theory on the structure of ecological networks. Specifically, we show that pollinator populations may collapse suddenly to extinction, due to a positive feedback mechanism that results from the positive interactions between plants and pollinators. Each pollinator population

described with our model is engaged in a unique positive feedback mechanism, of which the strength may vary substantially. Here, we show that such local positive feedback mechanisms may nonetheless provide the potential for a single community-wide collapse of pollinator populations, depending on the topology of mutualistic networks.

Our results can be understood intuitively by considering the “net effects” of species on each other and the way in which these effects are mediated by the topology of mutualistic networks. Pollinators have a direct negative effect on each other due to competition, while indirect positive effects may occur between pollinator species who interact with the same plant species. The extent to which pollinators interact with the same plant species increases with connectance and/or nestedness. A high nestedness of the mutualistic network may therefore promote the occurrence of indirect positive effects between pollinators. Earlier work has shown that these indirect positive effects may reduce the effective competition between pollinators, and promote the coexistence of species in nested communities (Bastolla et al. 2009).

In this study, we show that the relative strength of indirect facilitation between pollinators becomes stronger as the driver of pollinator decline, d_A , increases (Fig. 2.6). This corresponds to the increasingly popular ‘stress-gradient hypothesis’ which suggests that facilitative effects grow in importance as environmental stress increases (Bertness & Callaway 1994; Holmgren et al. 1997; He et al. 2013). A high nestedness of mutualistic networks may therefore not only minimize effective competition to a level required for species coexistence; under stressful conditions, it may even promote strong indirect facilitation between pollinators.

We found that pollinators who are part of highly connected and/or nested communities can maintain themselves substantially longer than pollinators who are part of communities with a low nestedness as the driver of pollinator decline, d_A , is increased. This large persistence of pollinator populations under increasingly stressful conditions is, most likely, the result of the aforementioned indirect facilitation. Pollinator species who are part of either a highly nested or highly connected community can maintain themselves under stressful conditions because they indirectly support each other.

On the other hand, when species can survive under stressful conditions because they indirectly support each other, they also increasingly depend on each other as conditions get more stressful. As a consequence, pollinators collapse simultaneously once the driver of pollinator decline, d_A , passes a critical point. What we see in our model is therefore a surprising relationship between the capacity of species to coexist, to survive under stressful conditions, and the risk for a single community-wide collapse. They are all the result of the indirect positive effects, which are promoted by a high connectance and/or nestedness of mutualistic networks. Importantly, once collapsed, highly connected and/or nested communities may not necessarily recover more easily. In fact, our model shows the contrary. Recovery of pollinator populations who form part of highly nested communities

require a quite large decrease in the driver of pollinator decline, d_A , in comparison to pollinator populations who form part of communities with a low nestedness.

Our findings may have large implications for our view on the sustainability of natural communities and the ecosystem services provided by them. Based on the insurance hypothesis, one expects ecosystem services to be more reliable when supported by a large number of species (Naeem & Li 1997; Yachi & Loreau 1999). Functional redundancy of species is often seen as a valuable ‘commodity’, because it makes ecosystems more reliable in terms of the ecosystem services they provide (see Naeem & Li 1997). Our analysis, however, illustrates that the functional overlap of pollinators, which is related to the connectivity and/or nestedness of mutualistic networks, may simultaneously increase the risk for a single community-wide collapse. A valuable ecosystem service, namely pollination, can therefore be lost suddenly, despite the fact that it is provided by a large number of species who are, when taking only their intrinsic properties into account, not equally sensitive to the driver of pollinator decline, d_A .

Our study is one of many small steps needed to bring theory on critical transitions and the structure of ecological networks together and we realize that this paper raises new questions that require further exploration. First, even though our model is substantially more complex than many others that study critical transitions, it is constrained to mutualistically interacting plant-pollinator communities. Multiple types of interactions co-occur in natural communities (Melián et al. 2009), and future studies should explore how the structuring of multiple types of interactions affect critical transitions. Secondly, our results underline the importance of developing early-warning signals for critical transitions in ecological networks (Scheffer et al. 2009). Third and finally, as the mechanisms we describe are generic, it is possible that a similar trade-off between persistence under severe conditions and potential for a systemic collapse occurs in other systems as well. This is reinforced by previous studies finding notable similarities between the structure of mutualistic networks and that of financial systems (Uzzi 1996; May et al. 2008; Saavedra et al. 2009; Haldane & May 2011; Saavedra et al. 2011).

A2.1 NULLCLINES

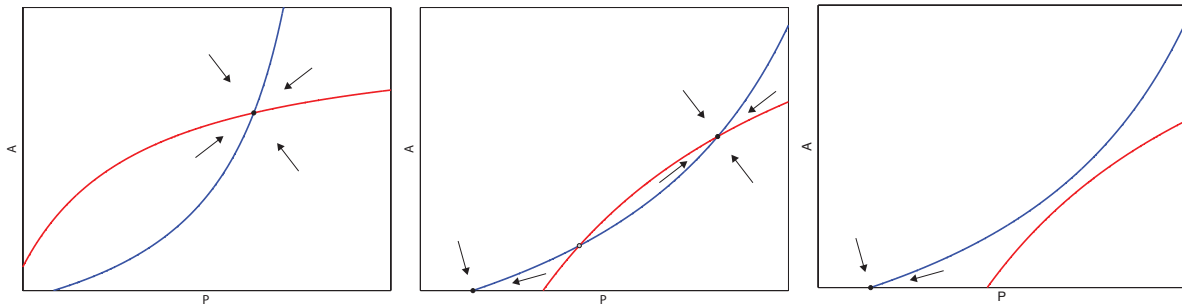


Figure A2.1: Nullclines of two mutualistically interacting species. Filled dots indicate stable equilibria, open dots indicate unstable equilibria. Fundamentally different configurations exist when (a) the driver of pollinator decline, d_A , is smaller than intrinsic growth rate r_A , (b) when the driver of pollinator decline, d_A , is bigger than intrinsic growth rate r_A and, (c) when the driver of pollinator decline, d_A , is substantially larger than intrinsic growth rate r_A . By increasing the driver of pollinator decline, d_A , we change from a regime with one stable state, presented in *a*, to the regime with two alternative stable states presented in *b*, until eventually a tipping point is reached where pollinators collapse to extinction. For a further analysis of models with two mutualistically interacting species see May (1978), Dean (1983), and Wright (1989)

A2.2 PLANT POPULATIONS

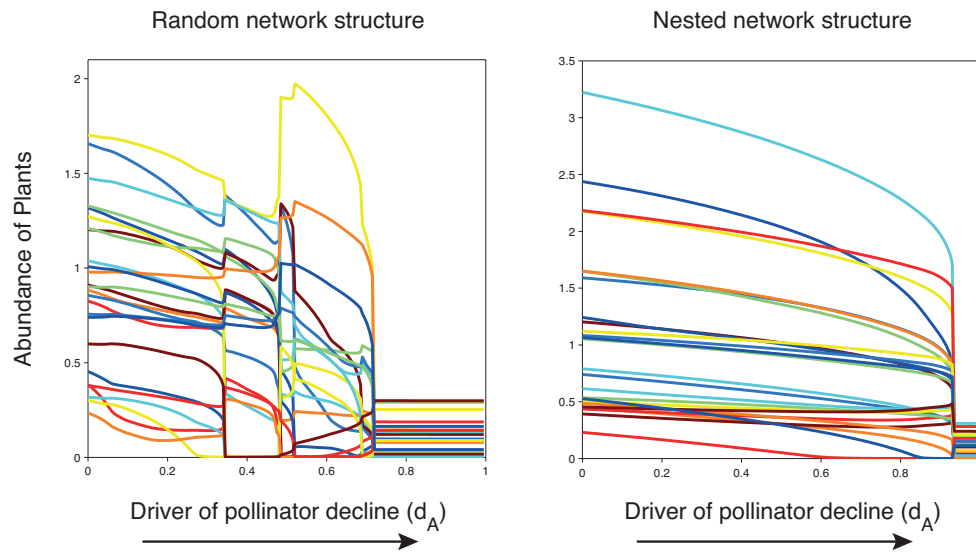


Figure A2.2: Collapse of plant populations when *increasing* the mortality d_A of pollinators. Results are shown for a random (left) and a nested (right, $N=0.6$) network. Parameter settings are the same as in Fig. 2.2.

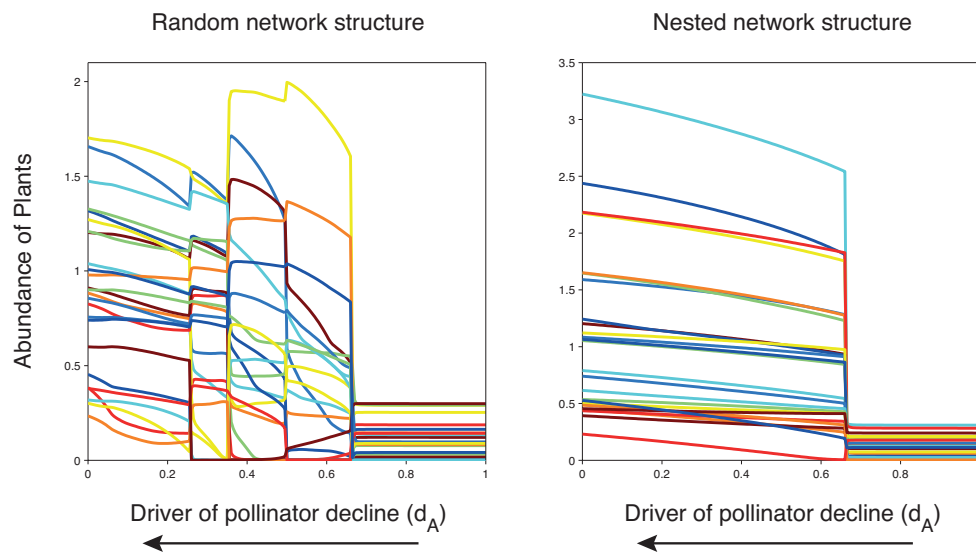


Figure A2.3: Re-establishment of plant populations when *decreasing* the mortality of pollinators d_A . Results are shown for a random (left) and a nested (right, $N=0.6$) network. Parameter settings are the same as in Fig. 2.3.

A2.3 NETWORK TOPOLOGY

We tested the extent to which our results depend on the specific number of species, connectance or fraction of forbidden links chosen (Fig. A2.4, A2.5, A2.6 and A2.7).

Furthermore, we show in Fig. A2.8 and A2.9 what our results look like if we do not allow any species to have less than 2 partners during any step of the algorithm we used to generate nested networks.

We only found qualitative differences in the behaviour of our model.

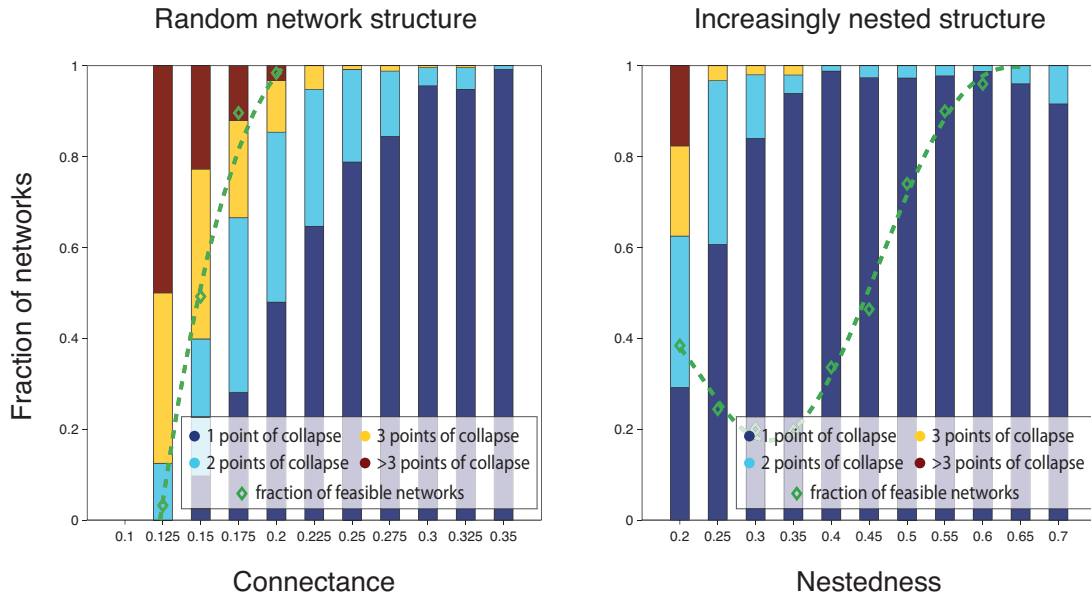


Figure A2.4: Results when using the same parameter settings as in Fig. 2.4, only now the community consists out of 35 plant and 35 pollinator species. As in Fig. 2.4, the coloured bars represent the fractions of feasible networks in which a certain number of collapses is found. The fraction of networks in which feasible solutions are found is indicated with the green diamonds.

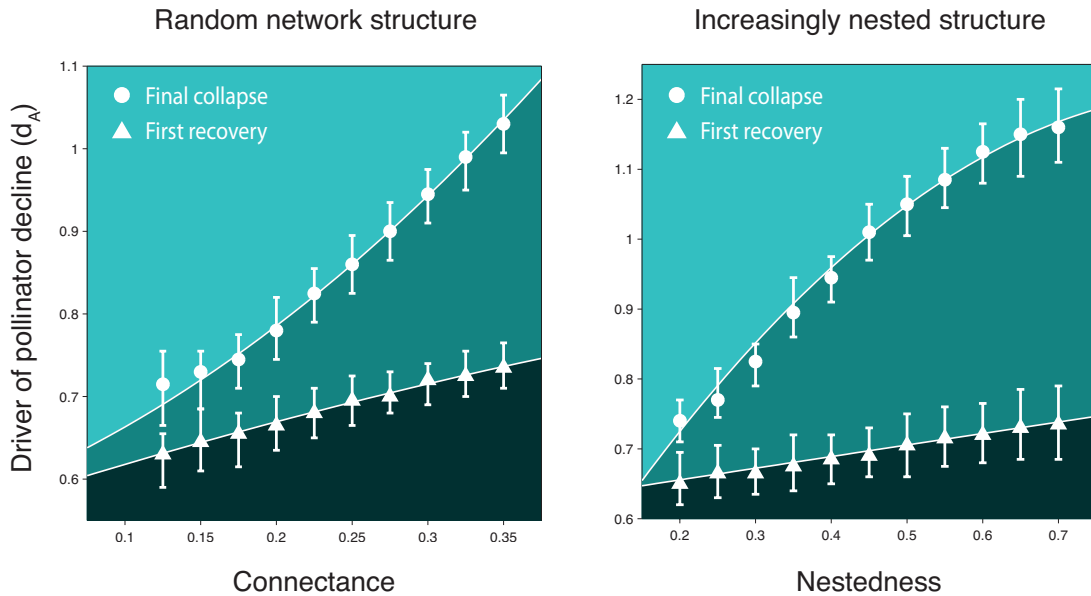


Figure A2.5: Points of collapse (circles) when the driver of pollinator decline, d_A , is increased, and points of recovery (triangles) when the driver of pollinator decline, d_A , is decreased. In case of multiple collapses and/or recoveries, the final point of collapse and the first point of recovery was plotted. Parameter settings are as in Fig. A2.4.

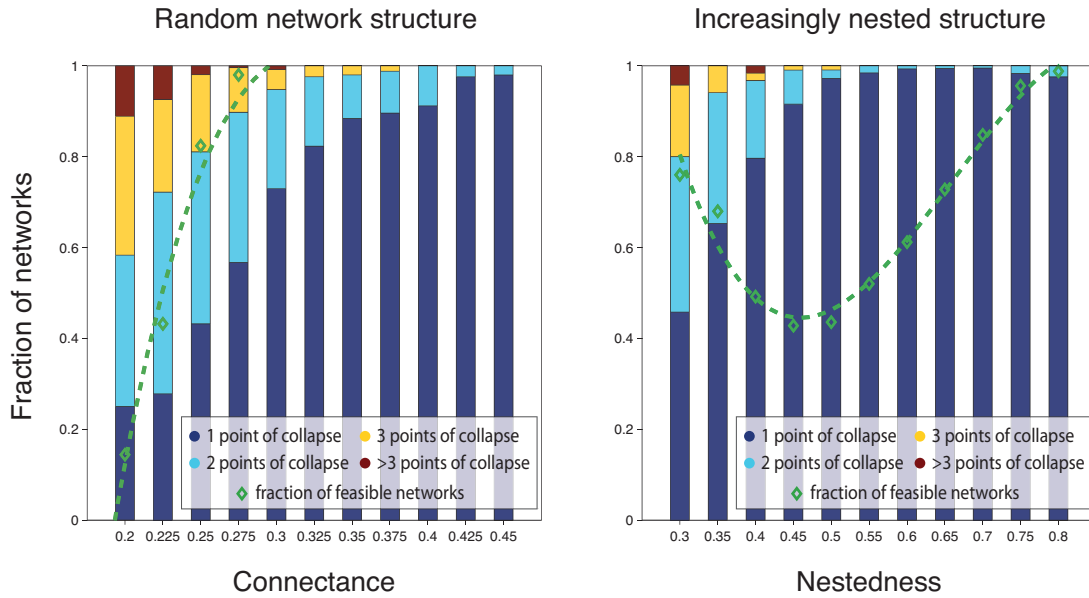


Figure A2.6: Results when using the same parameter settings as in Fig. 2.4, only now competition between species is a bit stronger, $C_{ij} \sim U(0.025, 0.075)$, and in communities with increasingly nested network topologies (right panel), the connectance is fixed to 0.25, and the fraction of forbidden links is fixed to 0.25. As in Fig. 2.4, the coloured bars represent the fractions of feasible networks in which a certain number of collapses is found. The fraction of networks in which feasible solutions are found is indicated with the green diamonds.

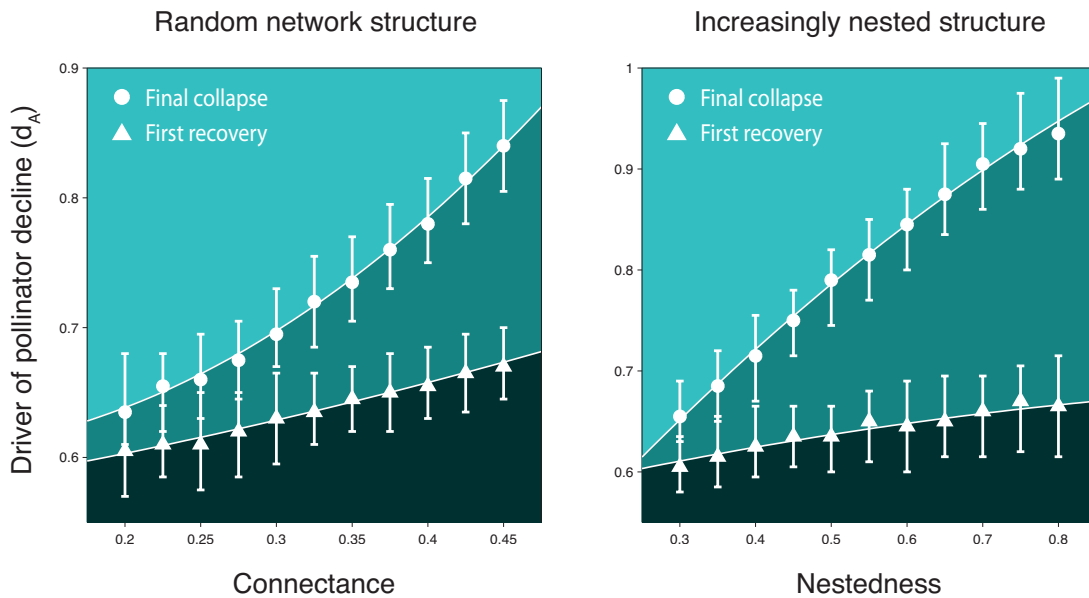


Figure A2.7: Points of collapse (circles) when the driver of pollinator decline, d_A , is increased, and points of recovery (triangles) when the driver of pollinator decline, d_A , is decreased. In case of multiple collapses and/or recoveries, the final point of collapse and the first point of recovery was plotted. Parameter settings are as in Fig. A2.6.

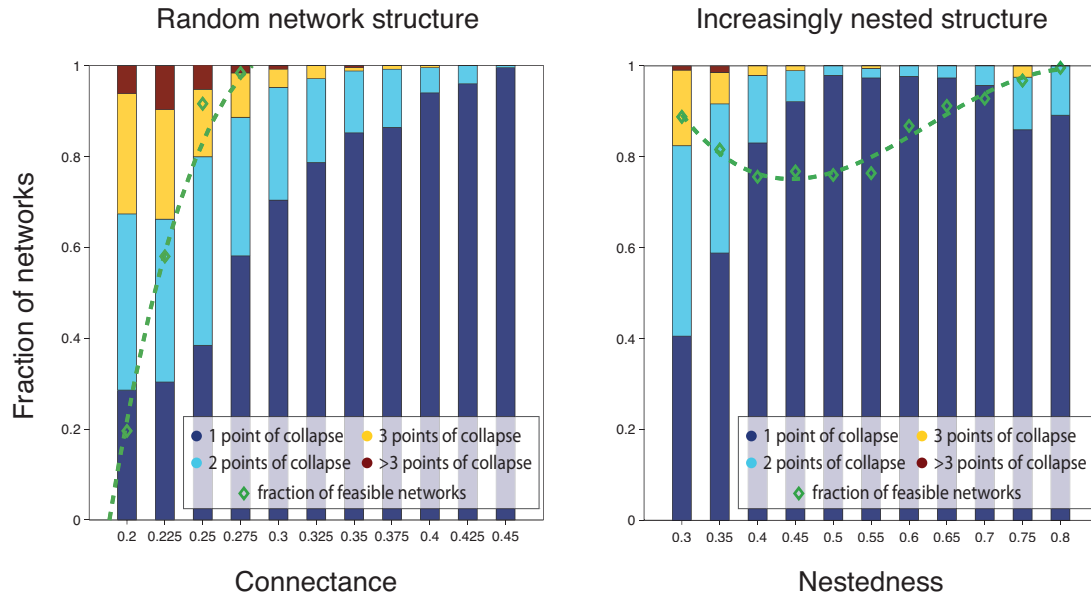


Figure A2.8: Results when using the same parameter settings as in Fig. A2.6, only now each species has at least two interactions. As in Fig. A2.6, the coloured bars represent the fractions of feasible networks in which a certain number of collapses is found. The fraction of networks in which feasible solutions are found is indicated with the green diamonds.

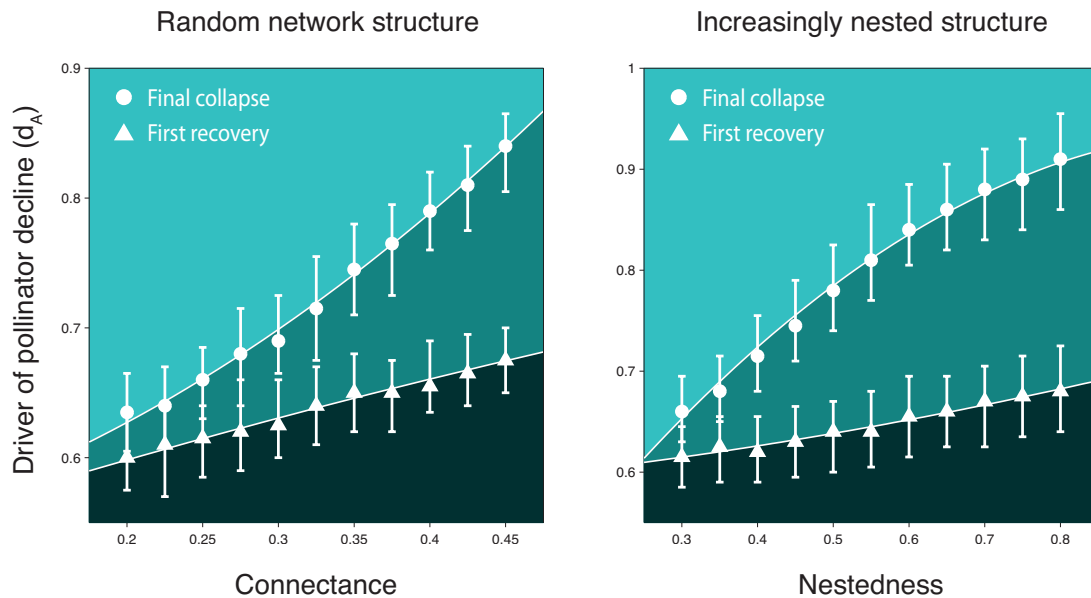


Figure A2.9: Points of collapse (circles) when the driver of pollinator decline, d_A , is increased, and points of recovery (triangles) when the driver of pollinator decline, d_A , is decreased. In case of multiple collapses and/or recoveries, the final point of collapse and the first point of recovery was plotted. Parameter settings are as in Fig. A2.8.



Chapter 3

Critical transitions in complex food webs

J. Jelle Lever,

Marten Scheffer,

Jordi Bascompte,

and Egbert H. van Nes

ABSTRACT

One of the main goals of studies on ecological networks is to understand how these often large and complex networks of interactions between species remain stable. While most of these studies try to identify network structural patterns that promote biodiversity, i.e. allow for a large number of coexisting species, less attention has been given to the specific ways in which biodiversity might be lost. In a time when ecosystems are under increasing pressure from anthropogenic drivers such as climate change, land use, and pollution, this question is however of great importance, in particular because critical transitions may occur towards other potentially less desirable states. Food-web theory and observations in real ecosystems suggest that destabilizing oscillatory dynamics caused by strong predator-prey interactions are damped by many weak interactions. Inspired by previous work on critical transitions and the structural stability of dynamical systems, we describe a variety of transitions, associated with different types of boundaries in parameter space, that may occur when such stabilizing, damping patterns are undermined and explore how structural network patterns, i.e. species number, connectance, and variability in interaction strength, might influence the occurrence of such transitions. These findings may have large implications for the way in which we evaluate the stability of complex ecosystems.

3.1 INTRODUCTION

That biodiversity is in decline is no longer in question (Vitousek et al., 1997; Millenium Ecosystem Assessment, 2005; Steffen et al., 2006; Rockström et al., 2009; Steffen et al., 2015). Which and when measures should be taken to prevent the extinction of species remains, however, subject of debate. Recent work has shown that changing environmental conditions may alter the strengths of interactions between species (Winder & Schindler, 2004; Suttle et al., 2007; Tylianakis et al., 2008; Doney et al., 2012; Blois et al., 2013; Burkle et al., 2013; Urban et al., 2016; Romero et al., 2018). Such changes may jumble structural patterns in the networks of trophic, mutualistic and/or other interactions that are crucial for the stable coexistence of species (Kareiva et al., 1993; McCann, 2000; Montoya et al., 2006; Bastolla et al., 2009). An increasing number of studies suggests therefore that a more holistic approach should be taken towards protecting biodiversity (Thompson, 1994; McCann, 2007; Gaston & Fuller, 2008; Tylianakis et al., 2010). Such an approach would not focus only on the well-being of endangered or iconic species, but tries to protect the natural communities in which they are embedded. Predicting the response of natural communities to changing environmental conditions is however difficult (but see **Chapter 4**). In particular, because this response depends in complex and, often, unknown ways on the intrinsic properties of species, the interactions between them, and the specific ways in they are affected by environmental change. This makes it hard to determine which ecosystems, species or interactions should be the focal point of efforts to maintain ecosystem stability.

Ecosystems may respond in various ways to changing environmental conditions. When conditions change gradually, the abundances of species may change likewise, in a smooth, gradual manner. Empirical studies of lakes, arid ecosystems, coral reefs, and tropical forests, have however shown that this is not always the case. Sudden, critical transitions towards alternative stable states may occur when critical points are passed (Scheffer et al., 2001). The most commonly studied cause of such transitions is a positive, reinforcing feedback that amplifies change when changing conditions or abundances pass a critical value. Such positive feedbacks are a necessary condition for the existence of alternative stable states (Thomas, 1981; Snoussi, 1998; Gouzé, 1998), and may, for example, occur in plant-pollinator communities where a decline in pollinator abundances may negatively affect plants, which in turn is bad for pollinators (Dean 1983; Wright 1989 and **Chapter 2**), or between a pair of competing species and in three-species omnivore loops in food webs (e.g. Van Nes & Scheffer 2004; Neutel & Thorne 2014 and Fig. 3.1.A-C). Critical transitions towards alternative stable states become increasingly likely when changing environmental conditions alter the relative strengths of feedbacks such that positive or other destabilizing feedbacks gain in strength relative to stabilizing, immediate negative feedbacks, and recovery from such transitions may require a relatively large change in conditions, a phenomenon known as ‘hysteresis’.

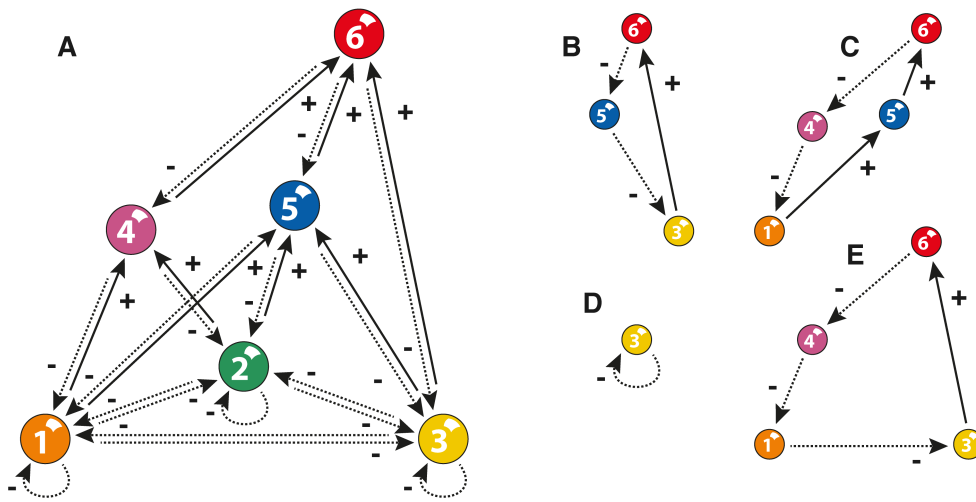


Figure 3.1: Examples of positive and negative feedback loops in a small food web. **(A)** The food web consisting of three primary producers, e.g. plants, 1-3, and three consumers, e.g. herbivores/omnivores, 4-6. primary producers compete with other producers. Consumers feed on other consumers and/or primary producers. **(B)** Positive feedback between species 3, 6, and 5 that may lead to an increase in the abundance of species 3 and 6, and a decrease in the abundance of species 5 or vice versa. **(C)** Positive feedback between species 1, 5, 6, and 4 that may lead to an increase in species 1, 5, and 6, and a decrease in species 4 or vice versa. **(D)** Negative feedback of species 3 on itself. This feedback is fast, because only a single species is involved. It has, therefore, a stabilizing effect on the dynamics of the network. **(E)** Negative feedback between species 1, 3, 6, and 4. This feedback is slow, because a relatively large number of species is involved in the feedback. It may, therefore, lead to oscillatory dynamics. Feedbacks are positive when there is an even number, and negative when there is an odd number of negative interactions in a feedback loop.

An early mathematical, theoretical foundation of transitions caused by an increase in the relative strength of a positive feedback was laid by the work of René Thom on catastrophe theory and the structural stability of dynamical systems. Thom (1972) describes seven ‘elementary catastrophes’ for processes controlled by up to four parameters (Thom, 1975). Despite some controversy in the past (Zahler & Sussmann, 1977), the cusp (two control parameters) and fold catastrophe (one control parameter), as described by Thom (1972), are now assumed to capture the essence of a wide variety of systems varying from ecosystems (May, 1977; Wilson & Agnew, 1992; Rietkerk & Van de Koppel, 1997; Scheffer et al., 2001), to human cells (Hasty et al., 2002; Ferrell Jr, 2002; Lee et al., 2002; Tyson et al., 2003; Angeli et al., 2004), and the climate (Hare & Mantua, 2000; Clark et al., 2002; Alley et al., 2003; Lenton et al., 2008). A particularly well known example in ecology is found in lakes where the equilibrium abundance of algae is controlled by lake depth and nutrient availability. When considering both these parameters, a cusp catastrophe may be obtained (see **Chapter 1** and Fig. 1.3). A fold catastrophe may be obtained when plotting the equilibrium abundance of algae against nutrient availability for a given depth,

i.e. for shallow lakes (Scheffer 1990; Scheffer et al. 1993, and Fig. 1.3.D).

Highly related to the work of René Thom, is the work of Buzz Holling who noted that for many ecosystems the important question is not how stable a system is in terms of the speed at which a system recovers from external perturbations, but how likely it is for a system to switch from one state to another under the influence of such perturbations (Holling, 1973). As a way to estimate such probability, he proposed to use the size of the domain of attraction in a system's phase space and later refers to the size of this domain as a measure of 'ecological resilience' (Holling, 1996). When conditions change such that a critical or 'bifurcation' point is approached, the minimum perturbation size required to cause a critical transition, as determined by the size of this domain, i.e. ecological resilience, goes to zero and a transition becomes inevitable (Fig. 1.4).

Positive feedbacks associated with a fold or cusp catastrophe are, however, not the only likely cause of instability in complex ecosystems. Feedbacks can be immediate, for example when members of the same species directly influence the growth of a population through intraspecific competition or facilitation. Delayed feedbacks may, for example, occur when they are mediated through other species, e.g. the indirect negative effect of prey species on themselves when promoting the growth of a predator population. Feedbacks in long loops, i.e. involving many species, tend to be slower than those in shorter loops. A system may exhibit oscillatory or other more complex dynamics when delayed negative feedbacks are strong relative to faster negative feedbacks (Levins, 1974; Puccia & Levins, 1985; Neutel & Thorne, 2014). Chaotic dynamics are found when there are two or more interacting sub-systems that, on their own, would show oscillatory dynamics (Goldbeter, 1996; Tyson et al., 2003; Novák & Tyson, 2008). Transitions towards such oscillatory or other more complex dynamics may occur when delayed negative feedbacks gain in strength relative to more immediate negative feedbacks (Marsden & McCracken, 1976; Kuznetsov, 1995).

Food webs of predator-prey interactions might be particularly susceptible to showing oscillatory or other more complex dynamics. A classical example is the 'paradox of enrichment' that may lead to oscillations in the abundances of predators and prey at high prey densities (Rosenzweig & MacArthur, 1963; Rosenzweig, 1971). Such oscillations may occur when increased nutrient availability reduces intraspecific competition among prey such that the destabilizing effect of the delayed, indirect negative feedback between predators and prey becomes apparent. Chaotic dynamics may occur in simple tritrophic food chains with, by definition, two delayed negative feedbacks of the aforementioned type (Hastings & Powell, 1991; McCann & Yodzis, 1994; De Feo & Rinaldi, 1998). The occurrence of such complex dynamics is best understood when considering such chains as coupled oscillators, i.e. one for each trophic interaction. In more complex food webs delayed negative feedback loops of more than two species may lead to oscillatory or other more complex dynamics as well (Fig. 3.1.D-E). Food-web theory and observations in real ecosystems suggests that

oscillatory or other chaotic dynamics are damped because subsets of strongly interacting species, that would show oscillatory dynamics in isolation, are embedded in food-webs with many weak interactions (McCann et al., 1998; Berlow, 1999; Neutel et al., 2002; Bascompte et al., 2005). Such an asymmetric distribution of interaction strengths may provide one of several answers to the question posed by May (1972, 1973) of what makes complex ecosystems of many species and interactions stable (Pimm, 1984; McCann, 2000). A wide variety of studies suggest, however, that changing environmental conditions may alter the strengths of trophic interactions (Winder & Schindler, 2004; Suttle et al., 2007; Tylianakis et al., 2008; Doney et al., 2012; Blois et al., 2013; Urban et al., 2016; Romero et al., 2018). Such changes may undermine the aforementioned damping effects and lead to critical transitions when delayed negative feedbacks gain in strength relative to more immediate negative feedbacks.

As mentioned previously, critical transitions become inevitable when changing environmental conditions change such that a critical or ‘bifurcation’ point is reached. At such a point, a system may be considered ‘structurally unstable’, i.e. an infinitely small change in parameters (conditions) may lead to a qualitative change in a system’s dynamical behavior, e.g. the existence of equilibrium points, limit cycles, or chaotic dynamics. The size of the area in a system’s parameter space within which a system shows the same qualitative behavior (in some domain within a system’s phase space) may be used as a measure of the extent to which a system’s dynamical behavior (within the aforementioned domain) is structurally stable (Thom, 1972; Alberch, 1989; Bastolla et al., 2005, 2009; Kuznetsov, 1995; Rohr et al., 2014). Questions on the structural stability of complex dynamical systems and the occurrence of critical transitions are thus closely related.

Inspired by previous work on critical transitions and the structural stability of dynamical systems, e.g. Thom (1972) and Kuznetsov (1995), we describe a series of catastrophes, i.e. different types of boundaries in parameter space, associated with the aforementioned changes in complex food webs. As a rough indication of which network structural properties might promote the occurrence of such catastrophes, we explore which properties, i.e. species number, connectance, and variability in interaction strengths, might influence the occurrence of such catastrophes. To illustrate that abrupt transitions towards alternative stable states, oscillatory or other more complex dynamics may occur when such boundaries are passed even under basic dynamical assumptions, we assume that the functional response of predators, i.e. the relation between a predator’s intake rate and prey availability, is linear. Parameters are assigned such that at a system’s nontrivial equilibrium, i.e. the equilibrium point at which all species have a non-zero abundance, the species’ growth, feeding and respiration rates follow allometric scaling laws, i.e. they depend on a species’ body mass. A species’ body mass depends, in turn, on a species’ position in a food web. Food-web topology, i.e. who interacts with whom, is determined by the niche model of Williams & Martinez (2000). Future work may build on this study to include also more complex, non-linear functional responses such that we may get a more

full understanding of the complex and potentially catastrophic ways in which changing environmental conditions may undermine food-web stability.

3.2 METHODS

We use a dynamic food-web model describing two species groups: primary producers and consumers. Primary producers, i.e. plants and other autotrophs, obtain resources from abiotic sources, e.g. soil nutrients and sunlight, while consumers, i.e. herbivores, omnivores, and carnivores, feed on other species. The dynamics of species i are described as follows:

$$\frac{dB_i}{dt} = R_i B_i \left(1 - \sum_{j \in \{prod.\}} \frac{c_{ij} B_j}{K_i} \right) + \sum_{k \in \{prey\}} J_i \psi_i \theta_{ki} B_k B_i - \sum_{l \in \{pred.\}} J_l \frac{\psi_l \theta_{il} B_i}{(1 - \delta_{il}) f_{il}} B_l - T_i B_i, \quad (3.1)$$

in which B_i represents the biomass of species i . The growth of primary producers is determined by growth rate R_i , carrying capacity K_i , and competitive interaction strength c_{ij} . Feeding rates and other biomass flows are determined by a consumer's maximum assimilation rate J_i , the fraction of a consumer's maximum assimilation rate realized per prey biomass ψ_i , relative feeding preference θ_{ki} , the fraction of killed prey biomass that is ingested or feeding efficiency f_{il} , the fraction of ingested biomass lost to feces δ_{il} , and the loss in consumer biomass production due to respiration T_i . Consumers may prey on primary producers, i.e. herbivore interactions, as well as on other consumers, i.e. carnivore interactions. Species j is a primary producer. Species k is a prey, and species l a predator of species i . R_i is assumed to be zero for consumers, while J_i and T_i are assumed to be zero for primary producers. The fraction of a consumer's maximum assimilation rate realized at a system's nontrivial equilibrium, ξ_i is determined by:

$$\xi_i = \sum_{k \in \{prey\}} \psi_i \theta_{ki} \hat{B}_k, \quad (3.2)$$

in which \hat{B}_k is the nontrivial equilibrium abundance of prey k . Parameters are assigned such that this fraction is smaller than one.

The intrinsic growth rate, R_i , of primary producers, a consumer's maximum assimilation rate, J_i , and respiration rate T_i , depend on a species' body mass, M_i , as follows:

$$\begin{aligned}
 R_i &= \alpha_R M_i^{-0.25}, \\
 J_i &= \alpha_J M_i^{-0.25}, \\
 T_i &= \alpha_T M_i^{-0.25},
 \end{aligned}
 \tag{3.3}$$

in which α_R , α_J , and α_T are allometric scaling coefficients. This way of assigning parameters facilitates comparison with empirical data, e.g. Huxley (1932), Kleiber (1932), Cohen et al. (1993), West et al. (1997), Enquist et al. (1999), Gillooly et al. (2001), Cohen et al. (2003), Ernest et al. (2003), Brown et al. (2004), Woodward et al. (2005), and Brose et al. (2006a), as well as with theoretical studies that make more complex assumptions when describing a consumer's functional response, e.g. Yodzis & Innes (1992), Brose et al. (2006b), Williams et al. (2007), Stouffer & Bascompte (2010), Purves et al. (2013), and Quévieux & Brose (2019). The entire model may be rewritten in a simpler form when determining the effective competitive and trophic interaction strengths, i.e. the combined effect of all parameters describing an interaction (see Appendix A3.1.1 in Supporting Information).

Food-web topology

The topology of our model food webs, i.e. who eats whom, is determined by the niche model of Williams & Martinez (2000). According to this model, species are randomly assigned a niche value taken from a uniform distribution. Consumers tend to eat prey with a similar or lower niche value, i.e. with niche values falling within a range of which the center is lower than a consumer's own niche value. The niche model of Williams & Martinez (2000) was shown to generate food webs with structural properties that are similar to those observed empirically in food webs (Williams & Martinez, 2000; Stouffer et al., 2005) and is based on the empirical observation that a single niche axis is often sufficient to explain who interacts with whom in complex food webs (Cohen, 1977; Cohen & Stephens, 1978; Cohen & Newman, 1985). With the help of this model we generate food webs with a predefined number of species, S , and average directed connectance, C , i.e. the number of trophic interactions, L , divided by the number of possible interactions, S^2 . Food-webs consisting out of more than one component are discarded from our analysis.

Coexistence and the body-mass of species

As the complexity of food webs, i.e. the number of species and/or interactions, increases, it becomes increasingly difficult to assign parameters such that species may coexist stably (May, 1972, 1973; Roberts, 1974; Gilpin, 1975). Assigning parameters such that species

may coexist stably in complex communities thus requires assumptions about the nonrandom way in these communities are organized. A primary condition for stable coexistence is that a community is feasible, i.e. the amount of resources available to species is sufficient to maintain a population while being predated upon by other species or suffering other losses. A food web may be considered feasible when the net biomass production at lower trophic levels is sufficient to maintain species at higher levels, and a food-web's nontrivial equilibrium is feasible when all nontrivial equilibrium abundances are larger than zero (Roberts, 1974; Gilpin, 1975). Such an equilibrium may be considered stable when the real part of the dominant eigenvalue of the Jacobian matrix corresponding to this equilibrium is smaller than zero (May, 1972).

Feasibility of the here studied model food webs is largely dependent on the specific way in which body masses are assigned. The intrinsic growth rate of producers and the maximum assimilation rate of consumers with a small body mass is larger than the net production and the maximum assimilation rate of larger producers or consumers. Two patterns in the body mass of species may therefore promote feasibility: 1) primary producers that are directly or indirectly preyed upon by many species, i.e. that have a low niche value, tend to be smaller than primary producers that need to sustain fewer species, and 2) predators are larger than prey. We are not aware of empirical studies that have explicitly described the first pattern, but it is known that the body mass of primary producers may vary widely which makes such a pattern likely. The body mass of consumers was, in line with the above described second pattern, found to increase with trophic level and predator-prey body-mass ratios were found to vary within some limited range in empirical food webs (Cohen et al. 1993, 2003; Emmerson & Raffaelli 2004; Woodward et al. 2005; Brose et al. 2006a, but see Carbone et al. 1999).

In this study, we take feasible, stable food webs as the starting point of our analysis and we assign body masses such that this is the case. Nontrivial equilibrium abundances, \hat{B}_i , and parameters that do not depend on a species' body mass are taken from predefined probability distributions (see parameter settings). To assign body masses, we use an algorithm that randomly updates body masses until a desired feasible, stable solution is reached (see Appendix A3.1.2). The outcome of this algorithm is a body-mass distribution that roughly follows the above described patterns. The feasibility and stability of the here studied model food webs depends on the relative differences in body mass and not on the absolute body mass of species.

Analysis and parameter settings

To explore how the response of ecosystems depends on the overall structure of food webs, we analyze several data sets each consisting of 2500 model-generated food webs. The structure of food webs, i.e. the topology and the distributions from which parameters are sampled, may differ among data sets. More specifically, we explore how differences in

species number, S , connectance, C , the distribution of relative feeding preferences, θ_{ik} , and the distribution of feeding efficiencies, f_{ik} , may affect the dynamical behavior of food webs.

Allometric scaling coefficients are, as in other studies, assigned as follows: $\alpha_R = 1$, $\alpha_J = 2.512$, and $\alpha_T = 0.314$ (consumers are assumed to be invertebrates, Brown et al. 2004; Brose et al. 2006b). The fraction of ingested biomass lost to feces, δ_{ij} , is taken from $U(0.4, 0.7)$ for herbivore interactions and from $U(0.05, 0.25)$ for carnivore interactions. Interspecific competitive interaction strengths, c_{ij} , are taken from $U(0.1, 0.5)$. Intraspecific competitive interaction strengths, c_{ii} , are one. Carrying capacities, K_i , are assigned such that they scale with a producer's intrinsic growth rate. We do this by assigning primary producers with R_i/K_i ratio, ρ_i , taken from $U(0.2, 1)$. R_i is determined by equation 3.3 and $K_i = R_i/\rho_i$. R_i/K_i ratios play an important role in ecological literature (MacArthur, 1962; Cody, 1966; MacArthur & Wilson, 1967; Pianka, 1970; Grime, 1979) and equal the effective intraspecific competitive interaction strength as described in Appendix A3.1.1.

Relative feeding preferences, θ_{ik} , are taken from a scaled, symmetric Dirichlet distribution. The distribution's concentration parameter α is, unless stated otherwise, assigned such that the expected variance in relative preference of consumers preying on two prey species is 0.03 ($\alpha = 2.875$). Preferences of other consumers are sampled from distributions with the same α . A consumer's minimum relative feeding preference is 0.1 divided by the number of prey, and the sum of all a consumer's relative preferences is one. Feeding efficiencies, f_{ik} , are taken from a scaled beta distribution with range (0.1, 1). Unless stated otherwise, shape parameters α and β are assigned such that the expected mean feeding efficiency is 0.75 and the expected variance 0.11.

Consumers are assumed to have a preference for, and prey more efficiently on species that are in the center of a consumer's niche range. Feeding preferences, θ_{ik} , and feeding efficiencies, f_{ik} , are therefore sorted such that this is the case. To make sure that our results do not critically depend on this assumption, we test networks in which this order is random as well.

Body masses are, with the help of the aforementioned algorithm (see Appendix A3.1.2), assigned such that the system's nontrivial equilibrium is stable, i.e. the real part of the Jacobian's dominant eigenvalue is smaller than $-1e-4$. The fractions of a consumer's maximum assimilation rate realized at a system's nontrivial equilibrium, γ_i , fall within the range (0.05, 0.75), and predator-prey body-mass ratios within (0.5, 20). Nontrivial equilibrium abundances, \hat{B}_i , are taken from a uniform distribution with range (1.5, 2.5). The fraction of a consumer's maximum assimilation rate realized per prey biomass is determined as follows:

$$\psi_i = \frac{\gamma_i}{\sum_{k \in \{prey\}} \theta_{ki} \hat{B}_k}. \quad (3.4)$$

When nothing is stated about the number of species, S , and connectance, C , we study food webs of 22 species with an average directed connectance of 0.16.

Alternative stable states

Because we assume a linear functional response there is only one single nontrivial equilibrium at which all species may coexist stably. In addition to this nontrivial equilibrium, trivial equilibria exist at which one or more species are extinct. Perhaps counterintuitively, because alternative stable states are usually separated by unstable equilibria in simple one- or two-dimensional models, multiple alternative stable states may exist in addition to a stable nontrivial equilibrium in systems with three or more species, even when assuming a linear functional response (Goh, 1977). Critical transitions away from a system's stable nontrivial equilibrium may occur towards such partially collapsed states when such trivial equilibria are stable. To determine the potential for such partial network collapses, we analytically determine for each subset of species whether a stable equilibrium exist at which all species belonging to a subset have positive abundances while the abundances of other species are zero (see Appendix A3.1.3).

The total feedback on each level

As mentioned in the introduction, feedbacks may have a different length depending on the number of species involved k . We determine the total feedback on each level k as follows:

$$F_K = \sum (-1)^{m+1} L(m, k), \quad (3.5)$$

where $L(m, k)$ is the product of each element in the Jacobian matrix at a system's nontrivial equilibrium, α_{ij} , corresponding to m disjunct, i.e. non-overlapping, loops together having k elements (Levins, 1974; Puccia & Levins, 1985). The total feedback on level k is thus determined by the strengths of feedbacks with length k and smaller. The first necessary condition for the local stability of a system's nontrivial equilibrium is that the total feedback, F_K , is negative at each level k . The second condition for stability is that the strength of slow negative feedbacks cannot be too large when compared to the faster negative feedbacks at lower levels (Levins, 1974; Puccia & Levins, 1985; Neutel & Thorne, 2014). By determining the total feedback, we may know at which level feedbacks might be destabilizing a system.

The total feedback on level k of a three-species system in which primary producer 1 has a direct negative effect on itself and where trophic interactions occur between species 1 and 2, 1 and 3, and 2 and 3, is as follows: $F_1 = \alpha_{11}$, $F_2 = \alpha_{12}\alpha_{21} + \alpha_{13}\alpha_{31} + \alpha_{23}\alpha_{32}$, and $F_3 = \alpha_{13}\alpha_{32}\alpha_{21} + \alpha_{12}\alpha_{23}\alpha_{31} - (\alpha_{23}\alpha_{32})\alpha_{11}$. Delayed negative feedbacks destabilize this system when $F_1 > 0$, or when $F_1F_2 + F_3 > 0$. More complex relationships exist in n -species systems, e.g. $F_1(F_1F_4 + F_5) - F_3(F_1F_2 + F_3) > 0$. Generally speaking, one may assume that a stable system requires that the total feedback on higher levels is not too large when compared to the total feedback on lower levels (Hurwitz, 1895; Gantmacher, 1959; Levins, 1974; Puccia & Levins, 1985).

As an intuitive measure of the extend in which a certain initial distribution of total feedbacks on different levels k , $F_{I,k}$, may or may not promote stability, we determine the threshold value, $F_{T,k}$, below or above which food webs with the same total-feedback distribution become unstable. $F_{T,k}$ is determined computationally by gradually in- or decreasing F_k by multiplying the total feedback at all levels with the same factor κ ($F_{T,k} = \kappa F_{I,k}$).

Boundaries to the area in which species may coexist stably

Boundaries to the area in which species coexist stably may occur when a species' abundance goes to zero, i.e. a loss of feasibility, or when a system's feasible, nontrivial equilibrium becomes unstable. In case of a transcritical bifurcation a system's nontrivial equilibrium may simultaneously become unfeasible and unstable. We refer to this case as a loss of feasibility because this is the ecologically relevant aspect of the bifurcation (equilibria with negative abundances are ecologically irrelevant). Because we assume a linear functional response, a fold bifurcation is not possible. Stability of a system's feasible, nontrivial equilibrium may, however, be lost when a system approaches a Hopf bifurcation. Such Hopf bifurcations may either be supercritical, in which case a stable limit cycle of increasing amplitude appears, or subcritical, in which case a system shifts abruptly to an alternative attractor. There are thus two different ways in which the system's feasible, nontrivial equilibrium may become unstable (when assuming codimension one, i.e. change in a single parameter). To illustrate how a food web's response depends on the nature of the boundary crossed, we study how the dynamical behavior of a simple six-species food webs with the topology in Fig. 3.1.A may depend on the top predator's relative feeding preferences, θ_{ki} . More specifically, we determine for the full network and for each subset of species the area in the top predator's parameter space where each set of species may coexist stably as well as the nature of the boundaries to areas with a single or multiple alternative stable states. We provide examples of three different parameter settings which are chosen such that the area in which a system's nontrivial equilibrium is stable exhibits a different type of boundary (see Appendix A3.1.4). Two cases of the specific way in which crossing a boundary may affect food web dynamics are explored for

each setting; one in which there is an alternative stable subset and one in which there is no alternative stable subset to which a food web may shift at the time of a transition. In total we thus distinguish six different ways in which a food web may respond to changing environmental conditions.

Studying the parameter space of large and complex food webs is complicated, in particular because all trophic interaction strengths as well as all other parameters may change simultaneously. For each of the 2500 model generated food webs belonging to a data set, we study therefore how a random change in the relative feeding preferences of consumers may alter the feasibility and stability of our model generated food webs. We do this by simultaneously altering the relative feeding preferences of all consumers, θ , as follows:

$$\theta_{ki}^* = \theta_{0,ki} + (\theta_{final,ki} - \theta_{0,ki})E, \quad (3.6)$$

in which $\theta_{0,ki}$ is the initial, $\theta_{final,ki}^*$ the final, and θ_{ki}^* the actual feeding preference of consumer species i . Environmental condition, E , is changed in a step-wise manner from 0 to 1 with steps of 0.0001. This approach is equivalent to choosing a random direction in parameter space and checking what kind of boundary to the area in which species may coexist stably is crossed. For each food web we explore 100 different directions, i.e. 100 randomly assigned values of $\theta_{final,ki}$. Like the initial feeding preferences, final feeding preferences are taken from a symmetric Dirichlet distribution such that the sum of all a consumer's relative feeding preferences is one. The distribution of final feeding preferences is assumed to be uniform, i.e. concentration parameter α of the Dirichlet distribution is one.

We assume the presence of alternative stable states at the system's initial conditions, i.e. at $E = 0$, to be indicative of the frequency at which alternative stable states are present when a boundary is crossed. To test whether this assumption is true, we determine whether alternative stable states are present one step before a boundary is reached and determine whether results are qualitatively the same. We also assume that our results are not crucially dependent on the assumption that the fraction of a consumer's maximum assimilation rate realized per prey biomass, ψ_k , stays the same as relative feeding preferences change. To test whether this assumption is true, we explore scenarios in which the fraction of a consumer's maximum assimilation rate realized per prey biomass, ψ_k , and/or the body mass of species changes as well. We do this by altering these fractions as follows:

$$\begin{aligned} \psi_i^* &= \psi_{0,i} + (\psi_{final,i} - \psi_{0,i})E, \\ M_i^* &= M_{0,i} + (M_{final,i} - M_{0,i})E, \end{aligned} \quad (3.7)$$

in which $\psi_{0,i}$ is the initial, $\psi_{final,i}$ the final, and ψ_i^* the actual feeding preference $M_{0,i}$ is the initial, $M_{final,i}$ the final, and M_i^* the actual body mass of consumer species i . $\psi_{final,i} = \kappa_i \psi_{0,i}$, and $M_{final,i} = \kappa_i M_{0,i}$. κ_i is taken from a uniform distribution with range (0.75,1.25).

We assume a food web to be unfeasible when the nontrivial equilibrium abundance of at least one species is smaller than 0.0001. We assume to be dealing with a loss of stability when the real part of at least one of the eigenvalues of the Jacobian matrix becomes larger than zero while all abundances are greater than 0.0001. In practice we were (nearly) always dealing with a pair of complex conjugate eigenvalues that would become larger than zero when a system is feasible, as is typical for Hopf bifurcations. When a Hopf bifurcation is found, we determine whether we are dealing with a supercritical or subcritical by determining the first Lyapunov coefficient. If the first Lyapunov coefficient is negative we are dealing with a supercritical Hopf bifurcation towards a stable limit cycle of which the amplitude increases as conditions change further. If the first Lyapunov coefficient is positive we are dealing with a subcritical Hopf bifurcation towards other potentially more complex dynamics (Marsden & McCracken 1976; Kuznetsov 1995).

3.3 RESULTS

The nature of different types of boundaries in parameter space and the associated critical transitions occurring in the here studied food webs is best understood when studying some stereotypical examples. To provide such examples, we explore the dynamic response of relatively simple food webs, i.e. with the topology in Fig. 3.1.A, to changes in the relative feeding preferences of the food-web's top predator (Fig. 3.2 and Appendix A3.1.4). Each example is associated with a different type of boundary in the top-predator's parameter space to the area in which all species may coexist stably, i.e. a loss of feasibility, a supercritical, or a subcritical Hopf bifurcation. Three types of areas in the predator's parameter space can be distinguished: areas with a single stable state, areas with multiple stable states, and areas in which no single combination of species may coexist stably. Areas with multiple, alternative stable states are of special interest as these are areas in which there is hysteresis. Oscillatory or other more complex dynamics occur in areas where there are no stable states, potentially allowing species to coexist in an 'unstable' manner, i.e. permanence (Hutson & Vickers, 1983; Hutson & Law, 1985). More complex possibilities exist when there are multiple alternative oscillatory, chaotic, or other complex attractors. In this study, we focus on such attractors only when they are directly associated with a shift towards instability of a system's feasible, nontrivial equilibrium. In addition to the here described catastrophes, specific points in parameter space may mark connecting points between different types of boundaries (Fig. A3.1). When such points exist, the behavior of a system is particularly (structurally) unstable in the sense that small differences in the specific way in which changing conditions affect parameters may cause a system to

respond in a fundamentally different way. Growth, feeding and respiration rates of all species and interactions are different in each example (see Appendix A3.1.4).

For each boundary type we indicate two directions away from an initial situation in which all species may coexist stably: a direction leading to a transition when no alternative subset of species is stable and a direction leading to a transition when an alternative subset is stable at the time of a transition (Fig. 3.2). Time series of all six species when conditions are changed along these directions are shown in Fig. 3.3. Perhaps surprisingly, we found that sudden transitions towards alternative stable subsets potentially leading to the loss of several species may be triggered by the decline of a single species, i.e. a loss of feasibility (Fig. 3.3.A). Recovery from such transitions may require a relatively large change in conditions, e.g. back towards the area in parameter space in which a system's nontrivial equilibrium is the only stable state. Although technically a Hopf bifurcation occurring when the abundance of a single species is nearly, but still slightly above zero, such transitions are associated with the gradual decline towards extinction of a single species after which the remaining subset of all-but-one species remains unstable (Fig. 3.3.A, direction 2). When this subset is stable, we are dealing with a transcritical bifurcation (Fig. 3.3.A, direction 1). Oscillatory dynamics with an increasing amplitude occur after a supercritical Hopf bifurcation is passed (Fig. 3.3.B). After such transitions a system may continue to oscillate until, in this example, a system's nontrivial equilibrium becomes stable again, or may shift towards an alternative stable subset once the amplitude of the oscillations is large enough to invoke a shift, e.g. when a limit cycle collides with a stable trivial equilibrium; a global bifurcation. Recovery from a such a shift may require a relatively large change in conditions. The, perhaps, most striking difference in dynamics is found when comparing dynamics after a subcritical Hopf bifurcation for the two cases with and without the presence of an alternative stable subset (Fig. 3.3.C). In the first case we found an abrupt transition towards chaotic or other complex dynamics. In the second case an abrupt transition occurred from one stable state to another. This last case shares some important characteristics with a classical fold bifurcation, i.e. it is a shift between alternative stable states and there is hysteresis. The cause of instability, i.e. an increase in the strength of a delayed negative feedback relative to more immediate negative feedbacks, is, however, fairly different.

A hint of what might happen after an impending regime shift may be found when studying the effect of changing environmental conditions on a system's feedbacks (see **Chapter 4**). An increase in the relative strength of the positive feedback in Fig. 3.1.B likely plays an important role in the existence of alternative stable states in Fig. 3.2.A and 3.2.B. This feedback promotes either an increase in species 5 (blue) and a decrease in species 3 (yellow) and 6 (red) as observed in Fig. 3.3.A.2, or a decrease in species 5 and increase in species 3 and 6 as observed in Fig. 3.3.B.2. A similar role might be played by the feedback in Fig. 3.1.C prior to the regime shift observed in Fig. 3.3.C.2 where it may promote the observed strong increase in species 1 (orange), 5 (blue), and 6 (red) and a decrease in species 4

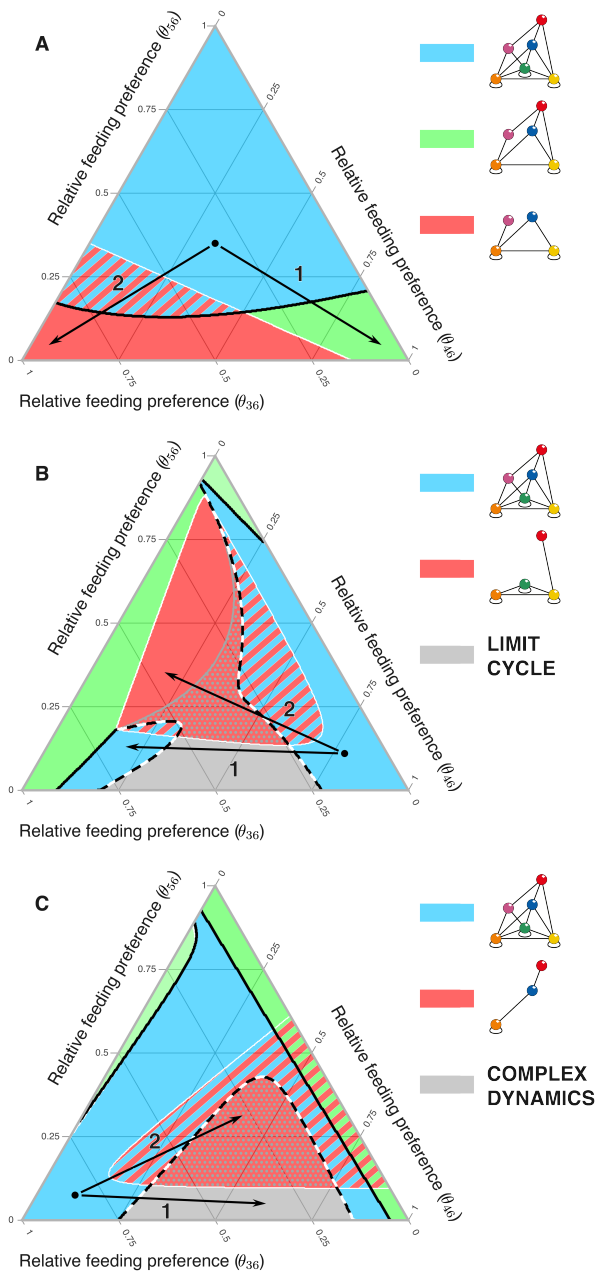


Figure 3.2: Boundaries in parameter space for three different parameter settings, e.g. feeding preferences, feeding efficiencies, and body masses of all species for food webs with the topology in Fig. 3.1.A. Results are shown for the relative feeding preferences of top predator 6 for prey species 5, 4, and 3. All species may coexist stably when relative feeding preferences remain within the blue area. Boundaries are crossed when a species' abundance goes to zero (black solid lines), i.e. a loss of feasibility, or when a feasible food web becomes unstable (striped lines). Areas in which subsets of species may coexist stably are shown in green when containing all but one species and in red when containing fewer species. Striped areas contain multiple alternative stable states. There are no stable states in fully grey areas. **(A)** A loss of feasibility leads to the gradual decline and extinction of a single species when change occurs along direction 1. A similar decline leads to an abrupt transition to an alternative stable subset when change occurs along direction 2. **(B)** A supercritical Hopf bifurcation leads to oscillatory dynamics when change occurs along direction 1. A similar loss of stability may lead, once the amplitude of oscillations is large enough, to an abrupt regime shift towards an alternative stable subset when change occurs along direction 2. **(C)** A subcritical Hopf bifurcation leads to complex dynamics when change occurs along direction 1. A similar loss of stability leads to an abrupt regime shift towards an alternative stable subset when change occurs along direction 2. Legends correspond to stable species combinations or types of dynamical behavior. See Appendix A3.1.4 for parameter settings. The panels are triangular because the sum of the top predator's three feeding preferences is one.

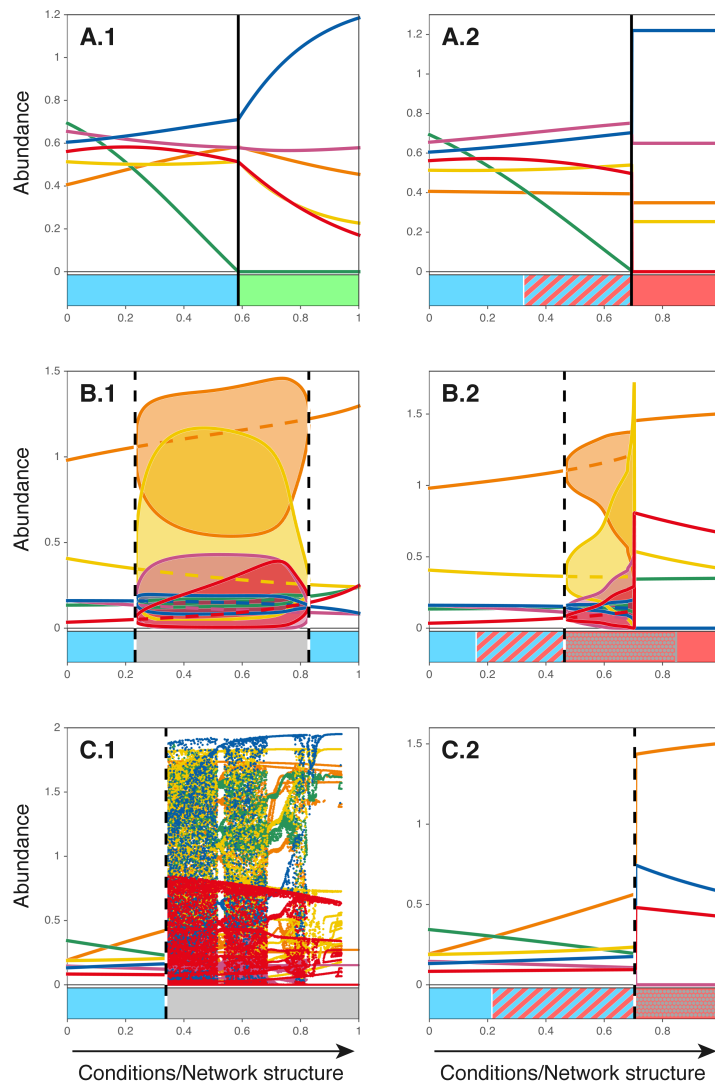


Figure 3.3: Time series of all six species when the top predator’s relative feeding preferences change along the arrows in Fig. 3.2. Each example corresponds to a different type of critical transition. The type of boundary crossed is different in panels A, B, and C. Panels 1 and 2 differ in the presence or absence of an alternative stable subset at the time of a transition. Bars below the time series correspond to the areas in Fig. 3.2. **(A)** The abundance of a single species (1) declines gradually and goes extinct, i.e. a loss of feasibility. In panel A.2 this gradual extinction is accompanied by the sudden collapse of a second species (6) and a shift towards a stable four-species subset (2,3,4,5). **(B)** The system approaches a supercritical Hopf bifurcation and shows oscillatory dynamics after it becomes unstable (see Fig. A3.2). In panel B.2 the cycle disappears when the system shifts to an stable four-species subset occurs (1,2,3,6). **(C)** The system approaches a subcritical Hopf bifurcation and shows complex dynamics after it becomes unstable (see Fig. A3.3). In panel C.2 this leads to an abrupt shift towards a stable three-species subset (1,5,6).

(purple). An increase in the relative strength of the delayed negative feedback in Fig. 3.1.E may promote the oscillatory dynamics observed in Fig. 3.3.B as the consecutive order in which species gain and lose in abundance over time corresponds to the way in which the species belonging to this loop relate to each other (Fig. A3.2). The complex dynamics in Fig. 3.3.C are resulting from the interplay between several delayed negative feedbacks.

The potential for large-scale critical transitions in complex food webs

The nature of a system's feedbacks, and thus its dynamical behavior, depends on the topology of food webs as well as on the distribution of trophic interaction strengths. In Fig. 3.4, we show how such different network structural patterns may affect the presence of alternative stable states. We found that, as the number of species or the connectance of food webs increases, alternative stable states become increasingly common (Fig. 3.4.A-B) and that the maximum number of species that could go extinct due to a regime shift towards such alternative states increases as well. Opposing effects are observed when studying the effect of an increase in the variance in relative feeding preferences and feeding efficiencies. When predators have an almost equally strong preference for all prey species, i.e. a low variance, we found alternative stable states to be relatively common (Fig. 3.4.C). A shift towards these states would lead to the loss of a relatively large number of species. A high variance in feeding efficiencies on the other hand, promotes the occurrence of alternative states and the extinction of species in case of a regime shift (Fig. 3.4.D).

In Fig. 3.5, we show the frequency at which different types of boundaries are crossed when gradually altering the relative feeding preferences of predators. The fractions of a consumer's maximum assimilation rate realized per prey biomass were, in this example, assumed to stay the same, i.e. $\psi_{final,k} = \psi_{0,k}$. We found that the structural patterns that were found to promote the existence of alternative stable states (Fig. 3.4) are also the ones promoting complex regime shifts to oscillatory, chaotic or other complex dynamics (Fig. 3.5). As the number of species or the connectance of food webs increases, for example, Hopf bifurcations become increasingly common (Fig. 3.5.A-B). Supercritical Hopf bifurcations to oscillatory dynamics tend to be more common than subcritical Hopf bifurcations to more complex dynamics. Despite this difference, subcritical Hopf bifurcations to complex dynamics may still occur frequently, e.g., slightly more than 30% of the regime shifts were found to be caused by a subcritical Hopf bifurcation in food webs with a relatively large number of species or a high connectance. As with the occurrence of alternative stable states, opposing effects are found when studying the effect of an increase in the variance in relative feeding preferences and feeding efficiencies (Fig. 3.5.C-D).

The average amount of change, dM , needed to cross a boundary, i.e. the value at which environmental condition M leads to species loss, is strongly influenced by the structure

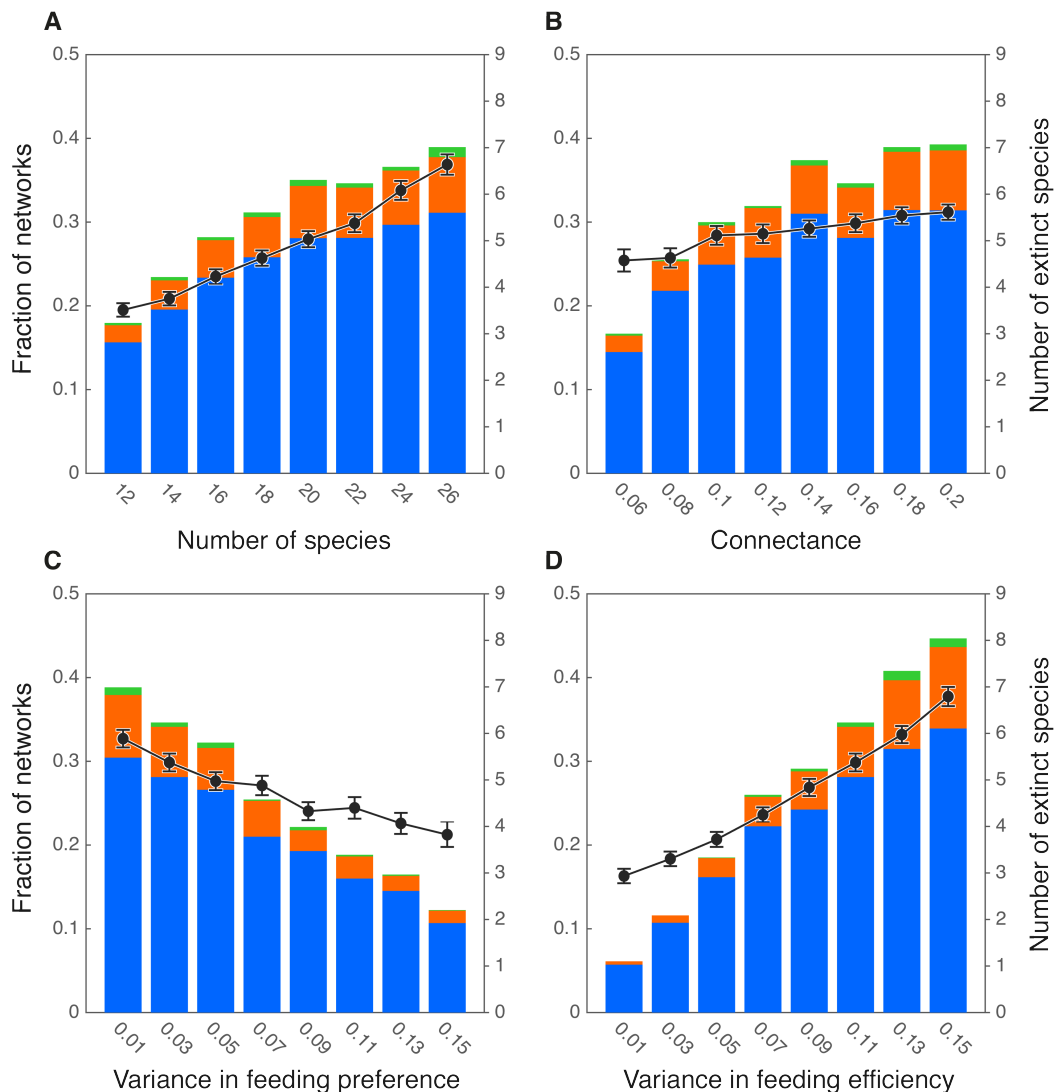


Figure 3.4: The fraction of food webs that exhibit two (blue), three (orange) or four or more (green) alternative stable states (left axis) and the maximum number of species that would go extinct in case of a regime shift towards one of these states, i.e. the total number of species minus the number of species in belonging to the smallest alternative stable subset (black, right axis). **(A-B)** As the number of species or the connectance of food webs increases, alternative stable states become increasingly common. The maximum number of species that could go extinct in case of a regime shift towards these states increases as well. **(C-D)** Two opposing effects are observed when studying the effect of an increase in the variance in relative feeding preferences and feeding efficiencies. When predators have an almost equally strong preference for all prey species, i.e. a low variance, we found alternative stable states to be relatively common. A shift towards these states would lead to the loss of a relatively large number of species. A high variance in feeding efficiencies on the other hand, promotes the occurrence of alternative states and the extinction of species in case of a regime shift.

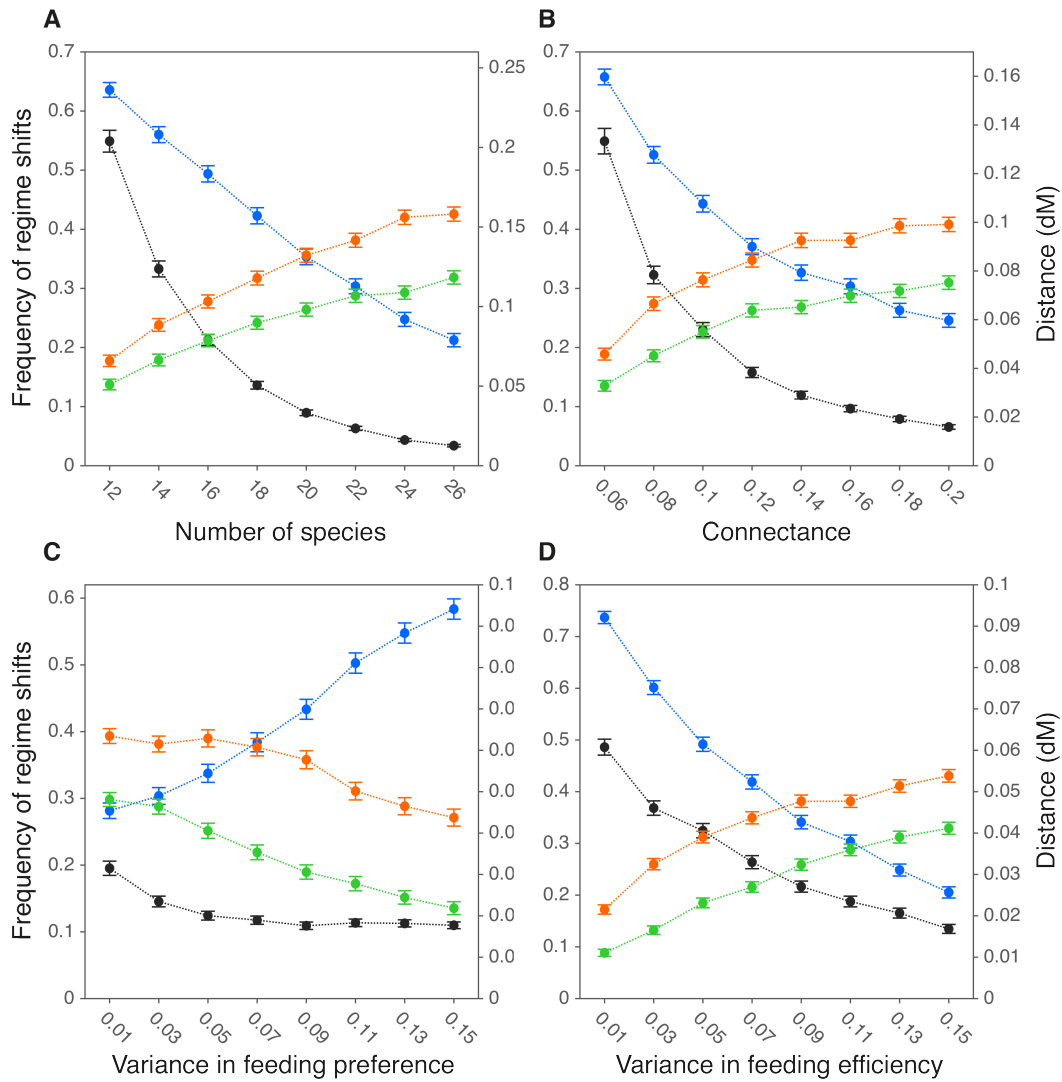


Figure 3.5: The frequency at which different types of boundaries are crossed under changing environmental conditions and the average amount of change needed to cross a boundary. Results are shown for a loss of feasibility (blue), supercritical transitions to oscillatory dynamics (orange), and subcritical transitions to more complex dynamics (green). The average amount of change needed to cross a boundary is indicated in black. **(A-B)** As the number of species or the connectance increases, complex transitions to oscillatory or other more complex dynamics become increasingly common. The amount of change needed to cause a regime shift becomes increasingly small. **(C-D)** A high variance in relative feeding preferences was found to promote sudden regime shifts to oscillatory or other more complex dynamics. The opposite is true for the variance in feeding efficiencies. The amount of change needed to cross a boundary was found to be relatively large when the variance in relative feeding preferences and when the variance in feeding efficiencies is low. Results are shown for a gradual change in the relative feeding preference of predators, other parameters are assumed to stay the same.

food webs. For three of the four structural patterns tested, we found that food webs that can handle a relatively large change in M are also the ones that tend to lose species due to a loss of feasibility, i.e. a gradual decline in abundance leading to extinction. A notable exception to this pattern, however, exists. When the variance in the feeding preferences of predators is low, we found abrupt regime shifts due to Hopf bifurcations to be relatively common and the amount of change needed to reach a bifurcation point to be relatively large. The mean growth rates of primary producers, the average connectance, and the average predator-prey body-mass ratios as observed in different data sets can be found in Fig. A3.5-A3.7.

Total feedback as an indicator of systemic risk

A more in-depth understanding of the interrelationship between network structural properties and the occurrence of abrupt regime shifts, i.e. super- and subcritical Hopf bifurcations, may be obtained when analyzing the nature of positive and negative feedbacks in complex food webs. The criterion that the strength of delayed negative feedbacks, i.e. in longer loops, cannot be too large compared to the more immediate negative feedbacks in shorter loops, as described in Hurwitz (1895) and Levins (1974), allows for a - not too large - increase in the strength of the total negative feedback on lower levels k . We indeed found that such an increase occurred in our model-generated food webs, such that the strength of the total negative feedback was usually largest around level 5-6 in food webs with 22 species (Fig. 3.6.A-B, A3.4 and A3.8). Above those levels a strong decline in total negative feedback with increasing level k was observed and required for stability. Notable differences were found in the strength of the total negative feedback on different levels k among data sets. Data sets containing food webs that were more likely to exhibit Hopf bifurcations showed a weaker total negative feedback across all levels k , with the exception of data sets that had different numbers of species. Within data sets we can also distinguish food webs that are highly likely and food webs that are unlikely to exhibit Hopf bifurcations, i.e. the frequency of Hopf bifurcations when food webs are subjected to change in a randomly chosen directions (Fig. 3.6.C-E). The total negative feedback of food webs that were likely to exhibit Hopf bifurcations was found to be weaker across all levels k as well.

The distribution of the median strength of total feedback across different levels, $F_{M,k}$, could vary somewhat among data sets, e.g. we found that as the average connectance increases in food webs of 22 species, the peak at which the total negative feedback is strongest, moved from level 6 to 5 (Fig. 3.6.A-B). In all cases we found on all levels k that, for a given distribution of median total feedback, an overall decrease in the total feedback would lead to instability below threshold value $F_{T,k}$, i.e. $F_{T,k} < F_{M,k}$ (Fig. A3.9). An overall increase in the strength of the total negative feedback never led to instability. Some distributions allow threshold values to be lower than other distributions.

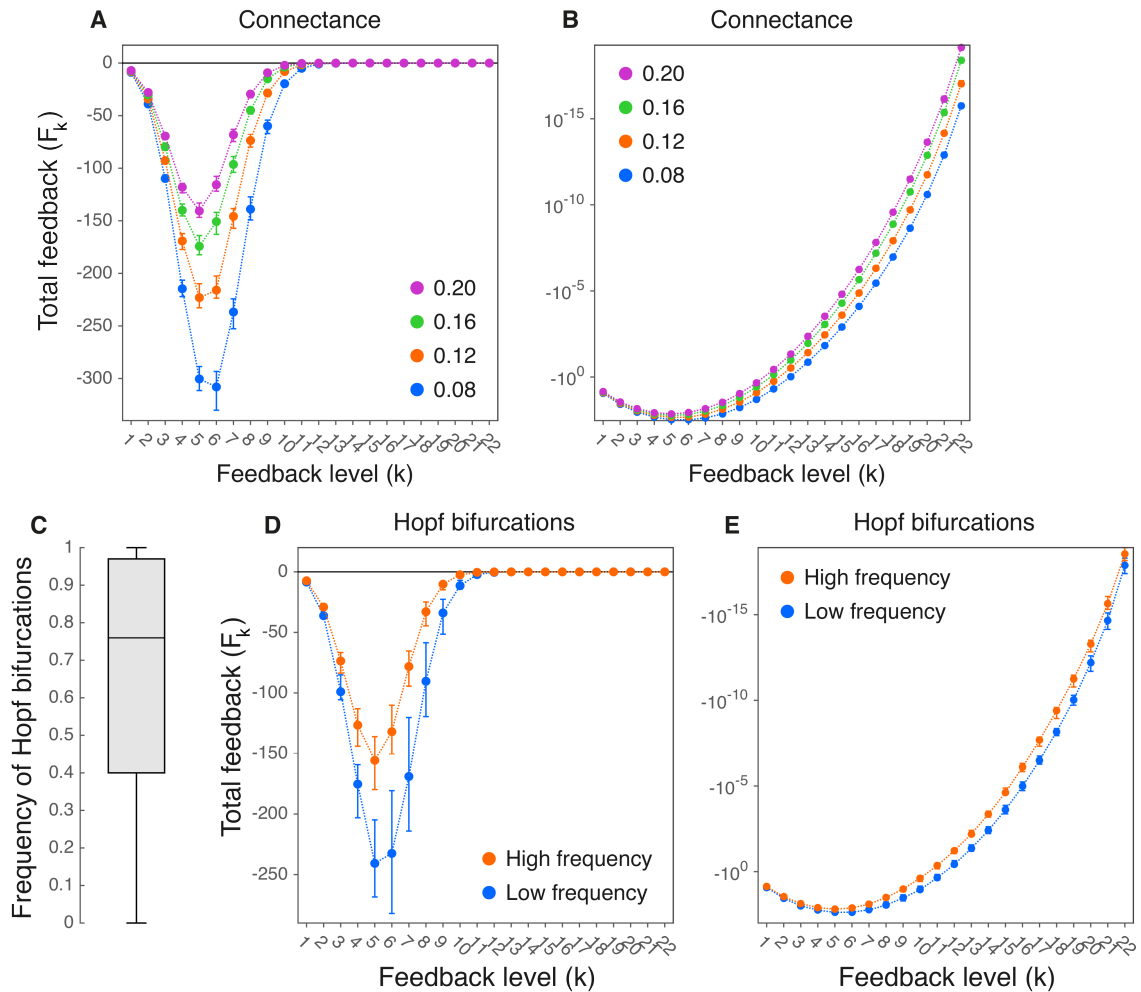


Figure 3.6: Interrelationships between the average directed connectance, the frequency of Hopf bifurcations, and the total feedback on different levels as observed in data sets of 2500 model-generated food webs. **(A-B)** The median total feedback as observed in data sets of food webs with a different average connectance. The total negative feedback of networks with a high connectance is weaker in particular around levels 4-6. **(C)** The frequency of Hopf bifurcations after gradually altering relative feeding preferences in each food web in a 100 different ways as observed in a single data set with average directed connectance 0.16. **(D-E)** The total feedback in networks belonging to the upper (orange) and the lower (blue) quartile in panel C. As in networks with a low connectance, the total negative feedback of networks that are likely to exhibit a Hopf bifurcation is generally weaker in particular around level 4-6. Panel A and B, and D and E contain the same data on a linear and a logarithmic scale.

The small shift in the level around which the total negative feedback is strongest to lower level 5 as observed with increasing connectance, was found to lower the threshold value $F_{T,k}$ suggesting that having a peak in total negative feedback on a lower level promotes stability. The increased stability arising from such a more optimal distribution does, however, not seem to make up for the loss in stability caused by an overall decrease in

the total negative feedback, as Hopf bifurcations were found to be increasingly common with increasing connectance.

3.4 DISCUSSION

The long-standing debate on the complexity and stability of ecosystems has mainly focused on the interrelationship between the number of species or interactions and the local stability of a system's nontrivial equilibrium (May, 1972, 1973; Pimm, 1984; McCann, 2000). As a consequence, relatively little is known about the specific ways in which biodiversity might be lost when environmental conditions change. By merging network theory with theory on critical transitions, we hope to provide a framework that allows us to better evaluate the risk of large, systemic changes in ecosystems under the influence of global environmental change. Our results show that complex transitions may occur even when assuming a linear relationship between the intake rate of predators and prey availability. The nature of such transitions is determined by the specific way in which feasibility or stability is lost and by the presence of alternative stable states at the time of a transition. Whether small changes in food-web parameters, e.g. growth, mortality, feeding and respiration rates, are likely to lead to catastrophic regime shifts depends on the size of the area in parameter space within which species may coexist stably and the nature of the boundaries to such an area. Systemic risk, i.e. the likelihood of a large and/or hardly reversible regime shifts, is high when a system's initial parameter values are close to a catastrophic boundary in parameter space.

By analyzing data sets of many model-generated food webs, we found that strong interrelationships exist between the complexity and the structure of food webs and the likelihood and nature of critical transitions occurring when the aforementioned boundaries are crossed. Complex food webs, i.e. with a large number of species and/or a high connectance, are more likely to exhibit alternative stable states and are also more likely to go through sudden transitions to oscillatory or other more complex dynamics. The same is true for food webs with a low variance in relative feeding preferences and a high variance in feeding efficiencies. We found that the structural properties we found to simultaneously promote the occurrence of alternative stable states and of transitions to oscillatory or other more complex dynamics are associated with an overall decline in the total negative feedback on all levels k , and we found that an overall decline in total negative feedback, i.e. while maintaining the same distribution across all levels k , leads to transitions to oscillatory or other more complex dynamics below a critical value $F_{T,k}$. Slight changes in distribution would decrease critical level $F_{T,k}$, suggesting that they have an opposing effect on the occurrence of the aforementioned transitions. A relatively weak total negative feedback across all levels k thus seems the most likely explanation for the increased occurrence of transitions to oscillatory or other more complex dynamics associated with the aforementioned network structural properties. A possible explanation for

the simultaneous increase in the occurrence of alternative stable states and of transitions to oscillatory or other more complex dynamics might be an increase in the strength of relatively short positive feedback loops, e.g. apparent competition. Positive feedbacks in short loops may lower the total negative feedback on all levels k larger than the length of these loops (the total feedback on level k is determined by the strengths of feedbacks with length k and smaller) and, as all other positive feedbacks, increase the potential for alternative stable states in the here studied systems.

We believe that, by assuming a linear functional response, we made a conservative estimate of the potential presence of alternative stable states and the occurrence of abrupt critical transitions, i.e. transitions to oscillating or other more complex dynamics. When assuming a non-linear response, multiple stable and unstable nontrivial equilibria may exist. Such unstable equilibria may lead to saddle-node, e.g. fold, bifurcations when colliding with the system's initial state and are associated with thresholds between the attraction basins of alternative stable states. In preliminary work (not shown here), we found that a non-linear functional response of predators may indeed promote the existence of alternative stable states and the potential for abrupt critical transitions. A non-linear functional response may simultaneously promote the occurrence of oscillating dynamics because it reduces the strength of a direct negative effect of prey species on themselves (as described by the Jacobian matrix). Future research should, however, further explore when and whether this is indeed the case, as the magnitude of the increase in the occurrence of alternative stable states and abrupt regime shifts was found to be highly sensitive to the specific function and parameter values chosen to describe predator-prey relationships.

Our findings may have large implications for the way in which we evaluate stability of food webs and the sustainability of the services they provide in the context of global environmental change. Our results suggest that, in addition to conservation efforts focused on the survival of rare or iconic species, it is of importance to monitor which changes are likely to undermine the overall stability of complex food webs. Two requirements for species coexistence should therefore be distinguished; feasibility and stability. A community is feasible when the amount of resources available to species is sufficient to maintain a population while being predated upon by other species. Stability requires that the relationships between species are such that they do not exclude each other. Conservation efforts have traditionally focused on preventing the decline of species abundances, i.e. on maintaining feasibility. Structural properties that promote feasibility, however, do not necessarily promote stability and vice versa. Conservation efforts that aim to prevent a decline in species abundances, i.e. a loss of feasibility, may thus pave the way for more large scale critical transitions when altering the interrelationships between species and the feedbacks providing stability to ecosystems as a whole.

This study is a first step towards a better understanding of the relationship between struc-

ture of complex food webs and the nature of critical transitions, and we realize that some important questions remain unexplored. First, we believe that a further development of the here presented theory could help identify the subsets of species that may cause instability and/or alternative stable states in food webs. The possibility to identify such (groups of) species could be of great importance in the context of nature conservation. Second, the number of ways in which parameters are assigned and the ways in which food web dynamics may be described provide a range of possibilities that is far too wide to be explored in a single study. Any study on complex food webs is, therefore, limited. In this study, we chose for mathematical simplicity, i.e. a linear functional response, while assigning ‘plausible’ parameters based on allometric scaling relationships. Future research could explore the impact of making more complex dynamical assumptions, in particular when describing predator-prey relationships, and will almost certainly show that a more accurate assignment of parameters is possible. By doing this, we hope to facilitate comparison with classical studies on food web stability that have used similar simple models as well as with empirical studies providing information on the flows of biomass through food webs. Future research should further explore which assumptions are crucial for our findings and which ones are of a lesser importance. Third and finally, the here described regime shifts may not only be important in the context of global environmental change. In principal, any complex system of many interacting components could exhibit the feedbacks and different types of critical transitions as described in this study. Some of the theoretical ideas used in this study were developed in the context of regulatory networks (Levins, 1974; Tyson et al., 2003; Novák & Tyson, 2008) and morphogenesis (Thom, 1975). Future research could further explore whether our findings are also of relevance for other types of complex systems.

A3.1 SUPPLEMENTARY METHODS

A3.1.1 LOTKA-VOLTERRA MODEL

The food-web model presented in the main text (equation 3.1) is equivalent to the following simple Lotka-Volterra model:

$$\frac{dB_i}{dt} = B_i(g_i + \sum_{j=1}^n \alpha_{ij} B_j), \quad (\text{A3.1})$$

in which B_i corresponds to the biomass of (basal or non-basal) species, g_i to a species' growth or respiration rate, and α_{ij} to the effective competitive or trophic interaction strengths. Growth or respiration rate $g_i = R_i$ for basal species and $g_k = -T_k$ for non-basal species.

Effective competitive interaction strengths between basal species i and j are determined as follows:

$$\alpha_{ij} = -R_i \frac{c_{ij}}{K_i}, \quad (\text{A3.2})$$

in which R_i is a basal species' intrinsic growth rate, c_{ij} the competitive interaction strength, and K_i a species' carrying capacity. Please note that competitive effect of species on themselves, α_{ii} , is equal to $-R_i/K_i$ because $c_{ii} = 1$. When assigning R_i/K_i ratio ψ_i (see parameter settings), we thus determine the strength of the effective intraspecific competition, α_{ii} .

The effects of prey species l on predator species k and of predator species k on prey species l are determined as follows:

$$\begin{aligned} \alpha_{lk} &= J_k \psi_k \theta_{lk}, \\ \alpha_{kl} &= -J_k \frac{\psi_k \theta_{lk}}{(1 - \delta_{lk}) f_{lk}}, \end{aligned} \quad (\text{A3.3})$$

in which J_k is the maximum assimilation rate of predator k at the system's non-trivial equilibrium, ψ_k , the total capture rate of predator k , and θ_{lk} , the relative preference of predator k for prey species l , f_{lk} is the fraction of killed prey biomass that is ingested and δ_{lk} the fraction of ingested biomass lost to feces.

A3.1.2 BODY-MASS ASSIGNMENT

To assign body masses, we use an algorithm that randomly updates body masses until a desired feasible, stable solution is reached. Initially, all consumers are assigned a body mass taken from a uniform distribution, i.e. $M_{k,0} \sim U(1,100)$. The body masses of consumers are at each iterative step simultaneously updated as follows:

$$M_{k,s+1} = \eta_{k,s} M_{k,s}, \quad (\text{A3.4})$$

in which $M_{k,s}$ is the body mass of consumer k at step s and $M_{k,s+1}$ its body mass at step $s + 1$. Random number $\eta_{k,s}$ is drawn from a uniform distribution with range $(0.9,1.1)$. The body masses, M_i , of primary producers are, at every iteration, assigned such that they meet the feeding demands of non-basal species:

$$M_i = \left(\sum_{j \in \{\text{prod.}\}} \frac{\rho_i c_{ij} \hat{B}_j}{\alpha_R} + \sum_{k \in \{\text{pred.}\}} J_k \frac{\psi_k \theta_{ik}}{(1 - \delta_{ik}) f_{ik} \alpha_R} \hat{B}_k \right)^{-4}, \quad (\text{A3.5})$$

in which ρ_i is the R_i/K_i ratio of primary producer i and \hat{B}_k the nontrivial equilibrium abundance of (producer or consumer) species k . Three stages can be distinguished while the algorithm updates the body mass of species. During each stage, updated body masses are either accepted, when they bring a system closer to a desired outcome, or rejected in which case body masses are assigned the values of the previous step. In the first stage, body masses are updated such that the fractions of the consumers' maximum assimilation rates realized at a system's nontrivial equilibrium, γ_k , fall within a predefined range. This range must lay somewhere between zero and one, e.g., $(0.05,0.75)$, i.e. the system is feasible. The fraction of the maximum assimilation rate of consumer k realized at a system's nontrivial equilibrium, γ_k , is *defined* as follows:

$$\gamma_k = \sum_{k \in \{\text{prey}\}} \psi_k \theta_{jk} \hat{B}_j, \quad (\text{A3.6})$$

in which \hat{B}_j is the nontrivial equilibrium abundance of prey species j . In the second stage, body masses are updated such that the dominant eigenvalue of the Jacobian at a system's nontrivial equilibrium is below a certain threshold value. This value is chosen below zero such that the system is stable. In the third stage, body masses are updated such that all predator-prey body-mass ratios fall within a predefined range. This prevents some unrealistically large or small predator-prey body-mass ratios from occurring. Changes in body mass that violate a criterion fulfilled in a previous stage are not accepted.

More specifically, we *determine* the fraction of a consumer's maximum assimilation rate realized at a system's non-trivial equilibrium, γ_k , as follows:

$$\begin{bmatrix} \gamma_k \\ \vdots \\ \gamma_l \end{bmatrix} = \begin{bmatrix} J_k \hat{B}_k - \frac{J_k \theta_{kk} \hat{B}_k \hat{B}_k}{(1 - \delta_{kk}) f_{kk} \sum_{j \in \{\text{prey}\}} \theta_{jk} \hat{B}_j} & \cdots & - \frac{J_l \theta_{kl} \hat{B}_k \hat{B}_l}{(1 - \delta_{kl}) f_{kl} \sum_{j \in \{\text{prey}\}} \theta_{jl} \hat{B}_j} \\ \vdots & \ddots & \vdots \\ - \frac{J_l \theta_{lk} \hat{B}_l \hat{B}_k}{(1 - \delta_{lk}) f_{lk} \sum_{j \in \{\text{prey}\}} \theta_{jk} \hat{B}_j} & \cdots & J_l \hat{B}_l - \frac{J_l \theta_{ll} \hat{B}_l \hat{B}_l}{(1 - \delta_{ll}) f_{ll} \sum_{j \in \{\text{prey}\}} \theta_{jl} \hat{B}_j} \end{bmatrix}^{-1} \begin{bmatrix} T_k \hat{B}_k \\ \vdots \\ T_l \hat{B}_l \end{bmatrix}, \quad (\text{A3.7})$$

in which maximum assimilation rate J_k and respiration rate T_k are determined with the allometric scaling relationships in equation 3.3 (see Methods). Other parameters are taken from a predefined probability distribution (see parameter settings).

After the initial assignment of body masses, the algorithm updates body-masses such that all γ_k fall within a predefined range. At each iterative step the differences between the realized γ_k , and the desired range ($\gamma_{min}, \gamma_{max}$) are determined. This difference is equal to $\gamma_{min} - \gamma_k$ when $\gamma_k < \gamma_{min}$, or $\gamma_k - \gamma_{max}$ when $\gamma_k > \gamma_{max}$. In this first stage, a change in body mass is accepted when the sum of these differences is smaller than at the previous step. When this is not the case, body masses are changed back to the body masses of the previous step. The network is discarded when the fractions of a predator's maximum assimilation rate, γ_k , are not with the desired range after 10.000 iterative steps.

When all fractions of a predator's maximum assimilation rate, γ_k , are within desired range ($\gamma_{min}, \gamma_{max}$), we determine the dominant eigenvalue of the Jacobian matrix at the system's non-trivial equilibrium. In this second stage, the algorithm continues to update body masses according to equations A3.4 and A3.5 (see Methods). A change in body mass is accepted when all assimilation rates, γ_k , remain within desired range ($\gamma_{min}, \gamma_{max}$) and when the real part of the dominant eigenvalue is lower than at the previous step. The algorithm continues to update body masses until the dominant eigenvalue is below a predefined minimum value (see parameter settings). This value is smaller than zero, such that the system's non-trivial equilibrium is stable. The network is discarded when the dominant eigenvalue is not below the desired value after 10.000 iterative steps.

Once a stable equilibrium is found, we determine for each interaction the predator-prey body-mass ratios as follows:

$$\nu_{jk} = \frac{M_k}{M_j}, \quad (\text{A3.8})$$

in which ν_{jk} is the predator-prey body-mass ratio of the interaction between predator species k and prey species j . At each of the following iterative steps, the algorithm determines the difference between the realized predator-prey body-mass ratio ν_{ik} , and desired range (ν_{min}, ν_{max}) . This difference is equal to $\nu_{min} - \nu_{ik}$ when $\nu_{ik} < \nu_{min}$, or $\nu_{ik} - \nu_{max}$ when $\nu_{ik} > \nu_{max}$. A different range might be used for herbivore, i.e., the prey is a basal species, and carnivore interactions, i.e., the prey is a non-basal species. A change in abundance is accepted in this third stage when all assimilation rates, γ_k , remain within desired range $(\gamma_{min}, \gamma_{max})$, when the real part of the dominant eigenvalue remains lower than the predefined minimum value, and when the sum of these differences is smaller than at the previous step. The network is discarded when the predator-prey body-mass ratios, ν_{ik} , are not with the desired range after 10.000 iterative steps. When all predator-prey body-mass ratios are within the desired range, we have obtained the final distribution of body-masses M_i .

The average connectance of the networks contained by a data set may differ from the assigned average directed connectance, C , because some of the networks generated by the niche model are discarded by the here described body-mass algorithm. To make sure that the eventual connectance of the networks contained by a data set does not deviate too much from the assigned connectance, we discard all networks that deviate more than ± 0.02 from the assigned average connectance, C .

A3.1.3 GLOBAL VS. LOCAL STABILITY

To determine whether a system's nontrivial equilibrium is globally or locally stable, we determine for each combination of species, S , whether a feasible, stable equilibrium can be found. Because we are dealing with a simple linear functional response, the equilibrium abundances of every subset can be determined analytically by constructing growth vector G_S and interaction matrix I_S :

$$G_S = \begin{bmatrix} g_i \\ g_j \\ \vdots \\ g_k \end{bmatrix}, \quad I_S = \begin{bmatrix} \alpha_{ii} & -\alpha_{ij} & \dots & \alpha_{ik} \\ \alpha_{ji} & \alpha_{jj} & \dots & \alpha_{jk} \\ \vdots & \vdots & \ddots & \vdots \\ \alpha_{ik} & \alpha_{jk} & \dots & \alpha_{kk} \end{bmatrix}, \quad (\text{A3.9})$$

in which g_i is a species' growth or respiration rate and α_{ij} the effective competitive or trophic interaction strength (see supplementary section A3.1.1). Only species and interactions between species that belong to subset S are included when constructing G_S and I_S . After constructing growth vector G_S and interaction matrix I_S , the equilibrium abundances of species, \hat{B}_S , can be determined as follows:

$$\hat{B}_S = -I_S^{-1}G_S \quad (\text{A3.10})$$

in which \hat{B}_S is a vector containing the equilibrium abundances of the species belonging to subset S . We consider the subset to be feasible when the abundances of all species belonging to the subset are larger than zero. When the subset is feasible, we evaluate the stability of the equilibrium point at which the abundances of species belonging to subset S are equal to B_S . The abundances of other species are zero. We do this by determining whether the eigenvalues of the Jacobian matrix are smaller than zero. The subset is thus only considered to be stable when the subset is both intrinsically stable, i.e., the properties of species and interactions belonging to the subset allow for stable coexistence, and when it cannot easily be invaded by species not belonging to the subset.

A3.1.4 PARAMETER SETTINGS SIX-SPECIES MODEL

To find intuitive examples of different types of boundaries, we explored the parameter space of the top-predator in the simple six-species food web in Fig. 3.1.A for a large number of randomly generated parameter settings. For illustrative purposes, we selected parameter spaces that were relatively simple in terms of the number of areas in which different subsets are stable, and we deliberately choose examples where the same boundary could be crossed either to an area in which an alternative subset is stable or to an area in which this is not the case. The parameter settings we ended up with are as mentioned below:

Fig. 3.2.A: $R_1 = 3.3555$, $R_2 = 6.6080$, $R_3 = 2.2813$, $K_1 = 1.8342$, $K_2 = 5.1387$, $K_3 = 1.3700$, $c_{12} = 0.2270$, $c_{13} = 0.2270$, $c_{21} = 0.2064$, $c_{23} = 0.2064$, $c_{31} = 0.4844$, $c_{32} = 0.2064$, $J_4 = 1.6062$, $J_5 = 1.7076$, $J_6 = 1.1427$, $\psi_4 = 0.3935$, $\psi_5 = 0.6612$, $\psi_6 = 0.2113$, $\theta_{14} = 0.9108$, $\theta_{15} = 0.2480$, $\theta_{24} = 0.0892$, $\theta_{25} = 0.3571$, $\theta_{35} = 0.4048$, $\delta_{14} = 0.55$, $\delta_{15} = 0.55$, $\delta_{24} = 0.55$, $\delta_{25} = 0.55$, $\delta_{35} = 0.55$, $\delta_{36} = 0.55$, $\delta_{46} = 0.15$, $\delta_{56} = 0.15$, $f_{14} = 0.6734$, $f_{15} = 0.6030$, $f_{24} = 0.2138$, $f_{25} = 0.1038$, $f_{35} = 0.7853$, $f_{36} = 0.6674$, $f_{46} = 0.7167$, $f_{56} = 0.2593$, $T_4 = 0.2008$, $T_5 = 0.2135$, and $T_6 = 0.1428$.

Fig. 3.2.B: $R_1 = 1.1023$, $R_2 = 0.2100$, $R_3 = 0.5569$, $K_1 = 1.7882$, $K_2 = 0.8971$, $K_3 = 2.7318$, $c_{12} = 0.3160$, $c_{13} = 0.4207$, $c_{21} = 0.3160$, $c_{23} = 0.1751$, $c_{31} = 0.4207$, $c_{32} = 0.1751$, $J_4 = 1.5681$, $J_5 = 1.3614$, $J_6 = 0.8867$, $\psi_4 = 0.2252$, $\psi_5 = 0.2253$, $\psi_6 = 0.6646$, $\theta_{14} = 0.8647$, $\theta_{15} = 0.3752$, $\theta_{24} = 0.1353$, $\theta_{25} = 0.2117$, $\theta_{35} = 0.4131$, $\delta_{14} = 0.55$, $\delta_{15} = 0.55$, $\delta_{24} = 0.55$, $\delta_{25} = 0.55$, $\delta_{35} = 0.55$, $\delta_{36} = 0.55$, $\delta_{46} = 0.15$, $\delta_{56} = 0.15$, $f_{14} = 0.5754$, $f_{15} = 0.2333$, $f_{24} = 0.7876$, $f_{25} = 0.3429$, $f_{35} = 0.1187$, $f_{36} = 0.6306$, $f_{46} = 0.3235$, $f_{56} = 0.8870$, $T_4 = 0.1960$, $T_5 = 0.1702$, and $T_6 = 0.1108$.

Fig. 3.2.C: $R_1 = 4.0681$, $R_2 = 0.8409$, $R_3 = 0.3336$, $K_1 = 1.7424$, $K_2 = 1.9634$, $K_3 = 1.8962$, $c_{12} = 0.1503$, $c_{13} = 0.2288$, $c_{21} = 0.1503$, $c_{23} = 0.4104$, $c_{31} = 0.2288$, $c_{32} = 0.4104$, $J_4 = 3.3152$, $J_5 = 2.8221$, $J_6 = 1.9674$, $\psi_4 = 0.7150$, $\psi_5 = 0.4486$, $\psi_6 = 0.6947$, $\theta_{14} = 0.6436$, $\theta_{15} = 0.2970$, $\theta_{24} = 0.3564$, $\theta_{25} = 0.6241$, $\theta_{35} = 0.0789$, $\delta_{14} = 0.55$, $\delta_{15} = 0.55$, $\delta_{24} = 0.55$, $\delta_{25} = 0.55$, $\delta_{35} = 0.55$, $\delta_{36} = 0.55$, $\delta_{46} = 0.15$, $\delta_{56} = 0.15$, $f_{14} = 0.1510$, $f_{15} = 0.8682$, $f_{24} = 0.8989$, $f_{25} = 0.6748$, $f_{35} = 0.2277$, $f_{36} = 0.7995$, $f_{46} = 0.1495$, $f_{56} = 0.9993$, $T_4 = 0.4144$, $T_5 = 0.3528$, and $T_6 = 0.2459$.

Fig. A3.1: $R_1 = 1.2729$, $R_2 = 4.5236$, $R_3 = 0.9246$, $K_1 = 1.5391$, $K_2 = 3.5850$, $K_3 = 1.2361$, $c_{12} = 0.4335$, $c_{13} = 0.2160$, $c_{21} = 0.4335$, $c_{23} = 0.1134$, $c_{31} = 0.2160$, $c_{32} = 0.1134$, $J_4 = 2.5666$, $J_5 = 2.5855$, $J_6 = 1.4720$, $\psi_4 = 0.3689$, $\psi_5 = 0.2276$, $\psi_6 = 0.2956$, $\theta_{14} = 0.0826$, $\theta_{15} = 0.0728$, $\theta_{24} = 0.9174$, $\theta_{25} = 0.6098$, $\theta_{35} = 0.3174$, $\delta_{14} = 0.55$, $\delta_{15} = 0.55$, $\delta_{24} = 0.55$, $\delta_{25} = 0.55$, $\delta_{35} = 0.55$, $\delta_{36} = 0.55$, $\delta_{46} = 0.15$, $\delta_{56} = 0.15$, $f_{14} = 0.8277$, $f_{15} = 0.1971$, $f_{24} = 0.1028$, $f_{25} = 0.6687$, $f_{35} = 0.7428$, $f_{36} = 0.9125$, $f_{46} = 0.1010$, $f_{56} = 0.6803$, $T_4 = 0.3083$, $T_5 = 0.3230$, and $T_6 = 0.1840$.

A3.2 SUPPLEMENTARY FIGURES

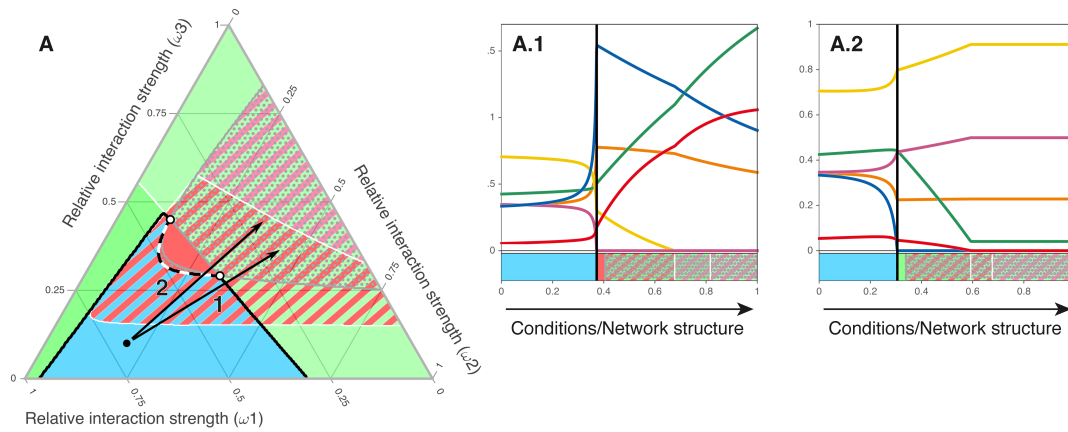


Figure A3.1: Specific points in parameter space (open circles) may mark connecting points between different types of boundaries. When such points exist, the behavior of the system is highly unstable in the sense that small differences in the way in which parameters change may cause the system to respond in a fundamentally different way. At these points two nullclines are parallel to each other in the network's state space, i.e., vertical bifurcation points.

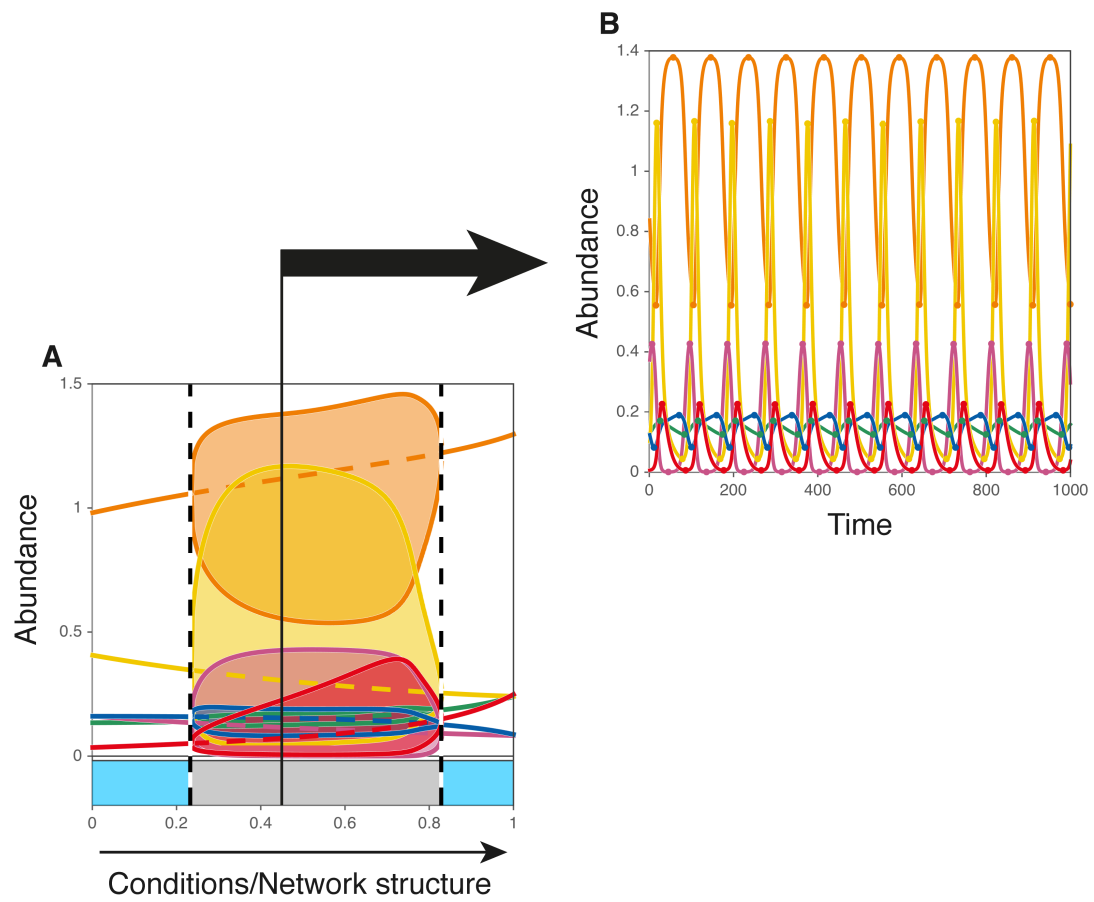


Figure A3.2: Oscillating dynamics after passing a supercritical Hopf bifurcation.

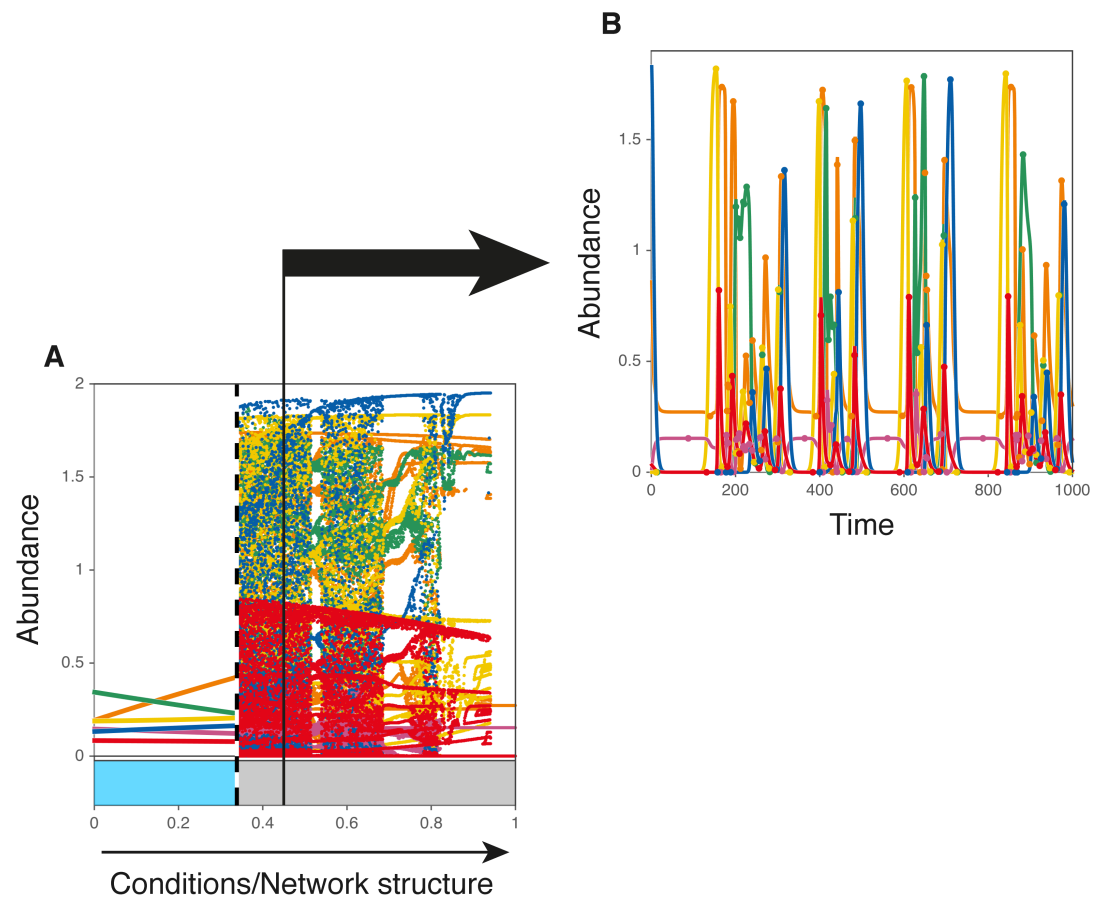


Figure A3.3: Complex dynamics after passing a subcritical Hopf bifurcation.

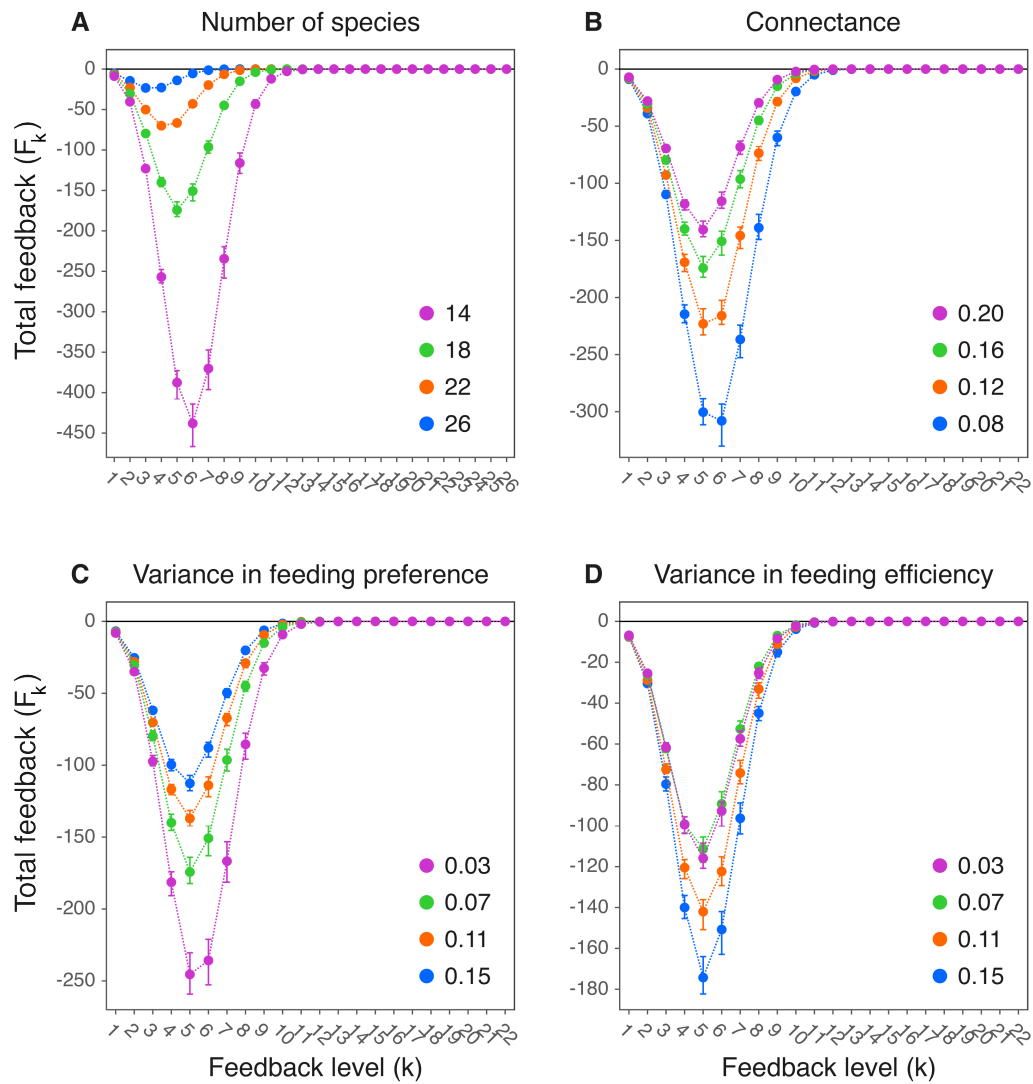


Figure A3.4: Median total feedback as observed in data sets of 2500 food webs for different network structural properties. Panels (A-D) correspond to the network structural patterns for which results are shown in Fig. 3.4 and Fig. 3.5.

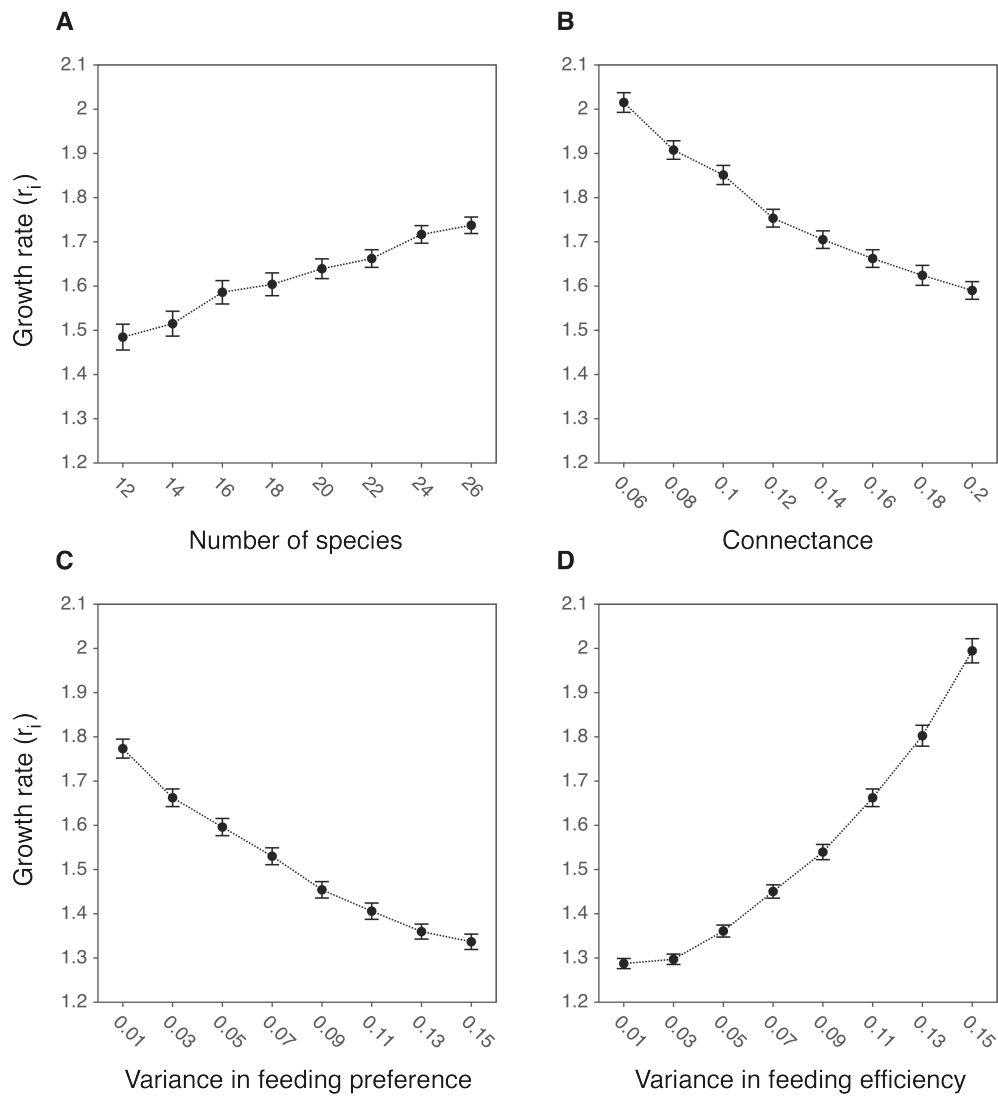


Figure A3.5: Average growth rate r_i as observed in data sets of 2500 food webs for different network structural properties. Panels (A-D) correspond to the network structural patterns for which results are shown in Fig. 3.4 and Fig. 3.5.

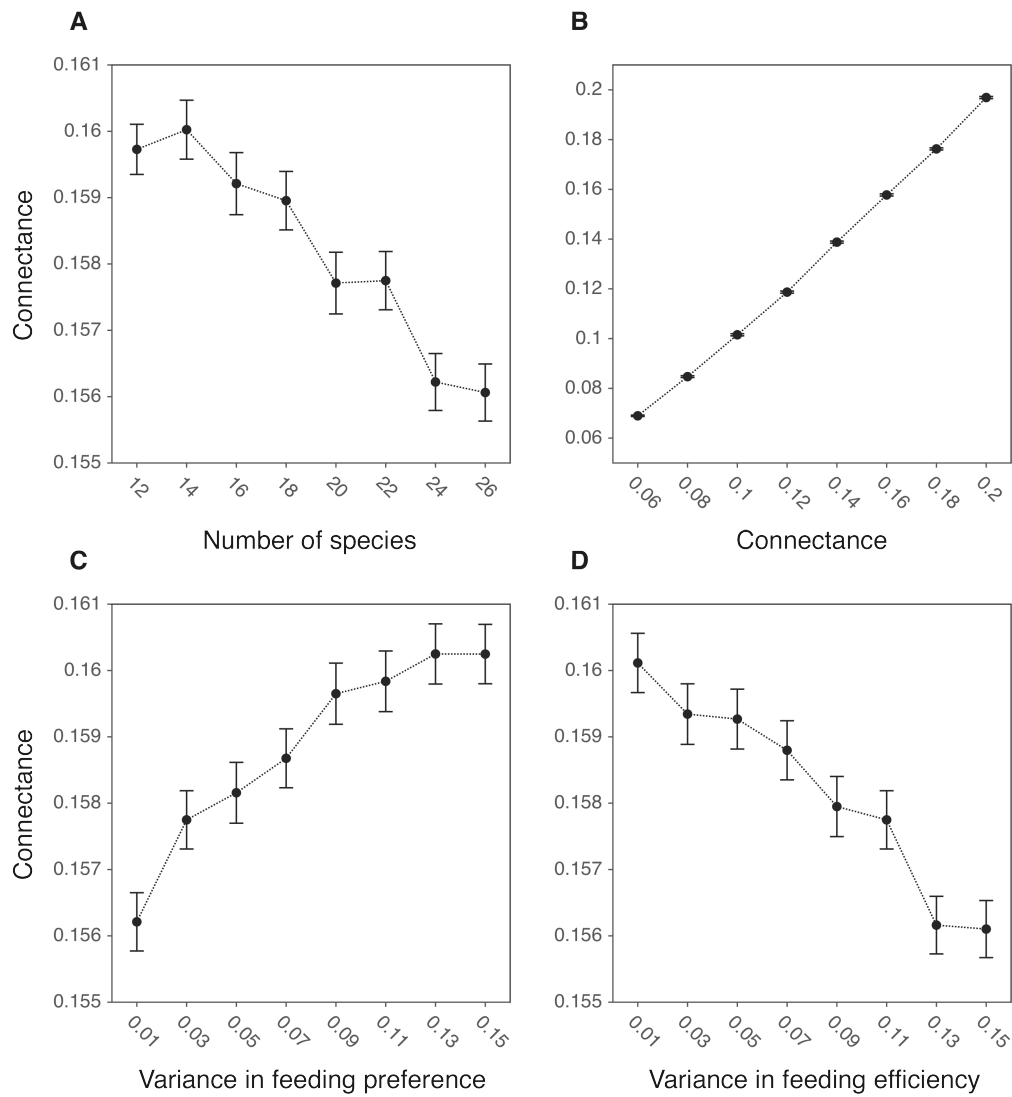


Figure A3.6: Average connectance as observed in data sets of 2500 food webs for different network structural properties. Panels (A-D) correspond to the network structural patterns for which results are shown in Fig. 3.4 and Fig. 3.5.

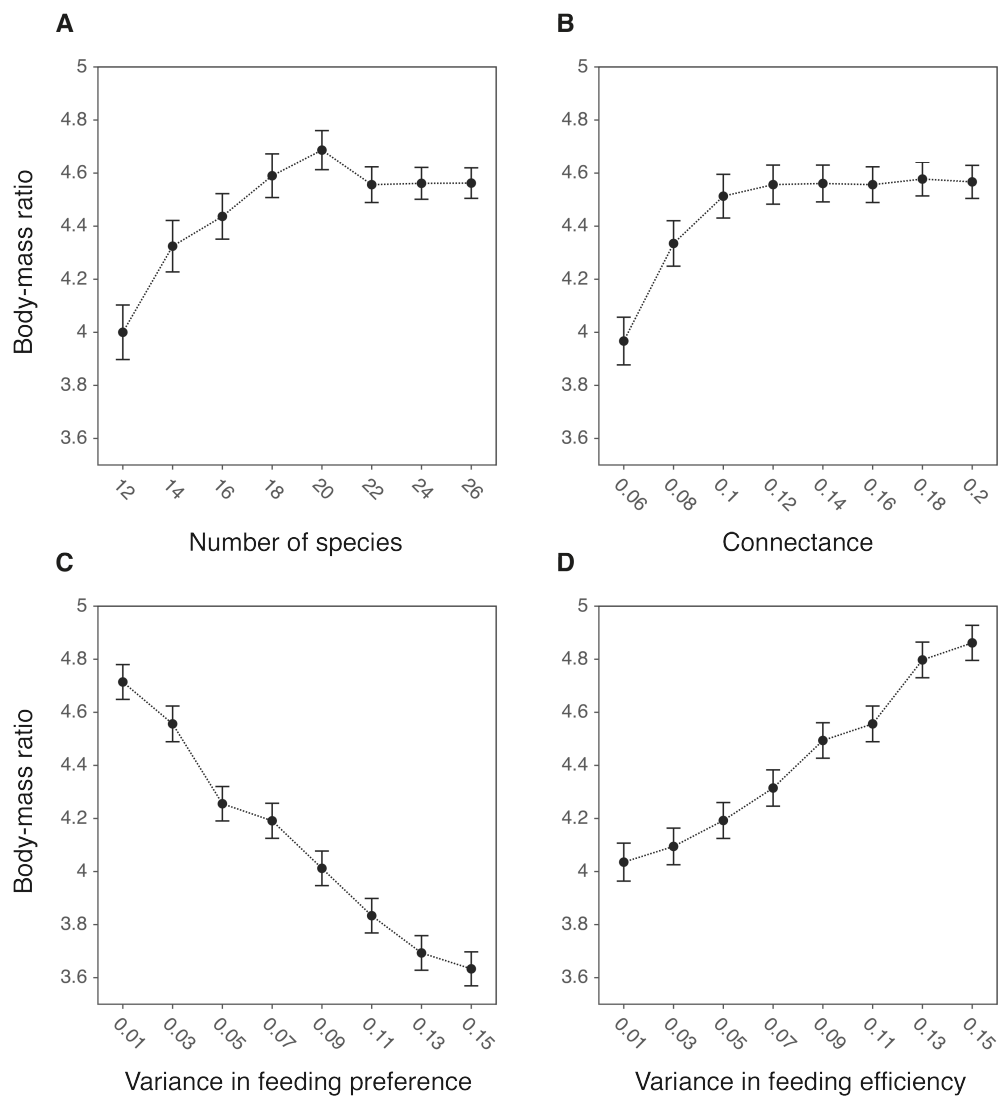


Figure A3.7: Average body-mass ratio as observed in data sets of 2500 food webs for different network structural properties. Panels (A-D) correspond to the network structural patterns for which results are shown in Fig. 3.4 and Fig. 3.5.

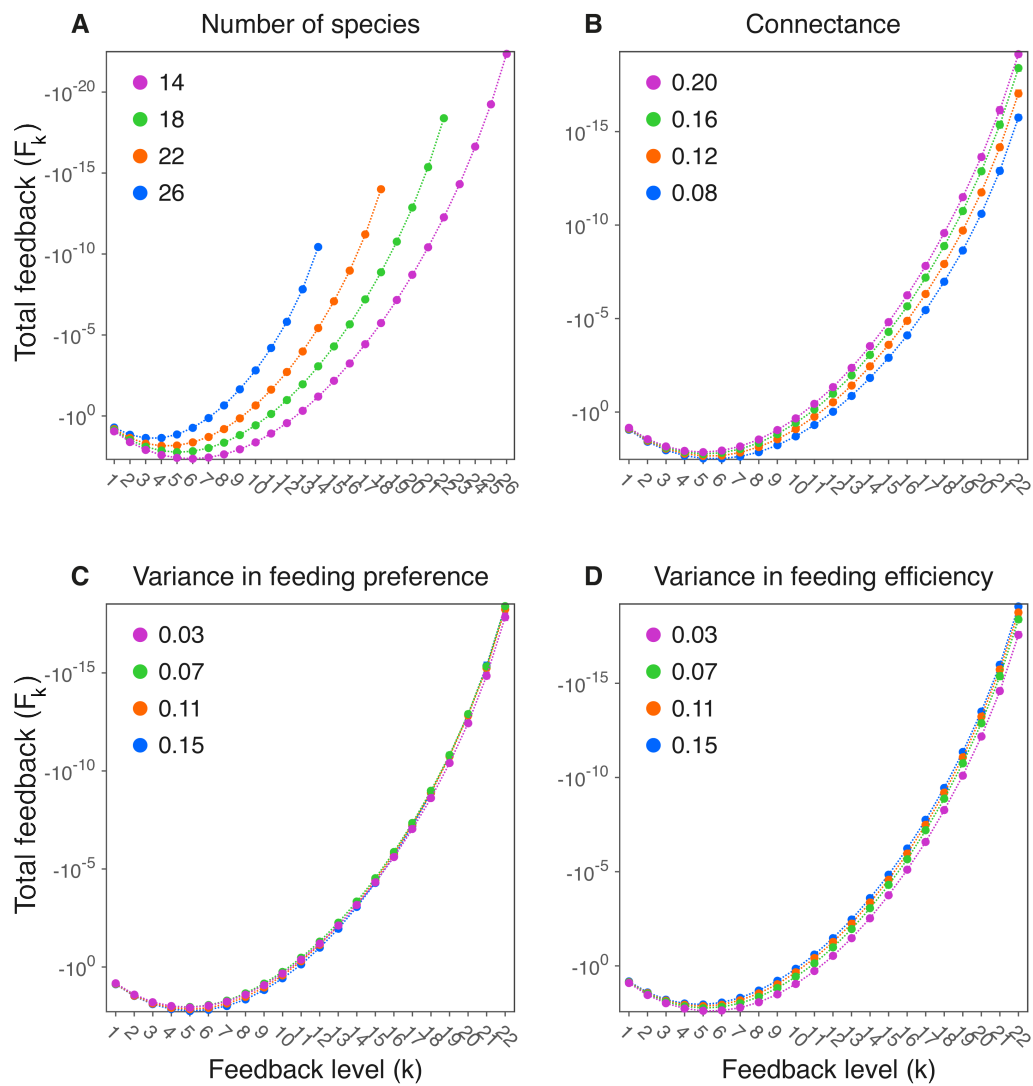


Figure A3.8: Median total feedback as observed in data sets of 2500 food webs for different network structural properties (log-scale). Panels (A-D) correspond to the network structural patterns for which results are shown in Fig. 3.4 and Fig. 3.5.

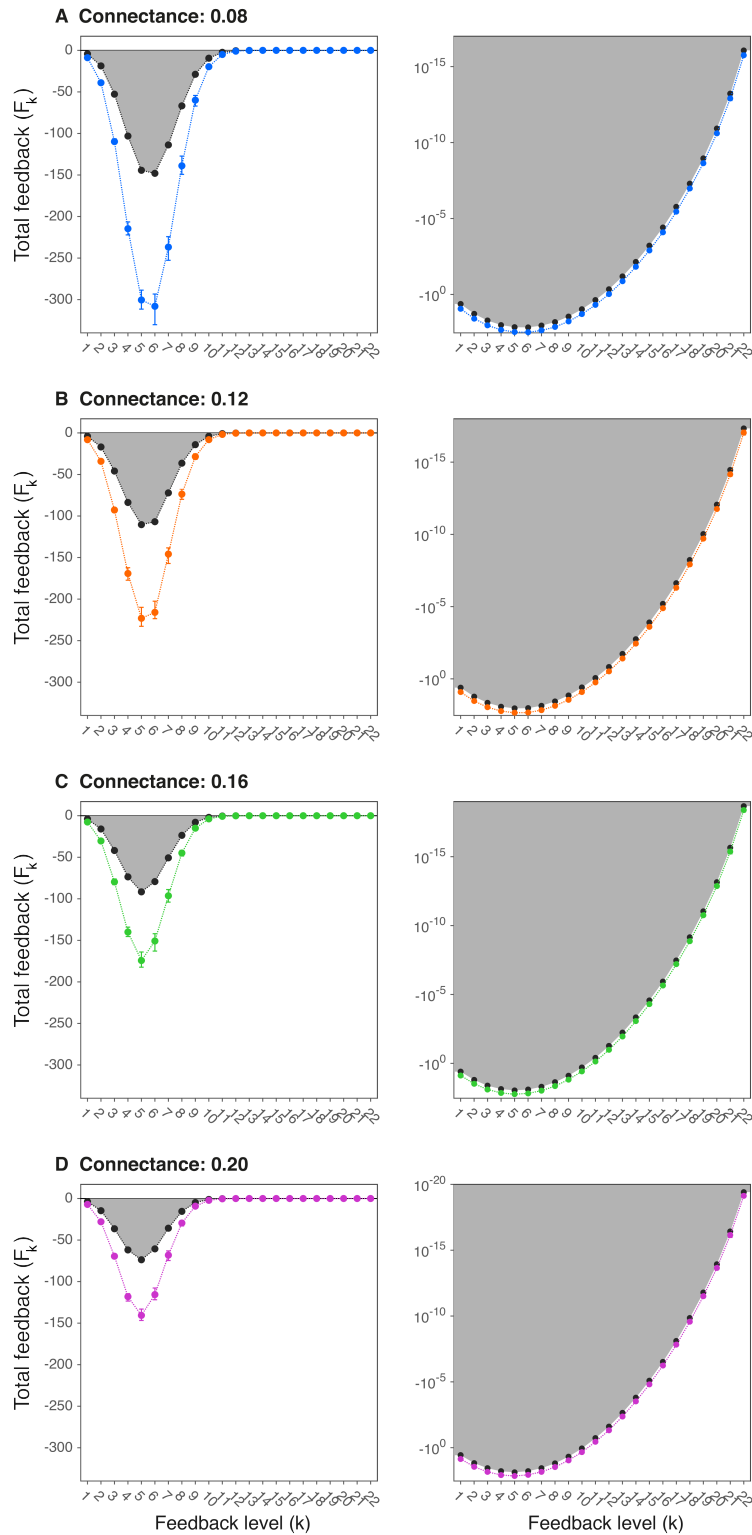


Figure A3.9: The median total feedback, $F_{T,k}$, as observed in data sets of 2500 food webs with a different average connectance, C , and the threshold values, $F_{T,k}$, below which food webs with the same total-feedback distribution become unstable. As in Fig. 3.6.A-B, results are shown for data sets with an average directed connectance of 0.08 (A), 0.12 (B), 0.16 (C), and 0.20 (D). Grey areas indicate unstable areas. Colored lines indicate the observed median total feedback on different levels k . The total negative feedback is stronger in food webs with a lower connectance and, despite a decline in the strength below which food webs with the same total-feedback distribution become unstable as connectance increases, a larger reduction of total feedback is needed to cause instability in food webs with a low connectance. An increase in feedback levels while maintaining the same distribution did not lead to instability.

Chapter 4

Foreseeing the future of mutualistic communities beyond collapse

J. Jelle Lever,

Ingrid A. van de Leemput,

Els Weinans,

Rick Quax,

Vasilis Dakos,

Egbert H. van Nes,

Jordi Bascompte,

and Marten Scheffer

This chapter is based on: Lever, J.J., Van de Leemput, I.A., Weinans, E., Quax, R., Dakos, V., Van Nes, E.H., Bascompte, J., & Scheffer, M. (2020). Foreseeing the future of mutualistic communities beyond collapse, *Ecology letters*, 23(1), 2-15.

ABSTRACT

Changing conditions may lead to sudden shifts in the state of ecosystems when critical thresholds are passed. Some well-studied drivers of such transitions lead to predictable outcomes such as a turbid lake or a degraded landscape. Many ecosystems are, however, complex systems of many interacting species. While detecting upcoming transitions in such systems is challenging, predicting what comes after a critical transition is terra incognita altogether. The problem is that complex ecosystems may shift to many different, alternative states. Whether an impending transition has minor, positive or catastrophic effects is thus unclear. Some systems may, however, behave more predictably than others. The dynamics of mutualistic communities can be expected to be relatively simple, because delayed negative feedbacks leading to oscillatory or other complex dynamics are weak. Here, we address the question of whether this relative simplicity allows us to foresee a community's future state. As a case study, we use a model of a bipartite mutualistic network and show that a network's post-transition state is indicated by the way in which a system recovers from minor disturbances. Similar results obtained with a unipartite model of facilitation suggest that our results are of relevance to a wide range of mutualistic systems.

4.1 INTRODUCTION

Empirical studies of lakes, arid ecosystems, coral reefs, and tropical forests suggest that remarkably sudden transitions to alternative stable states may occur when changing environmental conditions pass a critical value (Scheffer et al. 1993; Rietkerk & Van de Koppel 1997; Scheffer et al. 2001; Hirota et al. 2011). While the outcome of such transitions is relatively predictable when a few leading species or species groups determine the state of an ecosystem, this may not be the case when ecosystem dynamics are determined by many interacting species. Species traits as well as their sensitivity to changing conditions are known to be highly diverse, and many drivers of environmental change are known to have multiple simultaneous effects on species communities. A change in climate may, for example, affect the distribution, phenology, physiology, behavior, and relative abundances of species, and these changes may, in turn, affect the strengths of interactions between species (Kareiva et al. 1993; Memmott et al. 2007; Suttle et al. 2007; Tylianakis et al. 2008; Burkle et al. 2013; Høye et al. 2013; Usinowicz & Levine 2018). The specific ways in which interactions are arranged in complex ecological networks are known to be crucial for the stability of ecosystems (Kareiva et al. 1993; De Ruiter et al. 1995; McCann 2000; Solé & Montoya 2001; Neutel et al. 2002; Montoya et al. 2006; Bastolla et al. 2009; Rohr et al. 2014). Gradual changes in these patterns and other complex simultaneous effects of changing environmental conditions may therefore lead to regime shifts of which the outcomes are highly unpredictable (Scheffer et al., 2012).

The response of ecosystems to a change in environmental conditions is determined by the relative strengths of positive and negative feedback loops in the networks of interactions between species or between species and their environment. Immediate negative feedbacks, e.g. due to intraspecific competition, have stabilizing effects, while positive or ‘reinforcing’ feedbacks are destabilizing and a necessary condition for the existence of alternative stable states (Thomas 1981; Snoussi 1998; Gouzé 1998). Critical transitions towards such states may occur when changing conditions alter a system’s feedbacks such that destabilizing, positive feedbacks gain in strength relative to stabilizing, immediate negative feedbacks. A classic example is found in shallow lakes where an increase in algae leads to an increased turbidity and the suppression of aquatic plants. As a consequence, more nutrients become available to algae which enhances algae growth. A clear-water, plant-dominated state may therefore switch to a turbid, algae-dominated state when gradually increasing nutrient levels pass a critical value. Recovery from such transitions requires a relatively large reduction in nutrient availability, a phenomenon called ‘hysteresis’ (Scheffer et al. 1993). Other examples of such switching behavior are found in coral reefs, woodlands, deserts, and oceans (May 1977; Wilson & Agnew 1992; Scheffer et al. 2001), as well as in many other systems such as the climate (Hare & Mantua 2000; Scheffer et al. 2001; Clark et al. 2002; Alley et al. 2003; Lenton et al. 2008), the economy (Diamond & Dybvig 1983; Arthur 1989; Easley & Kleinberg 2010), and human cells (Hasty et al. 2002; Ferrell Jr 2002; Lee et al. 2002; Tyson et al. 2003; Angeli et al. 2004).

Mutually beneficial interactions are, perhaps, the most intuitive examples of positive feedback loops in complex ecological networks, metapopulations, or other complex environmental systems. Previous studies have emphasized the importance of such interactions in communities of flowering plants and animal pollinators or seed dispersers (Jordano, 1987; Bascompte et al., 2003). Mutually beneficial interactions between zooxanthellae, coral species and invertebrates occur in coral reefs where a diversity of coral species provide food, shelter and reproduction sites for other organisms (Moberg & Folke 1999; Wilson et al. 2006; Stella et al. 2011). Nutrient exchange with mycorrhizal fungi and nitrogen-fixing bacteria is fundamental for plant communities (Kiers et al. 2011), and mutualistic interactions are of importance for microbial communities where multiple species are involved in the degradation of organic substrates (Schink 2002; Stolyar et al. 2007). Indirect facilitation may occur between plant species when modifying harsh environments (Wilson & Agnew 1992; Callaway 1995; Holmgren et al. 1997; Rietkerk et al. 2004), and the exchange of individuals between habitat patches may be fundamental for metapopulations (Hanski 1998). Previous work suggested that critical transitions may occur due to the positive feedback resulting from such mutually beneficial relationships in plant-pollinator communities because a decline in pollinator abundances may negatively affect plant abundances, which in turn is bad for pollinators (see **Chapter 2**). Similar transitions may occur in metapopulations due to a ‘rescue effect’ (Hanski 1998) and in facilitative communities due to an ‘Allee effect’ (Rietkerk et al. 2004; Courchamp et al. 1999; Stephens et al. 1999). The observation that the relative strength of facilitative interactions tends to increase with environmental stress (Bertness & Callaway 1994; Maestre et al. 2009; Tur et al. 2016), suggests that competitive communities may become increasingly mutualistic as conditions change. The aforementioned positive feedbacks and associated critical transitions may thus also occur in communities where mutually beneficial interactions were not particularly strong under more advantageous conditions.

Here, we propose a new class of indicators that may allow us to detect the specific way in which species are affected by an increase in the relative strength of a positive feedback prior to a critical transition. The essence of our approach is that we seek the direction in a system’s phase space, i.e. a multidimensional space in which each axis corresponds to the abundance of a species, in which a system becomes increasingly sensitive to small subcritical disturbances. Earlier studies have shown that an increasingly slow recovery from small disturbances may be indicative of a loss of resilience prior to critical transitions (Wissel 1984; Van Nes & Scheffer 2007). Various indicators of this phenomenon known as ‘critical slowing down’ may therefore serve to detect an increase in the likelihood of critical transitions (Scheffer et al. 2009; Dakos et al. 2012). Here, we take advantage of the fact that resilience is not lost equally in all directions. Disturbances have a size (i.e. the total amount of change) and a direction (i.e. the relative amount of change in each species). The more similar a disturbance’s direction to the direction in which increasingly small perturbations may cause critical transitions, the stronger the effect of critical slowing

down. Provided that there are no oscillatory, chaotic or other complex dynamics, a system's future state will most likely lie in the same approximate direction.

To get an intuitive understanding of the principle behind our approach, consider a small plant-pollinator community of which the dynamics can be represented by a landscape of valleys, hills and ridges (Fig. 4.1.A and Appendix A4.2 in Supporting Information). In this landscape, every possible combination of pollinator abundances is represented by a unique point, while the speed and direction in which abundances change corresponds roughly to the slope of the landscape. The lowest points of the landscape's valleys or 'attraction basins' represent alternative stable states. As conditions change, the shape of the landscape changes and new basins appear. When a threshold comes close to the network's initial state, a small perturbation in the right direction can invoke a transition into another attraction basin. Eventually, the basin around the network's initial state disappears altogether and the system inevitably shifts into one of the alternative basins. The question we ask is whether we may know beforehand to which of the alternative attractors a system will most likely shift. The clue is that the slope of the initial state's attraction basin changes in a characteristic way before the transition occurs. A 'mountain pass' towards the system's future state is formed, marked by a 'saddle point' in the landscape. The initial state's attraction basin becomes increasingly shallow in the direction of this pass and the recovery from perturbations increasingly slow (Fig. 4.1.B-C and Fig. A4.2). This direction is what we refer to as the 'direction of critical slowing down' and is indicative of the relative gain or loss in abundance of each species after an impending critical transition.

To explore whether the direction of critical slowing down might be indicative of the future state of mutualistic communities, we use a model of a bipartite mutualistic network in which critical transitions are known to occur (see **Chapter 2**, Dakos & Bascompte 2014; Jiang et al. 2018). This model was originally developed to describe the interactions between flowering plants and animal pollinators or seed dispersers (Bastolla et al. 2009), but may describe any system characterized by competition within and cooperation between species groups. Previous work has shown that indirect facilitation occurs between pollinators when they interact with the same plant species (Moeller 2004; Ghazoul 2006; Bastolla et al. 2009). This indirect facilitation makes a network more resilient, i.e. the minimum size of perturbations or the amount of change in environmental conditions needed to cause a critical transition is larger. When pollinators continue to facilitate each other under increasingly harsh environmental conditions they may, however, also collapse simultaneously because they depend on each other for survival (see **Chapter 2**).

We generate time series in which the resilience of a network's initial state is gradually undermined by altering the relative strength of mutualistic interactions. Oscillatory, or other complex dynamics occurring after a threshold is passed may negatively affect the performance of the here proposed class of indicators but are unlikely in purely mutualistic

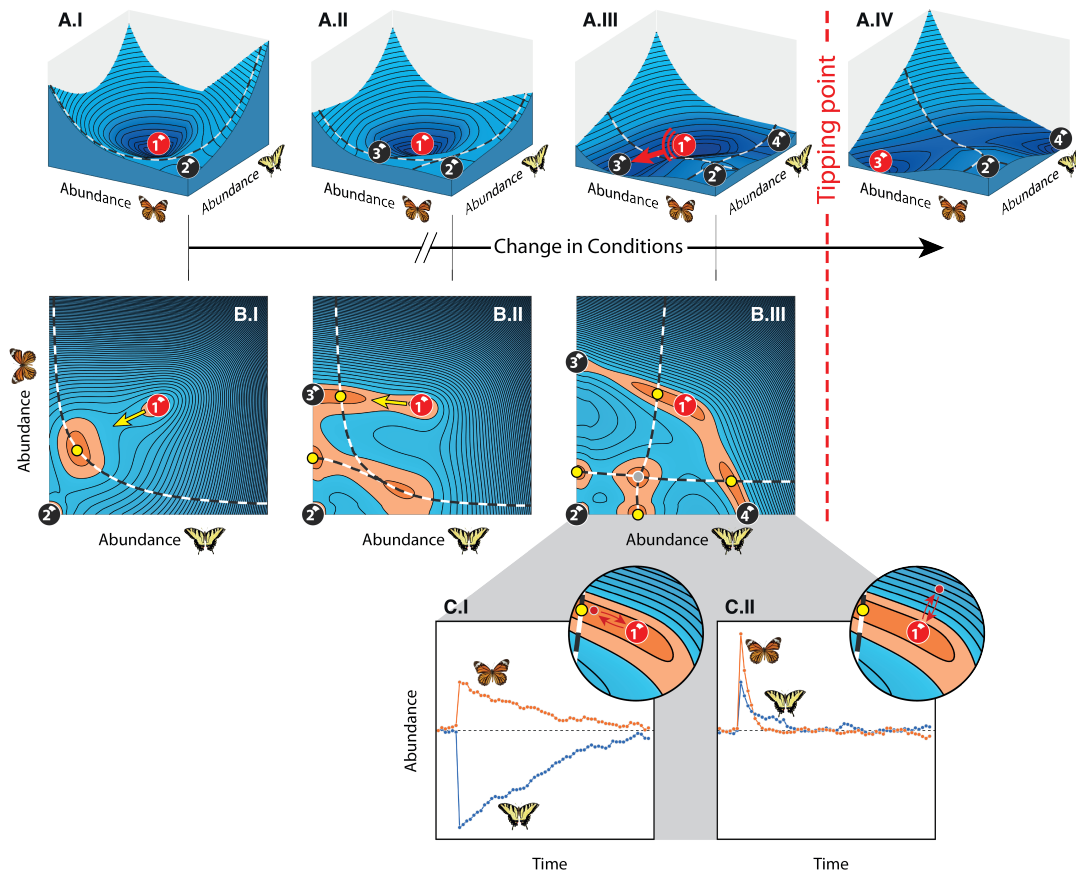


Figure 4.1: Stability properties for a small network of two pollinators (shown) and two plants (not shown). **(A)** Attraction basins (valleys) of alternative stable states (balls) are separated by thresholds (dashed curves). Initially, the only alternative to pristine state 1 is fully collapsed state 2 (A.I). When conditions change, two additional, partially collapsed states appear (states 3 and 4). The initial, pristine state loses resilience after state 3 appears (A.II-A.III). Eventually, the threshold towards state 3 approaches the pristine state so closely that a critical transition towards this state becomes inevitable (A.III-A.IV). **(B)** Alternative stable states, saddle points (yellow dots), and hilltops (grey dots) are surrounded by areas in which the landscape's slope, and thus the rate at which abundances change, is nearly zero (indicated in orange). Higher speeds are found further away from these points. The direction of slowest recovery changes substantially before future state 3 appears (yellow arrow, B.I-B.II). After state 3 appears, the system slows down in the direction of the saddle point on the approaching threshold (B.II-B.III). **(C)** Slow recovery from a perturbation towards the saddle point (C.I) as opposed to the much faster recovery from an equally large perturbation in another direction (C.II).

systems, i.e. systems in which all interspecific interactions are positive, because they require at least one delayed negative feedback, i.e. a negative feedback with a time lag, usually occurring as the result of an uneven number of negative interactions in feedback loops of two or more species (Levins 1974; Thomas 1981; Puccia & Levins 1985; Goldbeter

1996; Hastings & Powell 1991; Snoussi 1998; Gouzé 1998; McCann et al. 1998; Dambacher et al. 2003). Few real ecosystems can, however, be expected to be purely mutualistic. Different scenarios are therefore explored, varying from a scenario where positive feedbacks are the only cause of instability, i.e. in purely mutualistic systems, to scenarios in which the destabilizing effects of delayed negative feedbacks are stronger, i.e. in mixed systems with mutualistic and competitive interactions. To determine the direction of critical slowing down, we study changes in the fluctuations around the species mean abundances and determine whether they can be used to predict a network's post-transition state. To explore whether the results obtained with this model may hold for a wider class of mutualistic systems, we investigate whether similar results are obtained with a more general, unipartite model of competition and facilitation between species.

4.2 COMMUNITY MODEL

We use a dynamic model describing the interactions between two types of species: plants (P) and pollinators (A). As in Bastolla et al. (2009), species of the same type compete with each other, while species belonging to a different type interact mutualistically. The dynamics of species i belonging to a group of $S^{(A)}$ pollinator species are as follows:

$$\frac{dN_i^{(A)}}{dt} = \frac{R_i(N^{(P)})}{1 + h_i R_i(N^{(P)})} N_i^{(A)} - \sum_{j=1}^{S^{(A)}} c_{ij} N_j^{(A)} N_i^{(A)} - d_i N_i^{(A)} + \epsilon_i. \quad (4.1)$$

Plant dynamics are described by a similar formula, which can be found by exchanging indices A and P . Unless stated otherwise, this procedure can be applied to all formulas in this chapter.

Species i has abundance N_i , which may increase due to mutualistic interactions with members of the other species type. The rate at which the abundance of species i increases depends on the total amount of resources provided by mutualistic partners, $R_i(N^{(P)})$, i.e. nectar for pollinators and pollen for plants. As in Okuyama & Holland (2008) and Bastolla et al. (2009), we assume that species are limited in their capacity to process resources and become saturated when the amount of resources provided is high. The rate at which species become saturated is determined by saturation term h_i . The total mutualistic benefit, $R_i(N^{(P)})$, depends on the abundance of mutualistic partners as follows:

$$R_i(N^{(P)}) = \sum_{k=1}^{S^{(P)}} \gamma_{ik} N_k^{(P)}, \quad (4.2)$$

in which γ_{ik} is the mutualistic interaction strength, i.e. the rate at which resources become available to species i , due to its interaction with species k .

Species of the same type compete directly amongst each other, e.g. plants for soil nutrients and pollinators for nesting sites. Intraspecific competition, c_{ii} , is assumed to be substantially stronger than interspecific competition, c_{ij} , such that species do not easily outcompete each other. Independent of mutualistic and competitive interactions, several processes may simultaneously enhance or reduce population growth. We assume that the combined effect of these processes is negative, which is incorporated by mortality rate d_i .

Species experience small stochastic perturbations incorporated through noise term ϵ_i :

$$\epsilon_i = \delta_i \frac{dW}{dt}. \quad (4.3)$$

ϵ_i fluctuates in time due to a Wiener process, W , with mean zero and standard deviation δ_i . The Wiener process is a continuous-time stochastic process generating white noise. To prevent noise leading to negative abundances, we assume that $dN/dt = 0$ when $N < 0.001$.

Coexistence and relative mutualistic benefits

As the number of species and/or the strength of interspecific competition increases, it becomes increasingly difficult to assign parameters such that all species may stably coexist. In previous work, a trade-off was assumed between the number and the strength of mutualistic interactions which prevented species with many interactions from becoming overly abundant and outcompeting other species (see **Chapter 2**, Bastolla et al. 2009; Dakos & Bascompte 2014; Jiang et al. 2018). Here, we assume mutualistic interaction strengths to vary continuously, i.e. pollinators may interact with all plant species and vice versa, which allows us to explore gradual changes in interaction structure beyond the fixed structure of a predefined mutualistic network. A different kind of balancing relationship is therefore required, and mutualistic interaction strengths, γ_{ik} , are determined as follows:

$$\gamma_{ik} = \frac{\theta_{ik} R_i(\hat{N}^{(P)})}{\hat{N}_k^{(P)}}, \quad (4.4)$$

in which the relative mutualistic benefit, θ_{ik} , corresponds to the fraction of the total amount of resources provided by species k , and $R_i(\hat{N}^{(P)})$ to the total amount of resources received by species i at the system's nontrivial equilibrium, i.e. the equilibrium point at which all species have a non-zero abundance. There are different costs and benefits associated to different feeding strategies, e.g. being a specialist or a generalist or interacting

with specialists or generalists (Morales & Traveset, 2008; Tur et al., 2016). This way of assigning mutualistic interaction strengths makes sure that a species' total amount of resources received is independent from a species' relative feeding preferences, i.e. we assume the sum of these costs and benefits to be approximately the same for each strategy. The sum of a species' relative mutualistic benefits, $\sum_{k=1}^{S^{(P)}} \theta_{ik}$, is one. A change in relative mutualistic benefits does not affect the equilibrium abundances of species, because the total amount of resources provided to each species remains the same (see Appendix A4.5).

Changing environmental conditions and the direction in which resilience is lost

To test whether the direction of critical slowing down is indicative of a system's future state, we study our ability to predict a system's future state when changing conditions lead to substantial changes in the strength of positive feedbacks and the direction in which they have destabilizing effects. Such changes may occur when changing conditions fundamentally alter the ways in which species relate to each other.

Positive feedbacks and the direction in which resilience is lost can be studied when determining the elements of the Jacobian matrix at a system's nontrivial equilibrium. Each element in this matrix describes how a change in the abundance of species i affects the growth of species j , dN_j/dt . At a tipping point, the dominant eigenvalue of the Jacobian matrix is zero and the slope of the direction in which a system recovers slowest from perturbations is indicated by the eigenvector corresponding to this eigenvalue. The strength of the positive feedback between pollinator i and plant j can be determined by multiplying the Jacobian's off-diagonal elements; $\alpha_{ij} * \alpha_{ji}$. In a two-species system, a tipping point is reached when the strength of this feedback is equal to the multiplication of the two direct negative feedbacks; $\alpha_{ii} * \alpha_{jj}$. Similar relationships can be obtained when studying larger systems (Levins 1974; Thomas 1981; Puccia & Levins 1985; Goldbeter 1996; Snoussi 1998; Gouzé 1998; Dambacher et al. 2003; De Ruiter et al. 1995; Neutel et al. 2002; Neutel & Thorne 2014).

Some species contribute more to the instability caused by positive feedbacks than others. The effect of a temporary change in the abundance of mutualistic partners, as described by the Jacobian matrix, for example, is small when species are highly saturated, i.e. $R_i(\hat{N}^{(P)})$ and/or h_i is large. Positive feedbacks are therefore weak and the resilience of the here studied networks is high when relative mutualistic benefits, θ_{ik} , are distributed such that most resources are obtained from the same, highly saturated species (see Appendix A4.1 and Fig. A4.1). In more complex communities such a distribution resembles a nested structure as is commonly observed in mutualistic networks, as in those networks species tend to obtain resources from the same mutualistic partners as well (Bascompte et al. 2003 and Fig. A4.6.A). The interrelationships between saturated and non-saturated species are

asymmetrical as in Bascompte et al. (2006).

As a starting point for further research, we explore a scenario in which a change in the aforementioned distribution of relative mutualistic benefits, θ_{ik} , undermines the resilience of the mutualistic networks while keeping all other properties, e.g. nontrivial equilibrium abundances and the negative effects of inter- and intraspecific competition, constant (see Appendix A4.5). Increasingly strong positive feedbacks emerge when two or more non-saturated species start to interact increasingly strongly with each other. Eventually, this will lead to a full or partial network collapse depending on the specific way in which relative mutualistic benefits are changed. Conditions, M , affect relative mutualistic benefits as follows:

$$\theta_{ik}^* = \theta_{0,ik} + (\theta_{final,ik} - \theta_{0,ik})M, \quad (4.5)$$

in which $\theta_{0,ik}$ is the initial, $\theta_{final,ik}$ the final, and θ_{ik}^* the actual relative mutualistic benefit. Conditions, M , change from zero to one over time, t , such that $dM/dt = 1/T$, in which T is the total simulation time. Mutualistic interaction strengths, γ_{ik} , are updated as described in equation 4.4. The species and interactions involved in the positive feedback leading to a critical transition, the direction in which this feedback amplifies change, and the nature of a system's future state, are determined by the specific way in which interactions are altered.

In addition to the scenario in which only the relative mutualistic benefits change, we explore scenarios in which the nontrivial equilibrium abundances of species change as well due to a change in the total amount of resources received from mutualistic partners (see Appendix A4.5).

Determining the direction of critical slowing down

Although measuring the recovery rate from experimental perturbations is the most direct way to determine the direction of critical slowing down, an experimental approach may be impractical or even impossible when studying complex networks. The development of alternative methods to determine the direction of critical slowing down is therefore of importance. Previous studies suggested that small changes in the statistical properties of time series, e.g. an increase in variance, autocorrelation, skewness, and spatial correlation, may be used as an indicator of a change in the proximity to a tipping point (Scheffer et al. 2009; Dakos et al. 2012). Here, we explore whether changes in the statistical properties of time series may be used to predict the future state of mutualistic communities.

When assuming a continuous regime of random perturbations, a system will spend most time away from its equilibrium state in the direction in which it recovers slowest from perturbations (see Appendix A4.2). When approaching a tipping point, the distribution

of natural fluctuations around the species' mean abundances should therefore become increasingly elongated in the direction in which a system slows down (Fig. A4.3). To detect such change, we analyze our model-generated time series by determining the direction and magnitude of such asymmetry in a rolling window. This window has a fixed size and is moved along the time series as new data become available. To determine the direction in which abundances are distributed asymmetrically, we use a principal component analysis of which the first principal component corresponds to the line in the network's phase space along which variance is highest (see Held & Kleinen 2004; Chen et al. 2012; Suweis & D'Odorico 2014; Dakos 2018 and Chen et al. 2019 for related approaches). Abundances are distributed asymmetrically either in an up- or downward direction along this component. To determine the direction of our indicator, we orthogonally project the time series on the first principal component and determine the direction in which the projected time points are skewed (Fig. A4.4.A-E). The magnitude of the indicator is determined by the fraction of the total variance explained by the first principal component. This direction and magnitude together form a vector which is our indicator of a network's future state (Fig. A4.4.F).

A network's phase space has as many axes as there are nodes in a network. Our indicator thus has multiple components; one for each species (Fig. A4.4.F). Each component, or 'score on the indicator', gives an indication of the extent and direction in which the abundance of each individual species is distributed asymmetrically. The indicator accurately points towards the future state when its components, or 'scores', are directly proportional to the difference in abundance between a network's initial and future state. Species with a negative score are expected to decrease, while species with a positive score are expected to increase. Species with a relatively large score are expected to change more in abundance than species with a comparably smaller score. An increase in the indicator's magnitude is reflected by more extreme (positive or negative) scores.

To assess the quality of the prediction, we determine the angle between the indicator's slope, as determined by the first principal component, and the direction of the observed shift in abundance. As a measure of similarity, we take one minus the probability that the angle between two unrelated, random vectors is smaller (see Appendix A4.3). We consider the indicator's slope to be accurate when this measure of similarity is above 0.99. When time points are also skewed towards a network's future state, we consider the prediction to be fully accurate.

Simulations and parameter settings

We analyze several data sets consisting of 1000 model-generated time series in which the above described mutualistic networks approach a tipping point. For each time series, we compute the change in direction and magnitude of the indicator on the pollinator abundances (see Appendix A4.4). The distribution from which interspecific competitive

interaction strengths are sampled, the number of plant and pollinator species, and the way in which changing conditions affect nontrivial equilibrium abundances differ among data sets (see Appendix A4.5). The resilience of mutualistic networks is, in all cases, undermined by a change in the distribution of mutualistic benefits leading to a substantial increase in the relative strength of positive feedbacks or delayed negative feedbacks. Declining abundances may have an additional negative effect on resilience.

To explore the effects of oscillatory, chaotic or other complex dynamics, we analyze data sets of which the strength and variability in interspecific competitive interaction strengths, c_{ij} , varies. Delayed negative feedbacks become stronger as the strength and variability of interspecific competition increases. To provide a clue as to how (un)likely it is to find transitions to oscillatory, chaotic or other complex dynamics, we determine for each time series whether the system approaches a Hopf or a saddle-node bifurcation.

Networks were discarded from a data set when they were unstable at initial conditions, $M = 0$. We determined the frequency at which this occurred as a measure of how difficult it is to find a stable solution. The final distribution of relative mutualistic benefits, $\theta_{final,ik}$, was redrawn either when a network would become unstable within the range of conditions $M = (0, 0.5)$, or when a network would still be stable at $M = 1$.

A more general, unipartite model of competition and facilitation

To explore whether the indicator may work for a wider class of systems, we investigate whether similar results are obtained with a more general model of competition and facilitation. The positive feedback between plants and pollinators in the previously described communities can be seen as an Allee effect, i.e. a positive relationship between the growth and density of populations (Courchamp et al. 1999; Stephens et al. 1999). The indirect facilitation occurring between pollinators when interacting with the same plant species is not fundamentally different from the facilitation occurring between plant species when ameliorating the same harsh environment, or other forms of interspecific facilitation occurring in ecosystems. The most essential properties of a group of pollinator species may therefore be captured as follows:

$$\frac{dN_i}{dt} = r_i N_i \left(\frac{\sum_{j=1}^S \gamma_{ij} N_j}{A_i} - 1 \right) \left(1 - \frac{\sum_{j=1}^S c_{ij} N_j}{K_i} \right) - d_i N_i + \epsilon_i, \quad (4.6)$$

in which N_i is the abundance of species i . When the abundances of other species and mortality rates, d_i , are zero, species may grow in abundance until they reach carrying capacity K_i , or collapse to extinction when abundances are below critical abundance A_i . The speed at which species abundances change is determined by growth rate r_i . Facilitation is mediated by facilitation rate γ_{ij} . Strong interspecific facilitation allows species

to recover from large disturbances, i.e. below critical abundance A_i . Species with a high critical abundance A_i depend strongly on this facilitation, and a community's overall resilience is highest when such species are facilitated relatively strongly by species with a low A_i . The relative strength of interspecific competition is determined by c_{ij} . Other causes of abundance loss are incorporated through mortality rate d_i . Species are assumed to experience small stochastic perturbations, as in the bipartite mutualistic network model, through noise term ϵ_i .

The main difference between the here presented model and the previously described plant-pollinator model is that it is a unipartite model, i.e. it describes one set of interacting species. The means by which facilitation occurs are, in contrast to the above described plant-pollinator model, not explicitly described. Parameter settings and results can be found in Appendix A4.6 and A4.7.

4.3 RESULTS

We found that, when interspecific competitive interaction strengths are weak, instability nearly always arises from the positive feedback between plants and pollinators or from the Allee effect in the above described mutualistic or facilitative communities. Instability is caused by a saddle point approaching the communities' initial state and at least one species will collapse to extinction when a tipping point is passed. Other species may either gain or lose in abundance depending on the communities' initial properties and the way in which they are affected by changing environmental conditions (Fig. 4.2.A). Critical transitions were nearly always preceded by a period in which the indicator's magnitude would increase significantly, indicating that the distribution of fluctuating species abundances becomes increasingly asymmetric (see Appendix A4.7, Fig. 4.2.B-D and Fig. A4.7-A4.9). As with the small mutualistic network in Fig. 4.1, the indicated direction typically shifts towards a system's future state at the beginning of this period. The indicator thus consistently pointed towards a community's future state while increasing in magnitude prior to a critical transition, when interspecific competitive interactions were weak.

A notable exception to this general pattern occurred when competitive interaction strengths were taken from a low to intermediate range, e.g. $\sim U(0.02, 0.08)$. We found that, for such a range, full network collapses were not always indicated accurately. Transitions would lead either to the collapse of relatively few species or to a collapse of the entire network (Fig. A4.9). Both the inaccurate prediction of full network collapses and the absence of intermediate-size, partial network collapses may occur because critical transitions lead to a series of cascading, partial network collapses. The likelihood of an additional collapse increases as more species collapse (Solé & Montoya 2001; Memmott et al. 2004; Rezende et al. 2007). The most likely outcome of a series of cascading, partial network collapses is therefore a collapse of the entire network. In such a scenario, the indicator will accurately indicate the initial regime shift but will not foresee the cascade of partial net-

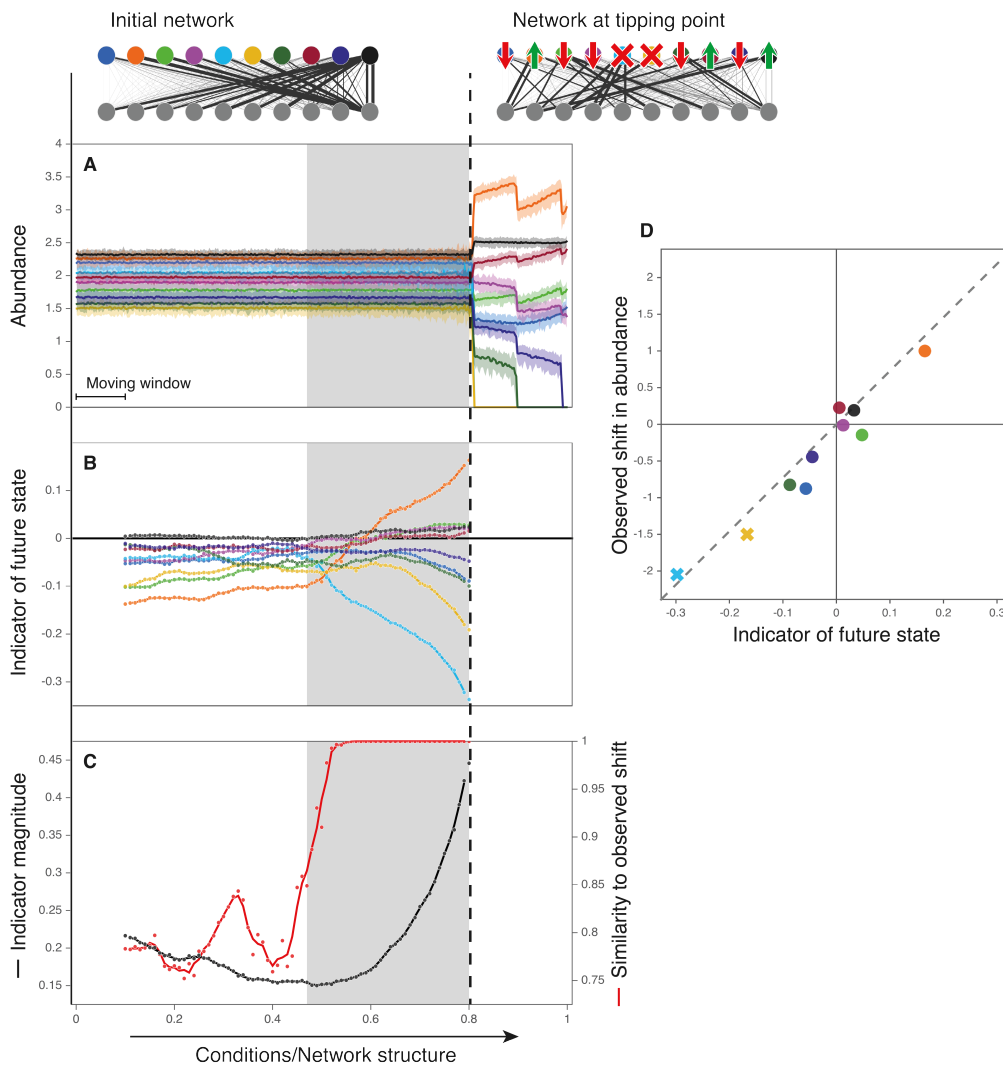


Figure 4.2: Directional slowing down in a mutualistic network as detected by our indicator. **(A)** Time series of species belonging to one part of a bipartite mutualistic network, i.e. the pollinators. At the tipping point two species collapse to extinction (light blue and yellow). **(B)** The indicator of the future state measuring the direction in which fluctuations are distributed asymmetrically. Scores on the indicator indicate the relative predicted gain or loss of each node. **(C)** The magnitude of the indicator, reflecting the extent to which fluctuations are distributed asymmetrically, plotted together with the accuracy measured as the similarity between its direction and the observed shift in abundance. Grey bands indicate the period in which the indicator's magnitude increases significantly. This period likely corresponds to the period in which the network rapidly loses resilience (as in Fig. 4.1.A.II-III). The accuracy increases rapidly at the beginning of this period. **(C)** The observed changes in abundance versus the scores on the indicator just before the tipping point. Extinct species are indicated with crosses. The observed shift is nearly proportional to the scores on the indicator as points are close to a straight line through the origin.

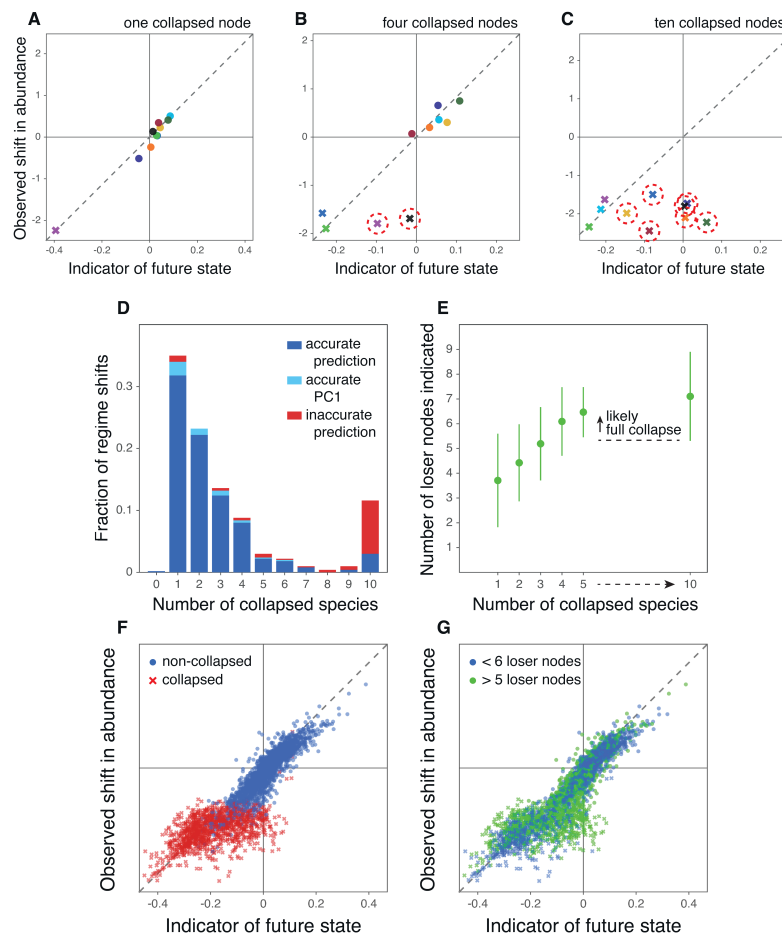


Figure 4.3: Cascading collapses and the indicator's performance when predicting the future state of mutualistic networks. **(A-C)** Examples of the relationship between the scores on the indicator and the observed shifts in abundance when a single, when four, and when all pollinator species collapse to extinction. The change in abundance of winners, losers and two or three collapsed species was almost always accurately indicated. The loss in abundance of additional species collapsing (red circles) was underestimated. **(D)** The fraction of regime shifts after which a certain number species collapsed to extinction. The fraction for which the change in abundance was not accurately indicated is shown in red. Inaccurate predictions (as in panel C) usually occurred prior to a full network collapse. **(E)** Relationship between the number of species collapsing and the number of species with a negative score on the indicator (mean and SD). When the number of species indicated to lose in abundance was high, we were often dealing with a full network collapse. **(F-G)** Combined plots of the 900 best indicated transitions in a data set of 1000 regime shifts. Species remaining after a regime shift (blue dots, panel F) are indicated more accurately than collapsing species (red crosses, panel F). Species of which the loss in abundance prior to a collapse was underestimated usually belonged to networks of which 5 or more species were indicated to lose in abundance (green dots and crosses, panel G). Competitive interaction strengths were taken from a low to intermediate range (i.e. 0.02-0.08).

work collapses immediately following it (Fig.4.3). In some time series, we observed that regime shifts consisted of several consecutive collapses (Fig. A4.10.A-B). The amount of time in between two consecutive collapses can, however, be extremely small. Also when cascades were not clearly visible, we suspect therefore that the inaccurate prediction of a full network collapse is caused by a cascading collapse.

Cascading, full network collapses were uncommon when interspecific competitive interaction strengths were drawn from other ranges (Fig. A4.9). When there is no competition between species, full network collapses are very common, well indicated and do not show signs of being caused by a cascade of partial network collapses (as in Fig. A4.10.C). When competitive interactions are strong, few species tend to collapse to extinction, while most or all other species gain in abundance from a transition. Apart from the specific range from which competitive interaction strengths were drawn, cascading collapses were found to become increasingly common when the noise level increases suggesting that they, in part, result from a low resilience of a system's future state (Fig. A4.11-A4.12). A relatively large number of species was usually indicated to lose in abundance when a, likely, cascading collapse occurred (e.g. 7 out of 10 on average, Fig. 4.3.E). As an alternative indicator of the likelihood of a cascading, full network collapse we propose therefore to use the number of species indicated to lose in abundance.

As the strength and variability of interspecific competition increases, Hopf bifurcations, leading to oscillatory, chaotic or other complex dynamics, become increasingly common. After such transitions, the system remains highly sensitive to small-scale stochastic perturbations and may end up in any of several potential future states (Fig. 4.4.A-B, and Fig. A4.13-A4.15). To which of these states a system will shift is determined by chance and thus hard to predict. For the highest competition level we tested, we found that such hard-to-predict regime shifts made up about 60% of a data set. Higher levels were not tested because, as the strength of competition increases, it becomes increasingly difficult to generate networks of which the initial, nontrivial state is stable. More specifically, we found that the probability of a network to be stable at initial conditions, $M = 0$, is nearly one when interspecific competitive interaction strengths were taken from the aforementioned lower ranges and below 0.01 when they were taken from the highest here reported range (Fig. A4.16). The indicator accurately indicated about 50% of the regime shifts in this 'worst-case scenario' (some of the hard-to-predict regime shifts were indicated accurately). When there is no competition between species, this percentage was nearly 100% (Fig. 4.4.C-D).

Qualitatively similar results were found when, in addition to a change in relative mutualistic benefits, the species' nontrivial equilibrium abundances changed as well (see Appendix A4.7 and Fig. A4.17). Full network collapses are more frequent when abundances tend to decrease and the period in which the indicator's magnitude increases prior to a critical transition tends to be somewhat shorter when abundances change over time. The exam-

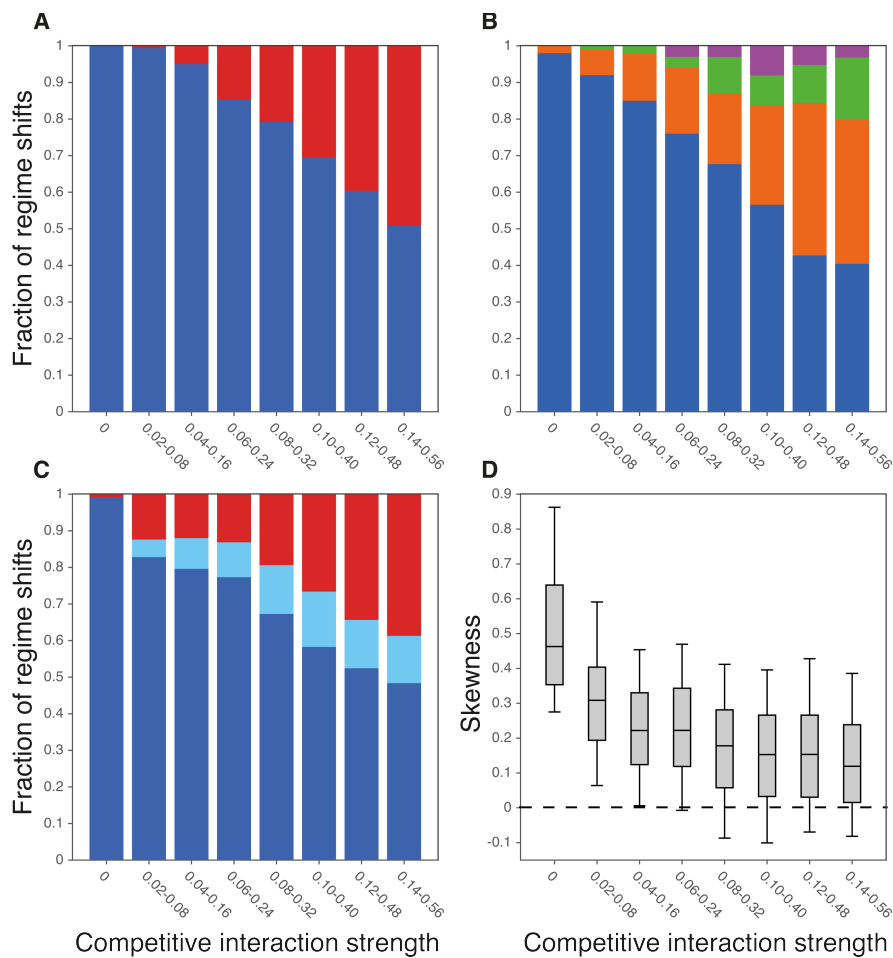


Figure 4.4: Hopf bifurcations and the predictability of a network's future state when sampling competitive interaction strengths from different parameter ranges (ranges are indicated on the x-axis). As the strength and variability of competition increases, Hopf bifurcations become increasingly frequent as well as the number of networks of which the future state is determined by chance. **(A)** The frequency of saddle-node (blue) and Hopf bifurcations (red) for different data sets. A high frequency of Hopf bifurcations indicates that transitions towards oscillatory, chaotic or other complex dynamics are common. **(B)** The fraction of cases in which, after five simulations in which a network's resilience was undermined in the exact same way, a network would always shift to the same state (blue), to one out of two states (orange), to one out of three states (green), or to one of four or more potential future states (purple). **(C)** The fraction of accurately indicated regime shifts (dark blue), the fraction accurately indicated by the first principal component, i.e. the slope of the indicator is accurate, but not by the direction in which time points are skewed (light blue), and the fraction of inaccurately indicated regime shifts (red). **(D)** The skewness of time points projected on the first principal component. A positive skewness means that time points are skewed in the direction of a network's future state. The skewness is shown for regime shifts that were accurately indicated by the first principal component.

ples in Fig. A4.18-A4.20 suggest that the direction of the first principal component is initially determined by the way in which abundances change over time. It may, therefore, take longer before the direction in which abundances are distributed asymmetrically is determined by the direction of critical slowing down. The application of a detrending method may prolong this period when trends are strong.

Qualitatively similar results were also found when analyzing data sets of communities with different numbers of species (see Appendix A4.7). Full network collapses became less common as the number of species increased, and Hopf bifurcations leading to oscillatory, chaotic or other complex dynamics became more frequent (Fig. A4.21-A4.22). These changes occurred, most likely, due to a change in the balance between intra- and inter-specific competition. Interaction strengths were assigned such that the relative difference between intra- and interspecific competitive interaction strengths remained approximately the same (see Appendix A4.5). The number of interspecific competitive interactions, however, increases as the number of species increases. The combined effect of all interspecific competitive interactions is therefore larger. Systems with many species may, due to the way in which we assigned competitive interaction strengths, therefore be comparable with smaller networks in which interspecific competition is relatively strong.

Simulations with the more general, unipartite model of facilitation between species gave roughly the same qualitative results as the bipartite plant-pollinator model (see Appendix A4.7). The resilience of communities of 10, 20 and 40 species was generally a bit lower than the resilience of plant-pollinator networks with the same number of plant and pollinator species. To prevent networks from collapsing almost immediately, we chose a lower noise level with standard deviation $\delta_i = 0.05$. A relatively low resilience may also explain the relatively high frequency of likely cascading collapses in facilitative communities of 10 species (Fig. A4.23). A different way of assigning critical abundances, A_i , could have increased the resilience of the here studied facilitative communities.

4.4 DISCUSSION

Human activities alter the Earth's climate and its ecosystems at unprecedented rates (Vitousek et al. 1997; Millenium Ecosystem Assessment 2005; Rockström et al. 2009; Intergovernmental Panel on Climate Change 2014; Steffen et al. 2015). These changes may jumble the patterns in the networks of interactions between species that hold complex species communities together (Kareiva et al. 1993; McCann 2007; Tylianakis et al. 2008). Monitoring and forecasting the effects of such changes thus requires a systems approach, i.e. an approach that explicitly studies the properties emerging from the complex and often unknown ways in which species relate to each other. Here, we try to make a further step towards developing such an approach by determining the direction in which destabilizing positive feedbacks undermine resilience. With model-generated time series we show that this direction is indicative of the future state of mutualistic communities,

potentially providing us with a tool to assess the impact of impending critical transitions in natural communities and other complex systems.

Ecologists have emphasized the importance of improving our ability to predict the future state of ecosystems previously, and predicting future developments in complex systems is common practice in various fields of research, e.g. economics, engineering, and climatology (Clark et al. 2001; Sutherland 2006; Coreau et al. 2009; Beckage et al. 2011; Novak et al. 2011; Evans et al. 2012, 2013; Purves et al. 2013; Petchey et al. 2015). Concerns about the forecastability of ecosystems and the limits to our capacity to predict the future state of ecosystems have however also been strong (Coreau et al. 2009; Beckage et al. 2011). Some of these concerns stem from a misunderstanding of why predictions are made. Making predictions is fundamentally different from describing a scientific law. Predictions are made when a limited amount of knowledge is available, and people rely on predictions even when they are known to often be inaccurate simply because better predictions are not available. Predictions may also be made when evaluating the risks associated with different ecological scenarios. In this spirit, we also see the indicator we propose here; as an indication of where a system's future state might lay. There is no absolute certainty as complex dynamics may occur after a critical threshold is passed.

Some general properties may, however, give a clue about the predictability of ecosystem dynamics. We found that, as the strength and variability of interspecific competition increases, dynamics change from a situation where positive feedbacks are the main cause of instability, to a mixed, intermediate situation, and, eventually, to a situation in which delayed negative feedbacks govern ecosystem dynamics. Our results suggest that the indicator performs well at predicting a system's future state when positive feedbacks are strong. Performance was reasonably good and transitions caused by positive feedbacks remained quite common in the aforementioned mixed situation, i.e. more than 50% accurate predictions. When dynamics were governed by delayed negative feedbacks, we found that the initial pristine state of the here studied systems was unlikely to be stable, i.e. the probability of a system's nontrivial equilibrium to be stable was below 0.01. The indicator could not be applied and the interplay between several delayed negative feedbacks was likely to lead to chaotic dynamics.

Ecosystems exhibit positive feedbacks when species have direct or indirect positive effects on themselves, i.e. in loops with an even number of negative interactions, and do not only occur as the result of mutually beneficial interactions. Positive feedbacks may, for example, also occur when species positively affect themselves by suppressing other species, e.g. between a pair of competing species and in three-species omnivore loops in food webs (e.g. Van Nes & Scheffer 2004 and Neutel & Thorne 2014). Despite a longstanding interest in the occurrence of complex ecosystem dynamics (May 1974; Hastings & Powell 1991; Huisman & Weissing 1999), no real classification of where and when to expect unpredictable, complex dynamics exists. As a first speculative proposal, we suggest that

all the various types of mutualistic communities are likely to exhibit relatively strong positive feedbacks and predictable dynamics. Terrestrial foodwebs, where the top-down effects of herbivory are relatively small (Cyr & Face 1993), may fall in the aforementioned mixed category, while aquatic food webs are more likely to exhibit chaotic dynamics (e.g. Benincà et al. 2008). Complex dynamics are likely to occur in competitive communities when competitive interaction strengths are variable and asymmetrical. When pairs of interacting species have similar competitive effects on each other, positive feedbacks between some pairs of species are more likely to be strong and dynamics may be fairly predictable (e.g. Van Nes & Scheffer 2004). Further research into where and when to expect complex dynamics will greatly improve our capacity to evaluate the performance of the here proposed indicator and the predictability of ecosystem dynamics in general. Such research may, for example, involve a further investigation of the interrelationship between the structural properties of ecological networks and the occurrence of different types of critical transitions and may include transitions that are not preceded by critical slowing down (see Grebogi et al. 1983 and Hastings & Wysham 2010).

Earlier studies explored different ways in which changing environmental conditions may lead to critical transitions in mutualistic networks, for example by increasing pollinator mortality rates (see **Chapter 2**, Jiang et al. 2018) or by declining mutualistic interaction strengths (Dakos & Bascompte 2014). In this work, assumptions were made that make the effects of these changes fairly simple from a dynamical perspective, e.g. the assumption that the intrinsic properties of species and the effects of changing environmental conditions are similar for all species, and the assumption that the structure of whom interacts with whom remains unchanged. As a consequence, there is little change in the direction of slowest recovery and the nature of the systems' alternative stable states. Here, we chose to study a more complex dynamical scenario because we wanted to test whether the direction of critical slowing down is indicative of a community's future state even when the direction of slowest recovery changes substantially prior to the period in which resilience is lost. There is no reason to assume that the indicator would perform worse at predicting a system's future state when changing conditions affect a group of similar species in one of the aforementioned more simple ways.

The here proposed indicator has a number of advantages compared to previous methods to predict the future state of ecosystems such as extrapolation and the use of mechanistic models. Extrapolation is risky, because it assumes trends to continue outside of the range in conditions for which data are collected, and the behavior of mechanistic models, e.g. aiming to simulate feeding, reproduction, death, and other rates with as much accuracy as possible, often depends on many unknown parameters, in particular when these rates depend on environmental conditions and species abundances. Using the direction of critical slowing down as an indicator of a system's future state has the advantage that it directly relates to an emerging property of complex ecosystems, i.e. the direction in which resilience is lost. As such, it avoids the often difficult process of parameter estimation

needed to develop mechanistic models, and it specifically aims to predict a system's future state when abrupt shifts away from existing trends, i.e. critical transitions, occur.

The above described results consider scenarios in which plenty of data are available. When time series are short, i.e. contain few data points, or when the rolling window used to analyze time series contains few data points, predictions become less accurate (Fig. A4.24-A4.29). This brings us to the question of how we may determine the data requirements in practice. In this context, it is important to consider the two different aspects of our analysis: 'critical slowing down' and 'the direction of slowest recovery'. Critical slowing down can only be detected over a longer time periods, i.e. in which conditions change, while the direction of slowest recovery can be determined for a given set of conditions, i.e. over a short period of time. When determining critical slowing down it is not necessary to monitor the abundances of all species per se, while this is important when determining the direction of slowest recovery. A more economical approach could thus be to monitor only few species for indicators of critical slowing down, e.g. using the methods in Scheffer et al. (2009) and Dakos et al. (2012), and to determine the direction of slowest recovery only once these indicators suggest that the system approaches a tipping point. In some cases, one may even consider to skip monitoring of critical slowing down indicators altogether and focus on determining the direction of slowest recovery in systems that are known to be under stress.

Two aspects could cause our approach to be less data-hungry than expected. First, we are only interested in the slope indicated by the first principal component and require, therefore, fewer data when compared to analysis in which also the higher-order components are of importance. Secondly, we expect the distribution of abundances to become highly asymmetric when a system approaches a tipping point. Dynamics become similar to a low-dimensional system and the number of observations needed to accurately determine the direction of slowest recovery becomes smaller when a system approaches a tipping point (Fig. A4.30). It remains, however, difficult to determine a priori what the data demands are.

Previous studies have proposed rules of thumb that give an indication of the minimum sample size required to perform principal component analysis, i.e. the method used to determine the slope of the indicator. Such rules are often a function of the number of variables, e.g. species abundances, and suggest that the minimum sample size required to perform a principal component analysis should be at least n , e.g. 2, 10 or 20, times more than the number of variables. Velicer & Fava (1998) and MacCallum et al. (1999) showed, however, that such rules of thumb are invalid and that the required sample size depends on the underlying correlation structure. A better approach to determine the minimum sample size is therefore to draw subsets from the data and compare results for the subset with those for the full set (Barrett & Kline 1981; Arrindell & Van der Ende 1985). When subsets give similar results to the full set, enough data is likely obtained. Methods to

determine the effect of a change in sample size may vary from a simple comparison of the direction indicated (as in Fig. A4.30) to more advanced bootstrapping techniques (as in Shaukat et al. 2016).

In this study, we chose to use time-series analysis because it links closely with previous work on early warning signals (Scheffer et al. 2009; Dakos et al. 2012), and because data collection efforts have, traditionally, focused on species abundances. For some ecosystems it may, however, be easier to monitor changes in the structural properties of ecological networks rather than in the specific way in which a system recovers from small perturbations. When such monitoring efforts could be used to estimate (changes in) the effective relationships between species as described by the different elements of the Jacobian matrix, we may be able to obtain a more direct measure of (changes in) the relative strengths of feedback loops in ecosystems, their proximity to a tipping point, and their likely future states. Our analysis suggests, for example, that the extent to which species are saturated and the relative benefits received from mutualistic partners play a crucial role in determining the resilience and future state of mutualistic communities. These properties might be measured in more direct ways, for example by determining the time spent by pollinators on handling and searching for nectar and their relative visitation rates to different plant species. Other theoretically-informed measures for other types of ecosystems may likely provide us with other potential indicators of the direction of critical slowing down.

In a time when humanity's biggest challenges and opportunities depend upon our capacity to manage complex natural systems, new tools to foresee the risks and opportunities associated with critical transitions are of increasing importance. Such tools may not only be useful when addressing the question of what a system's future state might be like, but may also help to address questions such as to what extent individual species or interactions are contributing to network resilience and which deliberate human interventions could prevent or alter the outcome of impending critical transitions. Such approaches are becoming increasingly useful as the availability of data on natural and other complex systems is rapidly increasing.

A4.1 EXAMPLE: UNDERMINING THE RESILIENCE OF A 3-SPECIES NETWORK

To illustrate how differences in the intrinsic properties of species and the arrangement of interactions between them may affect the overall resilience of mutualistic networks, we use a model in which one pollinator species interacts mutualistically with two plant species. The system's overall resilience is highest when this pollinator species obtains most resources from the more saturated plant species.

As conditions change from a situation in which pollinators obtain most resources from highly saturated plant species P_1 , i.e. with high saturation term h_1 , to a situation in which they obtain most resources from less saturated plant species P_2 , the network becomes increasingly sensitive to small-scale stochastic perturbations. Eventually, a critical transition occurs away from the initial pristine state of the network towards a fully collapsed network state in which both plant species and the pollinator species are extinct.

For illustrative purposes, we assume plants to be in steady-state and determine how changing conditions affect the relationship between the net growth of the pollinator species, $dN^{(A)}/dt$, and the abundance of the pollinator species, $N^{(A)}$ (Fig. A4.1). The net growth of the pollinator species is negative at low abundances. As a result, there are two alternative stable states; a pristine state in which the pollinator species has a positive abundance and a collapsed state in which the abundance of the pollinator species is zero. These two alternative stable states can be visualized more intuitively by a stability landscape of which the slope corresponds to the rate at which the abundance of the pollinator species changes, $dN^{(A)}/dt$, valleys to the attraction basins of the alternative stable states, and hilltops to the threshold between the two attraction basins. As conditions change, the attraction basin of the initial pristine state of the network becomes increasingly small and a small perturbation becomes sufficient to cross the threshold and cause a critical transition towards the alternative fully collapsed state of the network.

Parameter settings: $\hat{N}_i = 2$, $c_{ii} = 0.4$, $c_{ij} = 0.1$, $d_i = 0.2$, $h^{(A)} = 0.3$, $h_1^{(P)} = 0.3$, $h_2^{(P)} = 0.1$, and $\epsilon_i = 0.01$. Initial interaction strengths: ($M = 0$): $\theta_{0,11}^A = 1$, $\theta_{0,12}^A = 0$, $\theta_{0,11}^P = 1$, and $\theta_{0,21}^P = 1$. Final interaction strengths: ($M = 1$): $\theta_{final,11}^A = 0$, $\theta_{final,12}^A = 1$, $\theta_{final,11}^P = 1$, and $\theta_{final,21}^P = 1$.

A4.2 EXAMPLE: CRITICAL SLOWING DOWN IN A 4-SPECIES NETWORK

To illustrate the direction in which a community slows down prior to a critical transition and how this might be used to predict a community's future state, we use a model in which two pollinator species interact mutualistically with two plant species. As described in the main text, changing conditions undermine the resilience of this small network by altering relative mutualistic benefits, θ . As was the case with the earlier studied 3-species network (see Appendix A4.1), regime shifts occur in the here studied 4-species community because the community's initial pristine state is approached by a threshold (i.e. a boundary between two attraction basins, Fig. 4.1). As conditions change, the minimum size needed for perturbations to push the system over the approaching threshold becomes smaller. The likelihood of a transition caused by the small-scale stochastic perturbations incorporated in our model therefore increases and, eventually, a regime shift towards an alternative state becomes inevitable.

The outcome of a transition depends on the way in which changing conditions undermine a community's resilience. One, some or all species may collapse to extinction and remaining species may either gain or lose in abundance from a regime shift. Multiple thresholds separating the community's initial pristine state from different alternative stable states, or 'potential future states', may exist prior to a regime shift. Changing conditions may alter the number and nature of these alternative stable states, and the thresholds towards them may or may not approach the network's initial pristine state. Which alternative state eventually becomes the community's future state depends on which threshold towards which future state eventually approaches a community's initial state.

For illustrative purposes, we assume plants to be in steady state and determine how changing conditions affect the dynamics of the network. These dynamics can be visualized intuitively by a stability landscape of which the slope corresponds approximately to the rate at which the abundances of pollinator species change, $dN^{(A)}/dt$ (see methods below). Every possible combination of pollinator abundances is represented by a unique point in the stability landscape and alternative stable states are at the lowest point of the landscape valleys or 'attraction basins'. Thresholds between attraction basins are represented by ridges in the stability landscape. These thresholds are not equally high at all places and have local maxima at hilltops and local minima at saddle points in the network's stability landscape. Attraction basins are shallow in between alternative stable states and the saddle points on the thresholds that separate them. When approached by a threshold, the attraction basin of the initial pristine state becomes increasingly shallow and the network increasingly slow when recovering from perturbations in the direction of the saddle point on the approaching threshold.

For the here studied 4-species network (Fig. 4.1) we found that the network's pristine state is initially accompanied only by a fully collapsed state, i.e. a state in which the

abundance of all species is zero. The pristine state's distance from the threshold towards this state, however, remains large even when conditions change. A regime shift towards a fully collapsed state remains, therefore, unlikely. Changing conditions start to rapidly undermine the network's resilience only after the appearance of the first of two additional alternative stable states. These states correspond to partially collapsed network states in which the abundance of some but not all species is zero. Both thresholds towards both partially collapsed states approach the network's pristine state. One threshold, however, approaches the initial pristine state more closely than the other and eventually a regime shift, caused by the small-scale stochastic perturbations to which the network is permanently subjected, towards the partially collapsed state in the attraction basin behind this threshold becomes inevitable.

As conditions change there are two decisive moments which are both preceded by a particular change in the network's dynamics. The first is the moment at which the future state of the network comes into existence as an alternative stable state in the network's stability landscape, and the second is the moment at which the regime shift towards this alternative stable state actually occurs. The direction in which the network recovers slowly from perturbations changes substantially before the future state of the network comes into existence from a direction that roughly indicates a full collapse to a direction that indicates the future partially collapsed state of the network. The speed at which the network recovers from perturbations, however, remains approximately the same. After the future state of the network comes into existence, the network slows down dramatically when recovering from perturbations in approximately the same direction (Fig. A4.2).

Methods: To determine the rate at which pollinator abundances change as illustrated in Fig. 1.B, we analytically determined this rate, $v^{(A)}$, for different pollinator abundances at 200 by 200 grid points in the network's phase plane as follows:

$$v^{(A)} = \left(\sum_{i=1}^{S^{(A)}} \left(\frac{dN_i^{(A)}}{dt} \right)^2 \right)^{0.5}, \quad (\text{A4.1})$$

in which $N_i^{(A)}$ is the abundance and $dN_i^{(A)}/dt$ the net growth rate of pollinator species i . At the same grid points we determined the height of the stability landscape with an algorithm that keeps updating the height of the landscape until all slopes in between these points are within a certain margin of error from the pollinators net growth rate. This allows us to intuitively show the position of alternative stable states, which are found at the bottom of the landscapes valleys or 'attraction basins', and the thresholds between them, which correspond to hills or ridges in the landscape. The stability landscape produced with this algorithm, is a useful tool to intuitively illustrate the idea behind our method. As our system is non-gradient, it is not a way to determine the potential energy of the system.

Parameter settings: $\hat{N}_i = 2$, $c_{ii} = 0.4$, $c_{ij} = 0.1$, $d_i = 0.2$, $h_1^{(A)} = 0.1$, $h_2^{(A)} = 0.3$, $h_i^{(P)} = 0.3$, and $\epsilon_i = 0.04$. Initial interaction strengths: ($M = 0$): $\theta_{11}^A = 0.7$, $\theta_{12}^A = 0.3$, $\theta_{21}^A = 0.5$, $\theta_{22}^A = 0.5$, $\theta_{11}^P = 0.5$, $\theta_{12}^P = 0.5$, $\theta_{21}^P = 0.3$, $\theta_{22}^P = 0.7$. Final interaction strengths: ($M = 1$): $\theta_{11}^A \approx 0.83$, $\theta_{12}^A \approx 0.17$, $\theta_{21}^A \approx 0.10$, $\theta_{22}^A \approx 0.90$, $\theta_{11}^P \approx 0.90$, $\theta_{12}^P \approx 0.10$, $\theta_{21}^P \approx 0.17$, and $\theta_{22}^P \approx 0.83$

Conditions analyzed for Fig. 1 in the main text: $M = 0.31$, $M = 0.66$, and $M = 0.87$.

A4.3 SIMILARITY BETWEEN THE INDICATED AND OBSERVED SHIFT

As explained in the main text, the slope of the indicator is determined by the first principal component (Fig. A4.4.C), while the eventual (up- or downward) direction of the indicator along the first principal component is determined by the direction in which time points are skewed (Fig. A4.4.D-E). To assess the performance of our indicator, we evaluate the performance of the first principal component and the skewness of the projected time points independently. An accurate slope, means that the indicator performs well at predicting the relative gain or loss of species and which species shift in opposite directions (i.e. an ‘accurate PC1’). The indicated direction is, however, only fully ‘accurate’ when the actual winners and losers are also indicated correctly. This depends on the direction along the first principal component in which time points are skewed.

To evaluate the performance of the first principal component, we determine the difference between the slope of our indicator and the direction of the observed shift in abundance. We do this by determining the angle, θ , between the direction of the indicator and the observed shift as follows:

$$\theta = \cos^{-1} \frac{I \cdot \Delta N^{(A)}}{|I| |\Delta N^{(A)}|}, \quad (\text{A4.2})$$

in which I is the indicator of a network’s future state and $\Delta N^{(A)}$ the observed shift in pollinator abundances. $I \cdot \Delta N^{(A)}$ indicates that we take the dot product between these two vectors. To determine $\Delta N^{(A)}$, we take the mean abundances over 200 time steps at 500 steps before the tipping point and subtract it from the mean abundances 500 steps after the tipping point was found. Because we want to evaluate the accuracy of the first principal component, and not whether points are also skewed in the right direction, we take $-I$ as the input for the formula above when we find an angle $> \pi/2$ (i.e. > 90 degrees). Both I and $\Delta N^{(A)}$ are vectors of which the number of dimensions is equal to the number of species analyzed. The smaller the angle, the more similar the direction of the two vectors.

Two random vectors in a ten-dimensional space are more likely to be orthogonal than two random vectors in a three-dimensional space. More extreme small or large angles become less likely as the number of dimensions increases (Fig. A4.5). How ‘special’ it is to find a certain angle between the indicated and the observed shift thus depends on the number of dimensions in a system. As a measure of how different the indicated direction is from the observed regime shift, we determine for the observed angle, θ , the likelihood that two unrelated random vectors have an equal or smaller angle. As a measure of similarity, we take one minus this probability, and we consider the indicator’s slope to be accurate when this measure of similarity is above 0.99.

To determine the aforementioned probability, we use the following probability density function:

$$h(\theta) = \frac{1}{\sqrt{\pi}} \frac{\Gamma\left(\frac{S^{(A)}}{2}\right)}{\Gamma\left(\frac{S^{(A)}-1}{2}\right)} \cdot (\sin \theta)^{S^{(A)}-2}, \quad (\text{A4.3})$$

in which $S^{(A)}$ is the number of dimensions and $h(\theta)$ the probability density for a certain angle θ (ref. Cai et al. (2013)). Our method may be interpreted as a test whether the null hypothesis that I and N are two random vectors is true. This hypothesis is rejected when angle is found to be significantly smaller than the expected angle between two random vectors, when the one-sided p-value is smaller than 0.01 (i.e. similarity > 0.99).

To evaluate the tendency of time points to be skewed in the direction of a network's future state, we determine the skewness of the time points projected on the first principal component. When points are skewed in the direction of the network's future state, we report a positive skewness. When points are skewed in the opposite direction, we report a negative skewness. We consider a positive skewness as accurate and a negative skewness as inaccurate. A strong positive or negative skewness is considered more accurate or inaccurate than a weak positive or negative skewness.

A4.4 TIME SERIES ANALYSIS

Unless stated otherwise, we determine the dominant direction of fluctuations in a rolling window of 10% of the entire time series (e.g., 2000 out of 20,000 time points) to detect changes in the direction and extent in which time points are distributed asymmetrically. The choice of this window size is to some extent arbitrary. A too small window leads to irregular trends, while a too large window smooths out the trends. To test whether the size of the window chosen influences our results, we make additional analysis in which we use a window size of 0.005, 0.1, 0.5, 0.1, 5, 10, 20 and of 50% of the time series. The rolling window is moved along the time series with steps of 1% of the time series, independent of the window size. As time passes by, the direction and magnitude of the indicator is thus computed every 200 time steps in a window containing the last 2000 time steps when using a window size of 10% of a time series with a length of 20,000 time points.

Far from a tipping point, time points may be skewed only weakly. When this is the case, sudden shifts of nearly 180 degrees may occur in the direction of the indicator when time points are skewed in a different direction along the first principal component. Clearly, such large shifts in direction do not occur because the network's future state has changed. We, therefore, correct previously found indicator values such that there is no change larger than 90 degrees between two consecutive points at which the indicator's direction was determined. We assume the last direction in which time points were found to be skewed to be the accurate one.

To determine whether there is a significant increase in the indicator's magnitude, we determine the Kendall rank correlation coefficient, τ , for the last ten points at which the indicator's magnitude was computed. We consider the increase significant when this coefficient was positive and its p-value < 0.05 . Once a significant increase was found, we tested whether the increase remained significant by determining Kendall's correlation for the last eleven points the next time the indicator's magnitude is determined, for twelve points the time after that, and so on until the tipping point is reached. We would again look at the last ten points when the increase was found to not be significant anymore. By doing this, we could determine the range in conditions in which the indicator's magnitude increased significantly.

As a measure of a 'regime shift' we determined whether there was a change in abundance of more than 1.5 over a period of 1% of the entire time series (200 time steps). We did this by taking the mean abundances over a period of 200 time steps before this period and 200 time steps after this period and determining Euclidean distance between these two mean abundances. To make sure that this large shift in abundances was not a temporal large deviation from the species' mean abundances, we added as a second criterion that the abundance of at least one species should be near extinction, i.e. below 0.1.

We did not apply any preprocessing to handle trends in the time series. We expect

the indicator to be relatively robust against such trends, because trends only alter the direction of the first principal component when their effect on this direction is stronger than the effect of critical slowing down. Not applying any preprocessing is a good way to test this robustness. When using the indicator as part of a different study it may, however, be worth considering to apply a preprocessing method (see ref. Dakos et al. (2012)). It may improve the performance of the indicator, especially when trends are strong.

A4.5 ADDITIONAL INFORMATION BIPARTITE MUTUALISTIC NETWORKS

Nontrivial equilibrium abundances, \hat{N} , competitive interaction strengths, c , mortality rates, d , and saturation terms, h , are randomly sampled from predefined probability distributions, and the total amount of resources received by species i at the system's nontrivial equilibrium, $R_i(\hat{N}^{(P)})$, are assigned such that the rate at which abundances change at the system's nontrivial equilibrium, $d\hat{N}^{(P)}/dt$, is zero:

$$R_i(\hat{N}^{(P)}) = \frac{\sum_{j=1}^{S(A)} c_{ij} \hat{N}_j^{(A)} + d_i}{1 - h_i (\sum_{j=1}^{S(A)} c_{ij} \hat{N}_j^{(A)} + d_i)}. \quad (\text{A4.4})$$

The total amount of resources provided at the system's nontrivial equilibrium, $R_i(\hat{N}^{(P)})$, is thus approximately the same for highly specialized and more generalist species, provided that their losses due to competition, c , and mortality rates, d , and their nontrivial equilibrium abundances, \hat{N} , are similar.

The extent to which species are saturated is determined by the total amount of resources provided, $R_i(\hat{N}^{(P)})$, and the rate at which species become saturated as determined by saturation term h_i . In our simulations, we assume nontrivial equilibrium abundances, \hat{N} , and inter- and intraspecific competition, c_{ij} and c_{ii} , to be similar for all species. Highly saturated species are, therefore, the ones with a high h_i . Species are saturated relatively quickly, and, according to equation A4.4, the total amount of resources provided at the system's nontrivial equilibrium is high when species have a high h_i .

Parameters are assigned such that there are substantial differences in the extent in which species are saturated by drawing saturation terms, h_i , from a scaled beta distribution with range $\sim (0.05, 0.35)$ and shape parameters $\alpha = 1$ and $\beta = 5$. Due to this distribution, there are few highly saturated species, i.e. h_i close to 0.35, and many non-saturated species, i.e. h_i close to 0.05. Strong mutualistic interactions between non-saturated species lead to strong positive feedbacks. Non-saturated species thus need to obtain a relatively large share of resources from a few, highly saturated species for the network to be stable. Relative mutualistic benefits at initial conditions, $\theta_{0,ik}$, are therefore ordered such that larger benefits are obtained from the more saturated species. To make sure that the sum of all relative benefits is one, we take relative mutualistic benefits, $\theta_{0,ik}$, from a symmetric Dirichlet distribution. The distribution's concentration parameter, α , determines the extent in which species are specialized and is, for each species, taken from a uniform distribution between zero and one.

To explore how transitions towards oscillating, chaotic or other complex dynamics caused by delayed negative feedbacks may influence the performance of the indicator, we analyze

several data sets of which the strength and variability in interspecific competitive interaction strengths, c_{ij} , varies. The tested parameter ranges are: $c_{ij} = 0$, $c_{ij} \sim U(0.02, 0.08)$, $c_{ij} \sim U(0.04, 0.16)$, $c_{ij} \sim U(0.06, 0.24)$, $c_{ij} \sim U(0.08, 0.32)$, $c_{ij} \sim U(0.10, 0.40)$, $c_{ij} \sim U(0.12, 0.48)$, and $c_{ij} \sim U(0.14, 0.56)$. Intraspecific competition strengths, c_{ii} , are taken from $\sim U(0.9, 1.1)$. Delayed negative feedbacks become stronger as the strength and variability of interspecific competition increases. Simulations are made for communities of 10 plant and 10 pollinator species. Initial equilibrium abundances, $\hat{N}_{0,i}$, and mortality rates, d_i , are taken from $\hat{N}_{0,i} \sim U(1.5, 2.5)$ and $d_i \sim U(0.15, 0.25)$. Initial and final nontrivial equilibrium abundances are assumed to be equal, $\hat{N}_{final,i} = \hat{N}_{0,i}$.

Changing environmental conditions, M , lead to an increase in the relative mutualistic benefits received from some, and a decrease in the relative benefits received from other species. We assume the distribution of interaction strengths of the final network, at $M = 1$, to be quite heterogeneous (Fig. A4.6). We select, therefore, with a probability of 0.75, interactions of which the interaction strength goes to zero, $\theta_{final,ik} = 0$. To the remaining interactions, relative interaction strengths are assigned by taking them from a uniform Dirichlet distribution ($\alpha = 1$). The ‘diet breath’ of plants and pollinators thus tends to become more narrow as could be the case under various scenarios of global environmental change (Memmott et al. 2007; Burkle et al. 2013).

As conditions change, either a single eigenvalue or a pair of complex conjugate eigenvalues goes to zero. In the first case we are dealing with a saddle-point approaching the network’s initial state, caused by a positive feedback. In the second case, we are dealing with a Hopf bifurcation caused by a delayed negative feedback.

Data sets consist of 100 initial networks. For each network, 10 final distributions of relative mutualistic benefits, $\theta_{final,ik}$, were drawn, allowing us to determine the extent in which a community’s future state depends on the specific way in which relative mutualistic benefits are changed. Parameters were assigned such that this dependency is high. Networks were discarded from a data set when they were unstable at initial conditions, $M = 0$. We determined the frequency at which this occurred as a measure of how difficult it is to find a stable solution for the initial networks of a given data set. The final distribution of relative mutualistic benefits was redrawn either when the network would become unstable within the range of conditions $M = (0, 0.5)$, or when a network would still be stable at $M = 1$.

To test whether the indicator also works when equilibrium abundances change, we analyzed networks of 10 plant and 10 pollinator species of which the final equilibrium abundances are different. We do this by changing the nontrivial equilibrium abundances of species as follows:

$$\hat{N}_i^* = \hat{N}_{0,i} + (\hat{N}_{final,i} - \hat{N}_{0,i})M, \quad (\text{A4.5})$$

in which $\hat{N}_{0,i}$ is the initial, $\hat{N}_{final,i}$ the final, and \hat{N}_i^* the actual nontrivial equilibrium abundance of species i . The total amount of resources provided at the system's nontrivial equilibrium, and the strengths of mutualistic interactions are determined by equations 4.4 and A4.4. We tested three scenarios. One in which the nontrivial equilibrium abundances of species tend to increase, $\hat{N}_{final,i} \sim U(2, 3)$, one in which they stay the same on average $\hat{N}_{final,i} \sim U(1.5, 2.5)$, and one in which they tend to decrease $\hat{N}_{final,i} \sim U(1, 2)$. Competitive interaction strengths were taken from the following distributions: $c_{ii} \sim U(0.9, 1.1)$ and $c_{ij} \sim U(0.02, 0.08)$. Changing abundances affect all relationships as described by the Jacobian matrix. The main effect of a decline in abundance is, however, a reduction of the direct negative effects of species on themselves which undermines resilience. Increasing abundances tend to promote resilience.

To test whether the indicator may accurately indicate the future state of larger networks, we analyzed networks of 10 and 20, 10 and 40, 20 and 10, 20 and 20, 20 and 40, 40 and 10, 40 and 20, and 40 and 40 plant and pollinator species. We assigned competitive interaction strengths such that the rate at which species lose in abundance due to competition, $\sum_{j=1}^{S^{(A)}} c_{ij} N_j^{(A)} N_i^{(A)}$, is approximately the same for different numbers of species, as well as the relative difference between intra- and interpecific competition, c_{ij}/c_{ii} . When a species group consisted of 10 species we assumed $c_{ii} \sim U(0.9, 1.1)$ and $c_{ij} \sim U(0.02, 0.08)$. When a group consisted of 20 species $c_{ii} \sim U(0.67, 0.82)$ and $c_{ij} \sim U(0.015, 0.06)$, and when a group consisted of 40 species $c_{ii} \sim U(0.44, 0.54)$ and $c_{ij} \sim U(0.01, 0.039)$. Initial and final equilibrium abundances were assumed to be equal, $\hat{N}_{final,i} = \hat{N}_{0,i}$.

The amount of noise, determined by standard deviation δ , is assumed to be equal for all species. Unless stated otherwise, we assume standard deviation $\delta = 0.1$. Additional simulations were made with lower and higher noise levels, $\delta = 0.01$, $\delta = 0.05$, $\delta = 0.15$, and $\delta = 0.2$ to make sure that this does not qualitatively alter the results. Higher noise levels were not tested because they would lead to an almost immediate collapse. Unless stated otherwise, model generated time series had a length, T , of 20.000 time steps. Additional simulations were made in which time series had a length of 100, 200, 1.000, 2.000, 10.000, and 100.000.

A4.6 ADDITIONAL INFORMATION UNIPARTITE MODEL OF FACILITATION

Nontrivial equilibrium abundances, \hat{N} , interspecific facilitation rates, γ_{ij} , critical abundances A_i , interspecific competitive interaction strengths, c_{ij} , carrying capacities, K , and mortality rates, d , are randomly sampled from predefined probability distributions. Intraspecific facilitation rates, γ_{ii} , and intraspecific competition rates, c_{ii} , are one. To make sure that the rate at which abundances change at the nontrivial equilibrium, $d\hat{N}_i/dt$, is zero, we assign the intrinsic growth rates, r , as follows:

$$r_i = \frac{d_i \hat{N}_i A_i K_i}{(\sum_{j=1}^S \gamma_{ij} \hat{N}_j - A_i)(K_i - \sum_{j=1}^S c_{ij} \hat{N}_j) \hat{N}_i}. \quad (\text{A4.6})$$

The contribution of species to the overall resilience of a network is determined by critical abundance A_i . Species with a high critical abundance, A_i , collapse more easily and the overall resilience of the community is highest when such species are facilitated by species with a low critical abundance. A change from such a distribution to a more random distribution of facilitative interaction strengths will undermine resilience. To generate time series in which the resilience of the here described facilitative communities is undermined, we assume that conditions, M , affect facilitative interactions as follows:

$$\gamma_{ij}^* = \gamma_{0,ij} + (\gamma_{final,ij} - \gamma_{0,ij})M, \quad (\text{A4.7})$$

in which $\gamma_{0,ik}$ is the initial, $\gamma_{final,ik}$ the final, and γ_{ij}^* the actual facilitative interaction strength. Conditions, M , change from zero to one over time. We assume that the total amount of facilitation received, $\sum_{j=1}^S \gamma_{ij} \hat{N}_j$, remains equal as conditions change. We therefore determine the final facilitative interaction strength as follows:

$$\gamma_{final,ij} = \frac{\theta_{ij} \sum_{k=1}^S \gamma_{ik} \hat{N}_k}{\hat{N}_j}, \quad (\text{A4.8})$$

in which θ_{ij} is the fraction of the total facilitation received by species i from species j .

We assign parameters such that there are substantial differences in the critical abundances of species by drawing critical abundances, A_i , from a scaled beta distribution with $\alpha = 5$ and $\beta = 1$ and range $\sim (0, 1.5)$. Due to the beta distribution, there are few highly vigorous species (i.e. A_i close to 0) and many non-vigorous species (i.e. A_i close to 1.5). The initial facilitative interaction strengths are taken from the following uniform distribution: $\gamma_{0,ij} \sim U(0.2, 1.8)$. Initial facilitative interaction strengths are ordered such that species

receive most facilitation, i.e. highest $\gamma_{0,ij}$, from species with the lowest A_i . We assume that as conditions change, the strength of some facilitative interactions increases strongly while others approach zero. Final relative facilitative benefits, $\theta_{final,ik}$, are therefore selected with a probability of 0.75 and set to zero. To the remaining interactions, relative benefits are assigned by taking them from a uniform Dirichlet distribution ($\alpha = 1$). As with the model of mutualistically interacting species, we chose for this distribution of critical abundances, A_i , and facilitative interaction strengths γ_{ij} , because it leads to a high variety in potential future states to which a network may shift. Other parameters and equilibrium abundances are taken from the following uniform distributions: $\hat{N}_i \sim U(1.5, 2.5)$, $c_{ij} \sim U(0.04, 0.16)$, $d_i \sim U(0.15, 0.25)$.

Simulations were made with networks of 10, 20 and 40 species. As for the bipartite model of mutualistically interacting species, we assign parameters such that the rate at which abundance is lost due to competition, $\sum_{j=1}^S c_{ij}N_j/K_i$, remains approximately the same for different species numbers, as well as the relative difference between intra- and interspecific competition (see main text). Carrying capacities, K_i , were therefore taken from respectively $K_i \sim U(5, 6)$, $K_i \sim U(7.63, 9.15)$, and $K_i \sim U(12.89, 15.47)$, depending on the number of species.

The amount of noise, determined by standard deviation δ , is assumed to be equal for all species. For the results shown in this document we assume standard deviation $\delta = 0.05$. As with the model of mutualistically interacting species time series had a length, T , of 20.000 time steps.

A4.7 SUPPLEMENTARY RESULTS

Independent of the parameter ranges chosen, we found that regime shifts were preceded by a substantial period in which the indicator's magnitude increases significantly, i.e. the 'critical range'. Our indicator would, provided that the future state is indicated accurately, point towards a network's future state during a substantial part of this period (Fig. A4.7). In Fig. A4.8 we provide information about the critical ranges as observed in a single data set ($c_{ij} \sim U(0.02, 0.08)$). These results are exemplary for the other data sets and show that our indicator consistently indicates a network's future state during the period in which the network slows down.

Cascading collapses occur at an intermediate range of competitive interaction strengths most likely due to the nature of effective relationships between species, i.e. the combined effect of all direct and indirect interactions (Fig. A4.9). When there is no competition, effective relationships are positive and species collapse as one group. When competition is strong, most effective relationships are negative and species collapse independently. Cascading collapses are only likely when effective relationships are a mix of positive and negative relationships. When interspecific competitive interaction strengths, c_{ij} , were taken from $\sim U(0.02, 0.08)$, we found that such likely cascading, full network collapses took up a bit more than 12% of the data set. For specific parameter ranges not tested by us, this percentage may be higher.

In Fig. A4.10 we provide examples of two cascading collapses and one immediate network collapse. Species that collapsed a bit later, were also the ones for which the indicated loss in abundance was smallest, suggesting that the indicator indicates the initial regime shift accurately. The amount of time in between two consecutive partial network collapses can be extremely small. Also when cascades are not clearly visible, we suspect therefore that the inaccurate prediction of a full network collapse is caused by the occurrence of a cascading collapse.

In Fig. A4.13 we provide an example of a network for which the future state is hard to predict because it may shift to several alternative future states. When making five simulations in which relative mutualistic benefits, θ_{ik} , are changed in the exact same way by changing conditions, M , we found that the network shifted to four different future states. The future state of this network is determined by the only stochastic element in our model; the small-scale perturbations to which the network is permanently subjected. Our indicator accurately indicates two of the future states to which the network may shift, but does not indicate the other future states. A likely explanation for the several future states to which this system may shift is the fact that this system is approaching a Hopf bifurcation, leading to oscillating (Fig. A4.14), chaotic or other complex dynamics (Fig. A4.15). Such dynamics may explain a high sensitivity to perturbations in more than one direction.

In Fig. A4.18-A4.20, we show examples of time series in which not only the relative benefits, θ_{ij} , change over time. The nontrivial equilibrium abundances, \hat{N}_i , and thus the total gain from mutualistic interactions, $R_i(\hat{N}_i)$, changes as well. We found that a change in abundance over time does not have a strong effect on the performance of the indicator (Fig. A4.17). In comparison to data sets in which abundances stay (on average) the same, full network collapses are much less frequent when abundances increase and much more frequent when abundances decrease. Quite a large fraction of full network collapses is indicated accurately when abundances decrease. Cascading collapses may occur less frequently because all species experience a similar loss in resilience as a consequence of a decline in abundance. Another difference is that the length of the critical range tends to be a bit shorter when abundances in- or decrease.

In Fig. A4.21 and A4.22, we show that the indicator performs well, also when we apply our method to networks with different numbers of plant and pollinator species. Full network collapses become less common as the number of species increases, as well as the occurrence of cascading network collapses. An explanation for this effect of an increase in species number is that the loss in abundance due to competition with other species, $\sum_{j=1}^{S^{(A)}} c_{ij} N_j^{(A)} N_i^{(A)} - c_{ii} N_i^{(A)} N_i^{(A)}$, increases substantially as the number of species increases. Systems with many species may, therefore, be comparable with smaller networks in which interspecific competition is relatively strong. In those networks we also observed that full network collapses were less frequent. Increasing numbers of species did not have clear effect on the length of the critical range, nor on the fraction of the critical range in which the future state was indicated accurately by the slope of the indicator (Fig. A4.22). We did, however, find some effect on the skewness of time points projected on the first principal component. The frequency at which we found that points were skewed in the wrong direction increased as the number of species increases.

In Fig. A4.23, we show results for a more general model of competition and facilitation (see main text). The general behavior and performance of the indicator is similar to the results obtained with the mutualistic network model. The overall resilience of the networks tested seems a bit lower than the resilience of the mutualistic networks (this depends on parameter settings). To prevent networks from collapsing almost immediately, at $M \approx 0$, we chose a lower noise level of $\delta = 0.05$. This relatively low resilience may also explain the relatively high frequency of cascading collapses in networks of 10 species.

A4.8 SUPPLEMENTARY FIGURES

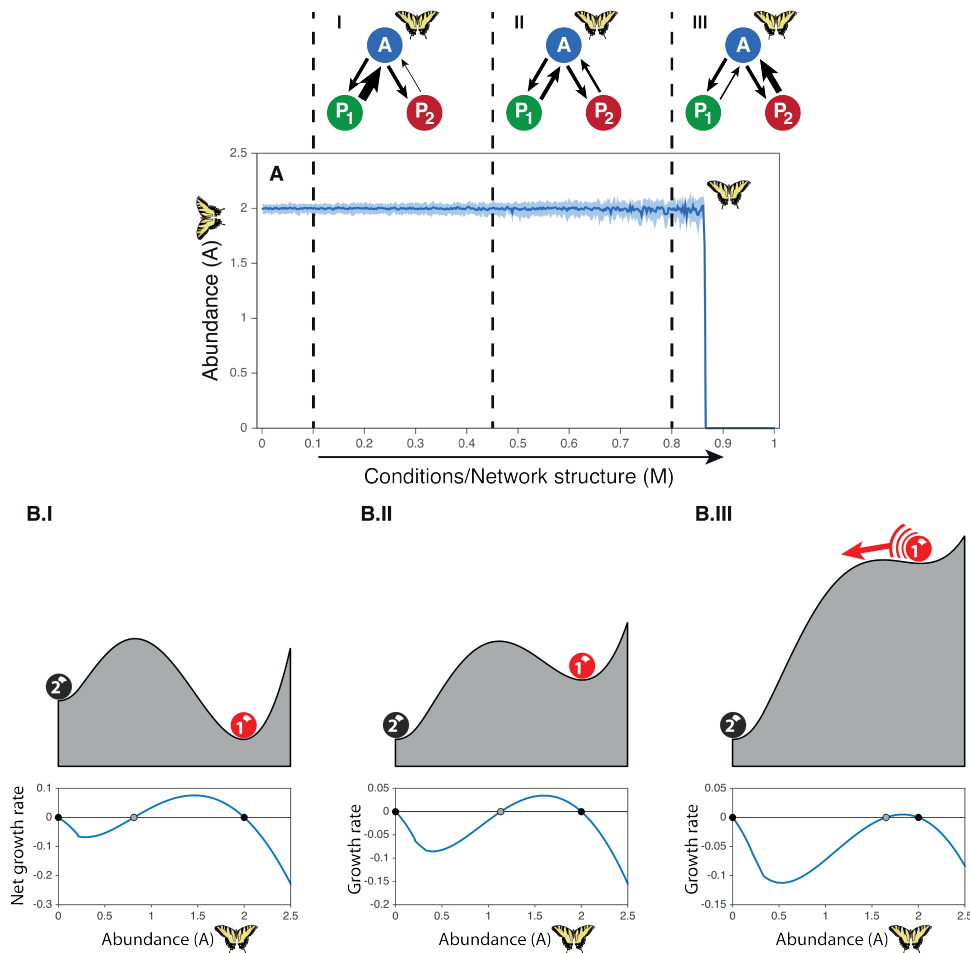


Figure A4.1: Changing conditions undermining the overall resilience of a small mutualistic network. The network consists out of one pollinator, A , and two plants species of which plant species P_1 is more saturated than plant species P_2 . For illustrative purposes, we assume plants to be in steady-state. **(A)** Time series of the pollinator species and the network at different conditions (I, II, and III). As indicated by the thickness of the network's arrows, changing conditions alter the relative mutualistic benefits, θ , such that the pollinator species becomes increasingly dependent on non-saturated plant species P_2 . This undermines the overall resilience of the network and leads to a full collapse of the network at which both plant species (not shown) and the pollinator species (shown) collapse to zero. **(B)** The net growth rate, dA/dt , and the stability landscape of the pollinator species at conditions I, II and III. As conditions change, the initial pristine state of the network, 1, is approached by a threshold, i.e. a hilltop in the stability landscape, and a small perturbation becomes sufficient to cause a regime shift towards fully collapsed state 2.

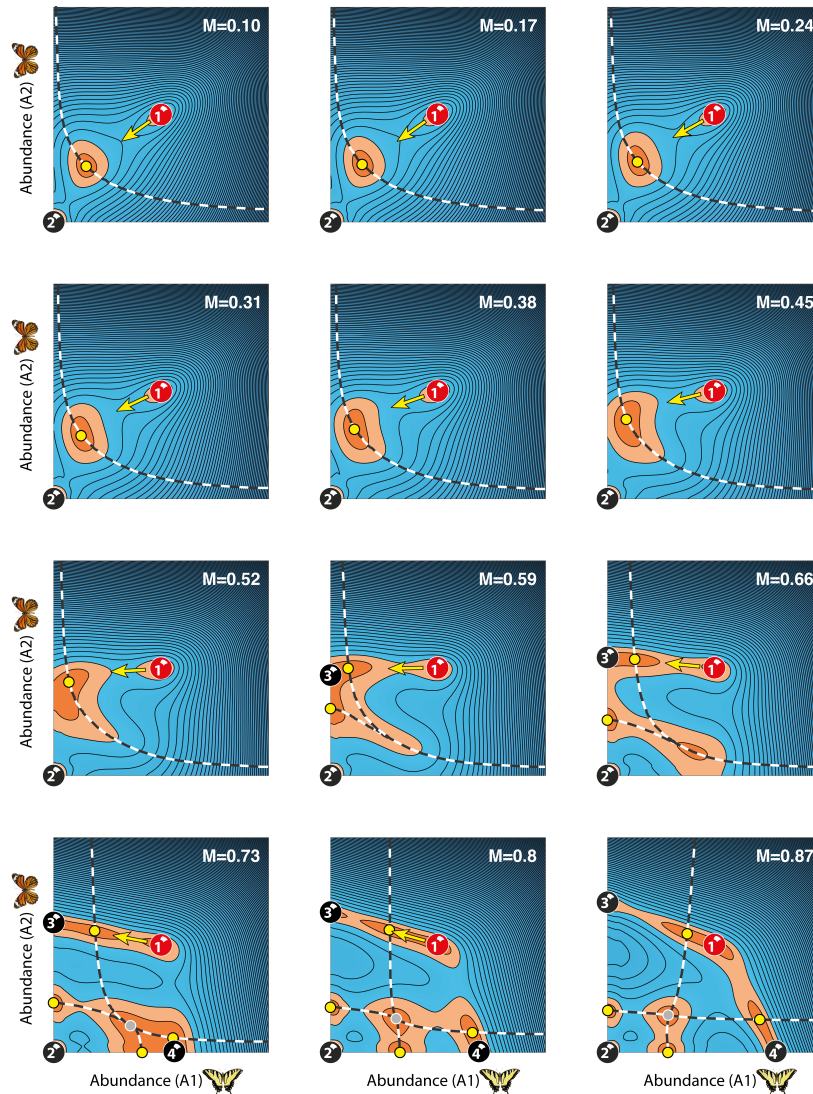


Figure A4.2: The slope of the small mutualistic network’s stability landscape reflecting the speed at which pollinator abundances change, v_a , at different conditions, M . As in Fig. 2 of the main text, alternative stable states (balls), saddle points (yellow dots), and hilltops (grey dots) are surrounded by areas in which the landscape’s slope, and thus the rate at which abundances change, is nearly zero (indicated in orange). Higher speeds (blue) are found further away from these points. The network recovers slowest from perturbations in the direction of the saddle point on the nearest threshold and slows down in the direction of the saddle point on the threshold approaching the network’s initial pristine state. Changing conditions alter the shape of the network’s stability landscape in a non-linear way. After a period in which there is almost no change ($M = [0, 0.31]$), the direction in which the network recovers slowest from perturbations (see yellow arrow) changes substantially from a direction that roughly indicates a full collapse to a direction indicating the future partially collapsed state of the network ($M = [0.31, 0.59]$). After the network’s future state comes into existence, the network slows down dramatically in approximately the same direction ($M = [0.59, 0.87]$).

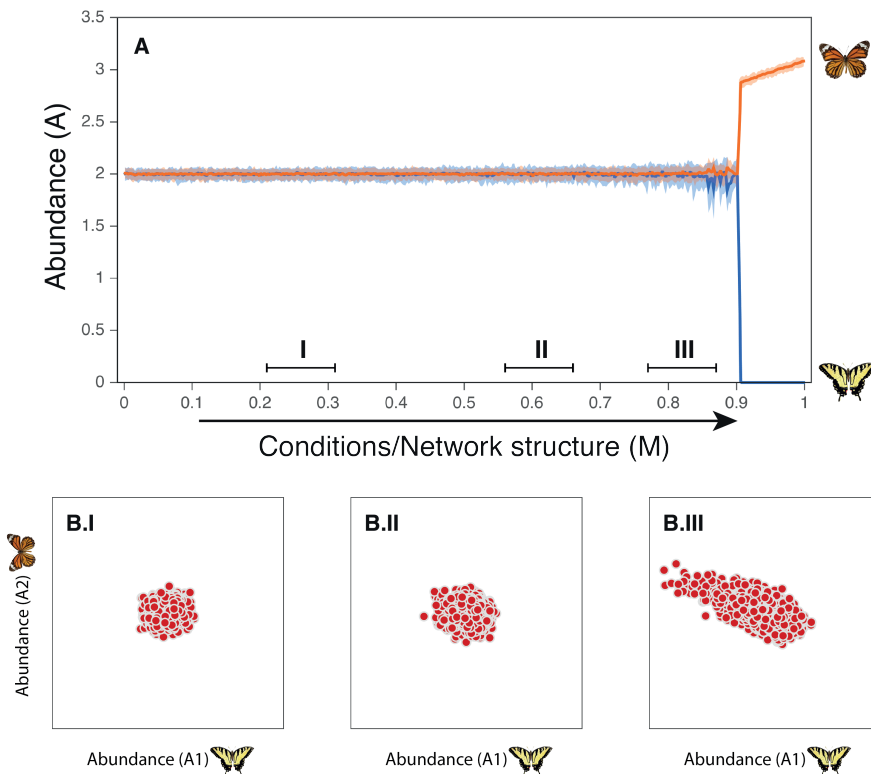


Figure A4.3: Example of a time series in which the small mutualistic network in Appendix A4.2 approaches a tipping point. Conditions at window I,II and III correspond to the conditions for which stability landscapes are shown in Fig. 1 of the main text. **(A)** At the tipping point ($M \approx 0.9$) one pollinator species collapses to extinction, while the other gains in abundance. **(B)** The distribution of points in the network's phase plane representing the abundances of species at different moments in time for time window I, II and III (see A). Far from the tipping point, in window I and II, deviations from the species' mean abundances are relatively small. Close to the tipping point, in window III, the distribution of points in the network's phase space is highly asymmetrical. Deviations from the mean abundances in time window III usually involve a simultaneous increase in the abundance of species A1 and a relatively larger decrease in the abundance of species A2, suggesting that this will also be the direction in which the network will shift once a threshold is passed.

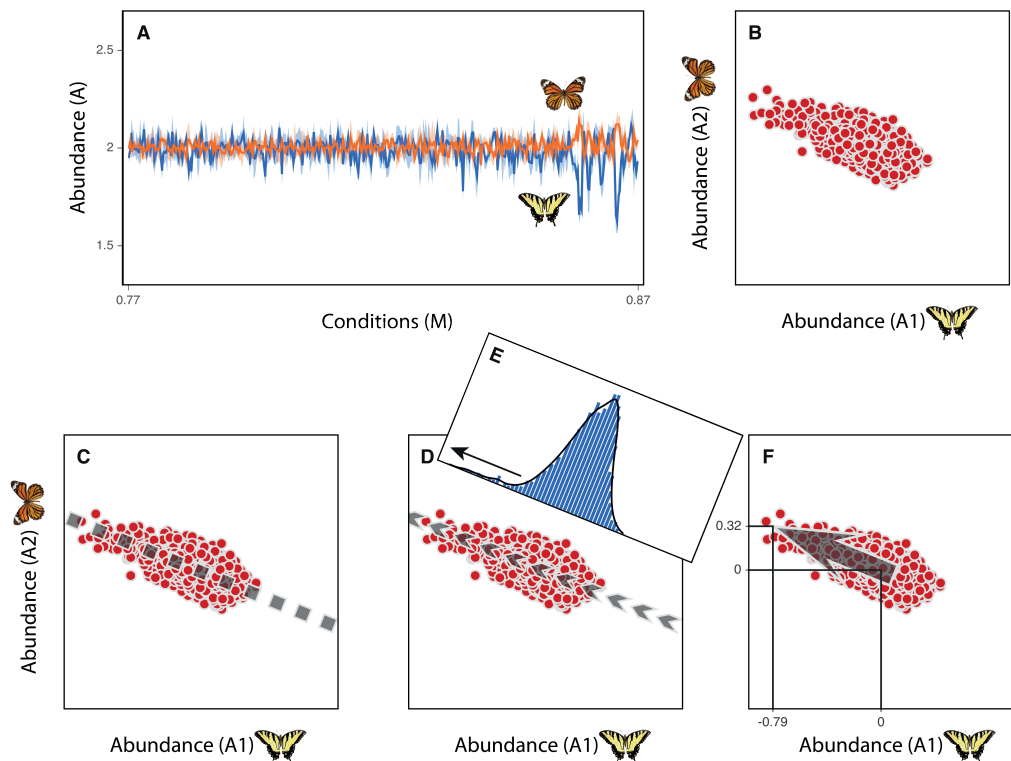


Figure A4.4: The measures of asymmetry together forming our indicator as they were determined for window III in Fig. A4.3. **(A)** Time series of the two pollinator species in the moving window. **(B)** Time points, representing species abundances at different moments in time, in the phase plane of the network. **(C)** The first principal component (grey dotted line) corresponding to the line in the phase plane along which variance is highest. **(D)** Direction along the first principal component (grey arrows) in which time points deviate the most from the species' mean abundance, i.e. the direction in which time points projected on the first principal component are skewed. **(E)** Distribution of the projected time points. **(F)** The indicator, corresponding to a vector in the phase plane of the network (grey arrow). The two components of this vector correspond to the species 'scores on the indicator'. In this example, we found a large negative score (-0.79) indicating a relatively large decline in abundance for the pollinator on the x-axis and a relatively smaller positive score (0.32) indicating a relatively smaller increase in abundance for the pollinator on the y-axis. The length of the indicator corresponds to the amount of variance explained by the first principal component.

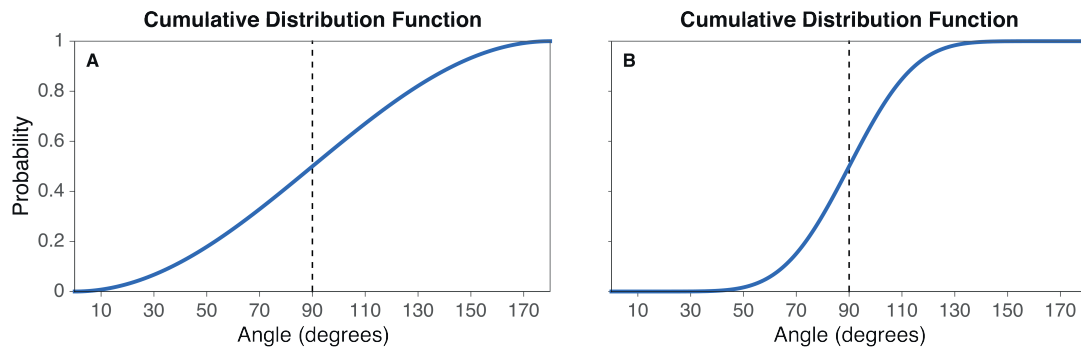


Figure A4.5: Cumulative distribution function of the angle between two random vectors. **(A)** Cumulative distribution function when these vectors have three dimensions. **(B)** Cumulative distribution function when these vectors have ten dimensions. As can be seen from the distributions, the probability of finding an angle of, for example, 40 degrees or less is much smaller in a high dimensional system. Cumulative distribution functions are determined with the help of the probability density function in ref. Cai et al. (2013).

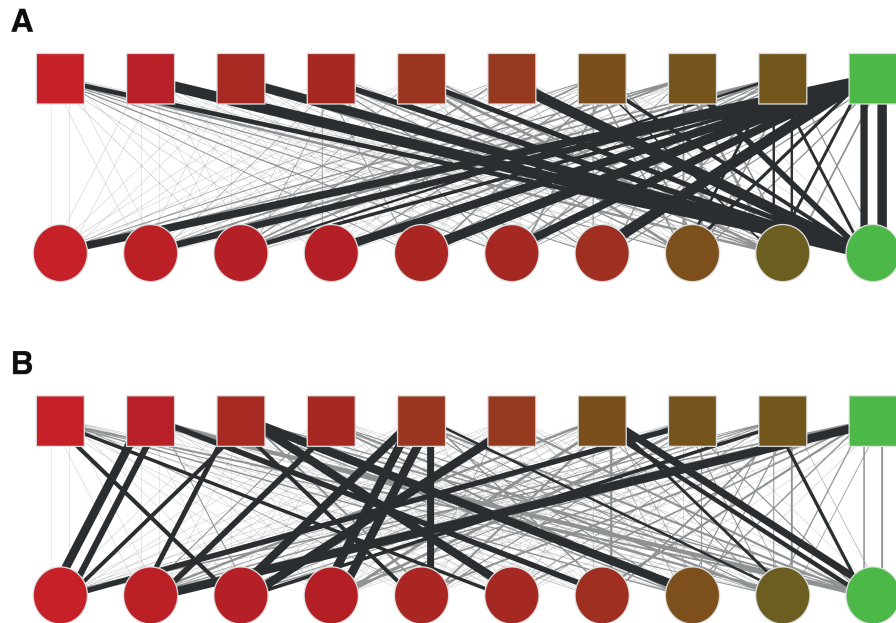


Figure A4.6: Example of (A) a highly resilient mutualistic network and (B) a network with a low resilience. Plant (circles) and pollinator species (squares) are ordered from highly saturated (green/left) to non-saturated (red/right). The thickness of the lines between nodes indicates relative mutualistic benefit θ_{ij} . In the highly resilient network species receive most of their resources from highly saturated species, while this is not the case in the network with a low overall resilience. The resilience of a network is undermined when relative benefits are changed from the situation in A to the situation in B.

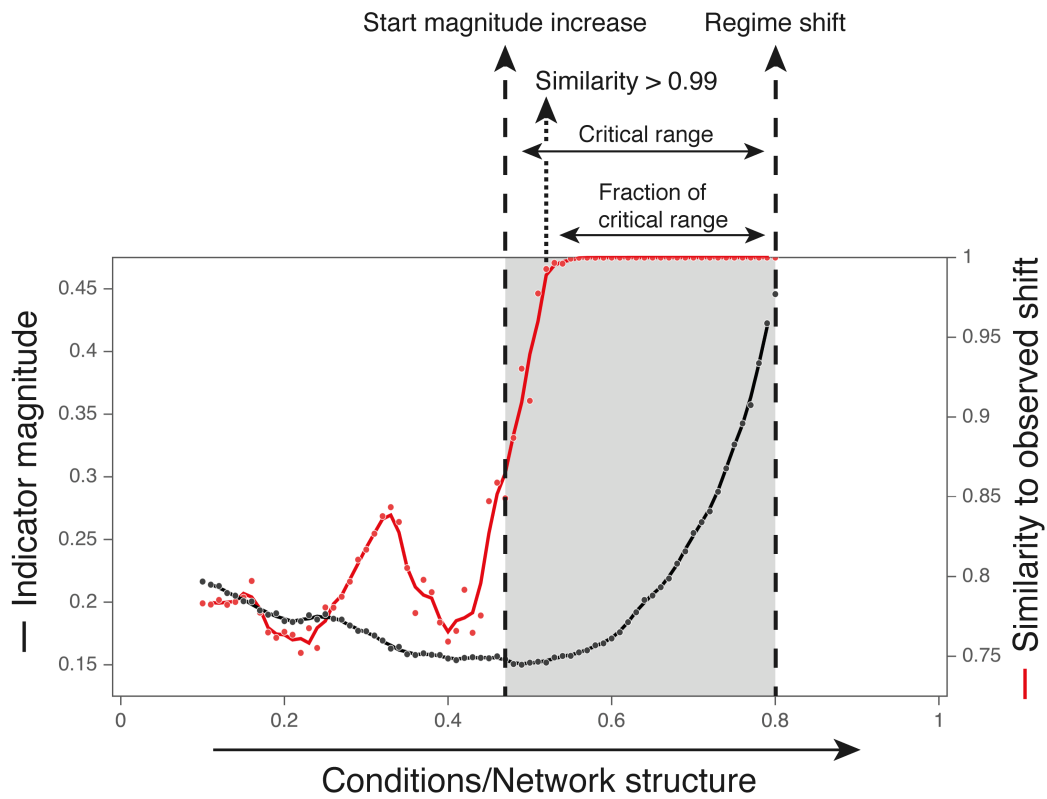


Figure A4.7: The critical range (grey band) in which the indicator's magnitude increases significantly and the fraction of this range in which the indicator's similarity to the observed shift in abundance is larger than 0.99. In the here shown example, the length of the critical period is $0.8 - 0.46 = 0.34$. The slope of the indicator accurately indicates the future state, i.e. similarity is > 0.99 , during a fraction of $0.29 / 0.34 = 0.85$ of this period. The full time series is shown in Fig. 2.

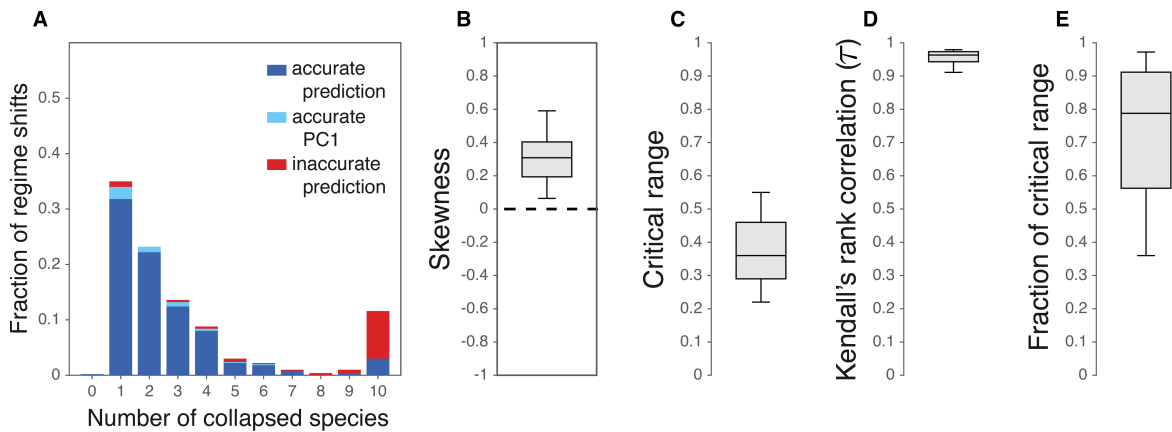


Figure A4.8: Overall statistics on the performance of the indicator when competitive interaction strengths, c_{ij} are taken from $\sim U(0.02, 0.08)$. **(A)** The performance of the indicator for different numbers of collapsed species. The fraction of regime shifts for which the change in abundance was not well indicated is shown in red. The fraction accurately indicated by the first principal component, but not by the direction in which time points are skewed is shown in light blue. Fully accurate predictions are indicated in dark blue. **(B)** The skewness of time points projected on the first principal component. A positive skewness means that time points were skewed in the direction of the network's future state. **(C)** The length of the critical range in which the indicator's magnitude increases significantly. **(D)** Kendall's rank correlation, τ , as determined for the critical range. **(E)** The fraction of the critical range in which the slope of the indicator accurately indicates the future state, i.e. in which the similarity between the first principal component and the observed shift in abundance is > 0.99 . Results in panels (B-E) are shown for regime shifts that were accurately indicated by the first principal component. Box plots show the median and the upper and lower quartiles. Whiskers correspond to the 9th and the 91st percentile.

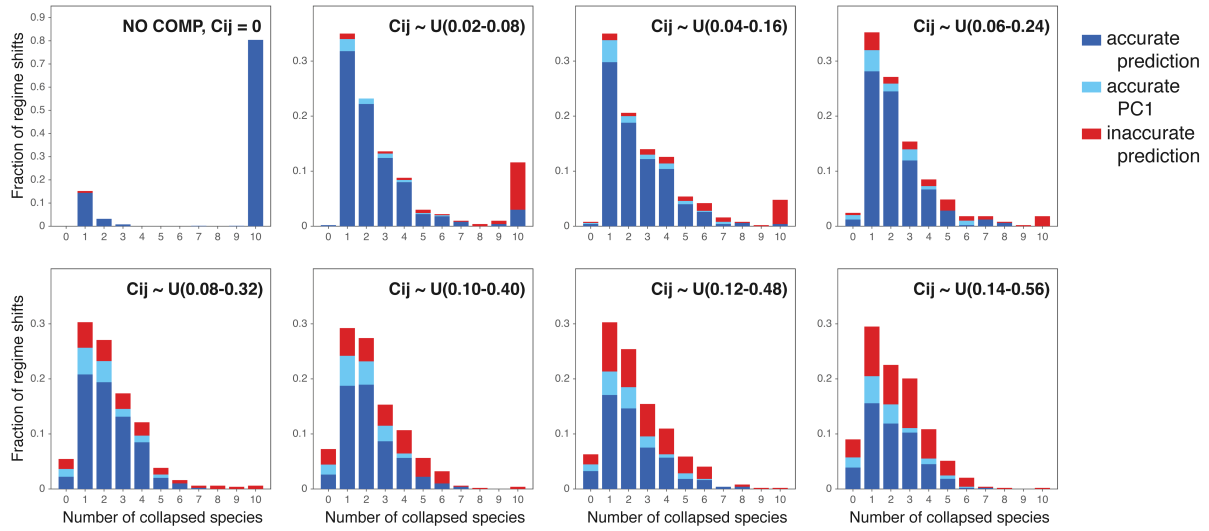


Figure A4.9: The number of pollinator species collapsing to extinction as observed in data sets of 1000 regime shifts. Each panel shows results when sampling competitive interaction strengths from a different parameter range (see ranges indicated). In the extreme case where there was no competition (top left panel), we found almost exclusively full network collapses (i.e. all ten pollinator species collapsed to extinction). As the strength of competition increases, full network collapses become less frequent. Partial network collapses tend to be small independent of the strength of competition, i.e. the most common partial collapse led to the extinction of only one single pollinator species. The fraction of regime shifts for which the change in abundance was not well indicated is shown in red. The fraction accurately indicated by the first principal component, i.e. the slope of the indicator is accurate, but not by the direction in which time points are skewed is shown in light blue. Fully accurate predictions are indicated in dark blue.

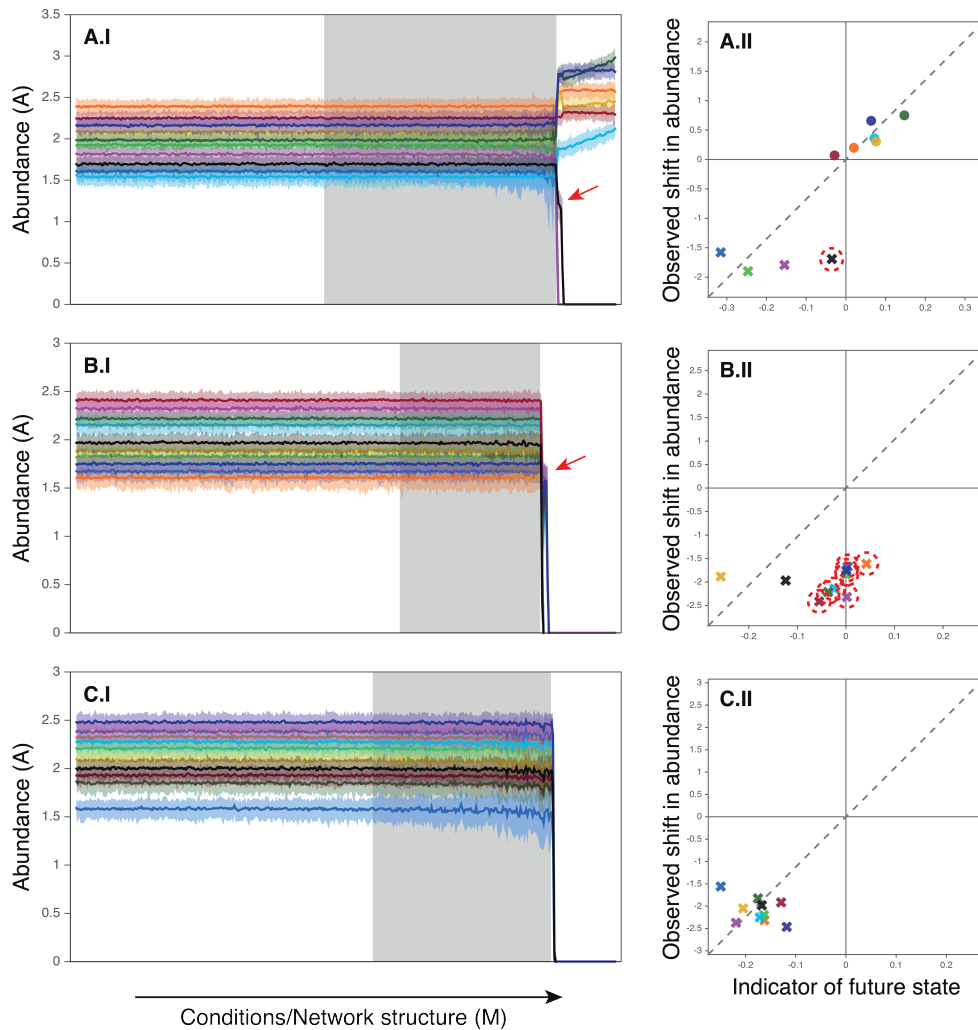


Figure A4.10: Two cascading collapses and one immediate collapse. **(A)** Example of a cascading collapse that eventually leads to the collapse of four pollinator species. Three species (blue, green and purple) collapse to extinction rapidly. A fourth (black) species collapses as well, but remains for a short while at a lower abundance before collapsing to extinction (red arrow, A.I). Out of the four species that collapse to extinction, the black species is also the one for which the indicated loss in abundance is smallest (red circle, A.II). **(B)** Example of a cascading collapse that eventually leads to a full collapse of the network (i.e. the most common outcome of a cascading collapse). Two species (black and yellow) collapse to extinction rapidly. The other species collapse as well, but remain for a short while at a lower abundance before collapsing to extinction (red arrow, b.I). The indicated loss in abundance of the rapidly collapsing species is much bigger than the loss indicated for the species that collapse a bit later (red circles, B.II). **(C)** Example of a full network collapse that was accurately indicated. All species collapse at approximately the same time (C.I). All species were indicated to lose in abundance (C.II).

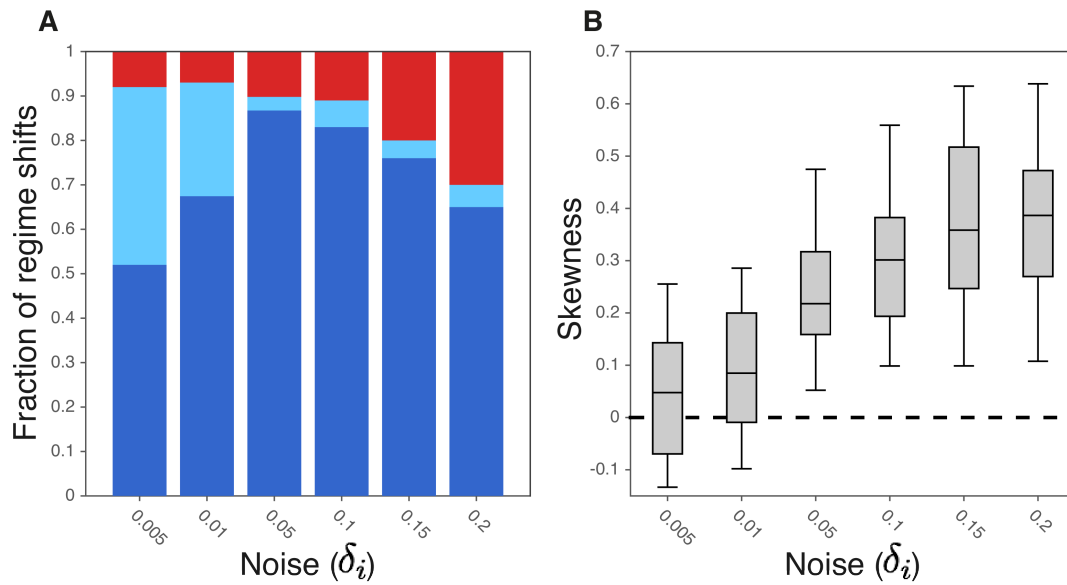


Figure A4.11: Performance of the indicator for different noise levels (noise levels, ϵ_i , are indicated on the x-axis). **(A)** The fraction of accurately indicated regime shifts (dark blue), the fraction accurately indicated by the first principal component, i.e. the slope of the indicator is accurate, but not by the direction in which time points are skewed (light blue), and the fraction of inaccurately indicated regime shifts (red). **(B)** The skewness of time points projected on the first principal component. A positive skewness means that time points are skewed in the direction of a network's future state. The skewness is shown for regime shifts that were accurately indicated by the first principal component.

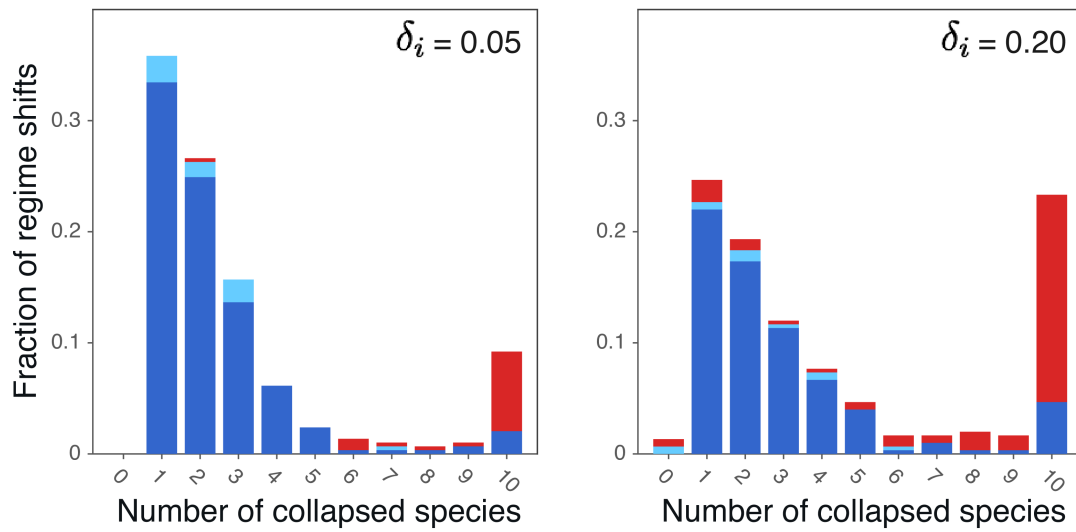


Figure A4.12: The number of pollinator species collapsing to extinction as observed in data sets of 1000 regime shifts when noise levels are low (left panel, $\epsilon_i = 0.05$) and when noise levels are high (left panel, $\epsilon_i = 0.2$). Full network collapses were found to occur more frequently when noise levels are high. The fraction of regime shifts for which the change in abundance was not well indicated is shown in red. The fraction accurately indicated by the first principal component, i.e. the slope of the indicator is accurate, but not by the direction in which time points are skewed is shown in light blue. Fully accurate predictions are indicated in dark blue.

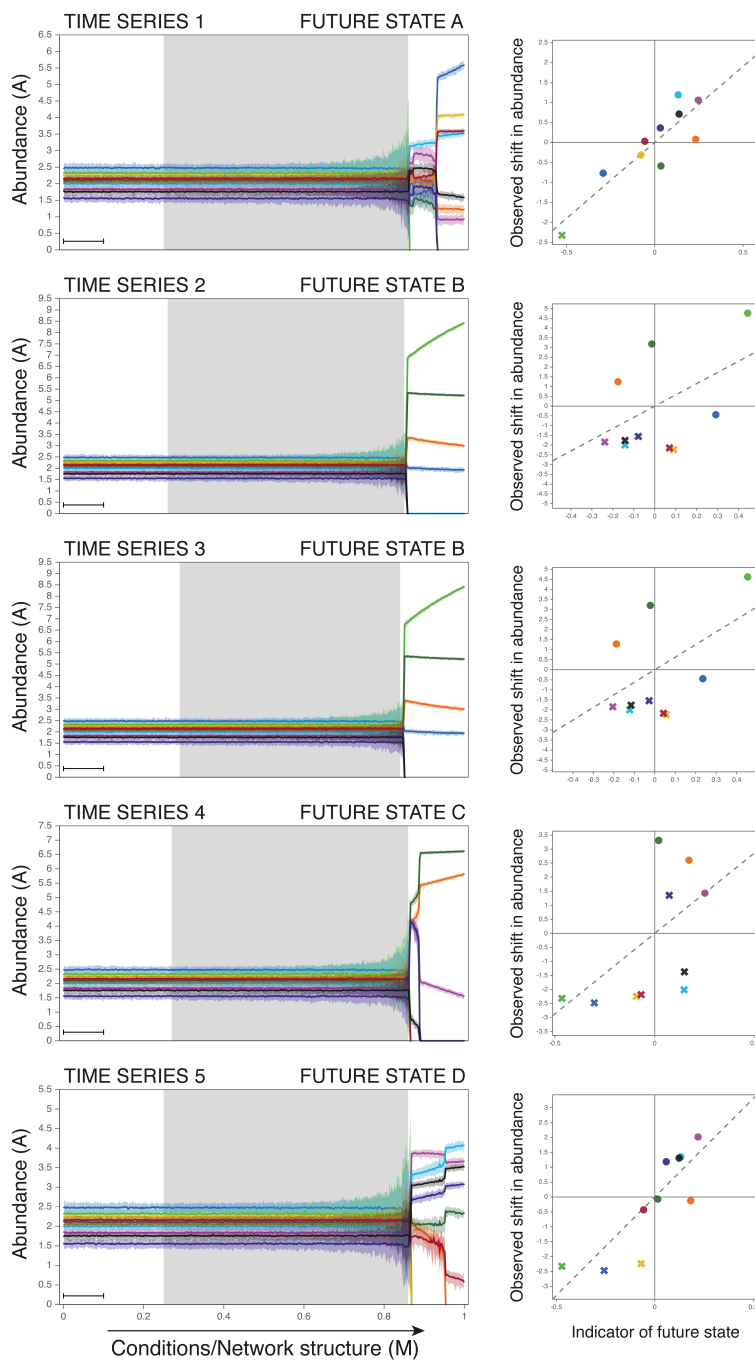


Figure A4.13: Five time series of a network that shows ‘unpredictable’ behavior. Even though the resilience of the network is undermined in the exact same way, the network may shift to several alternative future states. The future state of the network is determined by the only stochastic element in our model; the small-scale perturbations to which the network is permanently subjected. We found that this network may shift to (at least) four different future states (i.e. Euclidean distance between future states > 1.5). Of these future states, future state A and D are well indicated by the indicator (i.e. similarity > 0.99). The future state of the network is the same only in time series 2 and 3.

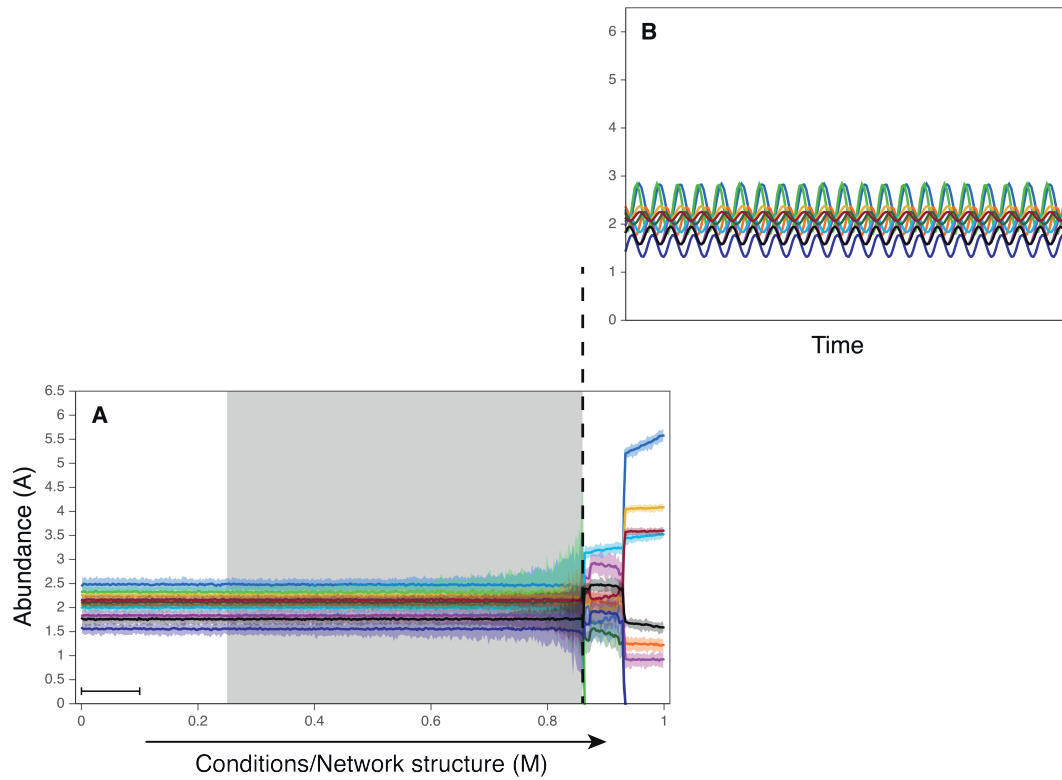


Figure A4.14: Example of a network approaching a supercritical Hopf bifurcation. **(A)** Time series of the network as conditions change. **(B)** Time series at fixed conditions just after the bifurcation point when assuming there are no external perturbations ($\epsilon = 0$). As can be seen from the dynamics we are dealing with a limit cycle. In the presence of external perturbations, the fluctuations caused by these dynamics are amplified and lead to a partial collapse of the network.

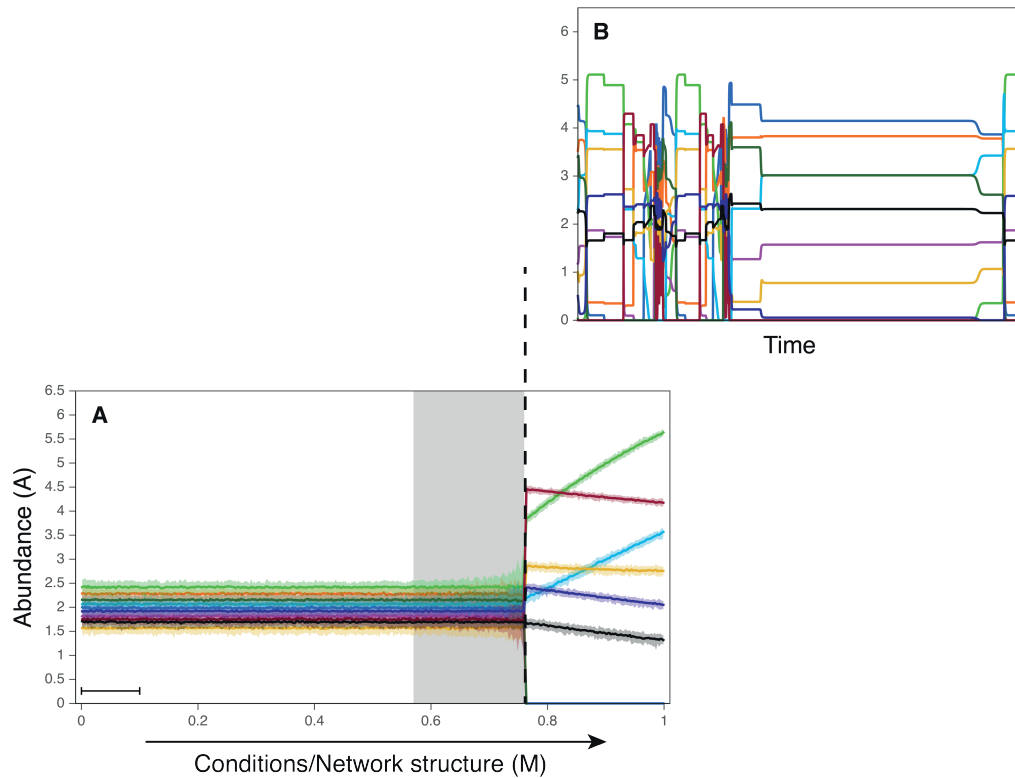


Figure A4.15: Example of a network approaching a subcritical Hopf bifurcation. **(A)** Time series of the network as conditions change. **(B)** Time series at fixed conditions just after the bifurcation point when assuming there are no external perturbations ($\epsilon = 0$) and when excluding the condition that populations of a size smaller than 0.001 have a zero growth rate ($dN/dt=0$). As can be seen from the dynamics we are dealing with chaotic/heteroclinic dynamics. The condition that populations of a size smaller than 0.001 have a zero growth rate leads to a partial collapse of the network. Which species are the first to cross this threshold is strongly influenced by the stochastic perturbations that are constantly disturbing the network.

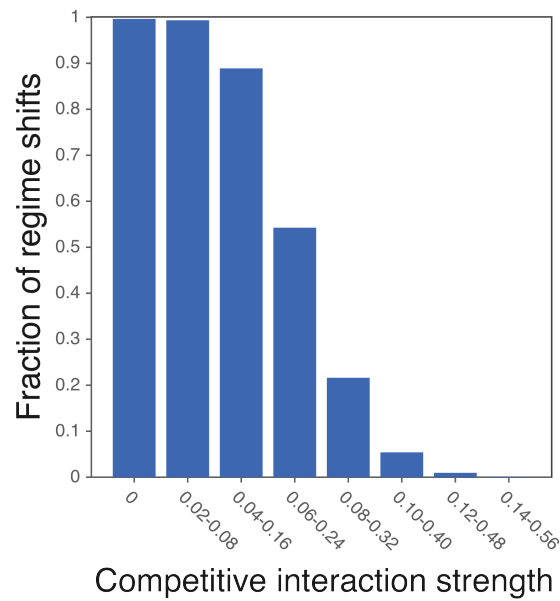


Figure A4.16: The probability of finding a stable solution at initial conditions, $M = 0$, when sampling competitive interaction strengths from different parameter ranges (ranges are indicated on the x-axis). As the strength of competition increases, it becomes increasingly difficult to find a stable solution. When there is no competition between species, the probability of finding a stable solution is nearly one. For the highest competition level we tested, i.e. (0.14,0.56), this probability was below 0.01. Results are shown for networks of 10 plants and 10 pollinators as described in Appendix A4.5.

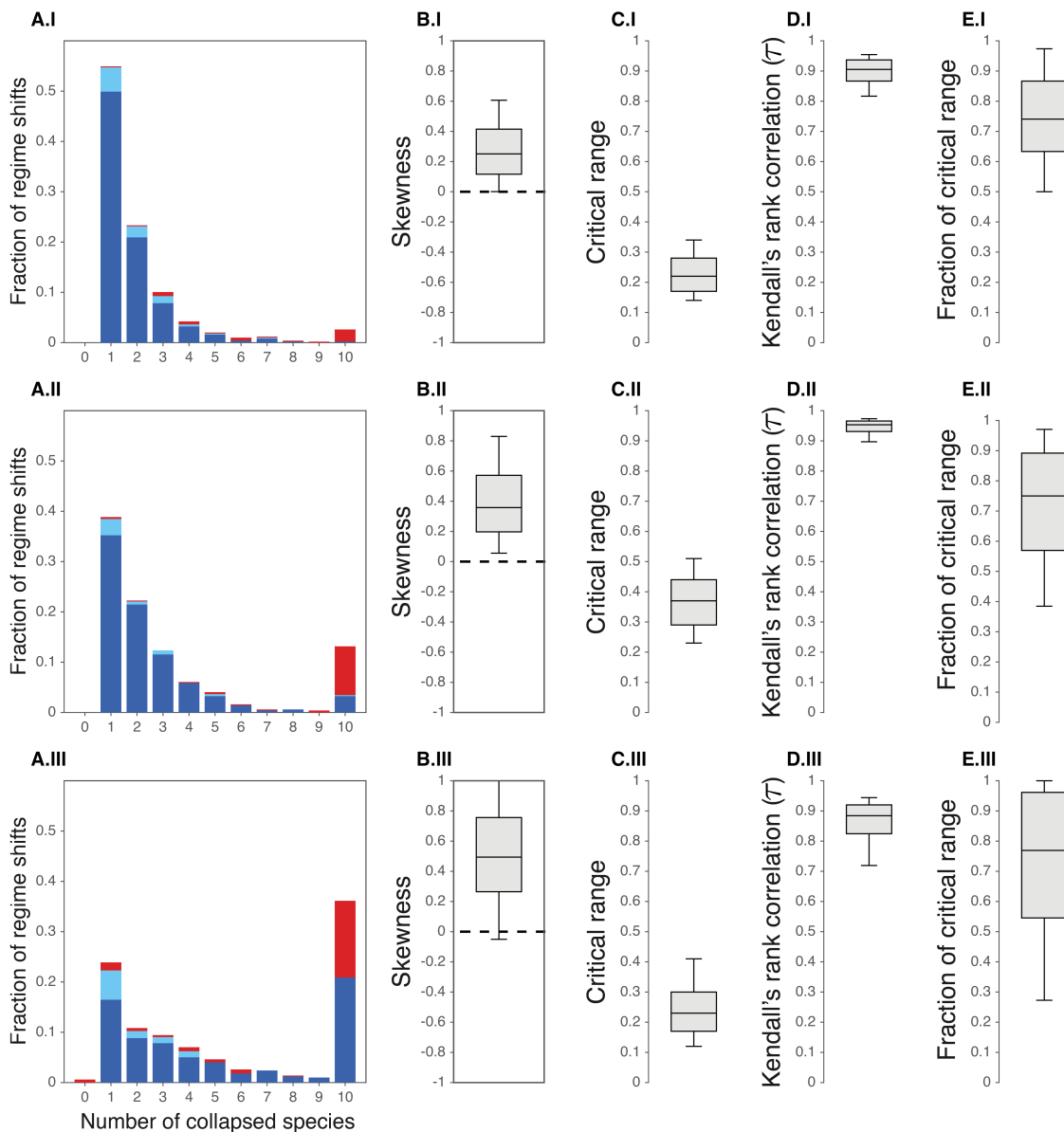


Figure A4.17: Overall statistics on the performance of the indicator when nontrivial equilibrium tend to increase (**I**), change but stay the same on average (**II**), and when abundances tend to decrease (**III**). Results are shown for data sets of 1000 regime shifts. As in Fig. A4.8 we show: (**A**) the performance of the indicator for different numbers of collapsed species, (**B**) the skewness of time points projected on the first principal component, (**C**) the length of the critical range in which the indicator's magnitude increases significantly, (**D**) Kendall's rank correlation, τ , as determined for the critical range, and (**E**) the fraction of the critical range in which the slope of the indicator accurately indicates the future state. Box plots show the median and the upper and lower quartiles. Whiskers correspond to the 9th and the 91st percentile.

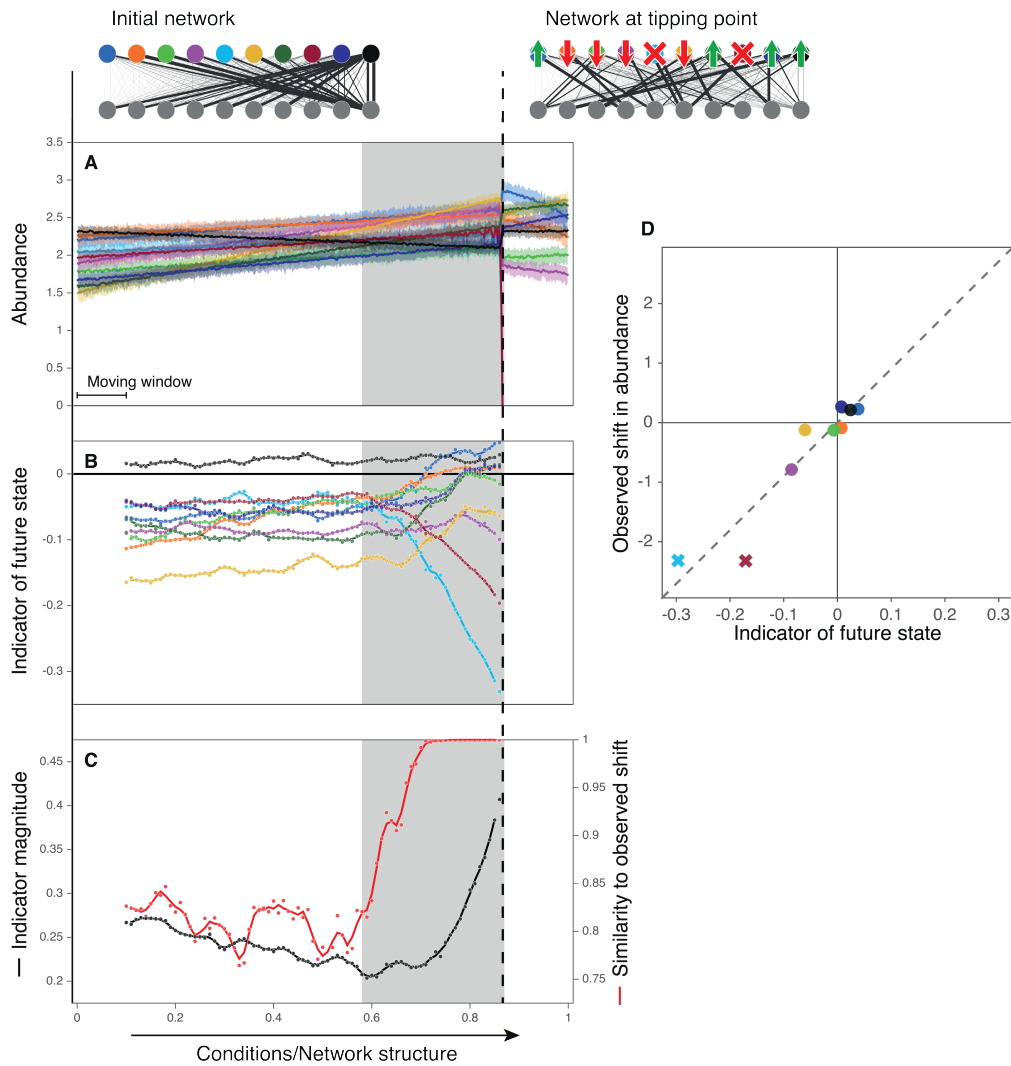


Figure A4.18: Directional slowing down when abundances tend to increase. **(A)** Time series of species belonging to one set of a bipartite mutualistic network, i.e. the pollinators. At the tipping point two species collapse to extinction (red and light blue). **(B)** The indicator of the future state measuring the direction in which fluctuations are distributed asymmetrically. **(C)** The magnitude of the indicator, reflecting the extent in which fluctuations are distributed asymmetrically, plotted together with the accuracy measured as the similarity between its direction and the observed shift in abundance. Grey bands indicate the period in which the indicator's magnitude increases significantly. **(D)** The observed changes in abundance versus the scores on the indicator just before the tipping point. Extinct species are indicated with crosses. The initial network, at $M=0$, is the same as in Fig. 4.2.

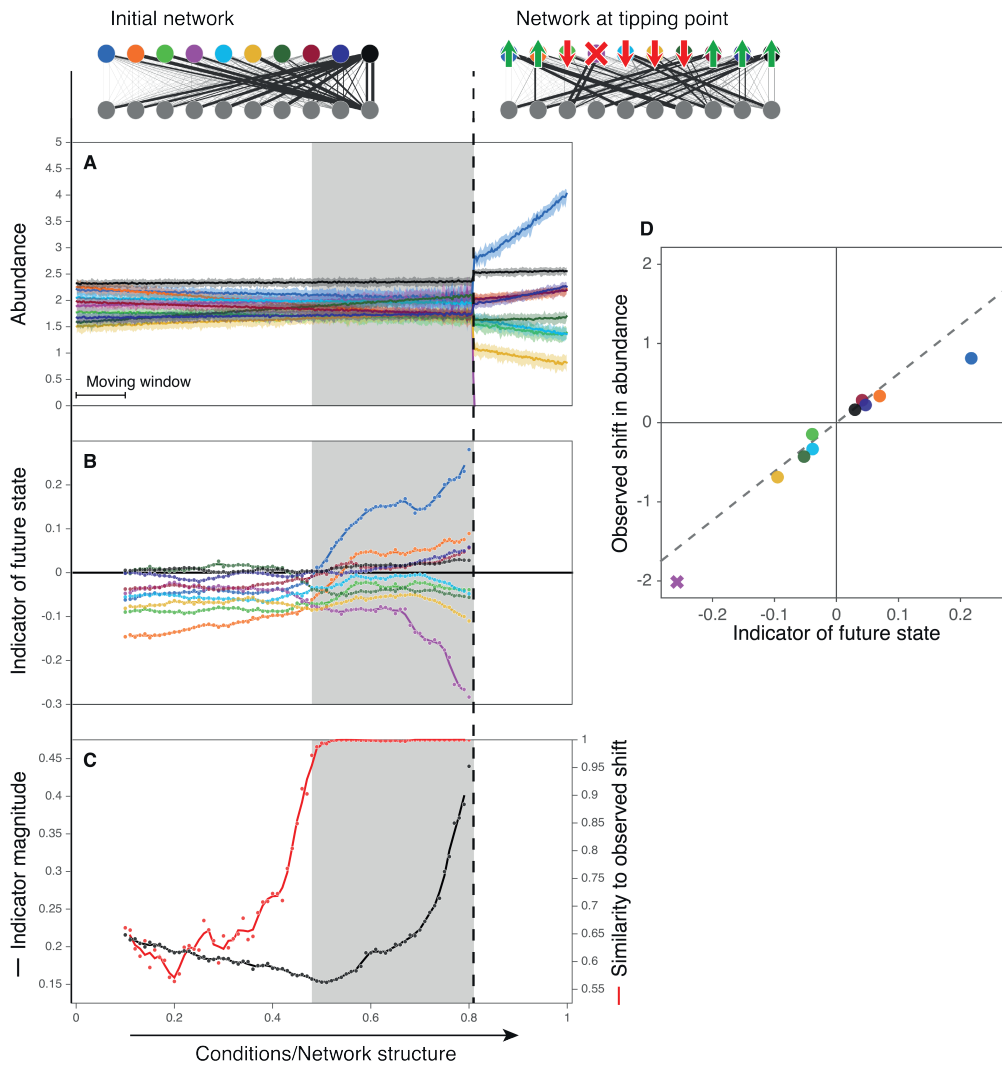


Figure A4.19: Directional slowing down when abundances change, but stay the same on average. **(A)** Time series of species belonging to one set of a bipartite mutualistic network, i.e. the pollinators. At the tipping point a single species collapses to extinction (purple). **(B)** The indicator of the future state measuring the direction in which fluctuations are distributed asymmetrically. **(C)** The magnitude of the indicator, reflecting the extent in which fluctuations are distributed asymmetrically, plotted together with the accuracy measured as the similarity between its direction and the observed shift in abundance. Grey bands indicate the period in which the indicator's magnitude increases significantly. **(D)** The observed changes in abundance versus the scores on the indicator just before the tipping point. Extinct species are indicated with crosses. The initial network, at $M=0$, is the same as in Fig. 4.2 and Fig. A4.18.

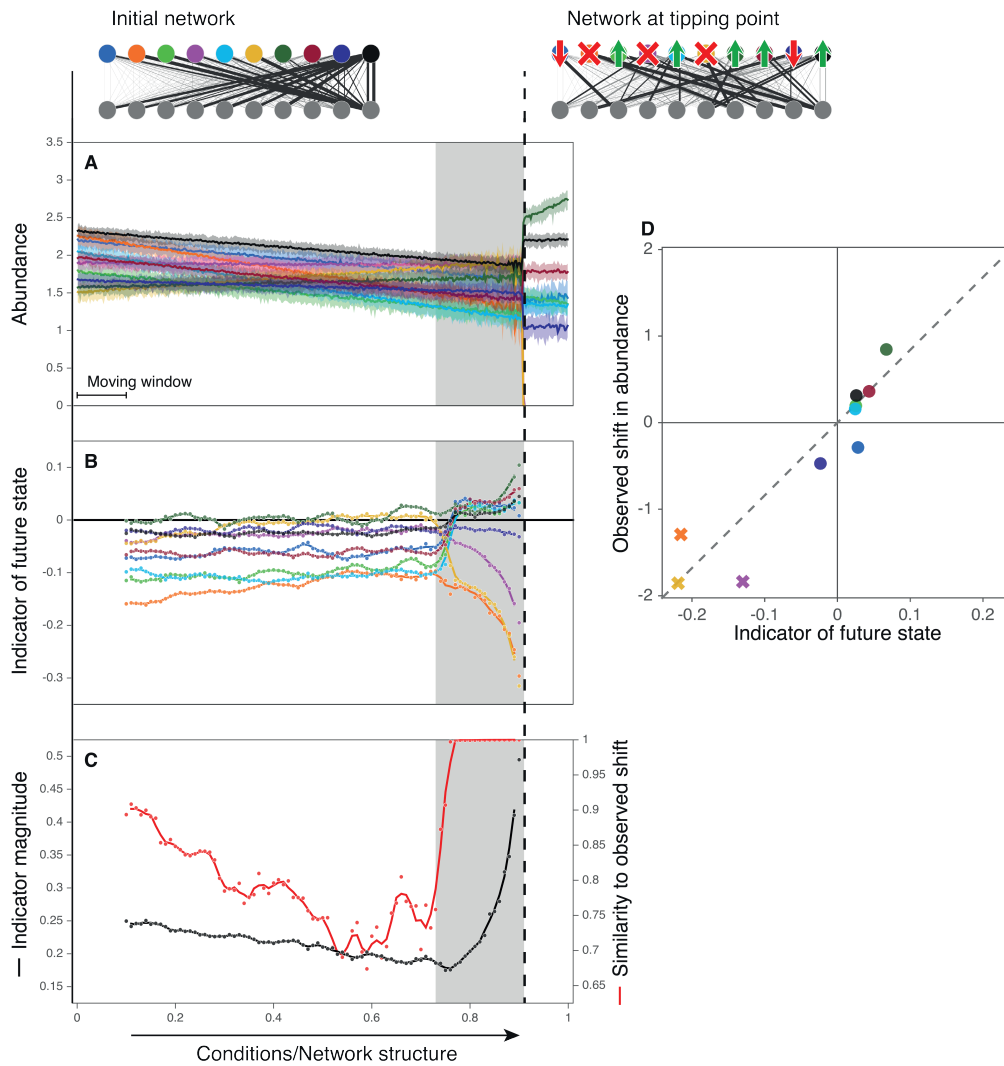


Figure A4.20: Directional slowing down when abundances tend to decrease. **(A)** Time series of species belonging to one set of a bipartite mutualistic network, i.e. the pollinators. At the tipping point three species collapse to extinction (yellow, purple and orange). **(B)** The indicator of the future state measuring the direction in which fluctuations are distributed asymmetrically. **(C)** The magnitude of the indicator, reflecting the extent in which fluctuations are distributed asymmetrically, plotted together with the accuracy measured as the similarity between its direction and the observed shift in abundance. Grey bands indicate the period in which the indicator's magnitude increases significantly. **(D)** The observed changes in abundance versus the scores on the indicator just before the tipping point. Extinct species are indicated with crosses. The initial network, at $M=0$, is the same as in Fig. 4.2, Fig. A4.19, and Fig. A4.18.

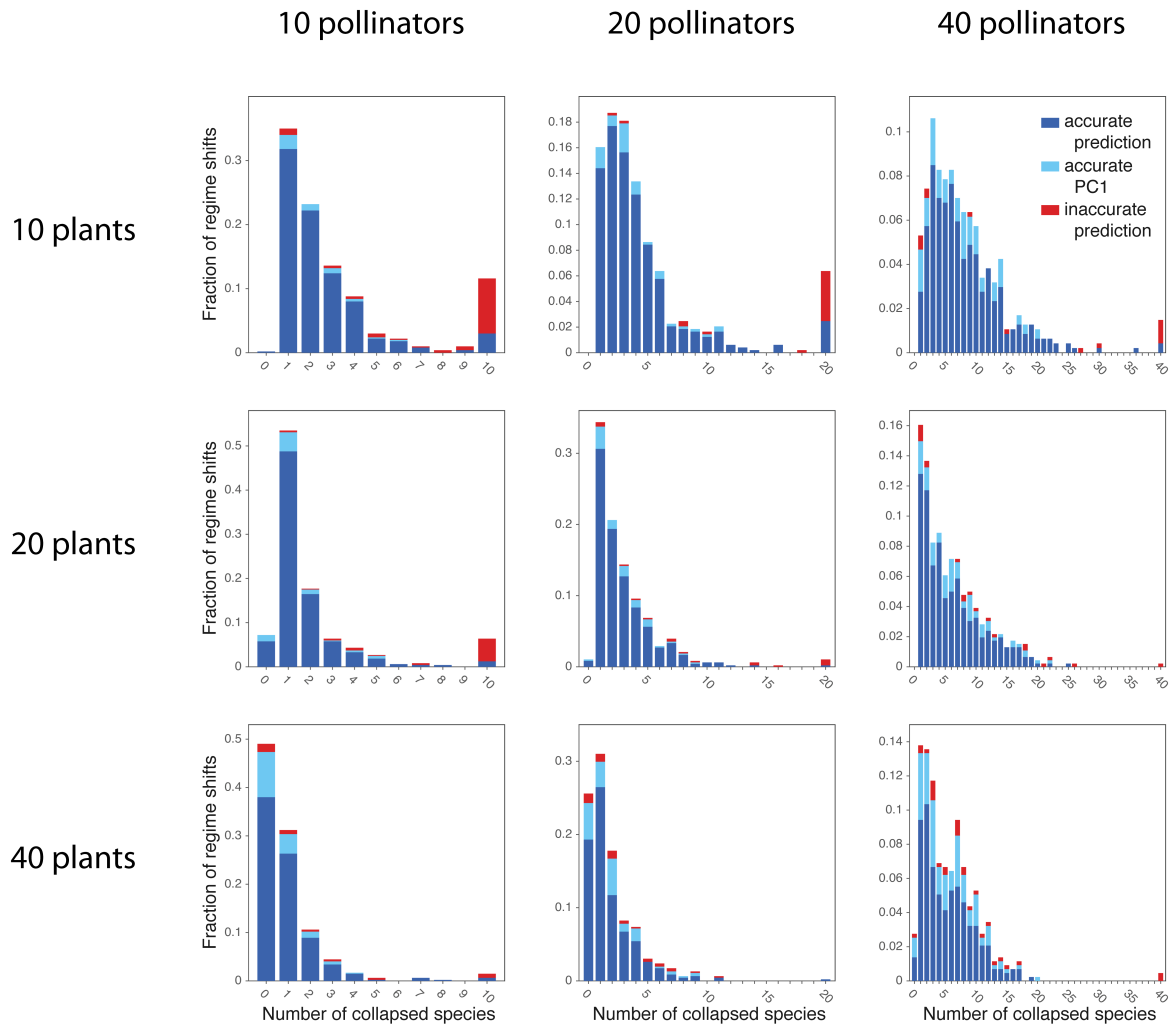


Figure A4.21: The performance of the indicator for networks of different size, i.e. for different number of plant (rows) and pollinator species (columns). Each panel shows the number of pollinator species collapsing to extinction as observed in data sets of 1000 regime shifts. The fraction of regime shifts for which the change in abundance was not well indicated is shown in red. The fraction accurately indicated by the first principal component, but not by the direction in which time points are skewed is shown in light blue. Fully accurate predictions are indicated in dark blue.

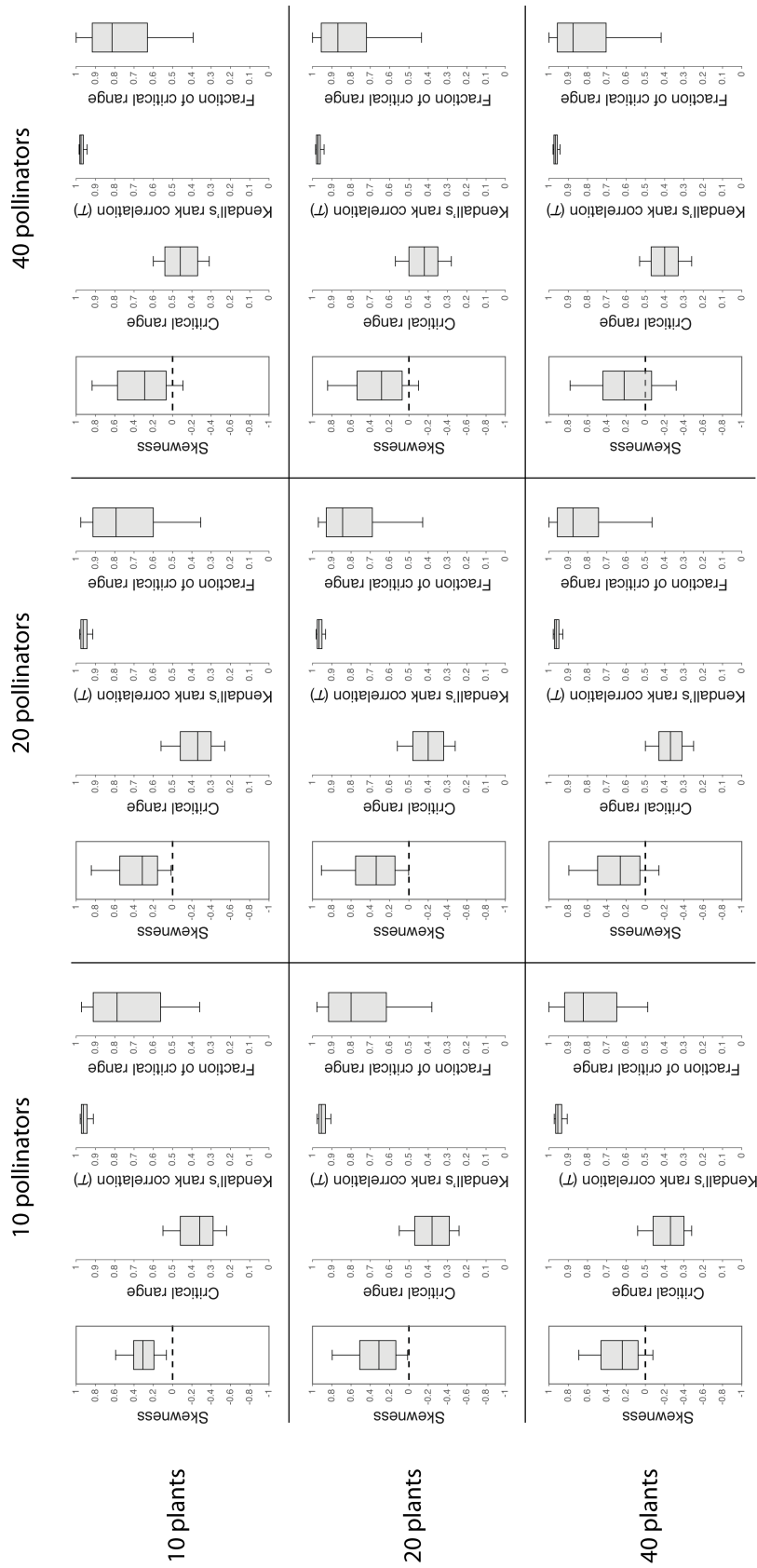


Figure A4.22: The performance of the indicator for networks of different size, i.e. for different number of plant (rows) and pollinator species (columns). Each panel shows the skewness of time points projected on the first principal component, the length of the critical range in which the indicator's magnitude increases significantly, Kendall's rank correlation, τ , as determined for the critical range, and the fraction of the critical range in which the slope of the indicator accurately indicates the future state. Results are shown for regime shifts that were accurately indicated by the first principal component. Results are shown for data sets of 1000 regime shifts. Box plots show the median and the upper and lower quartiles. Whiskers correspond to the 9th and the 91st percentile.

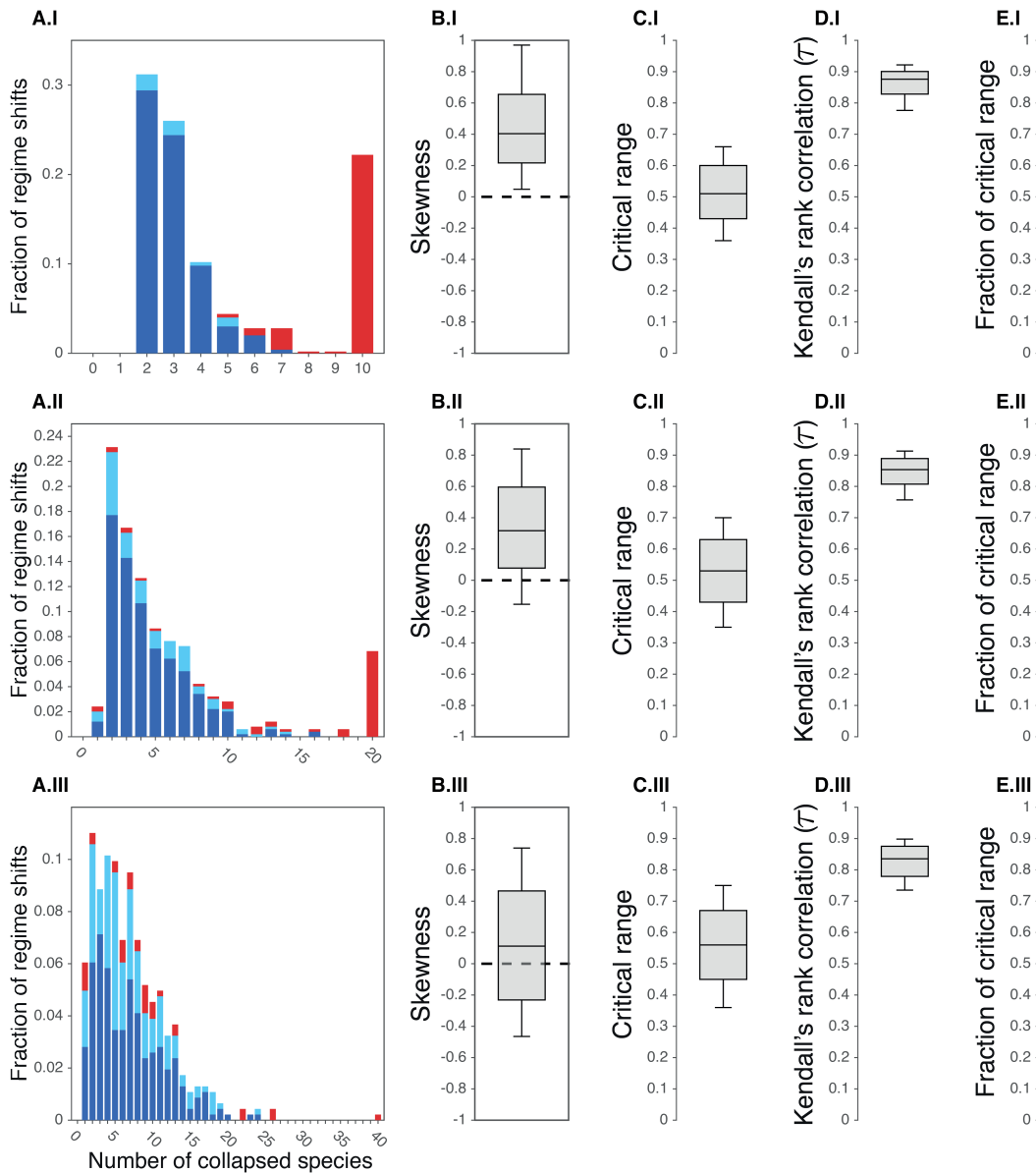


Figure A4.23: Overall statistics on the performance of the indicator when predicting the future state of a more general model of competition and facilitation. Results are shown for networks of 10 (I), 20 (II) and 40 species (III). (A) The performance of the indicator for different numbers of collapsed species. (B) The skewness of time points projected on the first principal component. (C) The length of the critical range in which the indicator's magnitude increases significantly. (D) Kendall's rank correlation, τ , as determined for the critical range. (E) The fraction of the critical range in which the slope of the indicator accurately indicates the future state, i.e. in which the similarity between the first principal component and the observed shift in abundance is > 0.99 . Results in panels (B-E) are shown for regime shifts that were accurately indicated by the first principal component. Box plots show the median and the upper and lower quartiles. Whiskers correspond to the 9th and the 91st percentile.

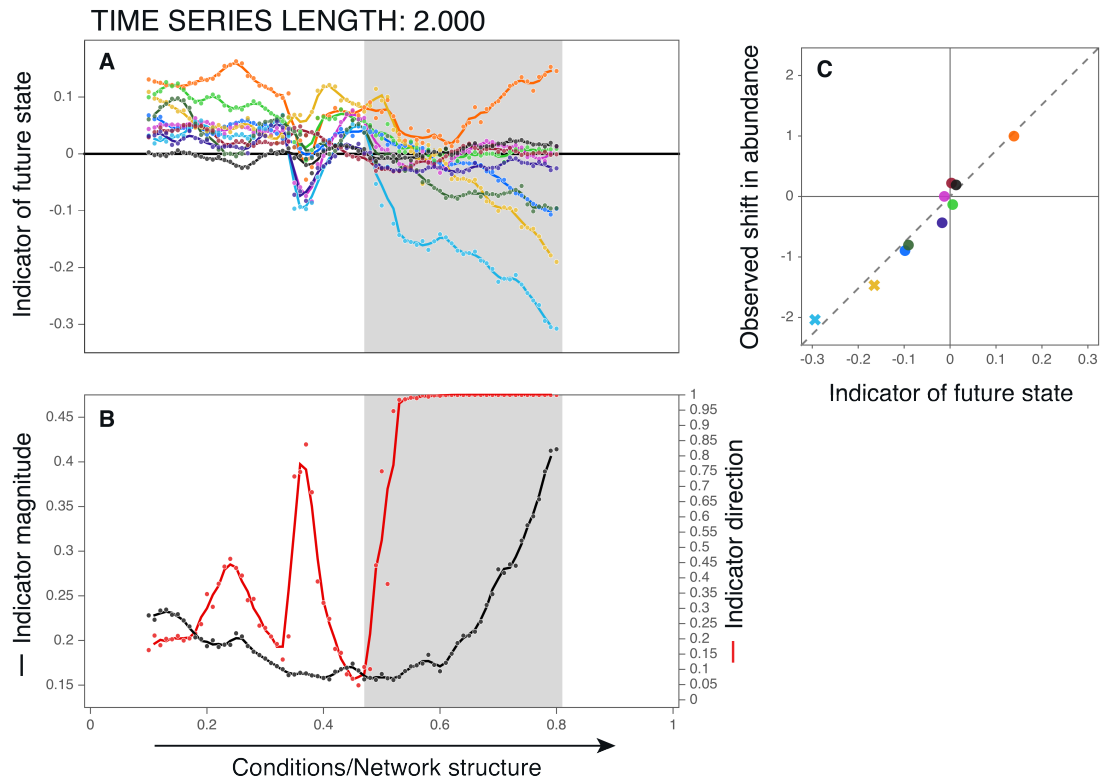


Figure A4.24: Directional slowing down as detected by the indicator when the total length of a time series is 2.000 time steps. **(A)** The indicator of the future state measuring the direction in which fluctuations are distributed asymmetrically. **(B)** The magnitude of the indicator, reflecting the extent in which fluctuations are distributed asymmetrically, plotted together with the accuracy measured as the similarity between its direction and the observed shift in abundance. Grey bands indicate the period in which the indicators magnitude increases significantly. **(C)** The observed changes in abundance versus the scores on the indicator just before the tipping point. Extinct species are indicated with crosses. The initial network, at $M = 0$, and the way in which this network is affected by changing environmental conditions, M , is the same as in Fig. 4.2. Changes in the direction and magnitude of the indicator are determined with a rolling window of 10% of the entire time series, i.e. 200 out of 2.000 time steps.

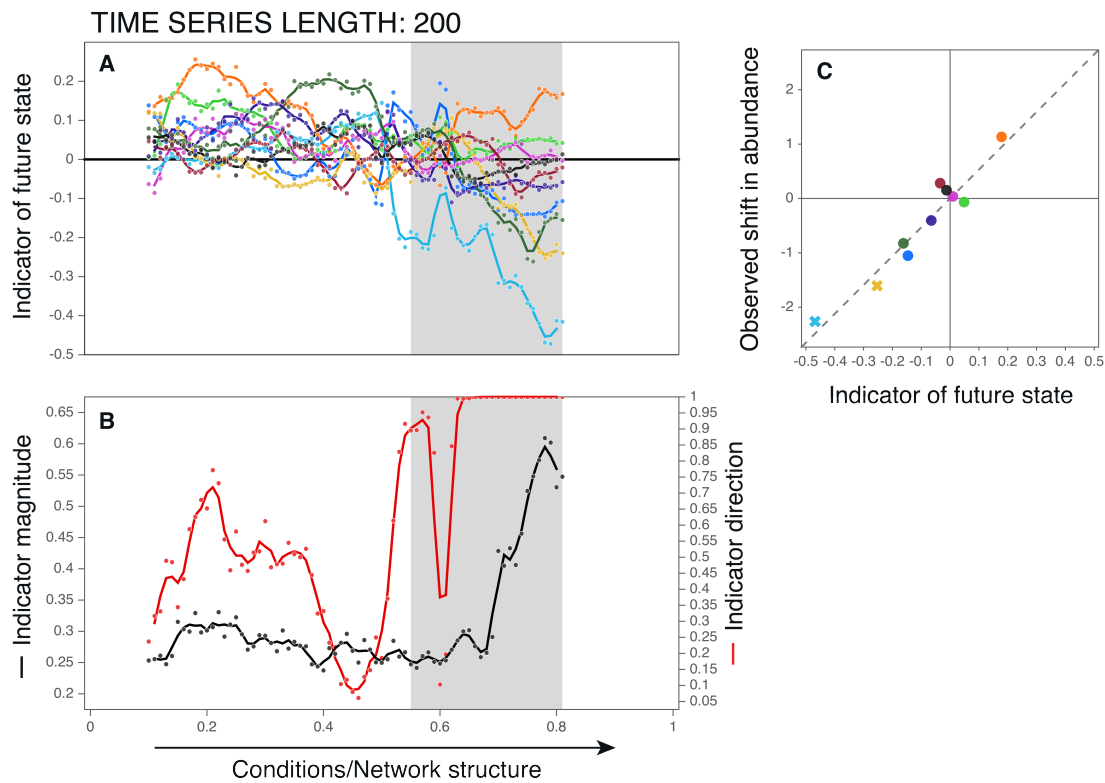


Figure A4.25: Directional slowing down as detected by the indicator when the total length of a time series is 200 time steps. **(A)** The indicator of the future state measuring the direction in which fluctuations are distributed asymmetrically. **(B)** The magnitude of the indicator, reflecting the extent in which fluctuations are distributed asymmetrically, plotted together with the accuracy measured as the similarity between its direction and the observed shift in abundance. Grey bands indicate the period in which the indicators magnitude increases significantly. **(C)** The observed changes in abundance versus the scores on the indicator just before the tipping point. Extinct species are indicated with crosses. The initial network, at $M = 0$, and the way in which this network is affected by changing environmental conditions, M , is the same as in Fig. 4.2. Changes in the direction and magnitude of the indicator are determined with a rolling window of 10% of the entire time series, i.e. 20 out of 200 time steps.

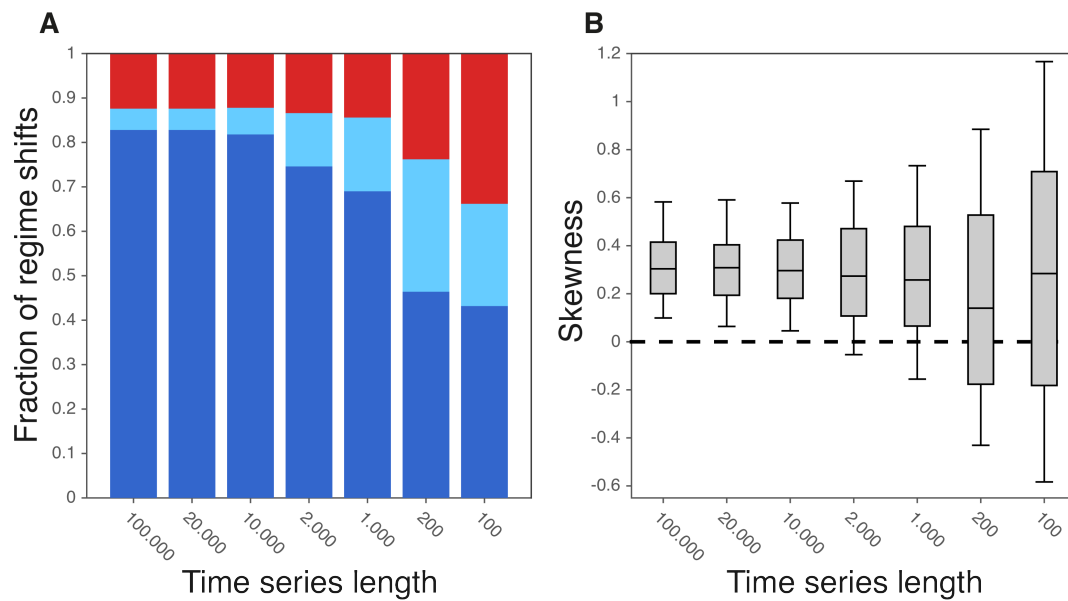


Figure A4.26: Performance of the indicator when time series have a different length (lengths are indicated on the x-axis). **(A)** The fraction of accurately indicated regime shifts (dark blue), the fraction accurately indicated by the first principal component, i.e. the slope of the indicator is accurate, but not by the direction in which time points are skewed (light blue), and the fraction of inaccurately indicated regime shifts (red). **(B)** The skewness of time points projected on the first principal component. A positive skewness means that time points are skewed in the direction of a network's future state. The skewness is shown for regime shifts that were accurately indicated by the first principal component. Changes in the direction and magnitude of the indicator are determined with a rolling window of 10% of the entire time series.

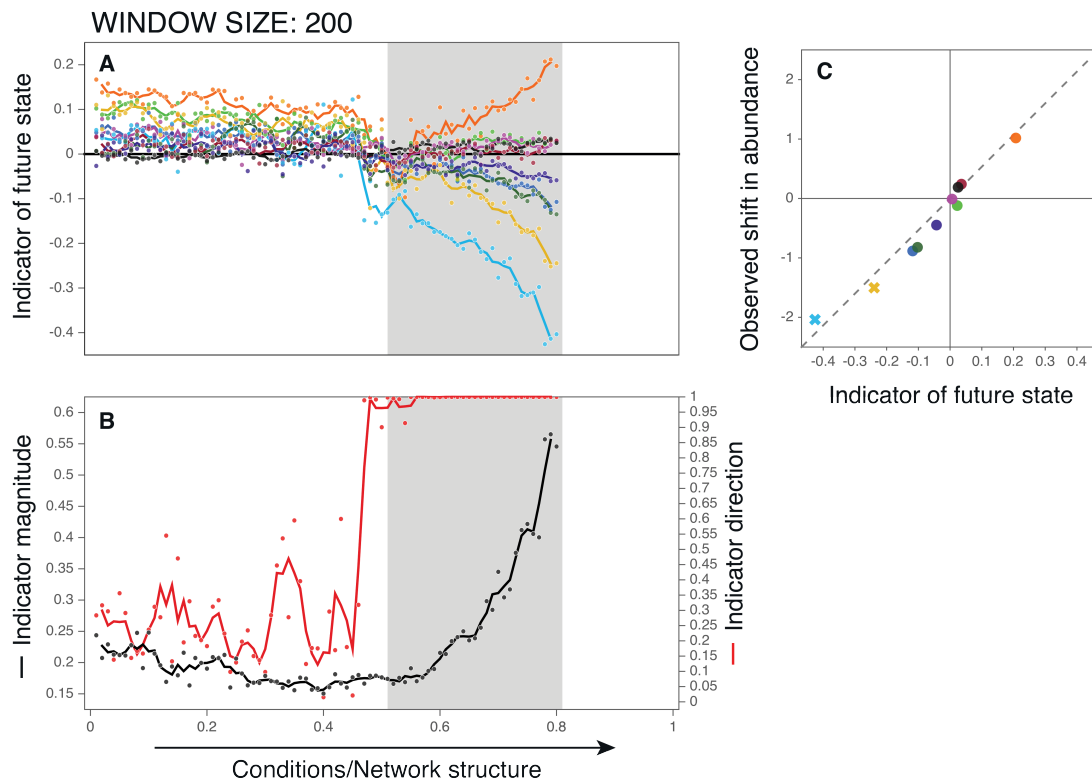


Figure A4.27: Directional slowing down as detected by the indicator when using a rolling window of 1% of the entire time series, i.e. 200 out of 20,000 time steps. **(A)** The indicator of the future state measuring the direction in which fluctuations are distributed asymmetrically. **(B)** The magnitude of the indicator, reflecting the extent in which fluctuations are distributed asymmetrically, plotted together with the accuracy measured as the similarity between its direction and the observed shift in abundance. Grey bands indicate the period in which the indicators magnitude increases significantly. **(C)** The observed changes in abundance versus the scores on the indicator just before the tipping point. Extinct species are indicated with crosses. The initial network, at $M = 0$, and the way in which this network is affected by changing environmental conditions, M , is the same as in Fig. 4.2.

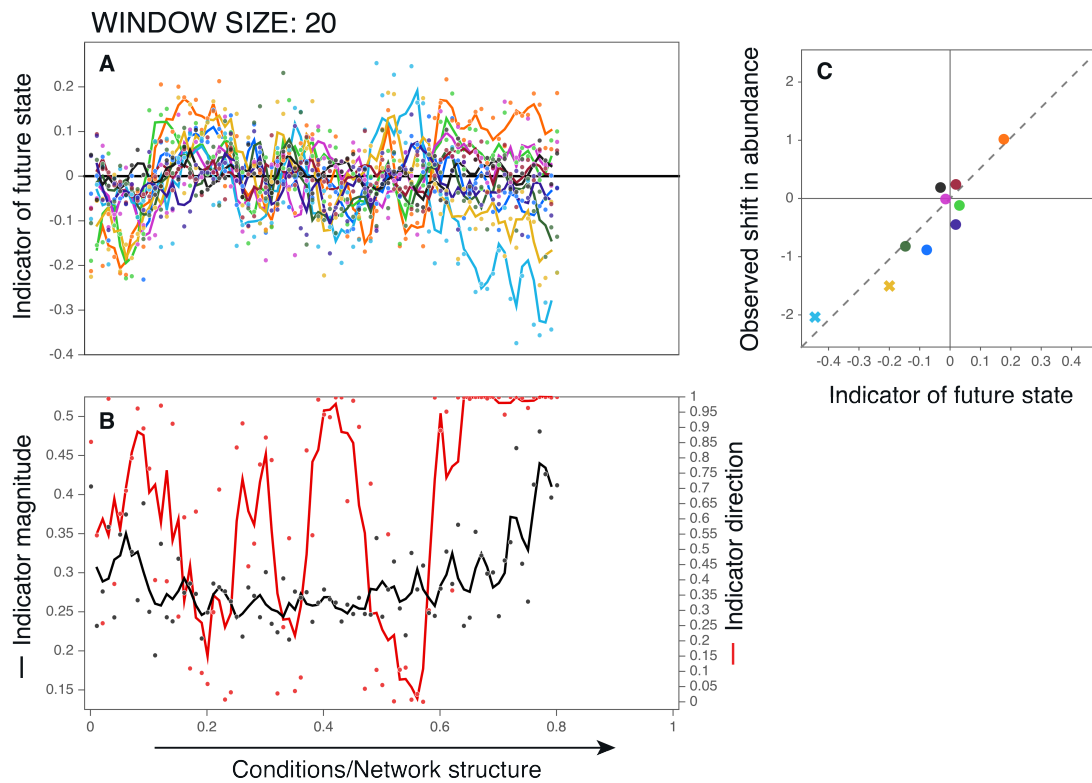


Figure A4.28: Directional slowing down as detected by the indicator when using a rolling window of 0.1% of the entire time series, i.e. 20 out of 20,000 time steps. **(A)** The indicator of the future state measuring the direction in which fluctuations are distributed asymmetrically. **(B)** The magnitude of the indicator, reflecting the extent in which fluctuations are distributed asymmetrically, plotted together with the accuracy measured as the similarity between its direction and the observed shift in abundance. No significant increase in the indicator's magnitude was detected. **(C)** The observed changes in abundance versus the scores on the indicator just before the tipping point. Extinct species are indicated with crosses. The initial network, at $M = 0$, and the way in which this network is affected by changing environmental conditions, M , is the same as in Fig. 4.2.

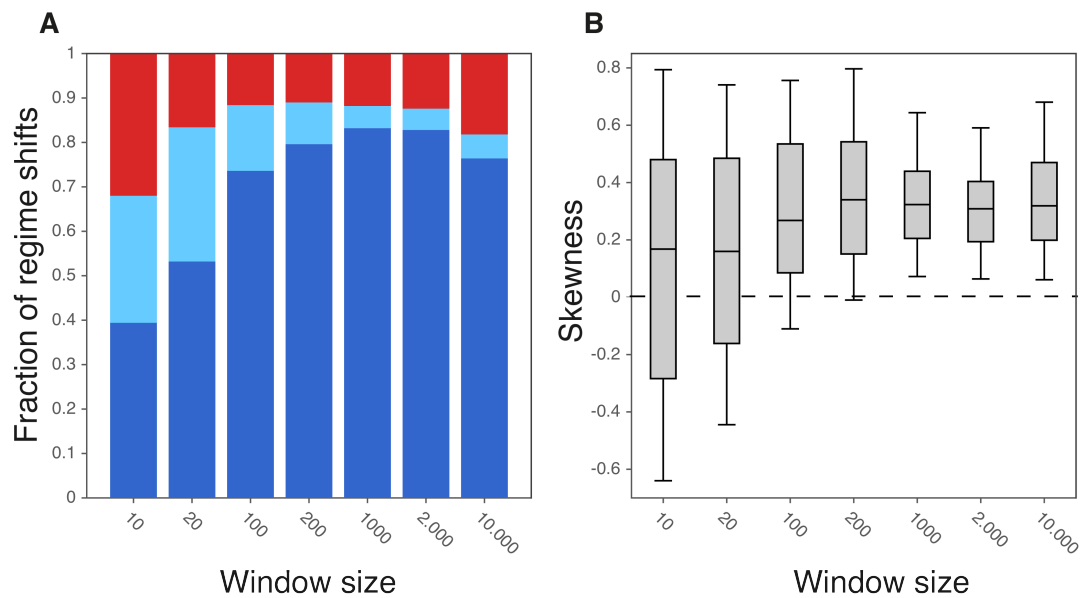


Figure A4.29: Performance of the indicator when the rolling window has a different length (lengths are indicated on the x-axis). **(A)** The fraction of accurately indicated regime shifts (dark blue), the fraction accurately indicated by the first principal component, i.e. the slope of the indicator is accurate, but not by the direction in which time points are skewed (light blue), and the fraction of inaccurately indicated regime shifts (red). **(B)** The skewness of time points projected on the first principal component. A positive skewness means that time points are skewed in the direction of a network's future state. The skewness is shown for regime shifts that were accurately indicated by the first principal component. Time series have a length of 20,000 time steps.

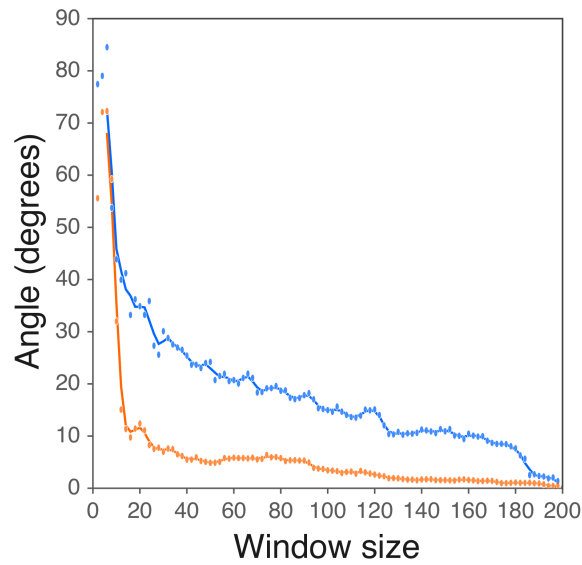


Figure A4.30: The extend in which the size of a rolling window affects the slope indicated by the first principal component far from a tipping point (blue) and close to a tipping point (orange). The y-axis corresponds to the difference in angle between the first principal component obtained for a window of 200 observations and for a window containing the number of observations indicated on the x-axis. The effect of an increasingly small window size on the direction of the first principal component is, in this example, much smaller close to a tipping point. Results are shown for the time series in Fig. 4.2.A at $M=0.1$ (blue) and $M=0.78$ (orange).



Chapter 5

Synthesis

J. Jelle Lever



The major, unanswered questions in ecology are often separated in two main classes: the fundamental ones, aiming to understand the basic processes shaping and occurring in ecosystems, and the applied ones, e.g. aiming to identify or reduce the risks associated with changing environmental conditions (Sutherland, 2006; Sutherland et al., 2013). In a time when ecosystems are confronted with rapid environmental change (Vitousek et al., 1997; Millenium Ecosystem Assessment, 2005; Rockström et al., 2009; Intergovernmental Panel on Climate Change, 2014; Steffen et al., 2015), it is, however, becoming increasingly clear that predicting the consequences of changing environmental conditions requires a fundamental understanding of the processes occurring in ecosystems. In particular, because such changes are likely to bring ecosystems outside of the range in conditions for which data are available. Questions on the stability of ecosystems in the context of such changes are thus both applied and fundamental, because their answers require the development of novel theories and hypothesis. Ecosystems are complex systems of many interacting species that may reorganize and shift towards alternative, potentially less desirable states when critical points are passed. Extrapolation of existing trends will thus not necessarily provide us with an accurate prediction of a system's future state. Detailed mechanistic models, on the other hand, might fail to incorporate the processes that are truly relevant for ecosystem dynamics, while more abstract models might be overly simplistic. Avoiding unnecessary details and/or strong simplifications requires a fundamental understanding of the key processes responsible for the stable coexistence of species, the services they provide, and the specific ways in which they might be undermined by changing environmental conditions.

Integrating basic with applied fields of research requires, in my view, an appreciation for the differences between the words 'complex' and 'complicated', and 'simple' and 'simplistic'. Complex systems are systems with emerging properties that result from the interactions between many components, while complicated systems are systems that are difficult to understand because of their complexity. Simple ideas may accurately describe the processes occurring in complex systems, but only when they are based on a basic understanding of how they work. When such understanding is absent, they must necessarily be simplistic. Life itself is an emerging property resulting from the chemical interactions and other processes involved in the functioning of complex organisms, and most biological and many non-biological systems have a complex nature. Approaches towards studying complexity in ecology, however, differ from other fields of research because it is the complexity of ecosystems itself or, more specifically, a diversity of species that is seen as an important, valuable property. We care less about complexity in other systems, e.g. we would be equally happy with a less complex brain as long as we remain equally intelligent, and in technological or societal systems, complexity is often something we wish to reduce when it is inefficient or costly. It is, perhaps, this admiration for the complexity as well as for the differences among ecosystems that may have promoted the idea that ecosystems are not only complex, but also complicated.

The idea that ecosystems are complicated, or at least that they are more complicated than many other complex systems is, in my view, debatable. Efforts made over the past 150 years, as described in **Chapter 1**, provide a - still incomplete - but increasingly clear image of what ecosystems are like. Ecosystems are unique, just like humans or other complex organisms, but they also have many properties in common. In particular, similarities were found in the properties determining ecosystem dynamics, such as recurring structural patterns in ecological networks and the body masses of species determining metabolic rates. The overall image that arises is one of intermediate complexity. The number of species involved in ecological networks is, for example, usually much smaller than the number of genes involved in gene regulatory networks, and ecosystem dynamics are not necessarily more complex than, for example, changes in local climate conditions. When studying ecosystems, we should thus not hesitate to apply the tools already available to study complex dynamical systems as they were often developed for other, more complicated systems.

Some fields of research are particularly likely to develop insights in the dynamics of complex systems that are of importance to ecology. Debates on whether complex morphologies and other species traits are the result of external processes and natural selection or the result of complex self-organizing processes held in the context of evolutionary developmental biology, are, for example, akin to discussions on what determines the structure and stability of ecosystems (Alberch, 1989; Kauffman, 1993; Bastolla et al., 2009; Rohr et al., 2014). We all know that oil droplets in water and soap bubbles are spherical and that snowflakes have complex structures that emerge without natural selection. In living systems it is, most likely, the interplay between natural selection and self-organization that determines the shapes and forms we eventually observe (Alberch, 1989; Kauffman, 1993). Such self-organization occurs because it is impossible for certain combinations of traits to co-occur within a single organism, just as certain combinations of species cannot co-exist in a single ecosystem. Such combinations are, like square droplets, intrinsically unstable. In **Chapter 2** we show that ecological network structures that promote such intrinsic stability may come with a trade-off in mutualistic plant-pollinator communities. Communities in which species indirectly support each other may survive longer under increasingly harsh circumstances. Once a tipping point is passed, however, species may also collapse simultaneously because they depend on each other for survival. Similar trade-offs may occur in other complex systems, such as in financial systems where similar network structural patterns were found (May et al., 2008; Saavedra et al., 2009). Such systemic shifts occur because of the specific way in which they are organized. Just like, when a soap bubble pops, it has consequences for all the molecules forming a bubble because of the specific way in which they interact with each other.

Other fundamental insights may come from studies on the interplay between network structural patterns and the dynamics of complex systems. The Belgian biologist René Thomas suggested in 1981, based on his analysis of ‘regulatory circuits’ or ‘feedback

loops' in gene regulatory networks, that alternative stable states may exist only when a system contains at least one positive feedback and that sustained oscillations may occur only when there is at least one negative feedback between two or more elements (Thomas, 1981). Conjectures that were later proven more rigorously by Snoussi (1998) and Gouzé (1998). Critical transitions between alternative stable states in ecosystems are typically associated with a gradual increase in the relative strength of positive feedbacks (Scheffer et al., 2001), and are certainly the most likely cause of instability in simple one-dimensional models of ecosystem dynamics as well as in networks of mutualistically interacting species, because the negative feedbacks required for oscillatory or other, more complex dynamics are weak. Positive feedbacks are, however, not the only likely cause of instability in other systems. The delayed negative effects of predators and prey on themselves when either increasing or decreasing the abundance of the species they interact with are, for example, a known cause of oscillations in the abundances of predators and prey (Rosenzweig & MacArthur, 1963; Rosenzweig, 1971; Levins, 1974; Puccia & Levins, 1985; Goldbeter, 1996). Chaotic dynamics may occur when two such oscillators are coupled, e.g. in a food chain (Hastings & Powell, 1991; McCann & Yodzis, 1994; De Feo & Rinaldi, 1998).

Observations in real food webs suggest that oscillatory or other, more complex dynamics caused by strong predator-prey interactions are damped by many weak interactions (McCann et al., 1998; Berlow, 1999; Neutel et al., 2002; Bascompte et al., 2005). In **Chapter 3** we describe different types of critical transitions that may occur when such stabilizing patterns are gradually undermined by changing environmental conditions. Perhaps surprisingly, we found that a gradual decline leading to the extinction of a single species may trigger abrupt regime shifts when the remaining set of species is unstable. Feasible food webs, i.e. food webs in which the amount of resources available to species is sufficient to maintain a population while being predated upon by other species, may also become unstable without such a decline in abundance. Stability may be lost when boundaries in parameter space are crossed leading to oscillatory or chaotic dynamics in the absence of alternative stable states, or to transitions to alternative stable subsets of species when such subsets are stable at the time of a transition. These findings are important because they point towards another potential cause of abrupt critical transitions in complex ecosystems, namely an increase in the relative strength of delayed negative feedbacks. Predicting a system's future state after such transitions is difficult, in particular when changing environmental conditions have multiple simultaneous effects on species and the interactions between them, i.e. when the effects of changing environmental conditions are complex. A scenario that seems particularly likely in the context of climate change which is known to simultaneously alter the distribution, phenology, physiology, behavior, and relative abundances of species. Changes that, in turn, may affect the strengths of interactions between species (Kareiva et al. 1993; Winder & Schindler 2004; Suttle et al. 2007; Tylianakis et al. 2008; Doney et al. 2012; Blois et al. 2013; Burkle et al. 2013; Urban et al. 2016; Romero et al. 2018; Usinowicz & Levine 2018).

Large-scale critical transitions caused by small but complex environmental changes are only likely when a system is close to a boundary in parameter space beyond which a shift occurs towards a fundamentally different state, e.g. a partly or fully collapsed state (Fig. 5.1 and **Chapter 3**). Knowing the proximity and nature of such boundaries is thus of great importance. The interrelationships between the properties of complex ecosystems, the size of the area, and the nature of the boundaries to the area within which species may coexist stably are, however, largely unknown (but see Bastolla et al. 2009, Rohr et al. 2014, and **Chapter 2**), which makes it difficult to assess the likelihood of large-scale critical transitions in complex ecosystems. Some general rules may, however, exist. Ecosystems in which species are limited by their capacity to handle resources provided by other species, e.g. a prey or a mutualistic partner, rather than by the amount of resources available, are less sensitive to changes in resource availability. This, in turn, makes a decline in abundance less likely and reduces the strength of destabilizing positive or negative feedbacks. Such ecosystems can thus be expected to be more like the situation depicted in Fig. 5.1.B.I or C.I. When species are less saturated, more in depth analysis are needed to be able to distinguish between the situation in Fig. 5.1.B.II and C.II.

Results in **Chapter 3** suggest that network structural properties such as the number of species and interactions, and the distribution of interaction strengths play an important role in the likelihood of large-scale critical transitions. Such general properties may thus give an indication of whether large-scale critical transitions are likely to occur in complex ecosystems. Other, more specific indicators of a system's likely future state may be obtained when studying of the specific way in which the relative strengths of destabilizing positive or negative feedbacks change under the influence of changing environmental conditions. The specific arrangement of positive and negative interactions in destabilizing negative feedbacks leading to oscillatory dynamics, for example, determines the order in which species increase and decrease in abundance, and the nature of positive feedbacks determines which species are likely to change in opposing directions when a system moves away from an unstable equilibrium (Fig. 5.2). The dynamics of complex ecosystems after impending critical transitions may thus, in part, be predicted when studying the specific nature of destabilizing feedbacks prior to such regime shifts.

Systems in which positive feedbacks are strong relative to delayed negative feedbacks are likely to behave more predictable than systems in which this is the other way around, simply because the amplifying effects of positive feedbacks are simpler than the complex dynamics that may occur due to several interacting delayed negative feedbacks. In **Chapter 4** we show that such relative simplicity may allow us to look beyond impending critical transitions and foresee the future state of communities in which mutually beneficial interactions are strong relative to other interaction types. To make such predictions, we build further on earlier work that has shown that system's recover increasingly slowly from perturbations prior to critical transitions, i.e. a phenomenon known as critical slowing down (Wissel, 1984; Van Nes & Scheffer, 2007). Such disturbances have a size (i.e.

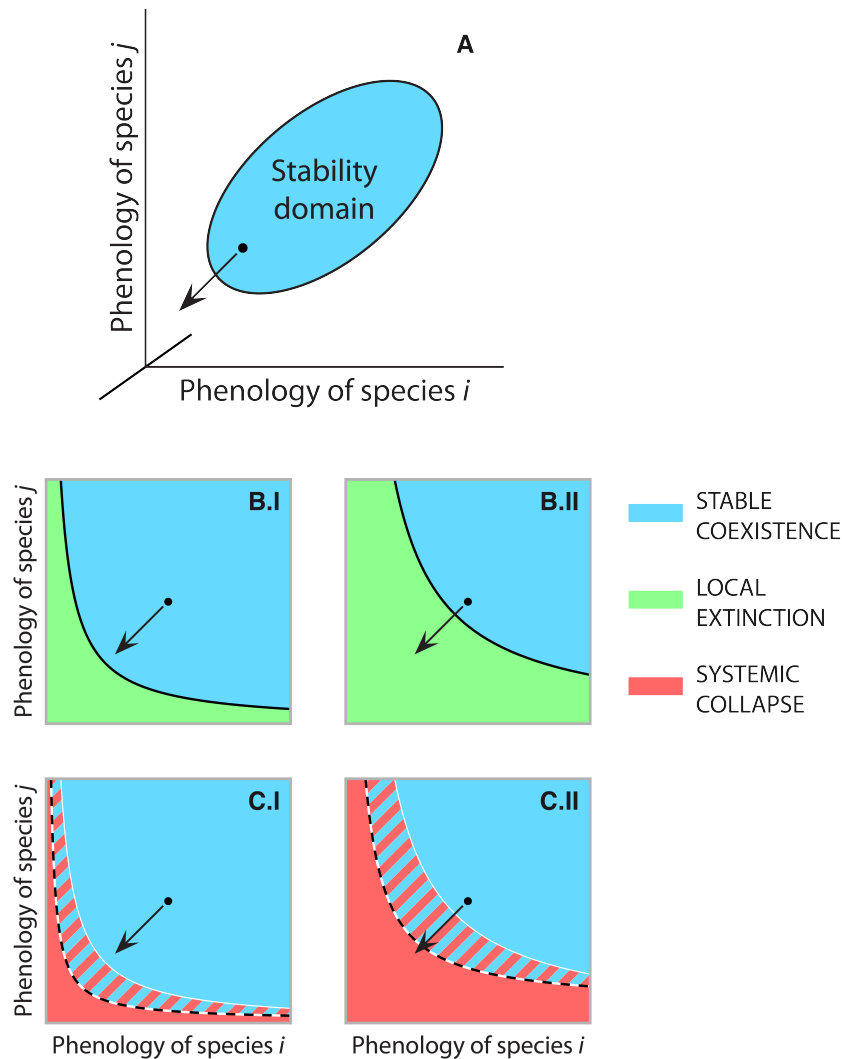


Figure 5.1: Complex, simultaneous effects of climate change on the phenology, e.g. the period of the year in which species are or become active, and the stable coexistence of species. **(A)** Stability domain within which all species may coexist stably. When such a domain is large, a system may handle a relatively large change in conditions. A possible effect of climate change away from an initial condition is indicated by a dot and arrow. **(B)** Example in which a similar change in conditions remains within the stability domain (B.I), and an example in which a boundary is crossed leading to the extinction of a single species (B.II). **(C)** Example in which a similar change in conditions remains within the stability domain (C.I), and an example in which a boundary is crossed leading to a partial or full collapse of an ecosystem (C.II). Striped areas indicate regions with alternative stable states. Recovery from such a collapse thus requires a relatively large change in conditions, i.e. hysteresis. Large, systemic transitions as a consequence of small but complex environmental changes are only likely in panel C.II. Similar graphs can be made for any change in environmental conditions and the multiple, simultaneous effects they might have on species and the interactions between them.

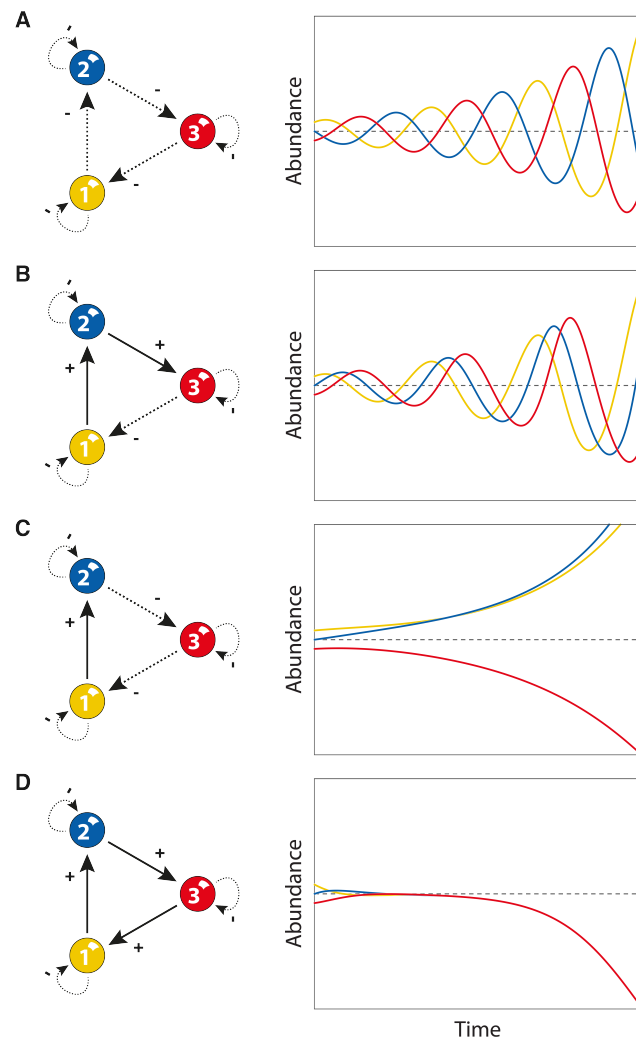


Figure 5.2: Destabilizing effects of three-species feedback loops around a system's unstable, nontrivial equilibrium. **(A)** Oscillatory dynamics caused by a negative feedback of three negative interactions. An increase in species 1 is, with some delay, followed by a decrease in species 2 which is followed by an increase in species 3 which, in turn, is followed by a decrease in species 1. **(B)** Oscillatory dynamics caused by a negative feedback of two positive and one negative interaction. An increase in species 1 is, with some delay, followed by an increase in species 2 which is followed by an increase in species 3 which, in turn, is followed by a decrease in species 1. **(C)** Amplifying effect caused by a positive feedback of one positive and two negative interactions. Species 1 and 2 increase while species 3 declines or vice versa (depending on initial abundances) **(D)** Amplifying effect caused by a positive feedback of three positive interactions. Species 1, 2, and 3 decline or increase together (depending on initial abundances). Feedbacks are negative when they consist of an odd number and positive when consisting of an even number of negative interactions. Species are assumed to have a direct negative effect on themselves which has a stabilizing effect. Dashed grey lines indicate nontrivial equilibrium abundances.

the total amount of change) and a direction (i.e. the relative amount of change in each species) in the phase space of complex systems. The more similar a disturbance's direction to the direction in which increasingly small perturbations may cause critical transitions, the stronger the effect of critical slowing down. Provided that there are no oscillating, chaotic or other complex dynamics, a system's future state will most likely lie in the same approximate direction. This 'direction of critical slowing down' may thus provide us with an indicator of a system's future state, and may help us assess whether impending critical transitions have large, systemic consequences. As an indicator of the direction of critical slowing down we propose to use the direction in which the distribution of fluctuating species abundances becomes increasingly asymmetrical, but other methods to determine this direction may be possible as well.

Some of the currently largest and unaddressed questions in ecology involve the inter-relationship between the fundamental processes allowing species to coexist in complex ecosystems and the ways in which these processes might be undermined by changing environmental conditions. While a relatively large number of studies has addressed the classical question posed by May (1972, 1973): "When will a large complex system be stable?", less attention has been given to the specific ways in which biodiversity might be lost. In a time when ecosystems are under increasing pressure from changing environmental conditions, this question is however of great importance. In particular, because critical transitions may occur towards other potentially less desirable states. In this thesis, I hope to have provided novel ideas and insights that might help to address the question of whether changing environmental conditions are likely to lead to large-scale systemic regime shifts in complex ecosystems. A distinguishing feature of such transitions is that they emerge from the specific ways in which species relate to each other and affect a large number of species rather than species in isolation. Assessing the probability and the potential consequences of such transitions requires a fundamental understanding of the specific ways in which species tend to relate to each other in complex ecosystems and how these relationships might change due to changing environmental conditions. An emerging property that may be referred to as 'systemic risk' (United Nations International Strategy for Disaster Reduction, 2009).

References

- Alberch, P. (1989). The logic of monsters: evidence for internal constraint in development and evolution. *Geobios*, *22*, 21–57.
- Albert, R., Jeong, H., & Barabási, A.-L. (2000). Error and attack tolerance of complex networks. *Nature*, *406*, 378–382.
- Allen-Wardell, G. et al. (1998). The Potential Consequences of Pollinator Declines on the Conservation of Biodiversity and Stability of Food Crop Yields. *Conserv. Biol.*, *12*, 8–17.
- Alley, R. B., Marotzke, J., Nordhaus, W. D., Overpeck, J. T., Peteet, D. M., Pielke, R. A., Pierrehumbert, R. T., Rhines, P. B., Stocker, T. F., Talley, L. D. et al. (2003). Abrupt climate change. *Science*, *299*, 2005–2010.
- Angeli, D., Ferrell, J. E., & Sontag, E. D. (2004). Detection of multistability, bifurcations, and hysteresis in a large class of biological positive-feedback systems. *Proc. Natl. Acad. Sci. U.S.A.*, *101*, 1822–1827.
- Arim, M., & Marquet, P. A. (2004). Intraguild predation: a widespread interaction related to species biology. *Ecol. Lett.*, *7*, 557–564.
- Arrindell, W. A., & Van der Ende, J. (1985). An empirical test of the utility of the observations-to-variables ratio in factor and components analysis. *Appl. Psychol. Meas.*, *9*, 165–178.
- Arthur, W. B. (1989). Competing technologies, increasing returns, and lock-in by historical events. *Econ. J.*, *99*, 116–131.
- Barabási, A.-L., & Albert, R. (1999). Emergence of scaling in random networks. *Science*, *286*, 509–512.
- Barrett, P. T., & Kline, P. (1981). The observation to variable ratio in factor analysis. *Personality Study & Group Behaviour*, *1*, 23–33.
- Bascompte, J., & Jordano, P. (2007). Plant-animal mutualistic networks: The architecture of biodiversity. *Annu. Rev. Ecol. Evol. Syst.*, *38*, 567–593.
- Bascompte, J., Jordano, P., Melián, C. J., & Olesen, J. M. (2003). The nested assembly of plant–animal mutualistic networks. *Proc. Natl. Acad. Sci. U.S.A.*, *100*, 9383–9387.

- Bascompte, J., Jordano, P., & Olesen, J. M. (2006). Asymmetric coevolutionary networks facilitate biodiversity maintenance. *Science*, *312*, 431–433.
- Bascompte, J., Melián, C. J., & Sala, E. (2005). Interaction strength combinations and the overfishing of a marine food web. *Proc. Natl. Acad. Sci. U.S.A.*, *102*, 5443–5447.
- Bastolla, U., Fortuna, M. A., Pascual-García, A., Ferrera, A., Luque, B., & Bascompte, J. (2009). The architecture of mutualistic networks minimizes competition and increases biodiversity. *Nature*, *458*, 1018–1020.
- Bastolla, U., Lässig, M., Manrubia, S. C., & Valleriani, A. (2005). Biodiversity in model ecosystems, i: coexistence conditions for competing species. *J. Theor. Biol.*, *235*, 521–530.
- Beckage, B., Gross, L. J., & Kauffman, S. (2011). The limits to prediction in ecological systems. *Ecosphere*, *2*, 1–12.
- Benincà, E., Huisman, J., Heerkloss, R., Jöhnk, K. D., Branco, P., Van Nes, E. H., Scheffer, M., & Ellner, S. P. (2008). Chaos in a long-term experiment with a plankton community. *Nature*, *451*, 822–825.
- Berlow, E. L. (1999). Strong effects of weak interactions in ecological communities. *Nature*, *398*, 330.
- Bersier, L.-F. (2007). A history of the study of ecological networks. In F. Kepes (Ed.), *Biological networks*. World Scientific Pub Co. Pte. Inc., Singapore.
- Bertness, M. D., & Callaway, R. (1994). Positive interactions in communities. *Trends Ecol. Evol.*, *9*, 191–193.
- Biesmeijer, J., Roberts, S., Reemer, M., Ohlemüller, R., Edwards, M., Peeters, T., Schaffers, A., Potts, S., Kleukers, R., Thomas, C. et al. (2006). Parallel declines in pollinators and insect-pollinated plants in Britain and the Netherlands. *Science*, *313*, 351–354.
- Blois, J. L., Zarnetske, P. L., Fitzpatrick, M. C., & Finnegan, S. (2013). Climate change and the past, present, and future of biotic interactions. *Science*, *341*, 499–504.
- Brose, U., Jonsson, T., Berlow, E. L., Warren, P., Banasek-Richter, C., Bersier, L.-F., Blanchard, J. L., Brey, T., Carpenter, S. R., Blandenier, M.-F. C. et al. (2006a). Consumer-resource body-size relationships in natural food webs. *Ecology*, *87*, 2411–2417.
- Brose, U., Williams, R. J., & Martinez, N. D. (2006b). Allometric scaling enhances stability in complex food webs. *Ecol. Lett.*, *9*, 1228–1236.
- Brown, J. H., Gillooly, J. F., Allen, A. P., Savage, V. M., & West, G. B. (2004). Toward a metabolic theory of ecology. *Ecology*, *85*, 1771–1789.
- Bryden, J., Gill, R. J., Mitton, R. A., Raine, N. E., & Jansen, V. A. (2013). Chronic sublethal stress causes bee colony failure. *Ecol. Lett.*, *16*, 1463–1469.

- Burgos, E., Ceva, H., Perazzo, R. P., Devoto, M., Medan, D., Zimmermann, M., & María Delbue, A. (2007). Why nestedness in mutualistic networks? *J. Theor. Biol.*, *249*, 307–313.
- Burkle, L. A., Marlin, J. C., & Knight, T. M. (2013). Plant-pollinator interactions over 120 years: loss of species, co-occurrence, and function. *Science*, *339*, 1611–1615.
- Cai, T., Fan, J., & Jiang, T. (2013). Distributions of angles in random packing on spheres. *J. Mach. Learn. Res.*, *14*, 1837–1864.
- Callaway, R. M. (1995). Positive interactions among plants. *Bot. Rev.*, *61*, 306–349.
- Camerano, L. (1880). Dell'equilibrio dei viventi mercé la reciproca distruzione. *Accademia delle Scienze di Torino*, *15*, 393–414.
- Camerano, L. (1994). On the equilibrium of living beings by means of reciprocal destruction. In S. A. Levin (Ed.), *Frontiers in mathematical biology* (pp. 360–380). Springer-Verlage, Berlin.
- Carbone, C., Mace, G. M., Roberts, S. C., & Macdonald, D. W. (1999). Energetic constraints on the diet of terrestrial carnivores. *Nature*, *402*, 286–288.
- Cattin, M.-F., Bersier, L.-F., Banašek-Richter, C., Baltensperger, R., & Gabriel, J.-P. (2004). Phylogenetic constraints and adaptation explain food-web structure. *Nature*, *427*, 835–839.
- Chase, J. M., Abrams, P. A., Grover, J. P., Diehl, S., Chesson, P., Holt, R. D., Richards, S. A., Nisbet, R. M., & Case, T. J. (2002). The interaction between predation and competition: a review and synthesis. *Ecol. Lett.*, *5*, 302–315.
- Chen, L., Liu, R., Liu, Z.-P., Li, M., & Aihara, K. (2012). Detecting early-warning signals for sudden deterioration of complex diseases by dynamical network biomarkers. *Sci. Rep.*, *2*.
- Chen, S., O'Dea, E. B., Drake, J. M., & Epureanu, B. I. (2019). Eigenvalues of the covariance matrix as early warning signals for critical transitions in ecological systems. *Sci. Rep.*, *9*, 2572.
- Clark, J. S., Carpenter, S. R., Barber, M., Collins, S., Dobson, A., Foley, J. A., Lodge, D. M., Pascual, M., Pielke, R., Pizer, W. et al. (2001). Ecological forecasts: an emerging imperative. *Science*, *293*, 657–660.
- Clark, P. U., Pisias, N. G., Stocker, T. F., & Weaver, A. J. (2002). The role of the thermohaline circulation in abrupt climate change. *Nature*, *415*, 863–869.
- Cody, M. L. (1966). A general theory of clutch size. *Evolution*, *20*, 174–184.
- Cody, M. L. (1974). *Competition and the structure of bird communities* volume 7. Princeton University Press, Princeton, NJ.
- Cohen, J., Briand, F., & Newman, C. (1990). *Community food webs: data and theory*

- volume 20. Springer, Berlin.
- Cohen, J. E. (1977). Food webs and the dimensionality of trophic niche space. *Proc. Natl. Acad. Sci. U.S.A.*, *74*, 4533–4536.
- Cohen, J. E. (1994). Lorenzo camerano's contribution to early food web theory. In S. A. Levin (Ed.), *Frontiers in mathematical biology* (pp. 351–359). Springer-Verlag, Berlin.
- Cohen, J. E., Jonsson, T., & Carpenter, S. R. (2003). Ecological community description using the food web, species abundance, and body size. *Proc. Natl. Acad. Sci. U.S.A.*, *100*, 1781–1786.
- Cohen, J. E., & Newman, C. M. (1985). A stochastic theory of community food webs i. models and aggregated data. *Proceedings of the Royal society of London. Series B. Biological sciences*, *224*, 421–448.
- Cohen, J. E., Pimm, S. L., Yodzis, P., & Saldaña, J. (1993). Body sizes of animal predators and animal prey in food webs. *J. Anim. Ecol.*, *62*, 67–78.
- Cohen, J. E., & Stephens, D. W. (1978). *Food webs and niche space*. 11. Princeton University Press, Princeton, NJ.
- Coreau, A., Pinay, G., Thompson, J. D., Cheptou, P.-O., & Mermet, L. (2009). The rise of research on futures in ecology: rebalancing scenarios and predictions. *Ecol. Lett.*, *12*, 1277–1286.
- Courchamp, F., Clutton-Brock, T., & Grenfell, B. (1999). Inverse density dependence and the allee effect. *Trends Ecol. Evol.*, *14*, 405–410.
- Cyr, H., & Face, M. L. (1993). Magnitude and patterns of herbivory in aquatic and terrestrial ecosystems. *Nature*, *361*, 148–150.
- Dai, L., Vorselen, D., Korolev, K. S., & Gore, J. (2012). Generic indicators for loss of resilience before a tipping point leading to population collapse. *Science*, *336*, 1175–1177.
- Dakos, V. (2018). Identifying best-indicator species for abrupt transitions in multispecies communities. *Ecol. Indic.*, *94*, 494–502.
- Dakos, V., & Bascompte, J. (2014). Critical slowing down as early warning for the onset of collapse in mutualistic communities. *Proc. Natl. Acad. Sci. U.S.A.*, *111*, 17546–17551.
- Dakos, V., Carpenter, S. R., Brock, W. A., Ellison, A. M., Guttal, V., Ives, A. R., Kéfi, S., Livina, V., Seekell, D. A., van Nes, E. H., & Scheffer, M. (2012). Methods for detecting early warnings of critical transitions in time series illustrated using simulated ecological data. *PLoS One*, *7*, e41010.
- Dambacher, J. M., Luh, H.-K., Li, H. W., & Rossignol, P. A. (2003). Qualitative stability and ambiguity in model ecosystems. *Am. Nat.*, *161*, 876–888.
- De Feo, O., & Rinaldi, S. (1998). Singular homoclinic bifurcations in tritrophic food

- chains. *Math. Biosci.*, 148, 7–20.
- De Ruiter, P. C., Neutel, A.-M., & Moore, J. C. (1995). Energetics, patterns of interaction strengths, and stability in real ecosystems. *Science*, 269, 1257–1260.
- Dean, A. M. (1983). A simple model of mutualism. *Am. Nat.*, 121, 409–417.
- Diamond, D. W., & Dybvig, P. H. (1983). Bank runs, deposit insurance, and liquidity. *J. Political Econ.*, 91, 401–419.
- Diaz, S., Chapin III, F., & Potts, S. (2005). Biodiversity regulation of ecosystem services. In *Ecosystems and human well-being*. Island Press, Washington, DC.
- Dodd, M. S., Papineau, D., Grenne, T., Slack, J. F., Rittner, M., Pirajno, F., O’Neil, J., & Little, C. T. (2017). Evidence for early life in earth’s oldest hydrothermal vent precipitates. *Nature*, 543, 60.
- Doney, S. C., Ruckelshaus, M., Emmett Duffy, J., Barry, J. P., Chan, F., English, C. A., Galindo, H. M., Grebmeier, J. M., Hollowed, A. B., Knowlton, N. et al. (2012). Climate change impacts on marine ecosystems. *Annu. Rev. Mar. Sci.*, 4, 11–37.
- Drake, J. M., & Griffen, B. D. (2010). Early warning signals of extinction in deteriorating environments. *Nature*, 467, 456–459.
- Easley, D., & Kleinberg, J. (2010). *Networks, crowds, and markets: Reasoning about a highly connected world*. Cambridge University Press, Cambridge.
- Elton, C. S. (1927). *Animal ecology*. University of Chicago Press, Chicago, IL.
- Elton, C. S. (1958). *The ecology of invasions by animals and plants*. University of Chicago Press, Chicago, IL.
- Emmerson, M. C., & Raffaelli, D. (2004). Predator–prey body size, interaction strength and the stability of a real food web. *J. Anim. Ecol.*, 73, 399–409.
- Enquist, B. J., West, G. B., Charnov, E. L., & Brown, J. H. (1999). Allometric scaling of production and life-history variation in vascular plants. *Nature*, 401, 907–911.
- Ernest, S., Enquist, B. J., Brown, J. H., Charnov, E. L., Gillooly, J. F., Savage, V. M., White, E. P., Smith, F. A., Hadly, E. A., Haskell, J. P. et al. (2003). Thermodynamic and metabolic effects on the scaling of production and population energy use. *Ecol. Lett.*, 6, 990–995.
- Evans, M. R., Bithell, M., Cornell, S. J., Dall, S. R., Díaz, S., Emmott, S., Ernande, B., Grimm, V., Hodgson, D. J., Lewis, S. L. et al. (2013). Predictive systems ecology. *Proc. Royal Soc. B*, 280, 20131452.
- Evans, M. R., Norris, K. J., & Benton, T. G. (2012). Predictive ecology: systems approaches. *Philos. Trans. Royal Soc. B*, 367, 163–167.
- Ferrell Jr, J. E. (2002). Self-perpetuating states in signal transduction: positive feedback, double-negative feedback and bistability. *Curr. Opin. Cell Biol.*, 14, 140–148.

- Forbes, S. A. (1925). The lake as a microcosm. *Ill. Nat. Hist. Surv. Bull.*, 15.
- Fortuna, M. A., & Bascompte, J. (2006). Habitat loss and the structure of plant-animal mutualistic networks. *Ecol. Lett.*, 9, 278–283.
- Gantmacher, F. R. (1959). *The Theory of Matrices*. Chelsea Publishing Company, London.
- Gardner, M. R., & Ashby, W. R. (1970). Connectance of large dynamic (cybernetic) systems: critical values for stability. *Nature*, 228, 784.
- Garibaldi, L. A., Steffan-Dewenter, I., Winfree, R., Aizen, M. A., Bommarco, R., Cunningham, S. A., Kremen, C., Carvalheiro, L. G., Harder, L. D., Afik, O. et al. (2013). Wild pollinators enhance fruit set of crops regardless of honey bee abundance. *Science*, 339, 1608–1611.
- Gaston, K. J., & Fuller, R. A. (2008). Commonness, population depletion and conservation biology. *Trends Ecol. Evol.*, 23, 14–19.
- Ghazoul, J. (2006). Floral diversity and the facilitation of pollination. *J. Ecol.*, 94, 295–304.
- Gillooly, J. F., Brown, J. H., West, G. B., Savage, V. M., & Charnov, E. L. (2001). Effects of size and temperature on metabolic rate. *Science*, 293, 2248–2251.
- Gilpin, M. E. (1975). Stability of feasible predator-prey systems. *Nature*, 254, 137.
- Glendening, G. E. (1952). Some quantitative data on the increase of mesquite and cactus on a desert grassland range in southern arizona. *Ecology*, 33, 319–328.
- Goh, B. S. (1977). Global stability in many-species systems. *Am. Nat.*, 111, 135–143.
- Goldbeter, A. (1996). *Biochemical oscillations and cellular rhythms: the molecular bases of periodic and chaotic behaviour*. Cambridge University Press, Cambridge.
- Gouzé, J.-L. (1998). Positive and negative circuits in dynamical systems. *J. Biol. Syst.*, 6, 11–15.
- Grebogi, C., Ott, E., & Yorke, J. A. (1983). Crises, sudden changes in chaotic attractors, and transient chaos. *Physica D*, 7, 181–200.
- Grime, J. P. (1979). *Plant strategies and vegetation processes*. John Wiley & Sons, New York, NY.
- Hairston, N. G., Smith, F. E., & Slobodkin, L. B. (1960). Community structure, population control, and competition. *Am. Nat.*, 94, 421–425.
- Haldane, A. G., & May, R. M. (2011). Systemic risk in banking ecosystems. *Nature*, 469, 351–355.
- Hanski, I. (1998). Metapopulation dynamics. *Nature*, 396, 41–49.
- Hare, S. R., & Mantua, N. J. (2000). Empirical evidence for north pacific regime shifts

- in 1977 and 1989. *Prog. Oceanogr.*, *47*, 103–145.
- Hastings, A., & Powell, T. (1991). Chaos in a three-species food chain. *Ecology*, *72*, 896–903.
- Hastings, A., & Wysham, D. B. (2010). Regime shifts in ecological systems can occur with no warning. *Ecol. Lett.*, *13*, 464–472.
- Hasty, J., McMillen, D., & Collins, J. J. (2002). Engineered gene circuits. *Nature*, *420*, 224–230.
- He, Q., Bertness, M. D., & Altieri, A. H. (2013). Global shifts towards positive species interactions with increasing environmental stress. *Ecol. Lett.*, *16*, 695–706.
- Held, H., & Kleinen, T. (2004). Detection of climate system bifurcations by degenerate fingerprinting. *Geophys. Res. Lett.*, *31*, L23207.
- Henry, M., Beguin, M., Requier, F., Rollin, O., Odoux, J.-F., Aupinel, P., Aptel, J., Tchamitchian, S., & Decourtye, A. (2012). A common pesticide decreases foraging success and survival in honey bees. *Science*, *336*, 348–350.
- Hirota, M., Holmgren, M., Van Nes, E. H., & Scheffer, M. (2011). Global resilience of tropical forest and savanna to critical transitions. *Science*, *334*, 232–235.
- Hofbauer, J., & Sigmund, K. (1988). *Evolutionary games and population dynamics*. Cambridge University Press, Cambridge.
- Holling, C. S. (1973). Resilience and stability of ecological systems. *Annu. Rev. Ecol. Evol. Syst.*, *4*, 1–23.
- Holling, C. S. (1996). Engineering resilience versus ecological resilience. In P. Schulze (Ed.), *Engineering within ecological constraints* (pp. 31–43). The National Academies Press, Washington, DC.
- Holmgren, M., Scheffer, M., & Huston, M. A. (1997). The interplay of facilitation and competition in plant communities. *Ecology*, *78*, 1966–1975.
- Holt, R. D. (1977). Predation, apparent competition, and the structure of prey communities. *Theor. Popul. Biol.*, *12*, 197–229.
- Holt, R. D., Grover, J., & Tilman, D. (1994). Simple rules for interspecific dominance in systems with exploitative and apparent competition. *Am. Nat.*, *144*, 741–771.
- Høye, T. T., Post, E., Schmidt, N. M., Trøjelsgaard, K., & Forchhammer, M. C. (2013). Shorter flowering seasons and declining abundance of flower visitors in a warmer arctic. *Nat. Clim. Change*, *3*, 759–763.
- Huisman, J., & Weissing, F. J. (1999). Biodiversity of plankton by species oscillations and chaos. *Nature*, *402*, 407–410.
- Hurwitz, A. (1895). Ueber die bedingungen, unter welchen eine gleichung nur wurzeln mit negativen reellen theilen besitzt. *Math. Ann.*, *46*, 273–284.

- Hutchinson, G. E. (1957). Concluding remarks. *Cold Spring Harbor Symp. Quant. Biol.*, *22*, 415–427.
- Hutchinson, G. E., Bonatti, E., Cowgill, U. M., Goulden, C. E., Leventhal, E. A., Mallett, M., Margaritora, F., Patrick, R., Racek, A., Roback, S. A. et al. (1970). Ianula: an account of the history and development of the lago di monterosi, latium, italy. *Trans. Am. Phil. Soc.*, *60*, 1–178.
- Hutson, V., & Law, R. (1985). Permanent coexistence in general models of three interacting species. *J. Math. Biol.*, *21*, 285–298.
- Hutson, V., & Vickers, G. (1983). A criterion for permanent coexistence of species, with an application to a two-prey one-predator system. *Math. Biosci.*, *63*, 253–269.
- Huxley, J. (1932). *Problems of relative growth*. Methuen and Co., Ltd., London.
- Intergovernmental Panel on Climate Change (2014). *Climate Change 2014: Synthesis Report. Contribution of Working Groups I, II and III to the Fifth Assessment Report of the Intergovernmental Panel on Climate Change* volume 5. IPCC, Geneva.
- Ives, A. R., & Carpenter, S. R. (2007). Stability and diversity of ecosystems. *Science*, *317*, 58–62.
- Jiang, J., Huang, Z.-G., Seager, T. P., Lin, W., Grebogi, C., Hastings, A., & Lai, Y.-C. (2018). Predicting tipping points in mutualistic networks through dimension reduction. *Proc. Natl. Acad. Sci. U.S.A.*, *115*, E639–E647.
- Jordano, P. (1987). Patterns of mutualistic interactions in pollination and seed dispersal: connectance, dependence asymmetries, and coevolution. *Am. Nat.*, *129*, 657–677.
- Jordano, P., Bascompte, J., & Olesen, J. M. (2003). Invariant properties in coevolutionary networks of plant–animal interactions. *Ecol. Lett.*, *6*, 69–81.
- Kareiva, P. M., Kingsolver, J. G., Huey, R. B. et al. (1993). *Biotic interactions and global change*. Sinauer Associates Inc., Sunderland, MA.
- Kauffman, S. A. (1993). *The origins of order: Self-organization and selection in evolution*. Oxford University Press, Oxford.
- Kefi, S., S., Rietkerk, M., Alados, C., Pueyo, Y., Papanastasis, V., ElAich, A., & de Ruiter, P. (2007). Spatial vegetation patterns and imminent desertification in mediterranean arid ecosystems. *Nature*, *449*, 213–217.
- Kiers, E. T., Duhamel, M., Beesetty, Y., Mensah, J. A., Franken, O., Verbruggen, E., Fellbaum, C. R., Kowalchuk, G. A., Hart, M. M., Bago, A. et al. (2011). Reciprocal rewards stabilize cooperation in the mycorrhizal symbiosis. *Science*, *333*, 880–882.
- Kleiber, M. (1932). Body size and metabolism. *Hilgardia*, *6*, 315–353.
- Klein, A., Vaissiere, B., Cane, J., Steffan-Dewenter, I., Cunningham, S., Kremen, C., & Tscharntke, T. (2007). Importance of pollinators in changing landscapes for world

- crops. *Proc. R. Soc. London, Ser. B*, 274, 303–313.
- Kondoh, M. (2008). Building trophic modules into a persistent food web. *Proc. Natl. Acad. Sci. U.S.A.*, 105, 16631–16635.
- Kuznetsov, Y. A. (1995). *Elements of applied bifurcation theory* volume 112. Springer-Verlage, New York, NY.
- Lafferty, K. D., Allesina, S., Arim, M., Briggs, C. J., De Leo, G., Dobson, A. P., Dunne, J. A., Johnson, P. T., Kuris, A. M., Marcogliese, D. J. et al. (2008). Parasites in food webs: the ultimate missing links. *Ecol. Lett.*, 11, 533–546.
- Law, R., & Morton, R. D. (1996). Permanence and the assembly of ecological communities. *Ecology*, 77, 762–775.
- Lawton, J. H., & Warren, P. H. (1988). Static and dynamic explanations for patterns in food webs. *Trends Ecol. Evol.*, 3, 242–245.
- Lee, T. I., Rinaldi, N. J., Robert, F., Odom, D. T., Bar-Joseph, Z., Gerber, G. K., Hannett, N. M., Harbison, C. T., Thompson, C. M., Simon, I. et al. (2002). Transcriptional regulatory networks in *saccharomyces cerevisiae*. *Science*, 298, 799–804.
- Lehman, C. L., & Tilman, D. (2000). Biodiversity, stability, and productivity in competitive communities. *Am. Nat.*, 156, 534–552.
- Lenton, T. M., Held, H., Kriegler, E., Hall, J. W., Lucht, W., Rahmstorf, S., & Schellnhuber, H. J. (2008). Tipping elements in the earth's climate system. *Proc. Natl. Acad. Sci. U.S.A.*, 105, 1786–1793.
- Levins, R. (1974). Discussion paper: the qualitative analysis of partially specified systems. *Ann. N.Y. Acad. Sci.*, 231, 123–138.
- Lindeman, R. L. (1942). The trophic-dynamic aspect of ecology. *Ecology*, 23, 399–417.
- Logofet, D. O. (1993). *Matrices and Graphs Stability Problems in Mathematical Ecology*. CRC Press LLC, Boca Raton, FL.
- Lorenz, E. N. (1963). Deterministic nonperiodic flow. *J. Atmos. Sci.*, 20, 130–141.
- MacArthur, R. (1955). Fluctuations of animal populations and a measure of community stability. *Ecology*, 36, 533–536.
- MacArthur, R. H. (1962). Some generalized theorems of natural selection. *Proc. Natl. Acad. Sci. U.S.A.*, 48, 1893–1897.
- MacArthur, R. H., & Wilson, E. O. (1967). *The theory of island biogeography* volume 1. Princeton University Press, Princeton, NJ.
- MacCallum, R. C., Widaman, K. F., Zhang, S., & Hong, S. (1999). Sample size in factor analysis. *Psychol. Methods*, 4, 84–99.
- Maestre, F. T., Callaway, R. M., Valladares, F., & Lortie, C. J. (2009). Refining the

- stress-gradient hypothesis for competition and facilitation in plant communities. *J. Ecol.*, *97*, 199–205.
- Marsden, J. E., & McCracken, M. (1976). *The Hopf bifurcation and its applications*. Springer-Verlag, New York.
- May, R., Levin, S., & Sugihara, G. (2008). Complex systems: ecology for bankers. *Nature*, *451*, 893–895.
- May, R. M. (1972). Will a large complex system be stable. *Nature*, *238*, 413–414.
- May, R. M. (1973). *Stability and complexity in model ecosystems* volume 6. Princeton University Press, Princeton, NJ.
- May, R. M. (1974). Biological populations with nonoverlapping generations: stable points, stable cycles, and chaos. *Science*, *186*, 645–647.
- May, R. M. (1976). Simple models with very complicated dynamics. *Nature*, *261*, 459–467.
- May, R. M. (1977). Thresholds and breakpoints in ecosystems with a multiplicity of stable states. *Nature*, *269*, 471–477.
- May, R. M. (1978). Mathematical aspects of the dynamics of animal populations. In *Studies in Mathematical Ecology. II Populations and Communities*. Mathematical Association of America, Washington, DC.
- May, R. M. (2006). Network structure and the biology of populations. *Trends Ecol. Evol.*, *21*, 394–399.
- McCann, K. (2007). Protecting biostructure. *Nature*, *446*, 29.
- McCann, K., Hastings, A., & Huxel, G. R. (1998). Weak trophic interactions and the balance of nature. *Nature*, *395*, 794–798.
- McCann, K., & Yodzis, P. (1994). Biological conditions for chaos in a three-species food chain. *Ecology*, *75*, 561–564.
- McCann, K. S. (2000). The diversity–stability debate. *Nature*, *405*, 228–233.
- Medan, D., Perazzo, R. P., Devoto, M., Burgos, E., Zimmermann, M. G., Ceva, H., & Delbue, A. M. (2007). Analysis and assembling of network structure in mutualistic systems. *J. Theor. Biol.*, *246*, 510–512. doi:doi: 10.1016/j.jtbi.2006.12.033.
- Melián, C. J., Bascompte, J., Jordano, P., & Krivan, V. (2009). Diversity in a complex ecological network with two interaction types. *Oikos*, *118*, 122–130.
- Memmott, J., Craze, P. G., Waser, N. M., & Price, M. V. (2007). Global warming and the disruption of plant–pollinator interactions. *Ecol. Lett.*, *10*, 710–717.
- Memmott, J., Waser, N. M., & Price, M. V. (2004). Tolerance of pollination networks to species extinctions. *Proc. R. Soc. London, Ser. B*, *271*, 2605–2611.

-
- Millenium Ecosystem Assessment (2005). *Ecosystems and human well-being* volume 5. Island Press, Washington, DC.
- Milo, R., Shen-Orr, S., Itzkovitz, S., Kashtan, N., Chklovskii, D., & Alon, U. (2002). Network motifs: simple building blocks of complex networks. *Science*, *298*, 824–827.
- Moberg, F., & Folke, C. (1999). Ecological goods and services of coral reef ecosystems. *Ecol. Econ.*, *29*, 215–233.
- Moeller, D. A. (2004). Facilitative interactions among plants via shared pollinators. *Ecology*, *85*, 3289–3301.
- Montoya, J. M., Pimm, S. L., & Solé, R. V. (2006). Ecological networks and their fragility. *Nature*, *442*, 259–264.
- Mora, C., Tittensor, D. P., Adl, S., Simpson, A. G., & Worm, B. (2011). How many species are there on earth and in the ocean? *PLoS Biol.*, *9*, e1001127.
- Morales, C. L., & Traveset, A. (2008). Interspecific pollen transfer: magnitude, prevalence and consequences for plant fitness. *Crit. Rev. Plant Sci.*, *27*, 221–238.
- Mougi, A., & Kondoh, M. (2012). Diversity of interaction types and ecological community stability. *Science*, *337*, 349–351.
- Naeem, S., & Li, S. (1997). Biodiversity enhances ecosystem reliability. *Nature*, *390*, 507–509.
- Neutel, A.-M., Heesterbeek, J. A., & de Ruiter, P. C. (2002). Stability in real food webs: weak links in long loops. *Science*, *296*, 1120–1123.
- Neutel, A.-M., & Thorne, M. A. (2014). Interaction strengths in balanced carbon cycles and the absence of a relation between ecosystem complexity and stability. *Ecol. Lett.*, *17*, 651–661.
- Novák, B., & Tyson, J. J. (2008). Design principles of biochemical oscillators. *Nat. Rev. Mol. Cell Biol.*, *9*, 981–991.
- Novak, M., Wootton, J. T., Doak, D. F., Emmerson, M., Estes, J. A., & Tinker, M. T. (2011). Predicting community responses to perturbations in the face of imperfect knowledge and network complexity. *Ecology*, *92*, 836–846.
- Odum, E. P. (1953). *Fundamentals of ecology*. Saunders, Philadelphia, PA.
- Odum, E. P. (1969). The strategy of ecosystem development. *Science*, *164*, 262–270.
- Odum, E. P., & Barrett, G. W. (2005). *Fundamentals of ecology*. (5th ed.). Thomson Brooks/Cole, Belmont, CA.
- Odum, H. T. (1957). Trophic structure and productivity of silver springs, florida. *Ecol. Monogr.*, *27*, 55–112.
- Odum, H. T. (1988). Self-organization, transformity, and information. *Science*, *242*,

- 1132–1139.
- Ohtomo, Y., Kakegawa, T., Ishida, A., Nagase, T., & Rosing, M. T. (2014). Evidence for biogenic graphite in early archaean isua metasedimentary rocks. *Nat. Geosci.*, *7*, 25–28.
- Okuyama, T., & Holland, J. N. (2008). Network structural properties mediate the stability of mutualistic communities. *Ecol. Lett.*, *11*, 208–216.
- Ollerton, J., Winfree, R., & Tarrant, S. (2011). How many flowering plants are pollinated by animals? *Oikos*, *120*, 321–326.
- Paine, R. T. (1966). Food web complexity and species diversity. *Am. Nat.*, *100*, 65–75.
- Paine, R. T. (1969). A note on trophic complexity and community stability. *Am. Nat.*, *103*, 91–93.
- Paine, R. T. (1980). Food webs: linkage, interaction strength and community infrastructure. *J. Anim. Ecol.*, *49*, 667–685.
- Petchey, O. L., Pontarp, M., Massie, T. M., Kéfi, S., Ozgul, A., Weilenmann, M., Palamara, G. M., Altermatt, F., Matthews, B., Levine, J. M. et al. (2015). The ecological forecast horizon, and examples of its uses and determinants. *Ecol. Lett.*, *18*, 597–611.
- Pianka, E. R. (1970). On r-and k-selection. *Am. Nat.*, *104*, 592–597.
- Pilosof, S., Porter, M. A., Pascual, M., & Kéfi, S. (2017). The multilayer nature of ecological networks. *Nat. Ecol. Evol.*, *1*, 0101.
- Pimm, S., & Lawton, J. H. (1978). On feeding on more than one trophic level. *Nature*, *275*, 542–544.
- Pimm, S. L. (1984). The complexity and stability of ecosystems. *Nature*, *307*, 321–326.
- Pocock, M. J., Evans, D. M., & Memmott, J. (2012). The robustness and restoration of a network of ecological networks. *Science*, *335*, 973–977.
- Poincaré, H. (1890). Sur le problème des trois corps et les équations de la dynamique. *Acta mathematica*, *13*, A3–A270.
- Potts, S., Biesmeijer, J., Kremen, C., Neumann, P., Schweiger, O., & Kunin, W. (2010). Global pollinator declines: trends, impacts and drivers. *Trends Ecol. Evol.*, *25*, 345–353.
- Prill, R. J., Iglesias, P. A., & Levchenko, A. (2005). Dynamic properties of network motifs contribute to biological network organization. *PLoS Biol.*, *3*, e343.
- Puccia, C. J., & Levins, R. (1985). *Qualitative modeling of complex systems an introduction to loop analysis and time averaging*. Harvard University Press, Cambridge, MA.
- Purves, D., Scharlemann, J. P., Harfoot, M., Newbold, T., Tittensor, D. P., Hutton, J., & Emmott, S. (2013). Ecosystems: time to model all life on earth. *Nature*, *493*, 295.
- Quévreur, P., & Brose, U. (2019). Metabolic adjustment enhances food web stability.

- Oikos*, 128, 54–63.
- Rezende, E. L., Lavabre, J. E., Guimarães, P. R., Jordano, P., & Bascompte, J. (2007). Non-random coextinctions in phylogenetically structured mutualistic networks. *Nature*, 448, 925–928.
- Ricker, W. (1963). Big effects from small causes: two examples from fish population dynamics. *J. Fish. Res. Board Can.*, 20, 257–264.
- Rietkerk, M., Dekker, S. C., de Ruiter, P. C., & van de Koppel, J. (2004). Self-organized patchiness and catastrophic shifts in ecosystems. *Science*, 305, 1926–1929.
- Rietkerk, M., & Van de Koppel, J. (1997). Alternate stable states and threshold effects in semi-arid grazing systems. *Oikos*, 79, 69–76.
- Roberts, A. (1974). The stability of a feasible random ecosystem. *Nature*, 251, 607–608.
- Rockström, J., Steffen, W. L., Noone, K., Persson, Å., Chapin III, F. S., Lambin, E., Lenton, T. M., Scheffer, M., Folke, C., Schellnhuber, H. J. et al. (2009). Planetary boundaries: exploring the safe operating space for humanity. *Ecol. Soc.*, 14, 32.
- Rohr, R. P., Saavedra, S., & Bascompte, J. (2014). On the structural stability of mutualistic systems. *Science*, 345, 1253497.
- Romero, G. Q., Gonçalves-Souza, T., Kratina, P., Marino, N. A., Petry, W. K., Sobral-Souza, T., & Roslin, T. (2018). Global predation pressure redistribution under future climate change. *Nat. Clim. Change*, 8, 1087–1091.
- Rosenzweig, M. L. (1971). Paradox of enrichment: destabilization of exploitation ecosystems in ecological time. *Science*, 171, 385–387.
- Rosenzweig, M. L., & MacArthur, R. H. (1963). Graphical representation and stability conditions of predator-prey interactions. *Am. Nat.*, 97, 209–223.
- Rosing, M. T. (1999). $\delta^{13}C$ -depleted carbon microparticles in 3700-ya sea-floor sedimentary rocks from west Greenland. *Science*, 283, 674–676.
- Saavedra, S., Reed-Tsochas, F., & Uzzi, B. (2009). A simple model of bipartite cooperation for ecological and organizational networks. *Nature*, 457, 463–466.
- Saavedra, S., Stouffer, D., Uzzi, B., & Bascompte, J. (2011). Strong contributors to network persistence are the most vulnerable to extinction. *Nature*, 478, 233–235.
- Scheffer, M. (1990). Multiplicity of stable states in freshwater systems. *Hydrobiologia*, 200, 475–486.
- Scheffer, M., Bascompte, J., Brock, W. A., Brovkin, V., Carpenter, S. R., Dakos, V., Held, H., Van Nes, E. H., Rietkerk, M., & Sugihara, G. (2009). Early-warning signals for critical transitions. *Nature*, 461, 53–59.
- Scheffer, M., Carpenter, S., Foley, J. A., Folke, C., & Walker, B. (2001). Catastrophic shifts in ecosystems. *Nature*, 413, 591–596.

- Scheffer, M., & Carpenter, S. R. (2003). Catastrophic regime shifts in ecosystems: linking theory to observation. *Trends Ecol. Evol.*, *18*, 648–656.
- Scheffer, M., Carpenter, S. R., Lenton, T. M., Bascompte, J., Brock, W., Dakos, V., Van de Koppel, J., Van de Leemput, I. A., Levin, S. A., Van Nes, E. H. et al. (2012). Anticipating critical transitions. *Science*, *338*, 344–348.
- Scheffer, M., Hosper, S., Meijer, M., Moss, B., & Jeppesen, E. (1993). Alternative equilibria in shallow lakes. *Trends Ecol. Evol.*, *8*, 275–279.
- Schink, B. (2002). Synergistic interactions in the microbial world. *Antonie van Leeuwenhoek*, *81*, 257–261.
- Shannon, C. E., & Weaver, W. (1949). *The mathematical theory of communication*. University of Illinois Press, Champaign, IL.
- Shaukat, S. S., Rao, T. A., & Khan, M. A. (2016). Impact of sample size on principal component analysis ordination of an environmental data set: effects on eigenstructure. *Ekológia (Bratislava)*, *35*, 173–190.
- Shelford, V. E. (1913). *Animal communities in temperate America: as illustrated in the Chicago region: a study in animal ecology*. 5. University of Chicago Press, Chicago, IL.
- Smith, S. H. (1968). Species succession and fishery exploitation in the great lakes. *J. Fish. Res. Board Can.*, *25*, 667–693.
- Snoussi, E. H. (1998). Necessary conditions for multistationarity and stable periodicity. *J. Biol. Syst.*, *6*, 3–9.
- Solé, R. V., & Montoya, M. (2001). Complexity and fragility in ecological networks. *Proc. Royal Soc. B*, *268*, 2039–2045.
- Steffen, W., Richardson, K., Rockström, J., Cornell, S. E., Fetzer, I., Bennett, E. M., Biggs, R., Carpenter, S. R., De Vries, W., De Wit, C. A. et al. (2015). Planetary boundaries: Guiding human development on a changing planet. *Science*, *347*, 1259855.
- Steffen, W., Sanderson, R. A., Tyson, P. D., Jäger, J., Matson, P. A., Moore III, B., Oldfield, F., Richardson, K., Schellnhuber, H.-J., Turner, B. L. et al. (2006). *Global change and the earth system: a planet under pressure*. Springer-Verlag, Berlin.
- Stella, J. S., Pratchett, M. S., Hutchings, P. A., & Jones, G. P. (2011). Coral-associated invertebrates: diversity, ecological importance and vulnerability to disturbance. *Oceanogr. Mar. Biol.*, *49*, 43–104.
- Stephens, P. A., Sutherland, W. J., & Freckleton, R. P. (1999). What is the allee effect? *Oikos*, *87*, 185–190.
- Stolyar, S., Van Dien, S., Hillesland, K. L., Pinel, N., Lie, T. J., Leigh, J. A., & Stahl, D. A. (2007). Metabolic modeling of a mutualistic microbial community. *Mol. Syst. Biol.*, *3*, 92.

-
- Stone, L., & Roberts, A. (1991). Conditions for a species to gain advantage from the presence of competitors. *Ecology*, *72*, 1964–1972.
- Stouffer, D., Camacho, J., Guimera, R., Ng, C., & Nunes Amaral, L. (2005). Quantitative patterns in the structure of model and empirical food webs. *Ecology*, *86*, 1301–1311.
- Stouffer, D. B., & Bascompte, J. (2010). Understanding food-web persistence from local to global scales. *Ecol. Lett.*, *13*, 154–161.
- Stouffer, D. B., Camacho, J., Jiang, W., & Amaral, L. A. N. (2007). Evidence for the existence of a robust pattern of prey selection in food webs. *Proc. Royal Soc. B*, *274*, 1931–1940.
- Sugihara, G. (1980). Minimal community structure: an explanation of species abundance patterns. *Am. Nat.*, *116*, 770–787.
- Sugihara, G. (1983). *Niche hierarchy: structure, organization and assembly in natural communities*. Ph.D. thesis Princeton University.
- Sutherland, W. J. (2006). Predicting the ecological consequences of environmental change: a review of the methods. *J. Appl. Ecol.*, *43*, 599–616.
- Sutherland, W. J., Freckleton, R. P., Godfray, H. C. J., Beissinger, S. R., Benton, T., Cameron, D. D., Carmel, Y., Coomes, D. A., Coulson, T., Emmerson, M. C. et al. (2013). Identification of 100 fundamental ecological questions. *J. Ecol.*, *101*, 58–67.
- Suttle, K., Thomsen, M. A., & Power, M. E. (2007). Species interactions reverse grassland responses to changing climate. *Science*, *315*, 640–642.
- Suweis, S., & D’Odorico, P. (2014). Early warning signs in social-ecological networks. *PLoS One*, *9*, e101851.
- Tansley, A. G. (1935). The use and abuse of vegetational concepts and terms. *Ecology*, *16*, 284–307.
- Thébault, E., & Fontaine, C. (2010). Stability of ecological communities and the architecture of mutualistic and trophic networks. *Science*, *329*, 853–856.
- Thom, R. (1972). *Stabilité structurelle et morphogénèse—Essai d’une théorie générale des modèles*. W.A. Benjamin, Inc., Reading, MA.
- Thom, R. (1975). *Structural Stability and Morphogenesis: An Outline of a General Theory of Models*, trans. D.H. Fowler. W.A. Benjamin, Inc., Reading, MA.
- Thom, R. (1977). Structural stability, catastrophe theory, and applied mathematics. *SIAM Rev.*, *19*, 189–201.
- Thomas, R. (1981). On the relation between the logical structure of systems and their ability to generate multiple steady states or sustained oscillations. In *Numerical methods in the study of critical phenomena* (pp. 180–193). Springer-Verlag, New York, NY.
- Thompson, J. N. (1994). *The coevolutionary process*. University of Chicago Press,

Chicago, IL.

- Tilman, D. (1982). *Resource competition and community structure*. Princeton university press, Princeton, NJ.
- Tilman, D., Lehman, C. L., & Bristow, C. E. (1998). Diversity-stability relationships: statistical inevitability or ecological consequence? *Am. Nat.*, *151*, 277–282.
- Tilman, D., Reich, P. B., & Knops, J. M. (2006). Biodiversity and ecosystem stability in a decade-long grassland experiment. *Nature*, *441*, 629–632.
- Tur, C., Sáez, A., Traveset, A., & Aizen, M. A. (2016). Evaluating the effects of pollinator-mediated interactions using pollen transfer networks: evidence of widespread facilitation in south andean plant communities. *Ecol. Lett.*, *19*, 576–586.
- Tylianakis, J. M., Didham, R. K., Bascompte, J., & Wardle, D. A. (2008). Global change and species interactions in terrestrial ecosystems. *Ecol. Lett.*, *11*, 1351–1363.
- Tylianakis, J. M., Laliberté, E., Nielsen, A., & Bascompte, J. (2010). Conservation of species interaction networks. *Biol. Conserv.*, *143*, 2270–2279.
- Tyson, J. J., Chen, K. C., & Novak, B. (2003). Sniffers, buzzers, toggles and blinkers: dynamics of regulatory and signaling pathways in the cell. *Curr. Opin. Cell Biol.*, *15*, 221–231.
- United Nations International Strategy for Disaster Reduction (2009). *Terminology on Disaster Risk Reduction*. UNISDR, Geneva.
- Urban, M. C., Bocedi, G., Hendry, A. P., Mihoub, J.-B., Pe'er, G., Singer, A., Bridle, J., Crozier, L., De Meester, L., Godsoe, W. et al. (2016). Improving the forecast for biodiversity under climate change. *Science*, *353*, aad8466.
- Usinowicz, J., & Levine, J. M. (2018). Species persistence under climate change: a geographical scale coexistence problem. *Ecol. Lett.*, *21*, 1589–1603.
- Uzzi, B. (1996). The sources and consequences of embeddedness for the economic performance of organizations: The network effect. *Am. Sociol. Rev.*, *61*, 674–698.
- Van Nes, E. H., Rip, W. J., & Scheffer, M. (2007). A theory for cyclic shifts between alternative states in shallow lakes. *Ecosystems*, *10*, 17–27.
- Van Nes, E. H., & Scheffer, M. (2004). Large species shifts triggered by small forces. *Am. Nat.*, *164*, 255–266.
- Van Nes, E. H., & Scheffer, M. (2007). Slow recovery from perturbations as a generic indicator of a nearby catastrophic shift. *Am. Nat.*, *169*, 738–747.
- Vandermeer, J. H. (1975). Interspecific competition: a new approach to the classical theory. *Science*, *188*, 253–255.
- Velicer, W. F., & Fava, J. L. (1998). Affects of variable and subject sampling on factor pattern recovery. *Psychol. Methods*, *3*, 231–251.

- Veraart, A. J., Faassen, E. J., Dakos, V., van Nes, E. H., Lürling, M., & Scheffer, M. (2011). Recovery rates reflect distance to a tipping point in a living system. *Nature*, *481*, 357–359.
- Vitousek, P. M., Mooney, H. A., Lubchenco, J., & Melillo, J. M. (1997). Human domination of earth's ecosystems. *Science*, *277*, 494–499.
- Walker, B., Holling, C. S., Carpenter, S., & Kinzig, A. (2004). Resilience, adaptability and transformability in social–ecological systems. *Ecol. Soc.*, *9*.
- Warren, P., & Lawton, J. (1987). Invertebrate predator-prey body size relationships: an explanation for upper triangular food webs and patterns in food web structure? *Oecologia*, *74*, 231–235.
- West, G. B., Brown, J. H., & Enquist, B. J. (1997). A general model for the origin of allometric scaling laws in biology. *Science*, *276*, 122–126.
- Whitehorn, P. R., O'Connor, S., Wackers, F. L., & Goulson, D. (2012). Neonicotinoid pesticide reduces bumble bee colony growth and queen production. *Science*, *336*, 351–352.
- Williams, R. J., Brose, U., & Martinez, N. D. (2007). Homage to yodzis and innes 1992: scaling up feeding-based population dynamics to complex ecological networks. In *From energetics to ecosystems: the dynamics and structure of ecological systems*. Springer, Dordrecht.
- Williams, R. J., & Martinez, N. D. (2000). Simple rules yield complex food webs. *Nature*, *404*, 180–183.
- Wilson, J. B., & Agnew, A. D. (1992). Positive-feedback switches in plant communities. In *Advances in Ecological Research* (pp. 263–336). Elsevier, Amsterdam volume 23.
- Wilson, S. K., Graham, N. A., Pratchett, M. S., Jones, G. P., & Polunin, N. V. (2006). Multiple disturbances and the global degradation of coral reefs: are reef fishes at risk or resilient? *Global Change Biol.*, *12*, 2220–2234.
- Winder, M., & Schindler, D. E. (2004). Climate change uncouples trophic interactions in an aquatic ecosystem. *Ecology*, *85*, 2100–2106.
- Wissel, C. (1984). A universal law of the characteristic return time near thresholds. *Oecologia*, *65*, 101–107.
- Woodward, G., Ebenman, B., Emmerson, M., Montoya, J. M., Olesen, J. M., Valido, A., & Warren, P. H. (2005). Body size in ecological networks. *Trends Ecol. Evol.*, *20*, 402–409.
- Wright, D. H. (1989). A simple, stable model of mutualism incorporating handling time. *Am. Nat.*, *134*, 664–667.
- Yachi, S., & Loreau, M. (1999). Biodiversity and ecosystem productivity in a fluctuating

- environment: The insurance hypothesis. *Proc. Natl. Acad. Sci. U.S.A.*, *96*, 1463–1468.
- Yodzis, P. (1981). The stability of real ecosystems. *Nature*, *289*, 674–676.
- Yodzis, P., & Innes, S. (1992). Body size and consumer-resource dynamics. *Am. Nat.*, *139*, 1151–1175.
- Zahler, R. S., & Sussmann, H. J. (1977). Claims and accomplishments of applied catastrophe theory. *Nature*, *269*, 759–763.

Summary

It is common knowledge that the millions of species that inhabit the Earth have adaptations that enable them to survive in different environments. Fish have gills which allow them to breathe under water, while the wings of birds allow them to fly. These adaptations are, as different as they may be, a different solution to the same problem: the problem of staying alive and reproduce in a world where species are under the constant pressure of natural selection. Perhaps less well known, but maybe not surprising when thought about carefully, is that the often complex networks of interactions between species, e.g. between plants and pollinators or between predators and prey, have certain non-random properties as well. These ‘network structural properties’, i.e. specific ways in which the interactions within networks are arranged most likely allow the often large numbers of species in ecosystems to coexist. Just like similar adaptations may be found in a wide variety of species, e.g. gills or gill-like organs in aquatic animals and wings on birds, insects, and bats, similar network structural properties may be found in a wide variety of ecosystems. Similarities that may occur simply because they are, like adaptations, a solution to the same problem: the problem of coexistence in systems where species heavily influence each other’s probability of survival.

While we are beginning to understand more about the structural properties of ecological networks, i.e. the networks of interactions between species, and how they might allow large numbers of species to coexist in complex ecosystems, the Earth and its ecosystems are changing at increasingly rapid rates due to human activities. In some cases, these changes are relatively simple in the sense that they affect a large group of species similarly, e.g. the effect of pesticides on a large group of insect pollinators, while in other cases these changes may be complex, e.g. the effects of climate change on the phenology and distribution of species which in turn leads to alterations in strengths of interspecific interactions in a way that is unique for each interaction. Ecosystems may respond in various ways to such changes (regardless of whether their effects are simple or complex). When conditions change gradually, the state of some ecosystems (e.g. the size of populations) may change likewise, in a smooth, gradual manner. Other systems may respond strongly to change within a narrow range of environmental conditions, but are relatively insensitive to change outside of this range. Particularly sudden shifts may occur when ecosystems have multiple alternative states. Such systems cannot change smoothly from

one state (e.g. large population sizes) to an alternative state (e.g. a state in which some or all species are extinct). Instead, a sudden shift or ‘critical transition’ occurs when environmental conditions pass a critical point. To return back to the original state after such a transition, a return to conditions prior to the transition is often not sufficient; instead, a larger change in conditions is needed until another critical point is reached at which the system shifts back to the original state, a phenomenon called ‘hysteresis’.

While the outcome of critical transitions is relatively predictable when a few leading species or species groups determine the state of an ecosystem, this may not be the case when ecosystem dynamics are determined by many interacting species. The consequences of critical transitions in such complex ecosystems might be severe, for example, when leading to the extinction of a large number of species. Not all critical transitions, however, will have dramatic consequences. Complex ecosystems may potentially shift to many different, alternative states. Some of those may imply minor, harmless changes in the state of a system, or invoke positive change, whereas others may have catastrophic consequences. The amount and type of change needed to cause a transition and a system’s future state after an impending critical transition depends in complex and often unknown ways on how ecosystems are organized, i.e. on the feedback mechanisms within it, and thus on the structure of ecological networks and/or how this structure might be changed by changing environmental conditions. Assessing or mitigating the risks associated with critical transitions in complex ecosystems thus requires a fundamental insight in the interrelationships between the structural properties of ecological networks, the dynamics of ecosystems, and the way in which these properties and dynamics might be affected by changing environmental conditions.

Despite a longstanding interest in ecological networks and more recent advances in detecting commonalities in the structure of ecological networks (**Chapter 1**), the common ground between studying the structure of ecological networks and the potential causes and consequences of critical transitions in complex ecosystems remains largely unexplored. One of the causes of this lack of exploration is, most likely, that stability is a multi-faceted concept that may be defined in various ways, e.g. the robustness of ecological networks to the random removal of species, a system’s temporal stability and/or speed of recovery from disturbances, and the amount of change in abundances or environmental conditions needed to cause a critical transition (**Chapter 1**). Most studies on the structure and stability of ecological networks have focused on stability concepts that are unrelated with critical transitions, while studies of critical transitions have often focused on the dynamics of individual populations rather than on the complex networks of interactions between species that maintain them.

In this thesis, we merge network theory with theory on critical transitions and show that an important trade-off between different aspects of stability may occur in pollinator communities (**Chapter 2**). The networks formed by the interactions between mutualistically

interacting plant and pollinator species are known to be highly nested, i.e. specialists tend to interact with a subset of the species interacting with the more generalist species. Earlier work has shown that such a structure may promote indirect facilitation, i.e. species indirectly support each other through interactions with other species, and the stable co-existence of species. We suggest, perhaps unsurprisingly, that such indirect facilitation also makes pollinator communities more resilient to changes in environmental conditions, e.g. an increase in the use of pesticides. This increase in resilience may, however, come at a cost; when pollinators continue to facilitate each other under increasingly harsh conditions they may eventually collapse simultaneously, because they depend on each other for survival. Recovery from such a simultaneous collapse may require a relatively large improvement of conditions. Findings that may have large implications for our view on the sustainability of pollinator communities and the services they provide in a time when pollinator populations are rapidly declining.

The most commonly studied cause of critical transitions in ecology is a positive, reinforcing feedback that amplifies change when changing conditions or abundances pass a critical value. In the aforementioned pollinator communities, for example, a decline in pollinator abundances may negatively affect plants, which in turn is bad for pollinators and leads to a further decline in pollinator abundances. Studies on the structure and stability of complex ecological networks, on the other hand, often put (implicitly) more emphasis on delayed negative feedbacks, i.e. negative feedbacks with a time lag, usually occurring as the result of an uneven number of negative interactions in feedback loops of two or more species, as a potential cause of instability. Food-web theory and observations in real ecosystems, for example, suggest that destabilizing oscillatory dynamics caused by strong predator-prey interactions are damped by many weak interactions. Transitions towards such dynamics, and more complex, chaotic dynamics, may occur when delayed negative feedbacks gain in strength relative to more immediate negative feedbacks (**Chapter 3**). Inspired by previous work on critical transitions and the structural stability of dynamical systems, we describe a variety of transitions, associated with different types of boundaries in parameter space, that may occur when such stabilizing, damping patterns are undermined. Inspired by previous work on critical transitions and the structural stability of dynamical systems, we describe a variety of transitions, associated with different types of boundaries in parameter space, that may occur when such stabilizing, damping patterns are undermined and explore how structural network patterns, i.e. species number, connectance, and variability in interaction strength, might influence the occurrence of such transitions. To illustrate that abrupt transitions towards alternative stable states, oscillatory or other more complex dynamics may occur even under basic dynamical assumptions, we assume that the functional response of predators, i.e. the relation between a predator's intake rate and prey availability, is linear. Future work may build on this study to include also more complex, non-linear functional responses.

The dynamics of ecosystems are determined by the interplay between many stabilizing

and destabilizing feedbacks and one may assume therefore that it will hardly be possible to detect a change in a system's proximity to a critical point. Earlier work has, however, shown that an increasingly slow recovery from small disturbances may be indicative of a loss of resilience prior to critical transitions. Various indicators of this phenomenon known as 'critical slowing down' may therefore serve to detect an increase in the likelihood of critical transitions. Predicting what comes after a critical transition is, however, terra incognita altogether. In **Chapter 4** we take a first step into this unexplored territory and show that the relative simplicity of the dynamics of mutualistic communities may allow us to look beyond impending critical transitions and foresee a community's future state. To make such predictions, we take advantage of the increasingly slow recovery from perturbations prior to critical transitions. Such disturbances have a size (i.e. the total amount of change) and a direction (i.e. the relative amount of change in each species) in the phase space of complex systems. The more similar a disturbance's direction to the direction in which increasingly small perturbations may cause critical transitions, the stronger the effect of critical slowing down. Provided that there are no oscillating, chaotic or other complex dynamics, a system's future state will most likely lie in the same approximate direction. This 'direction of critical slowing down' may thus provide us with an indicator of a system's future state, and may help us assess whether impending critical transitions may have large, systemic consequences. As an indicator of the direction of critical slowing down we propose to use the direction in which the distribution of fluctuating species abundances becomes increasingly asymmetrical, but other methods to determine this direction may be possible as well.

The major, unanswered questions in ecology are often separated in two main classes: the fundamental ones, aiming to understand the basic processes shaping and occurring in ecosystems, and the applied ones, e.g. aiming to identify or reduce the risks associated with changing environmental conditions (**Chapter 5**). In a time when ecosystems are confronted with rapid environmental change, it is, however, becoming increasingly clear that predicting the consequences of changing environmental conditions requires a fundamental understanding of the processes occurring in ecosystems. In particular, because such changes are likely to bring ecosystems outside of the range in conditions for which data are available. Questions on the stability of ecosystems in the context of such changes are thus both applied and fundamental because their answers require the development of novel theories and hypothesis. In this thesis, I hope to have provided novel ideas and insights that might help to address the question of whether changing environmental conditions are likely to lead to large-scale systemic regime shifts in complex ecosystems. An emerging property of complex ecosystems that may be referred to as 'systemic risk'.

Acknowledgements

These last pages in my PhD thesis are, perhaps, a good place to discuss the question of what gives a diploma value or purpose. Obviously, there are many possible answers to this question, and, in many cases, this answer will be highly personal and dependent on the diploma under consideration. Some diplomas have little value outside of the specific context within which they are awarded and are mostly there to provide students with a target towards which they can work and to acknowledge an achievement. I once received a diploma for being able to tie my shoelaces, for example. Other diplomas are more akin to a license, such as a diploma I received for my capacity to work in a lab safely, and may serve to make sure that only suitable candidates can access a particular job and/or participate in more highly specialized activities.

Doctoral degrees are, like most diplomas and their associated titles, a combination of an acknowledgement and a requirement, e.g. to apply for grants and continue a career in academia. I have, however, never been quite sure what to make of them, and would rather have worked towards separate diplomas for clearly defined skills such as producing and exploring novel ideas that fail, lecturing/educating, science communication (in a broad sense), computational/mathematical research methods, and being socially awkward. I think such diplomas could better represent someones competences and may thus contribute to a better system of requirements for a further career (in industry and academia). It could also remove the element of 'social status' associated with a doctoral degree. Something I'm not particularly fond of because the same status may not be awarded to people with equally valuable skills.

The skills I acquired while traveling between research labs in Seville, Wageningen, and Zurich, my increased knowledge of different European cultures, the great conversations with colleagues, colleagues that became friends, and the new perspectives we developed over the past years on as large a topic as 'how the world works' are, however, invaluable to me. They have changed me for life and I am grateful to more than are listed here.

First and foremost, I wish to express my gratitude to my (co-)promotors; Egbert, Jordi, and Marten. Your willingness to go along with the idea of an MSc student that was as vaguely defined as 'to serve as a bridge between your research labs' and 'to do something with critical transitions and the structure of ecological networks' meant, by definition,

that the probability of failure was higher. You've all invested lots of time, energy, and effort in me and my research regardless, and even though I was physically present in your labs only approximately half the time, you treated me as no less and, to my feeling, often as more than a full member of your research labs.

Egbert, I hope that one day you can tell me how you manage to always be available. Your contribution to this thesis has been enormous, and I am particularly grateful for your patience and feedback during the countless occasions in which I stormed into your office to discuss yet another possible solution for a problem we hardly knew existed. I learned a lot from you and your modesty deserves a statue.

Jordi, I admire your broad knowledge and capacity to place ideas into context. Even while I was an MSc student you took time to think about the ideas I had for further research, for example while walking back home in Seville, and helped me to further improve them or to understand why they were not so good after all. You acted as a mentor and made me more mature as a (scientific) thinker.

Marten, your playful nature is a constant reminder that creativity is a vital part of a scientific process. I value the discussions we had when exploring theoretical ideas and the time we spend together. You invited me into your (scientific) life and showed me, by example, how being a good scientist can be a lifestyle with sufficient moments of 'wandering' during which thinking is done by association.

Even though I am defending this thesis at the Wageningen University, I divided my time approximately equally between the labs of Jordi in Seville/Zurich and Marten in Wageningen and my research is greatly influenced by both environments. My fellow lab members at the Estación Biológica de Doñana in Seville, Antonio, Daniel S., Javier, Jessica, Miguel, Raúl, Maria C., Maria L., Rudolf, Serguei, Luisjo, Vasilis, and the lab's wider environment with, among others, Adrian, Ana, Andy, Arndt, Cande, Eva, Koldo, Pedro, Montse, Martha, Mireia, Pete, Shai, and Violeta, provided me with a home. Later I was, although more at a distance, joined by lab members at the University of Zurich such as Daniel W., Daniel T., Matthew, Nikos, Petra, Rodrigo, and Sabine. Some of you helped me to learn Spanish, others with coding/mathematics. We had inspiring scientific discussions. We complained about and enjoyed Sevillian culture. You gave me general advice on life, paperwork, and helped me to develop an international lifestyle. We spend many happy and joyful moments together, and, perhaps, one of the most important things you learned me is to let go of conventions. I had to re-invent myself and I hope to keep doing this permanently.

While re-inventing myself, I always found a safe-heaven at Wageningen University where I was lucky to be embedded in an environment full of kind, smart, and inspiring people. My fellow 'theoreticians', Arie, Babak, Bregje, Els, Ingrid, Pablo, Usman, Sanne G., Sebastian, and Xu, provided me with lots of feedback and food for thought, for example, during inspiring brainstorm sessions or one-to-one conversations. I think that, regardless of the

topic, anything we could discuss is interesting. Similarly inspiring discussions occurred within the ‘food-web group’ with Annette, Cassandra, Helen, Jan, Jeroen, Luuk, Robert, Sanne S., Sanja, and Wolf during the early stages of my research, and a wider warm daily environment was offered by my office mates Jochem and Marlies (thanks for taking care of the aquarium!) and other members of the Aquatic Ecology and Water Quality Management Group with, among others, Andrea, Andreu, Annelies, Ariadna, Bart, Bastiaan, Bernardo, Darya, Diego, Edwin, Els, Fee, Frits, Goraw, Gissell, Irene, Jacqui, Jeroen, John, Joke, Jordie, Kristina, Maíra, Marina, Milena, Merel, Nancy, Natalia, Nika, Noel, Miquel, Paul, Paula, Rudi, Sanne B., Sarian, Wendy, and Qinghua. We walked on ice, drank jenever at ‘De Zaaier’, sat in the sun, and went to festivals. We picked apples, had interesting conversations over lunch, and you explained and showed to me what research with actual organisms and chemicals can be like. I always felt supported by you as a group, for which I am deeply grateful.

Of course, life is not all about science, and I would like to thank all of my friends in, as a consequence of my research, various countries. Thank you for distracting me, the conversations we had, visiting me abroad, the evenings out, the evenings in, and all the other occasions in which we had fun or in which you were there for me. I especially want to thank Violeta with whom I spend a great part of the past years together. I will never look at the German ICE trains that allowed me to travel between Utrecht and Frankfurt, and Frankfurt and Zurich in the same way.

During my travels and PhD research, the knowledge that, when everything else fails, my family would be there to support me was important. I am thankful to my sisters, their husbands, and their children for being a part of their life even though, during substantial periods of time, I was and am living abroad. This is incredibly valuable to me. Papa and mama, thank you for stimulating my curiosity for science, music, and the world around me. Thank you for listening to me when I had doubts, and being there for me when I needed support. It is a luxury that I can take your support for granted.



About the author

Jelle Lever was born in 1984 in Maastricht, the Netherlands. He studied Biology (BSc) and Environmental Sciences (MSc) at Utrecht University where he obtained a broad general knowledge of biology and environmental policy. He wrote a BSc thesis on ‘Graadmeters voor Ecologische Natuurwaarde’, i.e. on methods to quantify the ecological value of natural areas, developed a strong interest for theoretical ecology while working on an MSc research project supervised by Yolanda Pueyo and Sonia Kéfi, and wrote his MSc thesis, supervised by Max Rietkerk and Jordi Bascompte, on ‘Competition, trophic interactions and the impact of habitat fragmentation on species richness’. One month before obtaining his MSc, Jelle started working on his PhD research under the supervision of Egbert van Nes and Marten Scheffer at Wageningen University and Jordi Bascompte at the Estación Biológica de Doñana in Seville and the University of Zurich. While working on this research, he divided his time approximately equally between the research labs of Jordi in Seville/Zurich and Marten in Wageningen and his work is greatly influenced by members of both labs. His current research interests vary from general theories on the stability and dynamics of complex systems to ecology, evolutionary developmental biology, conservation biology, and environmental policy.

Jelle has a variety of other interests. During his studies, Jelle was, for example, an active member of the Dutch United Nations Student Association in Utrecht for which he organized a large number of debates with on international politics and, prior to his studies at Utrecht University, Jelle followed preparatory schooling at the Utrecht School of the Arts (HKU) for a program to obtain a Bachelor of Music.

Jelle currently lives in Cambridge (UK) where he follows a teacher training programme at the University of Cambridge.



*Netherlands Research School for the
Socio-Economic and Natural Sciences of the Environment*

D I P L O M A

for specialised PhD training

The Netherlands research school for the
Socio-Economic and Natural Sciences of the Environment
(SENSE) declares that

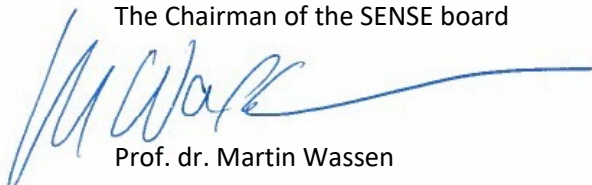
J. Jelle Lever

born on 8 April 1984 in Maastricht, The Netherlands

has successfully fulfilled all requirements of the
educational PhD programme of SENSE.


Wageningen, 19 February 2020

The Chairman of the SENSE board



Prof. dr. Martin Wassen

the SENSE Director of Education



Dr. Ad van Dommelen

The SENSE Research School has been accredited by the Royal Netherlands Academy of Arts and Sciences (KNAW)



K O N I N K L I J K E N E D E R L A N D S E
A K A D E M I E V A N W E T E N S C H A P P E N



The SENSE Research School declares that **J. Jelle Lever** has successfully fulfilled all requirements of the educational PhD programme of SENSE with a work load of 38.2 EC, including the following activities:

SENSE PhD Courses

- o Environmental research in context (2011)
- o Modelling critical transitions in nature and society (2014)
- o Research in context activity: 'Developing, publishing, and popularizing around subject of PhD research: www.systemicriskinecosystems.net' (2019)

Other PhD and Advanced MSc Courses

- o Models of Biological Processes and Environmental Quality, Wageningen University (2011)

External research visits at a foreign research institute

- o Visiting researcher, Estación Biológica de Doñana, Spain (2011-2014)

Management and Didactic Skills Training

- o Teaching Assistant MSc course 'Academic Consultancy' (2011), BSc course 'Food Web Ecology' (2011), and MSc course 'Classics and Trends' (2013), Wageningen University
- o Supervising two MSc students with thesis, Wageningen University (2013 and 2016)
- o Lecturer BSc course 'Kwaliteit van Leven', University of Amsterdam (2013-2015)
- o Lecturer BSc course 'Modelling Biological Systems', Wageningen University (2013-2014)
- o Lecturer PhD course 'Modelling critical transitions', SENSE Research School (2014)
- o Lecturer 'Dynamische Ecologie', Bètasteunpunt Wageningen – a course for secondary school teachers (2015)
- o Lecturer MSc course 'Introduction to Theoretical Ecology', University of Zurich (2015-2016)

Oral Presentations

- o *Critical transitions and the collapse of mutualistic networks. Ecological Society of America Annual Meeting, 05-10 August 2012, Portland, United States of America*
- o *Patterns of direct and indirect interactions prior to systemic shifts in ecological networks. Ecological Society of America Annual Meeting, 04-09 August 2013, Minneapolis, United States of America*
- o *Critical transitions in complex food webs, Conference on Complex Systems, 23-28 September 2018, Thessaloniki, Greece*
- o *Critical transitions in complex food webs, British Ecological Society Annual meeting, 16-19 December 2018, Birmingham, United Kingdom*

SENSE coordinator PhD education

Dr. ir. Peter Vermeulen

The research described in this thesis was financially supported by the Wageningen University, a Spinoza Prize awarded by the Dutch Research Council (NWO) to Marten Scheffer, and two European Research Council Advanced Grants awarded to Marten Scheffer and Jordi Bascompte.

Printing: Proefschriftmaken || www.proefschriftmaken.nl
Cover design: J. Jelle Lever

ISBN: 978-94-6395-263-7

DOI: <https://doi.org/10.18174/510243>

